UNIVERSITY OF CALIFORNIA
RIVERSIDE

Uncovering Mechanisms of Varicella Zoster Virus Pathogenesis Using a Rhesus Macaque Model

A Dissertation submitted in partial satisfaction
of the requirements for the degree of

Doctor of Philosophy

in

Microbiology

by

Nicole Justine Arnold

December 2016

Dissertation Committee:
Dr. Ilhem Messaoudi, Chairperson
Dr. Katherine Borkovich
Dr. Emma Wilson

The Dissertation of Nicole Justine Arnold is approved:

Committee Chairperson

University of California, Riverside

ACKNOWLEDGEMENTS

To Ilhem Messaoudi: Thank you for taking a chance on me and allowing me to join your lab. You have challenged me to do things that I thought that I could never do. Also, thank you for the countless pep talks during our individual meetings and words of encouragement when one of my papers would get rejected from a journal. I know you will make a great Mommy!

To the Messsaoudi Lab: Thank you guys so much for all of your help and support. I feel so lucky to have had such great lab mates that I can truly call my friends.

To Dr. Borkovich and Dr. Wilson: Thank you guys for agreeing to be on my committee. I truly do appreciate you guys for taking the time out of your day to give me great advice on becoming a great scientist. And to Dr. Borkovich, I wouldn't have even joined the PhD program if you wouldn't have recruited me so thank you for giving me the courage to undergo this challenge.

The text of this dissertation, in part or in full, is a reprint of the material as it appears in Clinical and Experimental Immunology 2016 (Chapter 1), Nature Scientific Reports 2016 (Chapter 2) and the Journal of Virology 2016 (Chapter 3). Chapter 5 is currently under review in the Journal of NeuroVirology. The co-author Ilhem Messaoudi listed in those publications directed and supervised the research that forms the basis for this dissertation.

This work was funded by the National Institute of Health (RO1AG037042-06).

DEDICATION

To my loved ones: I love you guys! **Mom**, thank you for watching Boe while I was at lab and for just being great supportive mother. **Dad,** thank you for the financial support and allowing me to get through grad school without having to be stressed financially. **Sisters and brothers,** thank you for always being there for me when I needed someone to talk to. **Nella,** thank you for always being there for me when I needed to get out and have some fun. You are such a great friend and I know I will always be able to count on you. **Kevin,** although we have only been together for 8 months I feel like you have made a positive impact in my life and I am thankful for all of the support you have given me.

In loving memory of Marvin Irvin Hunt, my grandpa and #1 fan.

ABSTRACT OF THE DISSERTATION

Uncovering Mechanisms of Varicella Zoster Virus Pathogenesis Using a Rhesus Macaque Model

by

Nicole Justine Arnold

Doctor of Philosophy, Graduate Program in Microbiology
University of California, Riverside, December 2016
Dr. Ilhem Messaoudi, Chairperson

Varicella Zoster Virus is neurotropic alpha herpesvirus that causes varicella (chickenpox) and establishes latency in the sensory ganglia. Reactivation results in herpes zoster (HZ, shingles), a painful and debilitating disease that affects 1 million people in the US each year. FDA approved vaccines reduce the incidence of both varicella and HZ; however, they induce short-lived immunity and are contraindicated for individuals who are immunosuppressed. The development of more efficacious vaccines has been hampered by the fact the VZV is a strictly human pathogen which has hindered the development of a robust translational animal model. Previous studies from our laboratory have shown that intrabronchial inoculation of rhesus macaques with simian varicella virus (SVV), the homolog of VZV, recapitulates the hallmarks of VZV infection in humans. In this dissertation, we use this animal model to investigate the host-pathogen interactions in the lung and sensory ganglia (sites of primary infection and latency) as well as the role that T cells play in SVV tropism and reactivation. First, we show that SVV infection causes severe lung damage characterized initially by significant immune infiltration, an up-regulation of genes involved in antiviral immunity and a down-regulation of genes involved in lung development. This robust host response correlates with a decrease in viral loads and is then

followed by an increase in genes important for tissue repair. Next, we show that SVV DNA and transcripts are detected in the ganglia 3 days post-infection (DPI), before the development of varicella. Interestingly, CD4 and CD8 T cells were also shown to infiltrate the sensory ganglia 3 DPI; before the development of cell mediated immunity, which suggests a role for T cells in SVV tropism into the ganglia. SVV acute infection of the ganglia induces robust gene expression changes indicative of an innate antiviral immune response along with a down-regulation of genes that play a role in the nervous system function. Interestingly, genes important for neuron development remained down-regulated 100 days post infection suggesting that SVV latency leads to a long-lived remodeling of the ganglia transcriptional profile. Next, given the crucial role that T cell play in SVV dissemination, we characterized the transcriptional changes that SVV infection induces within them. This analysis revealed that SVV alters expression of several genes that may support viral replication and dissemination. Lastly, we report that the decline of both CD4 and CD8 T cell immunity followed by stress can lead to SVV reactivation, which also causes long-lasting gene expression changes in the ganglia transcriptome, indicative of neuronal damage. These findings provide novel insights into the host pathogen interactions of VZV during acute infection and guide efforts toward more efficacious vaccines and therapeutics.

TABLE OF CONTENTS

Acknowledgements	**iv**
Dedication	**v**
Abstract	**xi**
List of Figures	**xi**
List of Tables	**xii**
Chapter 1: Introduction and Review of Literature	**1**
1.1 VZV genome and replication cycle	1
1.2 Acute VZV infection	2
1.2.1 Clinical manifestation of varicella	2
1.2.2 Acute VZV complications and treatment	3
1.3 Latency	4
1.4 Immunity	5
1.4.1 Immune system overview	5
1.4.2 Immune response during acute VZV infection	6
1.4.3 VZV Immune Evasion	8
1.5 Varicella vaccine	10
1.6 Reactivation	11
1.6.1 Clinical manifestations of Herpes Zoster	11
1.6.2 Herpes zoster complications and treatment	13
1.6.3 Immune response during reactivation	14
1.7 Herpes Zoster Vaccines	16
1.7.1 Live attenuated Zostavax®	16
1.7.2 Inactivated Adjuvant Subunit Vaccine	17

1.7.3 Heat inactivated vaccines 18

1.8 Animal models for VZV 20

1.8.1 Rodent Models 20

1.8.2 SCID-humanized mouse model 21

1.8.3 Nonhuman Primate models (NHP) 21

1.9 Simian Varicella Virus 22

1.9.1 Intrabronchial infection of SVV in rhesus macaques 22

1.9.2 Immune response to SVV in rhesus macaques 23

1.9.3 SVV Immune Evasion 25

1.10 Thesis Overview and Aims 25

CHAPTER 2: Genomic and functional analysis of the host response to acute simian varicella infection in the lung 27

Abstract 28

Introduction 29

Materials and Methods 31

Results 36

Discussion 63

CHAPTER 3: Acute simian varicella infection causes robust and sustained changes in gene expression in the sensory ganglia 69

Abstract 70

Introduction 71

Materials and Methods 73

Results 81

Discussion 110

CHAPTER 4: Simian Varicella Virus causes robust transcriptional changes in T cells that support viral replication 117

Abstract 118

Introduction 119

Materials and Methods 121

Results 123

Discussion 131

CHAPTER 5: Robust gene expression changes in the ganglia following subclinical reactivation in rhesus macaques infected with Simian Varicella Virus 135

Abstract 136

Introduction 137

Materials and Methods 139

Results 143

Discussion 162

CHAPTER 6: Discussion and Future Directions 166

6.1.1 SVV infection causes significant lung inflammation and lung injury 166

6.1.2 SVV reaches the site of latency before the appearance of rash 167

6.1.3 SVV induces transcriptional changes T cells in order to support viral replication 169

6.1.4 Both CD4 and CD8 T cells play a critical role in preventing reactivation 170

6.2 Final thoughts 173

REFERENCES 174

LIST OF FIGURES

Figure 1.1 Varicella Zoster Virus (VZV) immune response during reactivation **15**

Figure 2.1 SVV infection results in inflammation **37**

Figure 2.2 SVV infection induces secretion of cytokines, chemokines and growth factors **38**

Figure 2.3 SVV infection induces immune infiltration **40**

Figure 2.4 Immune cells proliferate and exhibit cytotoxicity in SVV infected lungs **41**

Figure 2.5 SVV infection results in robust changes in lung gene expression. **44**

Figure 2.6 Gene Validation **45**

Figure 2.7 DEGs detected 3 DPI play a role in innate immunity and lung development **47**

Figure 2.8 ImmGen heatmap showing the expression profile of the up-regulated genes found at day 3-post infection across different immune cell populations **50**

Figure 2.9 DEGs detected 7 DPI are involved in host defense **52**

Figure 2.10 ImmGen heatmap showing the expression profile of the up-regulated immune related genes found at day 7 post-infection across different immune cell populations **55**

Figure 2.11 DEGs detected 10 DPI are involved in cell cycle and organ development **57**

Figure 2.12 ImmGen heatmap showing the expression profile of the up-regulated genes at day 10 post-infection across different immune cell populations **60**

Figure 3.1 SVV viral DNA and immune infiltrates are detected in sensory ganglia as early as 3DPI **82**

Figure 3.2 Immunohistochemistry staining shows immune infiltration of T cells and macrophages **85**

Figure 3.3 SVV trafficking and replication is supported in T cells of the BAL **86**

Figure 3.4 SVV replicates in the ganglia before establishing latency at 7DPI **88**

Figure 3.5 SVV infection results in robust changes in gene expression **91**

Figure 3.6 Gene Validation **93**

Figure 3.7 Immunohistochemistry gene validation **95**

Figure 3.8 DEGs at 3 DPI play a role in axon transport, immunity and neuronal development **98**

Figure 3.9 DEGs at 7 DPI play a role in antiviral immunity and neuronal development **100**

Figure 3.10 DEGs at 10 DPI and 14 DPI are associated with neuronal development **105**

Figure 3.11 DEGS in latently infected ganglia tissue (100 DPI) play a role in the development of the nervous system and are associated with neurological diseases **109**

Figure 4.1 SVV causes robust gene expression changes in T cells **124**

Figure 4.2 Enrichment analysis revealed an up-regulation in gene regulation **126**

Figure 4.3 Enrichment analysis of down-regulated gene are involve with the immune system and antigen presentation **130**

Figure 5.1 Animal treatments and whole blood cell counts **144**

Figure 5.2 Thymectomy followed by depletion results in the loss of naïve T cells **145**

Figure 5.3 Depletion results in robust homeostatic proliferation **147**

Figure 5.4 SVV reactivation is detected in depleted animals in the absence of robust changes in immunity **149**

Figure 5.5 SVV reactivation results in substantial host transcriptional changes in the ganglia **151**

Figure 5.6 Gene validation **154**

Figure 5.7 Gene enrichment analysis of the up-regulated genes in reactivated animals **157**

Figure 5.8 Gene enrichment analysis of the down-regulated genes in reactivated animals **160**

Figure 6.1 SVV pathogenesis in a rhesus macaque **171**

LIST OF TABLES

Table 1.1 Pros and cons for Zostavax®, herpes zoster/subunit vaccine (HZ/su) and V212 vaccines **19**

Table 3.1 The number of differentially expressed genes (DEGs) found in the ganglia after SVV infection **90**

Table 3.2 Ten most statistically significant GO terms to which DEGs enriched at each time point **97**

Table 5.1 DRG-T Viral loads of the samples used for RNA-Seq analysis **153**

Table 5.2 Gene enrichment analysis of up-regulated and down-regulated genes **156**

CHAPTER 1: Introduction and Review of Literature

1.1 VZV genome and replication cycle

Varicella Zoster Virus (VZV) is one of 8 human herpes viruses and belongs to the alphaherpesvirus family together with HSV1 and HSV2. It has a linear double stranded DNA genome that is 124,885 base pairs long and encodes 71 unique open reading frames (ORFs)(1). The VZV genome has two isomeric forms consisting of one long and one short covalently linked segments with unique sequences bounded by inverted terminal repeats (ORF69 and ORF70). VZV shares approximately 40 conserved ORFs with other human herpesviruses that are essential for: viral replication (ORF18 and ORF19), DNA packaging (ORFs 25, 26, 30, 34, 42/45, 43 and 54), tegument structure (ORF9-ORF12, 22, 38, 44, 46, 53, 57, 64, and 69), capsid assembly (ORFs 20, 21, 23, 33, 40 and 41), and glycoproteins (gB(ORF31), gC(ORF14), gE(ORF68), gH(ORF37), gI(ORF67), gK(ORF5), gL(ORF60) and gN (ORF9a)) (1-3). Like other herpesviruses, the VZV virion contains an icosahedral-shaped nucleocapsid that encloses the viral DNA genome and a lipid envelope containing glycoproteins that facilitate viral entry (1).

VZV entry into cells is not well understood due to the difficulty in obtaining cell-free virus but is believed to occur through direct fusion with the plasma membrane or endocytosis (4). Previous studies have shown the VZV glycoproteins may interact with the mannose 6 phosphate receptors and/or heparin sulfate proteoglycan on the target cell surface (5). After viral entry, the virions are uncoated and nucleocapsids attach to nuclear pores and inject their genomic DNA into the nucleus where it circularizes. Successful lytic infection requires the use of the host's cellular machinery. Transcription of viral genes is accomplished using the host cell RNA polymerase (6). Gene expression occurs in a temporal manner with transcription of immediate early, early and then late genes (7). Immediate early and early genes encode for proteins involved in the

regulation of gene expression and viral replication while late genes encode for structural proteins such as nucleocapsids and glycoproteins (8). Viral mRNAs are transported to the cytoplasm where they are translated into proteins that are then transported back into the nucleus and used to complete the viral replication cycle. Nucleocapsids are then assembled in the nuclei of infected cells. Tegument proteins and glycoproteins are added in the cisternae of the trans-Golgi network (9). The virus is then released into the cytosol where it fuses with the plasma membrane to bud off. The replication cycle followed by the release of viral progeny takes 9-12 hours in human fibroblasts (7).

1.2 Acute VZV infection

1.2.1 Clinical manifestation of varicella

VZV is a highly contagious virus that is spread through the inhalation of saliva droplets containing viral particles or by direct contact with infectious fluid from vesicles (10, 11). It has an incubation period of 10-21 days, but shorter incubation periods have been observed in immunocompromised people (10, 12). It is believed that VZV initially replicates in the upper respiratory tract and tonsillar lymph nodes before dissemination to the skin. Previous studies proposed a dual viremia model where the virus first undergoes amplification in organs such as the liver and spleen followed by a secondary viremia during which the virus is transported to the skin (13). However, subsequent studies have shown that viral amplification in the spleen and liver is not necessary for viral dissemination to the skin.

Varicella usually occurs during childhood (1- 9 years old) and outbreaks have been shown to peak in late winter and early spring (14). Pain and burning sensation are usually the first symptoms of varicella; then fluid, virus-filled blisters begin to develop within 24 hours. Rash is

usually accompanied with fever, headache, fatigue and itching. Diagnosis of varicella is usually determined through visual inspection of the rash (15). Symptomatic relief usual consists of acetaminophen to control fever and topical medication to relieve the itch. Within 1-2 weeks, lesions begin to crust and sloth off (15).

1.2.2 Acute VZV complications and treatment

Primary infection of VZV in immune competent individuals usually resolves with no complications. However, in individuals who are immunocompromised, varicella can be severe and in some cases, fatal (16, 17). Adults aged 20 and above are 13 times more likely to be hospitalized and 25 times more likely to die compared to adolescents (18). Bacterial infection of skin lesions and pneumonia are the most common complications in both immune competent and immunocomprised children (16). Neurological complications are very rare and occur in 1-3 per 10,000 cases during acute infection (19). The most serious varicella-associated neurological complication is acute cerebellar ataxia, which can occur in 1 in 4000 – 1:100,000 varicella cases in children (depending on the age of the population studied) (20-22). Primary infection of varicella has also been associated with increased susceptibility to stoke in immune competent children (23) due to inflammation caused by VZV infecting endothelial cells lining the cerebral arteries (24).

Primary VZV infection in seronegative women during the first 8 to 20 weeks of gestation could result in fetal varicella syndrome, characterized by cutaneous scars, ocular malformations, and limb and central nervous system defects (25). This syndrome occurs in only 1-2% of births to mothers who contract varicella during pregnancy (26). In addition, acute VZV infection during the last two weeks of gestation can lead to congenital or neonatal varicella (25). Because of this

risk, women of childbearing age are screened for VZV-specific antibodies and vaccination is recommended if titers are below detection. Individuals who are at increased risk of severe varicella are often administered antivirals such as acyclovir or VZV-specific immunoglobulins (VariZIG) as prophylaxis following suspected exposure (27).

1.3 Latency

Like Herpes simplex 1 (HSV-1) and HSV-2, VZV establishes latency in sensory ganglia, and co-infection of the same neuron by multiple herpesviruses has been described (28, 29). The sensory ganglia is a bundle of nerve cell bodies in the intervertebral foramen that transmit sensory signals from the periphery to the central nervous system (30). The sensory ganglia are categorized based upon their location along the neuraxis: dorsal root ganglia (DRG) cervical, DRG thoracic, DRG lumbar sacral and trigeminal. VZV can also establish latency in enteric neurons (31), located in the lining of the gastrointestinal system and control autonomic activity (32).

There are two (non-mutually exclusive) theories on how VZV reaches the ganglia: 1) VZV enters into the nerve terminals from the vesicular rash hijacking the retrograde transport mechanism to the ganglia (33, 34); 2) VZV accesses the distal neurons through the hematogenous route, carried by infected T cells that gain access to the ganglia (35). Studies using fetal human skin xenografts in the severe combined immunodeficiency (SCID) mouse model showed that VZV can disseminate to the skin by infected tonsillar CD4+ T cells that express skin homing markers but not by infected skin fibroblasts (36-38). Other studies suggest that DCs infected at the respiratory mucosa transport VZV to the draining lymph nodes where they then infect T cells that can acquire memory and homing markers and travel to the skin (37, 39). Indeed, a recent study using

time of flight mass cytometry showed that in vitro VZV infection remodels tonsillar T cell with into activated skin-homing T cells (40, 41). Additional in vivo studies need to be done to clarify whether either or both theories are accurate.

During latency, VZV DNA is found in both satellite and neuron cells in sensory ganglia (42) as a circular episomal genome with limited viral gene transcription (43, 44). The most frequently expressed viral genes detected during latency include ORF4, ORF21, ORF29, ORF62, ORF63, and ORF66 (45-47). Interestingly, during latency, transcripts associated with these ORFs are found in the cytoplasm of neurons, whereas during acute replication in fibroblasts, they are found in the nucleus of the cell (48, 49). ORF4 and ORF63 were found to be required for the establishment of latency in a rat model where VZV-infected melanoma cells were injected directly into the spine (50, 51). Additional studies using rat neurons have shown that ORF63 may also play a role in preventing apoptosis (52).

1.4 Immunity

1.4.1 Immune system overview

The immune system consists of a network of cells that defend the host against foreign pathogens. It is comprised of two main arms: innate and adaptive immunity. The innate system is known as the first line of defense against pathogens and generates short-lived responses. It consists of neutrophils, which are able to kill infected cells by phagocytosis and by producing nitric oxide (53); eosinophils, basophils and mast cells that are important for fighting parasitic infections and mediating allergic responses (54); dendritic cells (DCs) and monocytes which are antigen-

presenting cells (APCs) that process foreign pathogens and present it to T cells leading to their activation (55); and Natural Killer (NK) cells which destroy virally infected and "altered" cells through the release of granzymes (56).

Unlike the innate immune system, the adaptive immune system develops life long immunological memory after its first response to a specific pathogen. This allows for a fast and enhanced response to subsequent exposures. The adaptive immune system consists of T cells and B cells. T cells are generated in the thymus where they differentiate into naïve CD4 or CD8 T cells (57). The main function of CD4 T cells is to modulate immune responses and to help B cells make antibodies (57). CD4 T cells can be further categorized as T helper (Th1), Th2, Th17, regulatory T cells (Tregs) and follicular helper (Tfh) CD4 T cells. Th1 responses produce proinflammatory cytokines such as IL-2, IFNγ and TNFα, which are important for killing intracellular pathogens such as viruses and intracellular bacteria (58). Th2 responses release cytokines IL-4, IL-5, IL-9, IL-10 and IL-13 which are important for killing parasites and helminth infections (58, 59). Th17 cells play an important role in killing extracellular pathogens. Tregs down-regulate the immune response after the pathogen has been cleared (60). Lastly, Tfh cells play a vital role in promoting germinal cell B cell responses (61). CD8 T cells are cytotoxic T cells that kill infected cells by producing granzymes and perforin (62) and secrete antiviral cytokines IFNγ and TNFα (63). With the help of cytokines produced by CD4 T cells, naïve B cells mature into plasma cells that secrete antibodies (57). Antibodies play an important role in fighting off pathogens by neutralizing microbes and opsonizing infected cells so that they can be phagocytosed and killed by macrophages and NK cells respectively (57).

1.4.2 Immune response during acute VZV infection

Both the innate and adaptive immune responses play a critical role in controlling VZV replication during acute infection. Early responses are mediated through NK cells and type 1 interferons. Indeed, patients who are deficient in NK cells or lack activated NK cells are at increased risk of severe or fatal varicella (64-67). NK cells can kill VZV-infected cells by secreting the antiviral factor granulysin, which induces apoptosis in infected cells (68). Type 1 and type 2 interferons (IFNs) have also been shown to inhibit VZV replication in human skin xenografts (38). Moreover, IFNα treatment reduces the number of new varicella lesions in cancer pediatric patients when administered within 72 hours after the appearance of the rash (69).

Complete resolution of acute VZV infection requires adaptive immune responses (70). Subjects with T cell deficiencies such as those with lymphoma, undergoing chemotherapy, or infected with Human Immunodeficiency Virus (HIV) experience severe varicella (71, 72). VZV-specific T cells can be detected in the blood 3 to 7 days after the appearance of rash and their frequency peaks 1-2 weeks later followed by a gradual decline (70, 73). T cell immunity to VZV is primarily a Th1 response with IL-2, IL-12, TNFα and IFNγ being the primary cytokines produced (74). IFNγ has been shown to induce clonal expansion of VZV specific T cells (75). Although a comprehensive analysis of the specificity of the primary anti-VZV T cell response has yet to be conducted, CD8 T cell responses to VZV immediate early genes ORF4, ORF62 and ORF63; tegument protein ORF10; single stranded DNA binding protein ORF29; and glycoproteins ORF67 (gI) and ORF68 (gE) have been described (1, 76-79).

Humoral immunity can be measured within 3 days after the appearance of the rash with the production of IgM, IgG, and IgA antibodies (80). The specificity of the antibody responses was

determined using a protein microarray that contained all 69 distinct VZV proteins and sera from subjects ranging from 2 to 70 years of age with no current symptoms of varicella or Herpes Zoster (HZ). This analysis showed that antibodies are primarily directed against VZV glycoproteins (ORF5, ORF14, ORF31, ORF37 and ORF68), capsid proteins (ORF20, ORF23, ORF40), tegument proteins (ORF53, ORF9, ORF11), proteins involved in viral replication and virion assembly (ORF25, ORF26, ORF28), immediate early transactivators (ORF12, ORF62 and ORF63), and membrane proteins ORF2 and ORF24 (81). The highest antibody responses were directed against ORF2, ORF12 and ORF62 (81).

Although both T and B cell responses are generated during acute varicella, early production of VZV-specific T cells, but not antibodies, correlates with reduced severity of clinical symptoms (70). In line with this observation, patients with agammaglobulinemia have uncomplicated varicella and are equally protected against a second episode of varicella as individuals with normal B cell responses (82). Moreover, treatment with VariZIG is most effective when given within 96 hours of exposure and recommended to be administered within 10 days of exposure (83).

1.4.3 VZV immune evasion

Like other viruses, VZV has developed mechanisms to evade the immune response. One of the ways that VZV is able to evade the innate response is by interfering with the interferon pathway. IFNα expression, a critical antiviral cytokine, is down-regulated of in VZV infected epidermal cells in skin xenografts of SCID-hu mice (84). This may be mediated by VZV IE63-mediated

inhibition of the key transcription factor STAT-1 activation (85). VZV ORF66 has also been shown to inhibit the IFNα signaling pathway in VZV-infected T cells (86) and VZV ORF61 has also been shown to degrade IRF3 in the IRF3-mediated IFNβ pathway (87).

The NFkB pathway, which is important for stimulating the expression of several genes involved in the immune response, can also be modulated by VZV. VZV ORF61 inhibits the NFkB pathway in DCs in vitro (88). In addition, VZV infections of epidermal cells, results in the sequesteration of NFkB subunits p50 and p65 in the cytoplasm, which in turn leads to the inhibition of IkBα degradation and prevents NFkB activation (89). VZV has also been shown to modulate I-CAM expression, which facilitates leukocyte recruitment, in VZV infected keratinocytes from HZ lesions (90). Furthermore, recent reports have suggested that VZV may interfere with the complement cascade in human T cells and DRG by up-regulating CD59 expression, which prevents the formation of the membrane attack complex (91).

VZV can also interfere with the adaptive immune reponse by interfering with antigen presentation. ORF66 has been shown to prevent MHC class I from reaching the cell surface by sequestering it in the golgi (92, 93). In addition, VZV can also down-regulate IFNγ-mediated MHC class II upregulation by inhibiting the expression of Stat1α and Jak2 proteins in the Jak/Stat pathway (94, 95) in human fibroblasts (HFs) and keratinocytes. Moreover, VZV can down-regulate MHC class I, CD80, CD83, CD86 and Fas expression on DC in vitro, which may inhibit their maturation and apoptosis (96, 97).

1.5 Varicella vaccine

Varivax® is a live attenuated vaccine that contains the Oka strain licensed for protection against varicella. The Oka strain was developed by Takahashi et al in 1974 by attenuating a VZV isolate from a child with primary varicella through 11 passages in human embryonic lung fibroblasts followed by 12 passages in guinea pig embryo fibroblasts and finally several additional passages in human diploid cells (98). The resultant attenuated Oka vaccine strain has 42 single-nucleotide polymorphisms (SNPs) compared to wild type VZV with 15 substitutions in ORF 68 alone (99). In the first clinical trial, hospitalized children with no history of varicella were vaccinated with the Oka stain vaccine in an attempt to stop the spread of chickenpox in the hospital. This trial proved to be successful (98).

Before the introduction of the varicella vaccine in the US in 1995 there were about 4 million cases each year in the US with about 11,000 hospitalizations and 50 to 100 deaths (100, 101). Medical costs for varicella were 5.2-6.1 million dollars per year (102). The introduction of the varicella vaccine led to an 88% reduction in the number of chickenpox cases (103). Initially, one vaccination was recommended, however the annual rate of breakthrough varicella significantly increased with time since vaccination from 1.6 cases per 1000 people within 1 year to 58 per 1000 people after 9 years (104). The results from this survey along with reports of breakthrough varicella in largely vaccinated school children populations led to the recommendation of a second dose of the Varivax® vaccine (105). The first vaccination is recommended at 12-15 months followed by a second dose at 4-6 years of age (103). The introduction of the second dose resulted in 98.3% efficacy (106). The vaccine is also 71-100% effective if given within 72 hours of exposure (107).

The varicella vaccine induces VZV-specific humoral and cellular responses. VZV-specific T cell responses are detected 2-3 weeks after immunization in children (108). An increase in the number of T cells expressing the activation markers CD25 and HLA-DR was observed 6 weeks after vaccination (109). VZV-specific antibodies are detected within 7-10 days after vaccination (110). Plasma levels of IL-2 at 2-4 days post vaccination, and IL-10 and IFNγ at 5 -7 days post vaccination are also increased (109, 111). These same cytokines are also produced in the PBMCs through natural infection of VZV (70). Antibodies are detected in 87.3% of children after one dose and 99% after a second dose (112).

Adverse reactions to the vaccine are minimal and include local reactions such as pain and inflammation at the site of infection (19 -24%) and rash (5 lesions in 3 -4 %). Although very rare, the vaccine can result in mild varicella and can be transmitted to other people (113). The vaccine is counter-indicated for people who are immunocompromised, pregnant or have serious allergic reactions to gelatin or neomycin. Varivax® may be administered to HIV infected children with a CD4+ cell count > 200 cells/uL (114). Although the current vaccine is effective in the prevention of clinical disease (varicella), it is still able to establish latency in the sensory ganglia (115). Furthermore, the vaccine strain was reported to reactivate in healthy children (116) and children with hematological malignancies who received bone marrow transplants (117).

1.6 Reactivation

1.6.1 Clinical manifestations of Herpes Zoster

VZV reactivation results in herpes zoster (HZ), a painful and often debilitating disease that affects 1 million individuals/year in the United States alone (118). During VZV reactivation, the virus travels ante-retrograde from the sensory ganglia to the skin nerve terminals where it infects

and replicates in keratinocytes, and epithelial cells, causing polykaryocytes (35) (Fig. 1.1). The first symptom of HZ is usually severe prodromal pain and burning which precedes the rash (119). Unlike varicella, the HZ rash is restricted to the dermatome innervated by the ganglia from which the virus reactivated (120).

The incidence of HZ dramatically increases after the age of 50 from an average of 3 cases per 1000 adults 40-50 years old, to 10 cases of HZ per 1000 adults aged 80 years or above (121). HZ also occurs frequently in individuals with autoimmune diseases, cancer, and organ transplant recipients who are receiving immunosuppressive drugs (66). Increased incidence of HZ has also been linked to physical trauma, inflammatory bowel disease, and diabetes (122, 123). Interestingly, African Americans are significantly less susceptible to HZ compared to Caucasians (124). In addition, numerous studies in the U.S and Europe have demonstrated that the incidence of HZ is significantly higher in women than men (125-129).

VZV can also reactivate without resulting in a rash. When accompanied by pain, this is referred to zoster sine herpete (130), which is difficult to diagnose and can only be confirmed by measuring VZV DNA in the cerebrospinal fluid (131). Asymptomatic reactivations can also occur during episodes of mild stress or immune suppression. For instance, infectious VZV DNA has been recovered from the saliva of astronauts during and after spaceflight in the absence of disease (132). VZV has also been hypothesized to reactivate from the enteric neurons resulting in enteric zoster, which causes gastrointestinal pain without a rash (32).

1.6.2 Herpes zoster complications and treatment

As with primary infection, HZ generally resolves with no complications, however, 26% of patients experience additional complications that are, on rare occasions, fatal (133). The most common complication is post-herpetic neuralgia (PHN, 19% of HZ cases), defined as chronic pain in the affected dermatomes lasting many months after resolution of the rash, presumably due to damaged nerve endings (133). Another serious complication is HZ ophthalmicus (1-10% of HZ cases) where reactivation from the first division of the trigeminal nerve leads to chronic ocular inflammation that could ultimately lead to blindness (133, 134). Additional rare complications include vasculopathy (which can occur with or without rash) where the virus infects the cerebral arteries and causes ischemic infarctions in the brain or spinal cord, leading to stroke, aneurysm and cerebral hemorrhaging (135). In immunocompromised individuals, VZV reactivation may also result in myelopathy where the virus infects the spinal cord or spinal arteries (136). VZV reactivation from the enteric neurons can lead to aganglionosis and ileus (137).

Treatment for most of these complications include antiviral therapy, however, the efficacy of antiviral drugs initiated later than 72 hours after the appearance of the rash is uncertain (138). Corticosteriods have also been shown to reduce morbidity, however, their efficacy is short lived and does not reduce the risk of PHN (139). Other treatments for PHN include antidepressants and antiepileptic drugs such as gabapentin (140, 141), opiate analgesic drugs, and topical anesthetic drugs such as lidocaine and capsaicin (142). VZV vasculopathy and myelitis are treated with intravenous acyclovir (135). Unfortunately, a large portion of patients do not respond to these treatments or only have moderate relief of pain or adverse side effects to the drugs (143).

1.6.3 Immune response during reactivation

As described above for varicella, it is believed that VZV-specific T cell immunity plays a more critical role in the prevention of VZV reactivation than antibodies. VZV antibody responses have been shown to be very stable with half-lives around 50 years, whereas VZV-specific T cells have been shown to decline with age (144, 145). Furthermore, studies have shown that frequency of VZV-specific CD4 T cells declines more dramatically with age compared to CD8 T cells (146). Although, our understanding of the specificity of the anti VZV response is very limited, T cell responses against the IE transactivators ORFs 62 and 63 are reduced in older individuals (77) and patients with malignancies (147).

During reactivation, VZV-specific T cell responses increase, peaking 3 to 6 weeks after the onset of the zoster rash and returning to pre-HZ levels by 3 years (118). Antibody titers also increase 6 fold 3 weeks after HZ and return to baseline levels by 6 weeks (118). VZV reactivation also results in a local immune response in the ganglia (Fig. 1.1). A study that examined ganglia collected from people who suffered from zoster 1 to 4.5 months before they died from other causes, reported presence of T cells (75% of which were non-cytolytic CD8 T cells), B cells, macrophages and Natural Killer (NK) cells, but no DCs in the ganglia (148). The recruitment of T and NK cells to the ganglia could potentially be due to VZV-induced expression of chemokine CXCL10 from neurons, which binds to CXCR3 on memory T cells and NK cells to induce their migration (149). Up-regulation of MHC-I and MHC-II molecules during reactivation has also been observed, suggesting a second mechanism for T cell retention and activation in the sensory ganglia (148). Skin biopsies collected during reactivation also show presence of CD4, CD8, NK cells and macrophages along with increased expression of IFNγ, TNF-α and IL-6 compared to non-lesioned skin biopsies from controls (90) (Fig. 1.1).

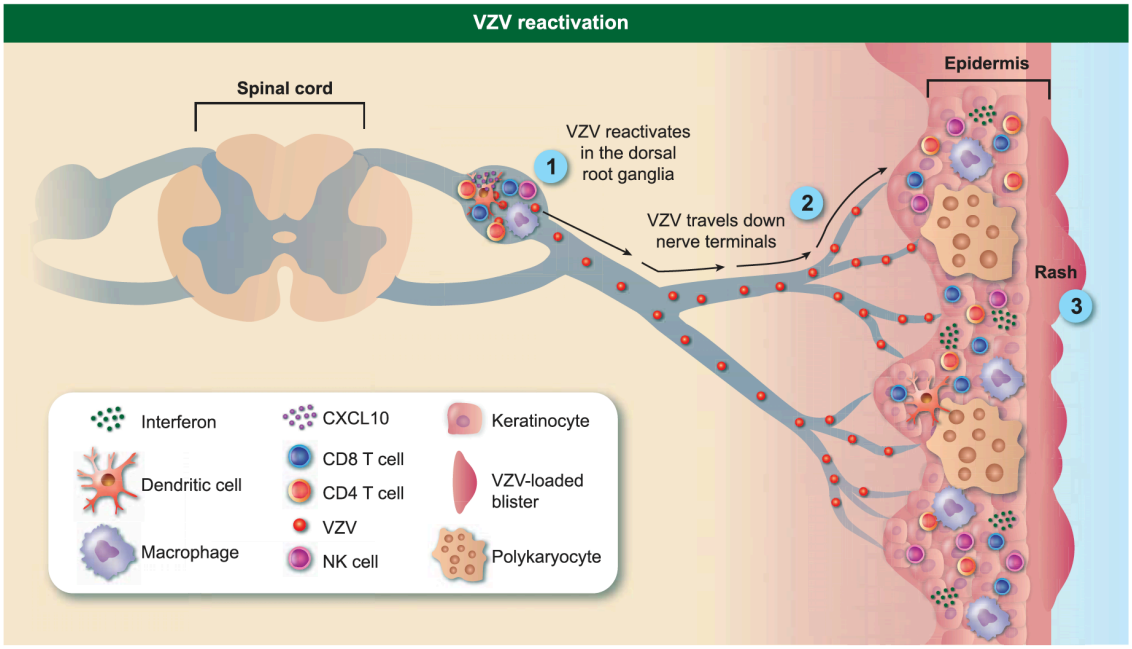

Figure 1.1 Varicella Zoster Virus (VZV) immune response during reactivation. When immune responses weaken, VZV reactivates by travelling anterograde towards nerve endings, replicates in keratinocytes and epithelial cells causing the formation of polykaryocytes, leading ultimately to a dermatomal rash. The local immune response in the ganglia is characterized by the infiltration of CD8, CD4, natural killer (NK) cells,macrophages and B cells. The immune response in the skin is characterized by CD4, CD8, NK cells and macrophages along with increased expression of interferon (IFN)-g, tumour necrosis factor (TNF)-a and interleukin (IL)-6.

1.7 Herpes Zoster Vaccines

1.7.1 Live attenuated Zostavax®

The Food and Drug Administration approved Zostavax® for the prevention in zoster in people 60 years of age and older in May 2006 (150). This vaccine contains 19,400 PFU/dose compared to the varicella vaccine Varivax®, which contains ~1,350 PFU/dose of live attenuated virus (121). Zostavax® was approved after the completion of the Shingles Prevention Study (SPS), a double blind, placebo controlled study that involved 38,546 people (151). Results from the SPS showed that Zostavax® reduced the incidence of disease by 51% and lowered the incidence of PHN and associated pain by 66.5% in subjects > 60 years of age (151). Efficacy of this vaccine decreases with increasing age with only 18% efficacy in individuals over the age of 80 (151). The FDA lowered the age requirement to 50 years in 2011 due to the increased efficacy in adults 50-59 (70%) (152, 153). Long-term efficacy of this vaccine was shown to drop to 21.1% for HZ and 35.4% for the PHN over the course of 7 to 10 years (154). A booster dose of Zostavax® 10 years after the first dose has been shown to enhance protection against HZ in people over the age of 70 (145). Therefore, like Varivax®, boosters may be recommended for Zostavax®.

Zostavax® vaccination induces a significant increase in VZV cell mediated responses compared to placebo recipients 6 weeks after vaccination, however, as described for efficacy, vaccine-induced increase in T cell responses negatively correlates with age of the recipient (155). Moreover, vaccine-induced cell mediated immunity declined dramatically one year post vaccination, and at the end of a 3 year follow up, T cell immunity had returned to almost pre-vaccination levels (151). A recent study showed that Zostavax® vaccination increases CD4 T cell responses to ORFs 40, 67, 9, 59, 12, 62, one month after vaccination. However, after 6 months, only CD4 T cells responses to ORFs 40, 59, 63 and 67 remained higher than pre-vaccination

levels (156). Interestingly, T cell responses to the VZV oka vaccine strain cross-recognize HSV-1 and HSV-2 antigens, which may indicate that the Zostavax® vaccine may provide some degree of protection against HSV as well (157). Zostavax® vaccination increases a humoral immune response to VZV, albeit to a lesser extent compared to levels achieved after HZ (118). Zostavax® can boost the antibody titers of individuals who previously had HZ, and the magnitude of this boost is negatively correlated with time since HZ episode (158).

Adverse reactions to Zostavax® mainly include pain and inflammation at the site of infection (159). Concomitant vaccine administration of zoster and influenza vaccine or pneumococcal vaccines does not adversely affect their immunogenicities (160, 161). Although Zostavax® vaccine has been proven to be safe for HIV-infected people with 15% CD4 T cells or a CD4 T cell count of 200 cells/μl, it is contraindicated for people who are: 1) taking steroids (40/per day for more than 7 days or 20mg/day for more than 14 days), 2) receiving biologics such as anti-TNFα (in the past 12 months) or 3) currently undergoing or underwent radiation or chemotherapy in the past 6 months (114, 162, 163). The Center for Disease Control (CDC) also recommends that newly vaccinated people avoid contact with individuals at high-risk for varicella complications such immune-compromised patients. Infectious viral DNA has been found in saliva from Zostavax® vaccinated individuals for up to 4 weeks post vaccination (164).

1.7.2 Inactivated Adjuvant Subunit Vaccine

Another potential strategy to develop a more efficacious vaccine is to generate a subunit vaccine that expresses immunogenic VZV proteins. Subunit vaccines can provoke a strong immune response while being safe for individuals for whom live attenuated vaccines are contraindicated. Two doses of a subunit vaccine (HZ/su) developed by GlaxoSmithKline using adjuvanted

recombinant glycoprotein E (ORF68) has shown great immunogenicity and efficacy in older individuals regardless of their age. A phase III HZ/su study that was recently completed with a total of 15,411 participants that received two doses of vaccine or placebo showed overall 97.2% efficacy rate among all three age groups tested (50-59, 60-69 and ≥70) in a 3.2-year follow up study (165). However, 81.5% of HZ/su recipients in the phase III study experienced pain at the site of injection and 66% of recipients had mild to moderate systemic reactions (grade 3 severity in 11.4% of the subjects) such as myalgia (most common), fatigue and headache (165). Glycoprotein E was selected for this subunit vaccine because it is the most abundant viral glycoprotein and also elicits robust CD4 T cell and antibody responses (166, 167). The adjuvant being used is ASO1, which is a liposome-based adjuvant system containing 3-O-desacyl-4'-monophosphoryl and saponin QS-21, which activates the Toll-like receptor 4 (TLR4) pathway and stimulates both antibody and Th1 responses (168). Two doses of HZ/su elicited a stronger anti-VZV gE, anti-VZV lysate antibody, and anti-VZV lysate CD4 T cell responses than two doses of Zostavax® in adults 50-70 year old over a 12-month follow up period (169). However, CD4 specific T cells and antibody levels to HZ/su dropped by almost half after 42 months (169). Three doses of the HZ/su vaccine was shown to be safe and immunogenic in hematopoietic cell transplants patients for up to 1 year and HIV patients for up to 18 months (170, 171).

1.7.3 Heat inactivated vaccines

Randomized, double blind, placebo controlled phase III studies are currently being conducted to test the safety and efficacy of a heat inactivated Varivax® (V212) vaccine targeted for bone marrow and hematopoietic- cell transplant recipients (172, 173). Study is expected to be completed end February 2017. Pros and cons for the Zostervax®, HZ/su and V212 vaccines are described in Table 1.1.

Vaccine	Pros	Cons
Live, attenuated vaccine **Zostavax®**	• Boosts both cellular and humoral immune responses	• Contraindicated for people with weakened immune systems • Potential for shedding and therefore transmission to people with weakened immune system • Vaccine needs to stay frozen in order to remain potent • Immunity and efficacy wane with increasing age and with time since vaccination
Subunit Vaccine **HZ/su**	• Only contains one viral protein, making it safe for immune deficient people and pregnant women	• Requires 2 doses • High incidence of adverse events due to the potency of the adjuvant
Heat inactivated **V212**	• Safe for immune deficient people and pregnant women • Does not require refrigeration	• Stimulates a weaker immune response than live vaccines • Requires 4 doses, making compliance an issue

Table 1.1 Pros and cons for Zostavax®, herpes zoster/subunit vaccine (HZ/su) and V212 vaccines

1.8 Animal models for VZV

1.8.1 Rodent Models

Guinea pigs have been used as an animal model of VZV infection, however, successful infection requires a guinea pig adapted strain that was passaged several times in fetal guinea pig cells (174-177). Subcutaneous and intranasal inoculation results in seroconversion, however, the development of rash is variable. Two studies which used the same intramuscular inoculation method in inbred weanling guinea pigs reported different results, with one reporting rash from 80% of infected animals 3 to 7 days post infection while the other study reported no clinical disease (175, 176). In addition, viremia is rarely detected and there is no evidence that VZV is infectious in guinea pigs (174, 177). However, studies using guinea pigs have provided evidence that VZV can be transmitted by aerosolized droplets (178) and that VZIG can be prophylactic for VZV (176). Furthermore, this animal model has shown that infected T cells can disseminate VZV to enteric neurons (179) suggesting that VZV may be linked to bowel related diseases such as gastric ulcers (180) and ulcerative colitis (181).

Rats have also been used as a model of VZV infection. However, subcutaneous, ocular and intraperitoneal inoculation result in seroconversion without clinical disease (182-185). Subcutaneous footpad inoculation of rats showed that VZV DNA can be detected the dorsal root ganglia (DRG) as early as 1-month post infection (182, 185). In addition, ORF 62 and ORF 63 transcripts which were previously reported in latently infected human ganglia (186-188) were found in the ganglia of rats 18 months after bilateral footpad inoculation (189). Rats have also been used to study pain associated with VZV such as PHN. In this model, Wistar rats inoculated subcutaneously in footpads experience hyperalgesia and allodynia in the infected footpad that decrease significantly 5 dpi and are resolved by 60 dpi (190, 191). Although rodent animal

models have provided insight into VZV pathogenesis, they don't severe as a robust translational animal model due to the fact that VZV inoculation doesn't result in disease or viremia.

1.8.2 SCID-humanized mouse model

Severe-combined immunodeficient humanized (SCID-hu) mice have been extensively used to investigate mechanisms of VZV pathogenesis (192). In this model a conjoint thymus liver (thy/liv) transplant or human fetal dorsal root ganglia (DRG) (193) is implanted under the kidney capsule. Human skin is also sometimes implanted as a dermal graft (194). Studies using the SCID-hu model have shown that T cells support viral replication (194) and that intravenous injection of VZV infected T tonsillar T cells but not VZV infected fibroblasts, results in the characteristic varicella rash in implanted human skin, showing that T cells play a vital role in VZV dissemination to the skin (84). Additional studies using this model have demonstrated that IFNα plays a critical role in inhibiting VZV replication in the skin explants. Direct inoculation of human fetal dorsal root ganglia (DRG) xenografts in this model showed that VZV replicates in the ganglia for 8 weeks, before establishing latency (193) and that both neurons and satellite cells are capable of being infected with VZV (84, 195). Although the use of SCID-hu mouse model has provided novel insight into key characteristics of VZV pathogenesis, this model presents significant shortcomings, notably the absence of an adaptive immune branch as well as the fact that the inoculation methods used do not mimic the natural route of infection.

1.8.3 Nonhuman Primate models (NHP)

As described for rodents, inoculation of NHPs with VZV does not result in disease. Subcutaneous VZV inoculation results in viremia in chimpanzees, however, the rash was limited to the site of infection (196). Oral-nasal-conjunctival inoculation of marmosets and intratracheal

inoculation of patas monkeys with VZV results in seroconversion in the absence of clinical disease or viremia (197, 198). Intratracheal or intrabronchial inoculation of cynologous and rhesus macaques with VZV also results in the development of both humoral and cellular immunity in the absence of rash and viremia (199, 200).

1.9 Simian Varicella Virus

Simian Varicella Virus (SVV) was first isolated in 1975 from an outbreak in vervet monkeys at the Tulane National Primate Center that was characterized by disseminated skin rash, fever, and 60% mortality rate (201). In contrast, reports of epizootics in macaques showed a much milder case of a varicella-like disease. Specifically, SVV outbreaks in pig-tailed, Japanese, cynomolgus, formosan rock and rhesus macaques in a Washington primate center resulted in only a 10% mortality (202, 203). SVV shares significant structural and genetic similarities with VZV. SVV and VZV genomes have comparable sizes (SVV: 124,138 bps versus VZV: 124,884bps) and G+C% content (SVV: 40.4% versus VZV: 46%). The two genomes share 70 to 75% DNA homology and 27% (ORF1) to 75% (ORF 31) similarity at the amino acid level (204, 205). The only major difference is found in the left terminus where the SVV genome contains an invertible 665bp that is absent in VZV (206). The similarities are so significant that vaccinating monkeys with VZV antigens resulted in protection from SVV (198).

1.9.1 Intrabronchial infection of SVV in rhesus macaques

Given the significant homology between SVV and VZV, our laboratory sought to develop an alternative NHP model Rhesus macaques were chosen for this model since SVV infection of other NHPs resulted in either severe and often fatal disease (207, 208) or persistent viremia (208, 209). To circumvent these challenges, other groups have utilized a model of natural infection of

cynonologous macques where naïve monkeys are exposed to intratrachelly infected monkeys. This model results in the development of rash and latency (210) however, antibody titers are lower than that seen in VZV seropositive patients viremia and seroconversion are not consistently observed and exact day of infection is not easily determined, which is a major confounder for longitudinal analysis of host responses (206, 210). In contrast, intrabronchial infection of rhesus macaques with SVV reproduces the cardinal features of VZV infection in humans including viremia, development of cellular and humoral immunity, and the establishment of latency in the sensory ganglia with limited transcriptional activity (49, 211-220).

1.9.2 Immune response to SVV in rhesus macaques

Following intrabronchial SVV infection, neutrophils infiltrate the lungs 7 DPI and their numbers peak 10 DPI, before returning to baseline 21 DPI. Plasmacytoid DCs, which play a role in producing the important antiviral factor IFNα peak at 7 DPI, while frequencies of myeloid dendritic cells (mDCs), which play a crucial role in T cell activation peak at 14 DPI in the BAL (221). Infiltration of immune cells in the BAL is accompanied by robust increases in chemokines (MCP-1 (CCL2), MIG (CXCL9), I-TAC (CXCL11), MIP-1α (CCL3), MIP-1β (CCL4), eotaxin, RANTES) that are chemotactic for monocytes, dendritic cells, NK cells, eosinophils and T cells at 7 DPI. Moreover, monocyte cytokines (IL-15, IL-1β, IL-6 and IL-12) also peak 7 DPI (221).

T cell proliferation peaks in the BAL and PBMC 10 DPI and SVV-specific T cell responses are first detected 7 DPI and their levels peak at 21 DPI. Similarly Th1 cytokine levels (IFNγ, TNFα and IL-2) also peak in the BAL at 7 DPI (217, 221). CD8 T cells are the dominant lymphocyte population in the BAL during acute infection and their relative frequency remains significantly

increased for up to 126 DPI (221), but both CD8 and CD4 T cells display cytolytic activity in the BAL and PBMC (221). B cell proliferation peaks at 10 DPI in the BAL and 14 DPI in the PBMC and correlates with peak SVV-specific antibody IgG antibody titers (217, 221).

Using this model we showed that CD4 T cells play a critical role in controlling acute infection (219) as well as the establishment of latency (220). We also characterized the specificity of the T cell response to SVV during acute infection and latency using IFNγ ELISPOT (222). Our data show a robust and broad T cell response during acute infection with CD8 T cell responses directed mostly against immediate early and early viral proteins, while CD4 T cell responses were directed primarily against SVV late genes. During latent infection, T cells responses were significantly reduced in magnitude and breadth compared to those observed during acute infection (222). Interestingly, T cell responses against ORF4, ORF11, ORF19, ORF31, and ORF 37 were maintained into latency albeit at lower levels whereas T cells responses to ORF10, ORF20, ORF29, ORF31, ORF62, ORF63 and ORF68 showed a significant decrease of about 83% between primary and latent infection (222). These observations provide a potential explanation for the success of the subunit vaccine HZ/su, which contains adjuvanted ORF68 protein and can potentially aid in the development of a multivalent subunit vaccine.

Studies using this model have also shed light on VZV trafficking to the ganglia. African green macaques (AGMs) infected with SVV expressing enhanced green fluorescent protein show that SVV primarily infects memory T cells that can infiltrate the ganglia (223). This study also showed the infiltration of DCs and macrophages into the ganglia during acute SVV infection of AGMs (224). Moreover, as described for VZV in humans, CD4 and CD8 T cells infiltrate the ganglia during SVV reactivation, which correlates with CXCL10 expression (225). However,

given the severity of SVV infection in AGMs and the differences between AGMs and human immune systems, these studies need to be validated in the rhesus macaque model, which more faithfully recapitulates human disease.

1.9.3 SVV immune evasion

Like VZV, SVV has also developed strategies to escape the immune system. SVV ORF61 has also been shown to interfere with the NFkB signaling pathway by preventing the phosphorylation of IkBα and blocking β-TrCP, which is part of the E3 ubiquitin ligase complex that mediates IkBα degradation (226). In vitro studies have also shown that SVV can interfere with type I interferon signaling by down-regulating the expression of IRF9 and inhibiting Stat2 phosphorylation (227). Furthermore, in vivo studies in rhesus macaques have show that SVV ORF61 can inhibits IFNα production and expression of interferon stimulated gene (228).

1. 10 Thesis Overview and Aims

Rhesus macaques infected with SVV serve as a powerful tool to investigate the host pathogen during VZV infection. Since VZV is respiratory pathogen and the main complications of acute VZV infection is pneumonia. I used this robust animal model to first characterize the host response during SVV acute infection in the lung parenchyma. Furthermore, it is unclear how VZV reaches the ganglia during acute infection; therefore, the second aim of my dissertation was to define the host response and kinetics of VZV latency in the ganglia. Since VZV primarily infects T cells that are believed to play a role in trafficking VZV to the skin and ganglia, I also investigated how SVV alters the SVV transcriptome. Finally, although VZV reactivation is believed to occur due to the loss of CD4 specific T cells; this hypothesis has not been formally tested. Therefore, my last aim of my dissertation was to investigate the role that T cell

senescence plays in preventing HZ. Data from these studies provide novel insight in the VZV-host pathogen interactions and have the potential to guide efforts to improve vaccines and therapeutics.

CHAPTER 2: Genomic and functional analysis of the host response to acute simian varicella infection in the lung

Nicole Arnold[1], Thomas Girke[2], Suhas Sureshchandra[3], Christina Nguyen[4], Maham Rais[4] and Ilhem Messaoudi[1,3,4*]

[1]Graduate Program in Microbiology, University of California-Riverside, CA, USA

[2] Department of Botany and Plant Sciences, University of California-Riverside, CA, USA

[3]Graduate Program in Genetics, Genomics and Bioinformatics, University of California-Riverside, CA, USA

[4]Division of Biomedical Sciences, School of Medicine, University of California-Riverside, Riverside, CA

A version of this chapter is published in Nature Scientific Reports:
Arnold N, Girke T, Sureshchandra S, Nguyen C, Rais M, Messaoudi I (2016b). Genomic and functional analysis of the host response to acute simian varicella infection in the lung. Sci Rep 6: 34164.

ABSTRACT

Varicella Zoster Virus (VZV) is the causative agent of varicella and herpes zoster. Although it is well established that VZV is transmitted via the respiratory route, the host-pathogen interactions during acute VZV infection in the lungs remain poorly understood due to limited access to clinical samples. To address these gaps in our knowledge, we leveraged a nonhuman primate model of VZV infection we developed where rhesus macaques are intrabronchially challenged with the closely related Simian Varicella Virus (SVV). Acute infection is characterized by immune infiltration of the lung airways, a significant up-regulation of genes involved in antiviral-immunity, and a down-regulation of genes involved in lung development. This is followed by a decrease in viral loads and increased expression of genes associated with cell cycle and tissue repair. These data provide the first characterization of the host response required to control varicella virus replication in the lung and provide insight into mechanisms by which VZV infection can cause lung injury in an immune competent host.

INTRODUCTION

Varicella zoster virus (VZV) is a neurotropic alpha herpes virus and the causative agent of varicella and herpes zoster. VZV is primarily acquired through the inhalation of infectious virus particles or via direct contact with skin lesions (229). Although varicella is a benign self-limiting disease, adults (especially smokers and pregnant women) and immunocompromised persons frequently develop serious complications, notably varicella pneumonia (VP) (230, 231), which can result in acute respiratory distress syndrome (ARDS) in severe cases (232).

Mechanisms of VZV pathogenesis and the host response to VZV infection in the lungs is poorly understood because of limited access to human lung biopsies during acute infection and the strict host species specificity of VZV. Simian Varicella Virus (SVV) shares 70-75% DNA homology with VZV (204) and intra-bronchial infection of rhesus macaques (RM) recapitulates the clinical features of primary VZV (217). Recent studies from our group have reported the presence of a vigorous anti-SVV response characterized by effector memory CD8 T cell infiltration, a robust CD4 T cell response, and production of antiviral cytokines/chemokines and growth factors in the bronchoalveolar lavage (BAL) (221). However, we still do not have a clear understanding of the host response to varicella virus within the lung tissue. Here, we leveraged this animal model to characterize SVV-induced immune response as well as changes in lung histopathology and gene expression during primary varicella infection. Our results show that SVV infection results in lung injury as evidenced by focal hemorrhaging, collapse of airways, and reduced expression of genes with a role in lung development and/or function. SVV infection also induces a robust immune response as evidenced by immune cell infiltration, production of pro-inflammatory cytokines and chemokines, and increased expression of genes involved in host defense. The development of this

immune response correlates with decreased SVV viral loads. Moreover, as viral loads decrease, a shift towards increased expression of genes with a role in tissue regeneration and increased levels of growth factors is observed. Collectively, these data increase our understanding of mechanisms of host defense and the development of respiratory complications during VZV infection.

MATERIALS AND METHODS

Animals and sample collection

Fourteen colony-bred Rhesus macaques (Macaca mulatta, RM) 3-5 years of age and of Indian origin were used in these analyses. Animals were housed and handled in accordance with the Oregon National Primate Research Center (ONPRC) Institutional Animal Care and Use Committee (IACUC protocol #0779). The ONPRC Institutional Animal Care Use Committee approved all experimental protocols. The ONPRC has been continuously accredited by the American Association for Accreditation of Laboratory Animal Care since 1974 (PHS/OLAW Animal Welfare Assurance # A3304-01). Eleven RM were inoculated with 4×10^5 PFU SVV as previously described (217) and euthanized 3 (n=3), 7 (n=3), 10 (n=2), and 14 (n=3) days post-infection (DPI); and 3 were controls. Animals were either housed single or paired in caging that allowed for social interactions in a temperature and humidity controlled environment. Food and water were available ad libitum and enrichment was provided daily. All procedures were done under Ketamine anesthesia to minimize animal suffering. Necropsy was carried out in accordance with the recommendation of the American Veterinary Association guidelines for euthanasia. Blood, bronchial alveolar lavage (BAL) and lung tissues were collected at necropsy. Tissues were then flash frozen or stored in trizol at -80°.

Luminex analysis

Lung tissue was homogenized using 1.0mm Silicon Carbide Beads (BioSpec Products Inc, Bartlesville, OK). Lung homogenate and BAL supernatants were analyzed using the Non-Human Primate ProcartaPLex Cytokine/Chemokine/Growth Factor 37-Panel (eBioscience, Inc, San Diego, CA) which measure the expression levels of: monocyte chemoattractant protein 1 (MCP-1; CCL2), IL-1β, IL-2, IL-10, IL-12p70, IL-4, IL-5, IL-6, IL-7, IL-8, IL-12, IL-13, IL-15, IL-

17A, IL-18, IL-23, interferon gamma-induced protein 10 (IP-10; CXCL10), macrophage inflammatory protein 1 alpha (MIP-1α; CCL3) and beta (MIP-1β;CCL4), IL-1 receptor agonist (IL-1RA), TNF-α, Stem Cell Factor (SCF), Eotaxin (CCL11), Fibroblast Growth Factor 2 (FGF-2), B lymphocyte chemoattractant (BLC;CXCL13), Brain-derived neurotrophic factor (BDNF), granulocyte-colony stimulating factor (G-CSF), Granulocyte macrophage colony-stimulating factor (GM-CSF), IFNα, IFNγ, interferon-inducible T cell Alpha chemoattractant (I-TAC; CXCL11), nerve growth factor beta (NGFβ), platelet-derived growth factor-BB (PDGF-BB), soluble CD40 ligand (sCD40L), stromal cell-derived factor 1(SDF-1α;CXCL12a), vascular endothelial growth factor A (VEGF-A) and D (VEGF-D).

Isolation of immune cells

Lung tissue was digested using 150U/ml collagenase, 60U/ml DNAse, 60U/ml hyaluronidase and 0.2U/ml elastase for 1 hour at 37°C with shaking. The digested tissue was then homogenized using a cell strainer to generate a single cell suspension. Cells were isolated using a 30% percoll gradient, then stained with antibodies directed against: CD4 (Tonbo Biosciences, San Diego, CA), CD8β (Beckman Coulter, Brea, CA), CD28 (Tonbo Biosciences), CD95 (BioLegend, San Diego, CA), CCR7 (BD Pharmingen, San Diego, CA) CD20 (Southern Biotech, Birmingham, AL), IgD (Southern Biotech), and CD27 (Biolegend) as previously described (221). A second sample was stained using antibodies against: CD3 (BD Pharmingen), CD20 (Biolegend), CD14 (BioLegend), HLA-DR (Biolegend), CD11c (Biolegend), and CD123 (Biolegend) as previously described (221). Samples were analyzed using the LSRII instrument (Becton, Dickinson and Company, San Jose, CA) and Flowjo software (TreeStar, Ashland, OR).

DNA/RNA Extraction

DNA was extracted from lung tissue using the Qiagen genomic DNA extraction kit (Qiagen, Valencia, CA) and from BAL and blood using the ArchivePure DNA cell/tissue kit (5 PRIME, Gaithersberg, MD). Viral DNA loads were determined exactly as previously described (217) by real-time PCR using primers and probes specific for ORF21 and ran on the ABI StepOne (Applied Biosystems, Foster City, CA). RNA was extracted from lung tissue homogenized in trizol using a bead beater and zirconia/silica beads followed by extraction using the Ambion Purelink RNA Mini Kit (Life Technologies, Carlsbad, CA).

Histological and Immunohistochemistry Analysis

Hematoxylin and Eosin (H&E) staining of 5μm lung tissue sections were deparaffinized with Histo-Clear II (National Diagnostics, Atlanta, Georgia) and rehydrated. Tissue was then stained with Hematoxylin for 2 minutes followed by Eosin for 40 seconds and then hydrated back to Histoclear and covered with coverslips using Omnimount (National Diagnostics, Atlanta, Georgia). For immunohistochemistry analysis, antigen retrieval was done using a pressure cooker in citrate buffer for 20 minutes. Sections were then blocked in 1% bovine serum albumin (BSA) and 5% normal goat or horse serum for 1hr followed by avidin and then biotin for 15 minutes. Tissues were then stained with primary antibodies CD3 (1:200 dilution, Dako M0452, CD20 (1:300 dilution, Dako M0755), CD68 (1:75, Dako, Ki67 1:150 dilution, Dako MIB-1), granzyme B (1:200 dilution, Millipore, Temecula, CA) and VZV glycoprotein B (1:200 dilution, antibodies-online.com clone SG2-2E6). Color development was done with ImmPACT DAB (Vector labs,

Burlingame, CA) and counter stained with Hematoxylin QS (Vector Laboratories, Burlingame, CA). Slides were then covered with coverslips using Omnimount (National Diagnostics, Atlanta, Georgia). Images were taken on the Leica DM5500 B (Leica Biosystems, Buffalo Grove, IL) microscope.

mRNA Library Preparation

One microgram of RNA was used to generate RNA libraries using the using the New England Biolab (NEB) Next Ultra Direction RNA Prep kit for Illumina (Ipswich, MA) and AMPure XP beads (Beckman Coutler, Brea, CA). Each library was made with a unique index primer to allow for multiplexing and then sequenced on the Illumina HiSeq2500 (Illumina, San Diego, CA) platform at single-ends 100bps as previously described (233).

RNA-Sequencing analysis

Sequence analysis was performed as previously described (233). Due to the limited number of animals used in the this study, use used a stringent cutoff of with differentially expressed genes (DEGs) being defined as those with a fold change ≥ 3 and a false discovery rate (FDR) ≤ 0.05 compared to naïve animals. Enrichment analysis was performed using MetaCore software (GeneGo, Philadelphia, PA). Gene clusters were predicted by STEM using k-means clustering of median normalized reads and maps were generated using ggplot package in R. GEO accession number SRP072466.

Gene Validation

Gene validation was done using RNA from the same samples used for RNA-Seq. RNA was reverse-transcribed using 100mM dNTPs (Applied Biosystems) and multiscribe reverse transcriptase (Applied Biosystems) to produce cDNA. Expression was determined using Taqman gene expression assays (Thermo Fisher, Waltham, MA) of BST2, IFITM1, IGJ, MX1 and a housekeeping gene (RPL32). Taqman gene expression assays with 50ng of cDNA and a housekeeping gene (RPL32) was carried out in duplicates on the ABI StepOne instrument (Applied Biosystems,). Expression of mRNA was normalized to expression levels of RPL32 using ΔCt values as previously described (233).

Statistical Analysis

Statistical analysis was conducted using GraphPad Prism software (GraphPad, Software, Inc., La Jolla, CA). Significant values were determined using one-way ANOVA with an alpha value of 0.05 or less.

RESULTS

SVV infection results in significant lung inflammation

Eleven rhesus macaques were intrabronchially inoculated with $4x10^5$ PFU of SVV into their right bronchus and euthanized 3 (n=3), 7 (n=3), 10 (n=2) and 14 (n=3) days post infection (DPI). Viral loads peaked in the BAL and infected right lung 3 DPI and in the uninfected left lung and blood 7 DPI, followed by cessation of viral replication 14 DPI (Fig. 2.1A). In line with viral replication kinetics, the lungs showed severe focal hemorrhaging and firm nodules 7 DPI, which resolved 14 DPI (Fig. 2.1B). Similarly, H&E staining revealed damage to the alveolar walls and perivascular infiltration of lymphocytes and macrophages that peaked 7-10 DPI, indicative of viral pneumonia, which also resolved 14 DPI (Fig. 2.1C). To determine the association between viral replication and viral antigen, lung tissue slides were stained with anti-VZVgB (which shares 71% amino acid identity with SVVgB). As described for viral DNA loads, VZVgB staining peaked 7 DPI (Fig. 2.1D).

The concentration of chemokines, cytokines and growth factors in BAL supernatants and lung homogenates were measured using Luminex technology. Levels of the B cell chemoattractant BLC, eosinophil attractant eotaxin, granulocyte chemoattractants IL-8 and MIP1α, as well as T cell chemokines I-TAC and MIG increased 3-10 DPI (Fig. 2.2A). Levels of IL-6, which plays a critical role in viral clearance, also increased 3-10 DPI (Fig. 2.2B). In addition, levels of the potent antiviral cytokine IFNα were increased 3 and 7 DPI (Fig. 2.2B), while levels of IFNγ, IL-18 (induces IFNγ production by T cells), IL-1β, and its antagonist IL-1RA were increased only 7 DPI (Fig. 2.2B). Moreover, levels of growth factors VEGF-D and PDGF-BB were increased 3-14

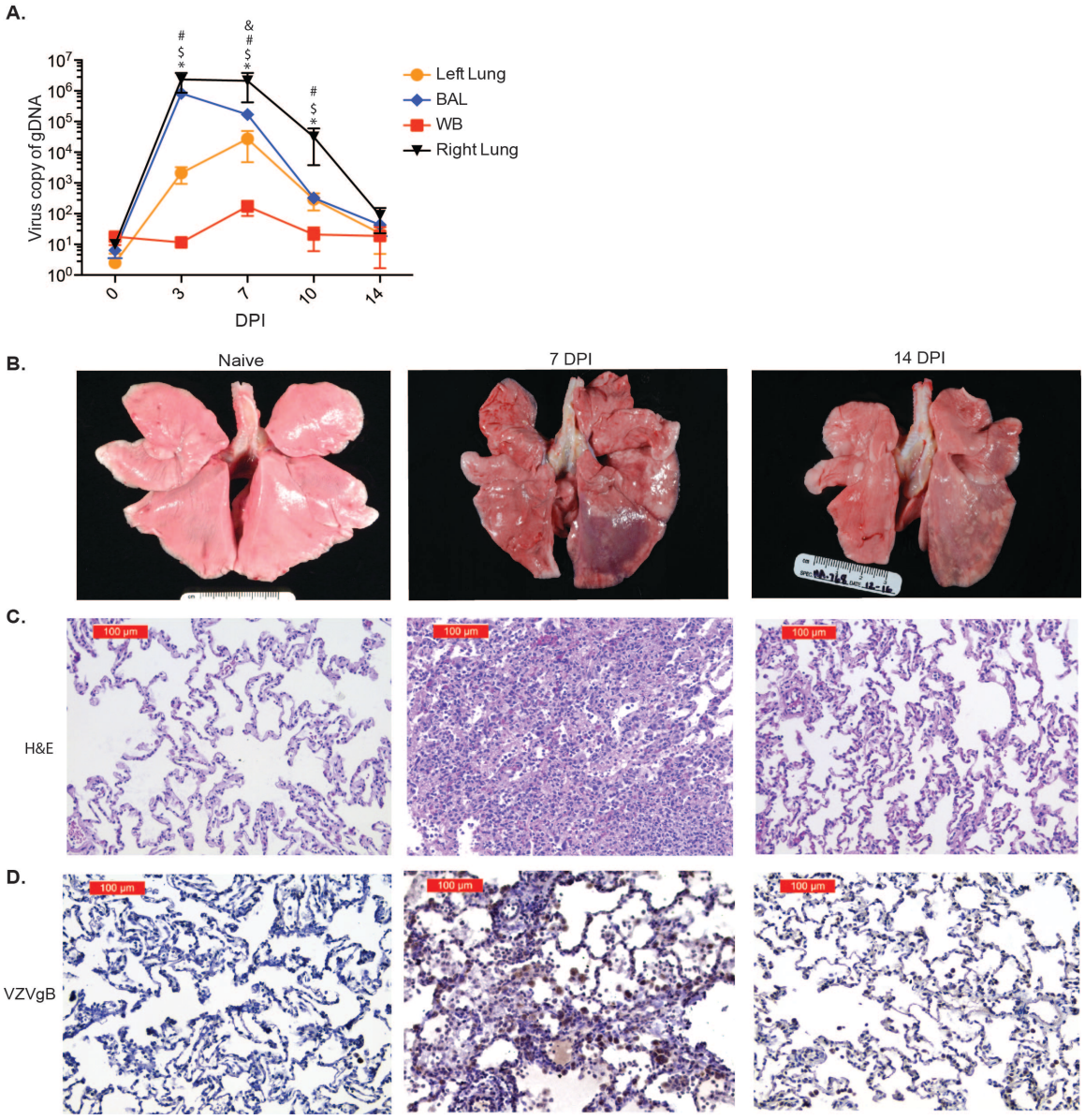

Figure 2.1 SVV infection results in inflammation. (A) SVV viral loads in lung biopsies, bronchial alveolar lavage (BAL) and blood (WB) were measured by quantitative PCR using primers and probes specific for SVV *ORF21* (BAL: n=14 (0 days post infection, DPI), n= 11 (3 DPI), n=8 (7 DPI), n=5 (10 DPI), n=3 (14 DPI); Lung: n=3 (0 DPI), n= 3 (3 DPI), n=3 (7 DPI), n=2 (10 DPI), n=3 (14 DPI); WB: n=14 (0 DPI), n= 11 (3 DPI), n=8 (7 DPI), n=5 (10 DPI), n=3 (14 DPI)) (#, $p<0.05$ for left lung; $, $p<0.05$ for BAL; &, $p<0.05$ for WB; *, $p<0.05$ for right lung relative to day 0). (B) SVV infection results in focal hemorrhage during peak viral replication that largely resolved 14 DPI. (C) H&E staining shows immune infiltrates and lung consolidation during peak viral replication. (D) VZVgB staining showing high levels of viral antigen 7 DPI that were decreased 14 DPI.

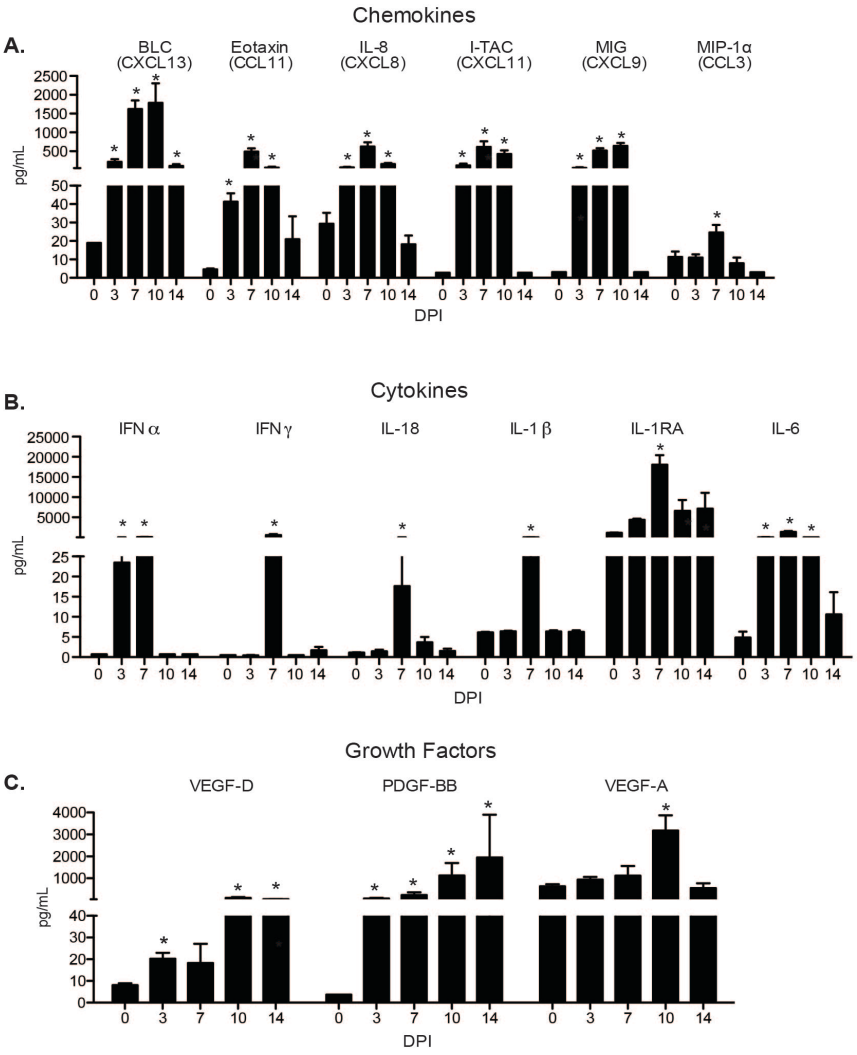

Figure 2.2 SVV infection induces secretion of cytokines, chemokines and growth factors. Levels of (A) chemokine, (B) cytokines and (C) growth factors in the BAL were measured using Luminex technology. BAL: n=14 (0 days post infection, DPI), n= 11 (3 DPI), n=8 (7 DPI), n=5 (10 DPI), n=3 (14 DPI) Mean pg/ml ± SEM (*, $p<0.05$ compared to day 0).

DPI and those of the pro-angiogenic factor VEGF-A were increased 10 dpi (Fig. 2.2C). In contrast, the lung homogenates showed no significant change in protein levels of chemokines, cytokines or growth factors.

SVV infection leads to the recruitment of T cells and phagocytes

Given the increased concentration of T cell, B cell and granulocyte chemokines in the BAL, we characterized immune cells that infiltrated the lungs during acute varicella (Fig. 2.3). As we previously reported (221), CD20 cells were rare whereas CD4 and CD8 T cells were abundant pre-infection in BAL. After SVV infection, the frequency of CD8 T cells in the BAL increased 10 and 14 DPI (Fig. 2.3A). In contrast, frequencies of both B and T cells were low in naïve lungs, but increased as early as 3 DPI, with CD8 T cells showing the largest increase 10 and 14 DPI (Fig. 2.3B). T cell activation was indicated by the increased prevalence of highly differentiated CD8 EM T cells and CD4 CM T cells 7 to 14 DPI and CD4 EM 7-10 DPI (Figs. 2.3C,D). We also observed an increased frequency of plasmacytoid dendritic cells (pDCs), myeloid dendritic cells (mDCs), and macrophages (MACs) 3 - 7 DPI in both BAL and lung (Figs. 2.3E,F).

To further characterize the immune infiltrates, immunohistochemistry (IHC) was used to determine changes in distribution and frequency of CD3, CD20, CD68, Ki67 and granzyme B (GRZMB) positive cells (Fig. 2.4). Intensity of CD3, CD20 and CD68 staining increased 3 DPI and peaked 7 DPI (Fig. 2.4B). Peak staining of GRZMB and Ki67 was also observed at 7 DPI and correlated with increased frequency of memory T cells detected by flow cytometry (Fig. 2.4B). By 14 DPI, CD20 and granzyme B staining was substantially reduced, while CD3, CD68, and Ki67 expression remained higher than baseline (Fig. 2.4C).

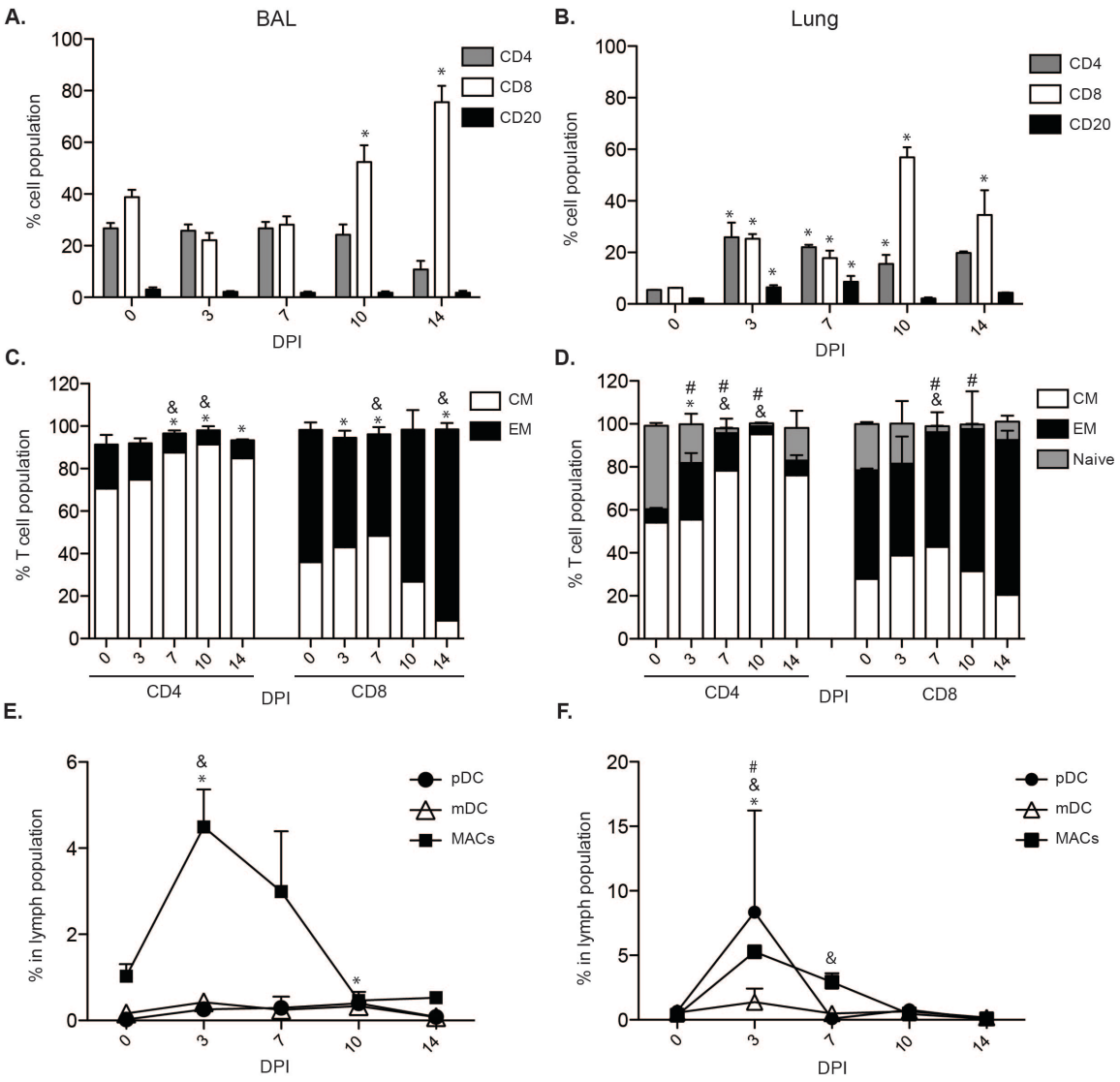

Figure 2.3 SVV infection induces immune infiltration. (A-B) The frequencies (means ± SEM) of CD4, CD8 and CD20 positive cells in (A) BAL and (B) the lungs (*, p< 0.05 compared to day 0). (C-D) The percentage of naïve, central memory (CM) and effector memory (EM) CD4 and CD8 T cells in the (C) BAL (&, p< 0.05 for CM; *, p< 0.05 for EM compared to day 0) and (D) lungs (& = p< 0.05 for CM; *= p< 0.05 for EM; # = p< 0.05 for naïve compared to day 0). (E-F) The percentage of plasmacytoid DCs (pDCs), myeloid DCs (mDCs), and macrophages (MACs) in (E) BAL and (F) lungs (& = p< 0.05 for MACs; * = p< 0.05 for pDCs; # = p< 0.05 for mDCs). BAL: n=14 (0 days post infection, DPI), n= 11 (3 DPI), n=8 (7 DPI), n=5 (10 DPI), n=3 (14 DPI); Lung: n=3 (0 DPI), n= 3 (3 DPI), n=3 (7 DPI), n=2 (10 DPI), n=3 (14 DPI). Tissues used were from the infected right lobe.

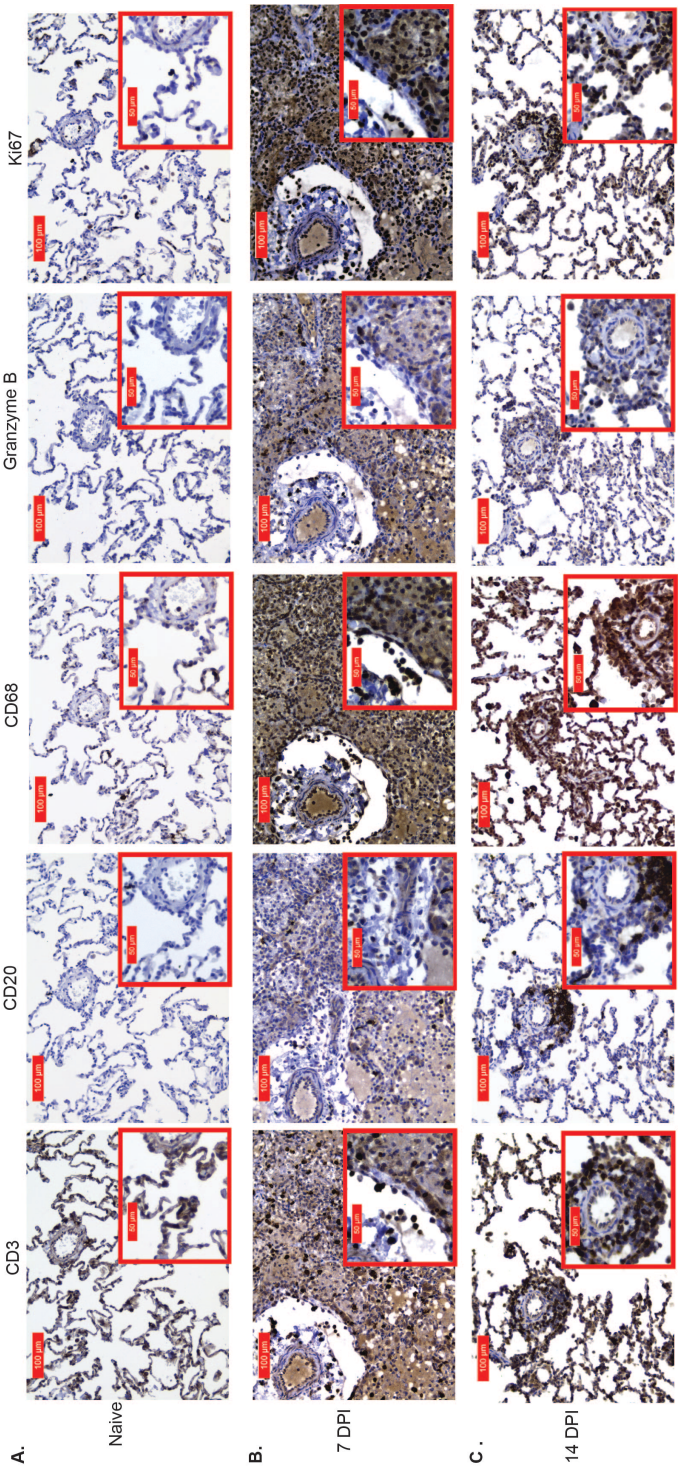
A.
Naive
B.
7 DPI
C.
14 DPI
CD3
CD20
CD68
Granzyme B
Ki67

(Previous page) Figure 2.4 Immune cells proliferate and exhibit cytotoxicity in SVV infected lungs. CD3, CD20, CD68, granzyme B and Ki67 staining in lung sections from (A) naïve, (B) 7 DPI and (C) 14 DPI at 20X and 40X magnification.

SVV infection induces robust changes in gene expression

RNA-Seq was used to characterize the host gene expression changes in the lungs during acute varicella. The number of differentially expressed genes (DEGs) correlated tightly with viral loads, with the highest number of DEGs detected 7 DPI (Fig. 2.5A). Changes in gene expression were validated for a subset of genes using qRT-PCR (Fig. 2.6). The 54 DEGs that were differentially expressed 3, 7 and 10 DPI (Fig. 2.5B) segregated into 3 clusters. Cluster 1 contained 30 DEGs whose expression gradually increased until it peaked 10 DPI (Fig. 2.5C). Several of these genes are involved in cell cycle such as cyclin kinase subunit 2 (*CKS2*), Ribonucleoside-diphosphate reductase subunit M2 (*RRM2*), and topoisomerase II alpha (*TOP2A*). Cluster 2 contained 7 DEGs whose expression was substantially increased as early as 3 DPI and remained high until 10 DPI before decreasing back to baseline 14 DPI (Fig. 2.5D). Several of these DEGs play a role in antiviral defense such as granzyme A (*GZMA*), *GZMB*, 2'-5'-Oligoadenylate Synthetase-Like (*OASL*), and *CXCL9*. Cluster 3 contained 15 genes that remained down-regulated throughout acute infection (Fig. 2.5E). These genes are involved in several cellular processes such as migration (fascin actin-bundling protein 1, *FSCN1*), division (Glypican 1, *GPC1*), and tight junction organization (nectin-1, *PVRL1*, an alpha herpesvirus entry mediator (234)). To gain a better understanding of the biological implications of the gene expression changes we detected, functional enrichment of DEGs that have human homologs was carried out using Metacore software.

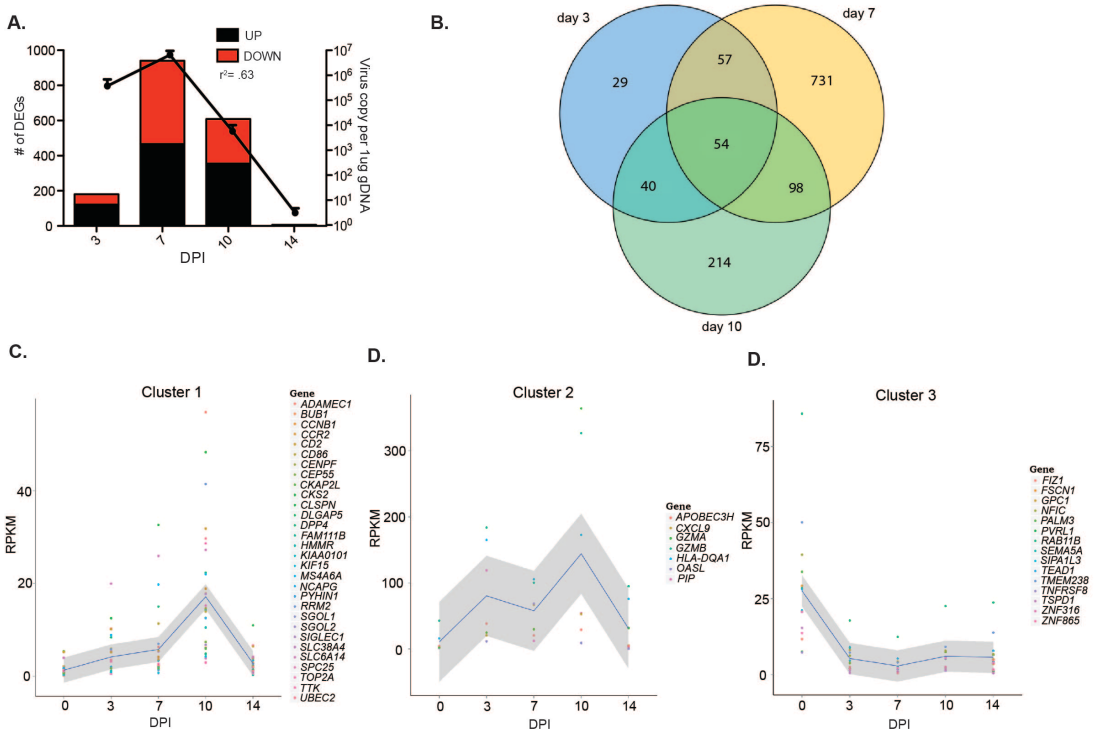

Figure 2.5 SVV infection results in robust changes in lung gene expression. (A) The number of DEGs correlates with viral loads. (B) Venn diagram of DEGs detected 3, 7 and 10 DPI. (C-E) Gene clusters of the 52 common DEGs with human homologs.

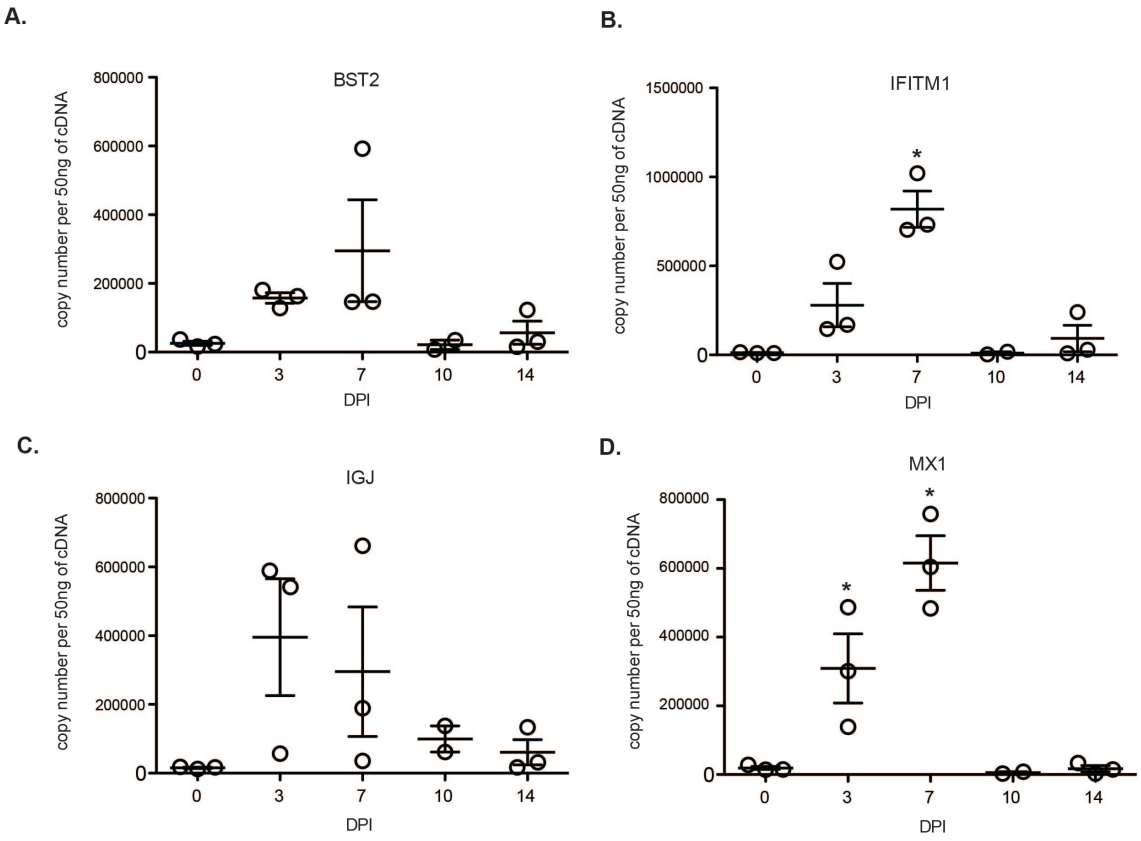

Figure 2.6 Gene Validation. Taqman expression assays were done on (A) BST2 (B) IFITM1 (C) IGJ and (D) MX1. Statistical significance was determined using one-way ANOVA. Error bars show the standard error of the mean (*, $p<0.05$ compares to 0 DPI).

DEGs 3 DPI play a role in innate immunity and lung development

Most of the 106 DEGs that were up-regulated 3 DPI mapped to Gene Ontology (GO) terms associated with antiviral immunity (Fig. 2.7A). Several genes that enriched to the GO process "immune system process" are part of a network regulated by Signal Transducers and Activators of Transcription 1 (*STAT1*; FC 4) (Fig. 2.7B). Most of these DEGs have antiviral function such as interferon-stimulated genes (ISGs) *ISG15* (FC 8), *MXA* (FC 7), and *GBP1* (FC 7) as well as dsRNA sensors *DDX60* (FC 5) and *RIG-I* (FC 4) (235) (Fig. 2.7B). Other *STAT1* regulated DEGs in our dataset are involved in apoptosis, such as granzyme A (*GZMA*; FC 83), granzyme K (*GZMK*; FC 35), and Fas ligand (*FASL*; FC 12) (236). Other DEGs play a role in chemotaxis, e.g. *MIG* (*CXCL9*, FC 32), *IP10* (*CXCL10*, FC 17), and *ITAC* (*CXCL11*, FC 14) (237). Additional highly up-regulated genes include the immune-modulatory prolactin induced protein (*PIP*; FC 51) and lymphocyte differentiation antigen immunoglobulin J *(IGJ*, FC 38).

The 54 down-regulated genes primarily mapped to GO terms associated with lung development (Fig. 2.7C) such as iroqouis homeobox 3 (*IRX3*; FC7) (238), nuclear factor I/C (*NFIC*; FC 8) (239) and WNT frizzled class receptor 5 (*FZD5*; FC8) (240). The 23 down-regulated DEGs that mapped to biosynthetic pathways play a role in DNA binding and transcriptional regulation, notably zinc finger protein 865 (*ZNF865*; FC 9) and 316 (*ZNF316*; FC 9), and parathymosin (*PTMS*; FC8) (Fig. 2.7D) (241, 242).

Given the immune changes in immune infiltrates into the lung 3 DPI, we wanted to gain a better understanding of which immune cells are expressing these DEGs. To that end, we used the Immunological Genome Project (ImmGen), a database maintained by a collaborative group of immunologists and computational biologists that aim to determine the patterns of gene expression

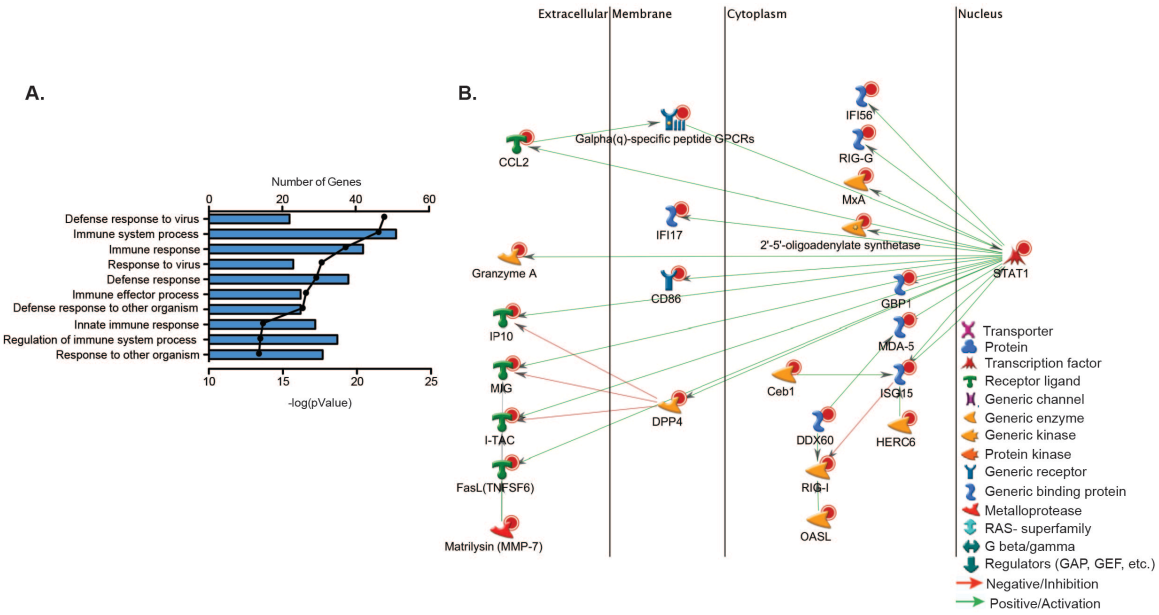
A.
Number of Genes
0
20
40
60
Defense response to virus
Immune system process
Immune response
Response to virus
Defense response
Immune effector process
Defense response to other organism
Innate immune response
Regulation of immune system process
Response to other organism
10
15
20
25
-log(pValue)
B.
Extracellular
Membrane
Cytoplasm
Nucleus
CCL2
Galpha(q)-specific peptide GPCRs
IFI56
RIG-G
MxA
IFI17
2'-5'-oligoadenylate synthetase
Granzyme A
CD86
STAT1
GBP1
IP10
MDA-5
MIG
Ceb1
ISG15
DPP4
DDX60
HERC6
I-TAC
RIG-I
FasL(TNFSF6)
OASL
Matrilysin (MMP-7)
Transporter
Protein
Transcription factor
Receptor ligand
Generic channel
Generic enzyme
Generic kinase
Protein kinase
Generic receptor
Generic binding protein
Metalloprotease
RAS- superfamily
G beta/gamma
Regulators (GAP, GEF, etc.)
Negative/Inhibition
Positive/Activation

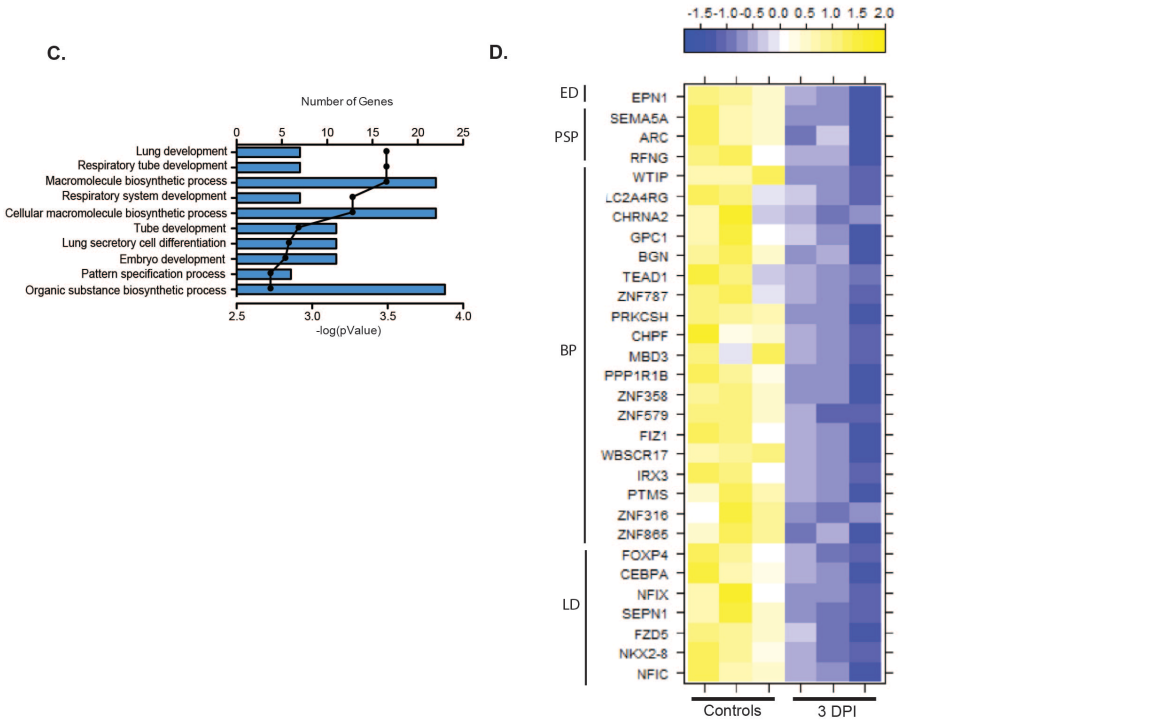
C.
Number of Genes
0
5
10
15
20
25
Lung development
Respiratory tube development
Macromolecule biosynthetic process
Respiratory system development
Cellular macromolecule biosynthetic process
Tube development
Lung secretory cell differentiation
Embryo development
Pattern specification process
Organic substance biosynthetic process
2.5
3.0
3.5
4.0
-log(pValue)
D.
-1.5 -1.0 -0.5 0.0 0.5 1.0 1.5 2.0
ED
PSP
BP
LD
EPN1
SEMA5A
ARC
RFNG
WTIP
LC2A4RG
CHRNA2
GPC1
BGN
TEAD1
ZNF787
PRKCSH
CHPF
MBD3
PPP1R1B
ZNF358
ZNF579
FIZ1
WBSCR17
IRX3
PTMS
ZNF316
ZNF865
FOXP4
CEBPA
NFIX
SEPN1
FZD5
NKX2-8
NFIC
Controls
3 DPI

(Previous page) Figure 2.7 DEGs detected 3 DPI play a role in innate immunity and lung development. (A) Bar graph shows the number of genes mapping to each of the 10 most statistically significant GO terms to which the 106 up-regulated genes enriched. Line represents the –log(p-value) associated with each GO term. (B) Network of DEGs mapping to the GO process "immune system" that directly interact. (C) Bar graph shows the number of genes mapping to each of the 10 most statistically significant GO processes to which the 54 down-regulated genes enriched. Line represents the –log(p-value) associated with each GO term. (D) Heat map of the 30 down-regulated DEGs that enriched to the GO terms described in (D) grouped by the GO term to which they mapped: ED= Embryo development, PSP= pattern specification process, BP= biosynthetic process and LD= Lung development.

of specific immune cells in the mouse (243, 244). This analysis showed that a group of genes that play a role in the cell cycle progression (e.g. *Top2a*, *BUB1*, *CEP55*, *SPC25* and *CENPF*) were highly expressed by B cells, dendritic cells and T cells (Fig. 2.8, cluster 1). We also identified 2 additional clusters of genes that were mainly expressed by MACs (e.g. *ADAMDEC1*, *IgJ, SIGLEC1*, *CXCL9* and *CXCL10*) (Fig. 2.8, cluster 2a,b). Two small clusters are expressed by NK cells (e.g. *GZMB*, *GZMA* and *SAMD3*) (Fig. 2.8 cluster 3a,b), and an additional cluster of antiviral genes was seen in the neutrophils (e.g. DDX60, OAS2, and RASD2) (Fig. 2.8, cluster 4). These data correlate with our flow cytometry analysis (Fig. 2.3), which report significant increases in T cells, B cells, MACs and DC numbers at 3 DPI in the lung.

In line with our functional analysis, few of the DEGs down-regulated at 3 DPI mapped to immune cell populations. These include *FSCN1* (pathogen recognition molecule (245)) and *ARC* (apoptosis (246)) highly expressed in dendritic cells, and *SEPN1* (oxidation-reduction homeostasis (247)), highly expressed in neutrophils (data not shown).

DEGs detected 7 DPI primarily map to host defense

The 380 up-regulated DEGs detected 7 DPI primarily mapped to GO terms related to host defense (Fig. 2.9A). Over 100 DEGs involved in anti-viral immunity had a fold change >10 including: *CCL8* (FC 129), *CXCL10* (FC 129), *CCL20* (FC 77), *CCL2* (FC 63), *ISG15* (FC 59), 2'-5'-oligoadenylate synthetase-like (*OASL*, FC 44), *RIGG* (FC 32), *GBP1* (FC 30), and *IL8* (*CXCL8*, FC 28) (Fig. 2.9B). Additional immune related DEGs that didn't map to the 10 most significant GO processes include *FAM26F* (FC 92), involved in IFNγ production by NK cells (248), Pentraxin 3 (*PTX3*, FC 71) involved in complement activation (249), and tissue inhibitors

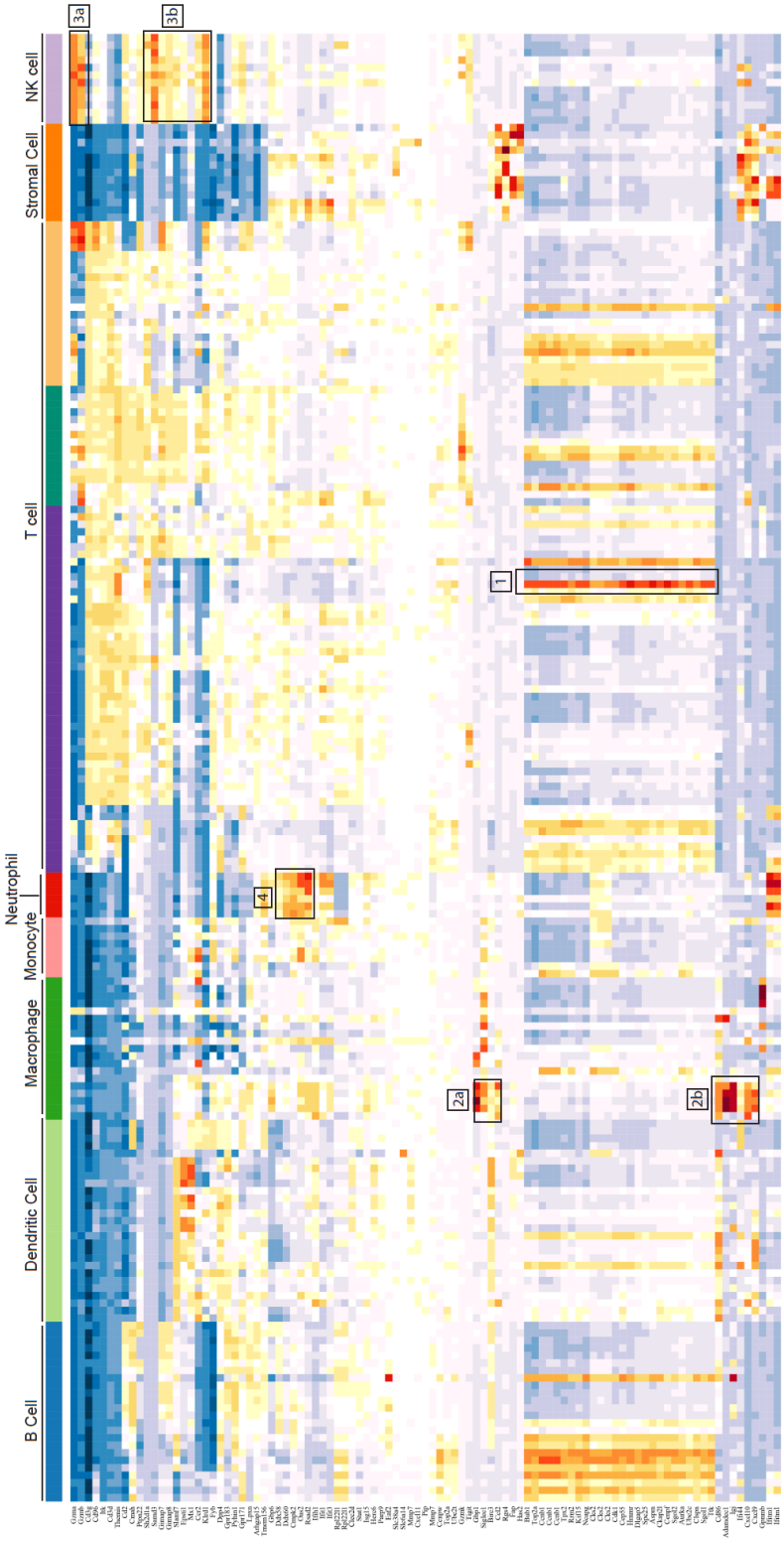
B Cell
Dendritic Cell
Macrophage
Monocyte
Neutrophil
T cell
Stromal Cell
NK cell
1
2a
2b
3a
3b
4

(Previous Page) Figure 2.8 ImmGen heatmap showing the expression profile of the up-regulated genes found at day 3-post infection across different immune cell populations. Each row represents a gene and corresponding microarray ID and columns represent an immune cell type and study. Colors represent expression levels where red indicates the likelihood that the gene of interest is highly expressed by a specific cell type and blue represents low expression. Cluster 1 shows genes involved in the cell cycle (e.g. *Top2a*, *BUB1*, *CEP55*) mapping to B cells, dendritic cells and T cells. Cluster 2a,b shows genes that are highly expressed in macrophages (*ADAMDEC1*, *IgJ*, *IFI44*, *CXCL9* and *CXCL10*). Cluster 3 shows antiviral genes *DDX60*, *OAS2* and *RSAD2* highly expressed in neutrophils. Cluster 4a,b shows genes *GZMB* and *GZMA* highly expressed in NK cells.

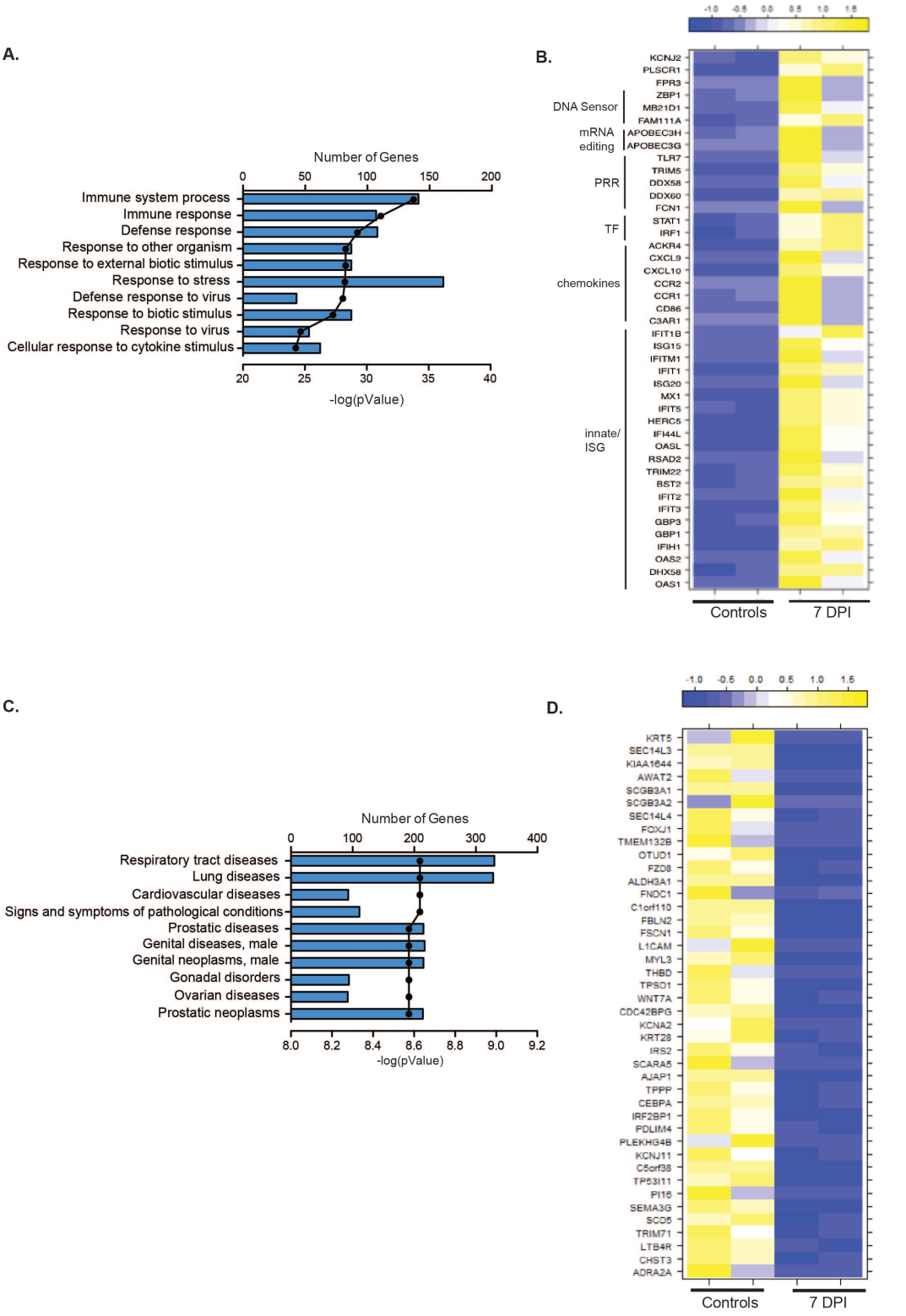
A.
Number of Genes
0
50
100
150
200
Immune system process
Immune response
Defense response
Response to other organism
Response to external biotic stimulus
Response to stress
Defense response to virus
Response to biotic stimulus
Response to virus
Cellular response to cytokine stimulus
20
25
30
35
40
-log(pValue)
B.
-1.0
-0.5
0.0
0.5
1.0
1.5
KCNJ2
PLSCR1
FPR3
ZBP1
MB21D1
FAM111A
APOBEC3H
APOBEC3G
TLR7
TRIM5
DDX58
DDX60
FCN1
STAT1
IRF1
ACKR4
CXCL9
CXCL10
CCR2
CCR1
CD86
C3AR1
IFIT1B
ISG15
IFITM1
IFIT1
ISG20
MX1
IFIT5
HERC5
IFI44L
OASL
RSAD2
TRIM22
BST2
IFIT2
IFIT3
GBP3
GBP1
IFIH1
OAS2
DHX58
OAS1
DNA Sensor
mRNA editing
PRR
TF
chemokines
innate/ ISG
Controls
7 DPI
C.
Number of Genes
0
100
200
300
400
Respiratory tract diseases
Lung diseases
Cardiovascular diseases
Signs and symptoms of pathological conditions
Prostatic diseases
Genital diseases, male
Genital neoplasms, male
Gonadal disorders
Ovarian diseases
Prostatic neoplasms
8.0
8.2
8.4
8.6
8.8
9.0
9.2
-log(pValue)
D.
-1.0
-0.5
0.0
0.5
1.0
1.5
KRT5
SEC14L3
KIAA1644
AWAT2
SCGB3A1
SCGB3A2
SEC14L4
FOXJ1
TMEM132B
OTUD1
FZD8
ALDH3A1
FNDC1
C1orf110
FBLN2
FSCN1
L1CAM
MYL3
THBD
TPSD1
WNT7A
CDC42BPG
KCNA2
KRT28
IRS2
SCARA5
AJAP1
TPPP
CEBPA
IRF2BP1
PDLIM4
PLEKHG4B
KCNJ11
C5orf38
TP53I11
PI16
SEMA3G
SCD5
TRIM71
LTB4R
CHST3
ADRA2A
Controls
7 DPI

(Previous page) Figure 2.9 DEGs detected 7 DPI are involved in host defense. (A) Bar graph shows the number of genes mapping to each of the 10 most statistically significant GO terms to which the 380 up-regulated genes enriched. Line represents the –log(p-value) associated with each GO term (B) Heat map of the genes that mapped to the GO process "response to virus" grouped by function (PRR=pathogen recognition receptor; TF= transcription factor; ISG= immune stimulated gene). (C) Bar graph shows the number of genes mapping to each of the 10 most statistically significant disease pathways to which 400 down-regulated genes enriched. Line represents the –log(p-value) associated with each GO term. (D) Heat map of the DEGs with a FC >8 that enriched to "respiratory tract diseases" and "lung diseases".

of metalloproteinases 1 (*TIMP1*, FC 26). Other highly up-regulated DEGs play a role in respiratory diseases such as Hyaluronan synthase 2 (*HAS2*; FC 71) associated with asthma and tissue fibrosis (250), and metallothionein 2A (*MT2A*, FC 24) involved in lung cancer (251).

Of the 400 down-regulated DEGs 7 DPI, 300 enriched to GO terms "respiratory tract diseases" and "lung diseases" (Fig. 2.9C). The most down-regulated gene was keratin 5 (*KRT5*, FC 35), an intermediate filament protein involved in lung regeneration (252) (Fig. 2.9D). Down-regulated DEGs with a role in lung function include: insulin receptor substrate 2 (*IRS2*, FC 9), an anti-inflammatory agent in the lung (253); and *SEC*14-like 3 (*SEC14L3*, FC 33), a lipid packing sensor expressed by alveolar cells and involved in the prevention of lung collapse (254).

ImmGen analysis of the up-regulated immune genes revealed clusters that are highly expressed by DCs (e.g. *MX1*, *IFIH1*, and *IL-15RA*); MACs (e.g *CCR1*, *CD86* and *IL-1β*); NK cells (*GZMA* and *GZMB*); neutrophils (e.g *OAS2*, *RSAD2* and *TNFSF13B*) and T and B cells (e.g. *RRM2*, *KPNA1* and *EZH2*) (Fig. 2.10, clusters 1-5). We also observed a cluster of inflammatory genes (e.g. *CCL1*, *CXCL1*, *CXCL9*, *CXCL10* and *IFITM1*) that were highly expressed by stromal cells (Fig. 2.10, cluster 6a,b). In line with our functional enrichment, only 1 down-regulated gene (*SEPN1*) was expressed by immune cells (data not shown).

DEGS at 10 DPI are involved in tissue regeneration

At 10 DPI, most of the 300 up-regulated DEGs enriched to GO terms associated with cell cycle (Fig. 2.11A). Several of these DEGs are part of a network regulated by transcription factors Myb-related protein B (*b-Myb*, FC 9, S- phase (255)) and forkhead box M1 (*FOXM1*, FC 11, S- and M-phase (256)) (Figure 2.11B) and modified by serine/threonine kinase, cyclin-dependent kinase

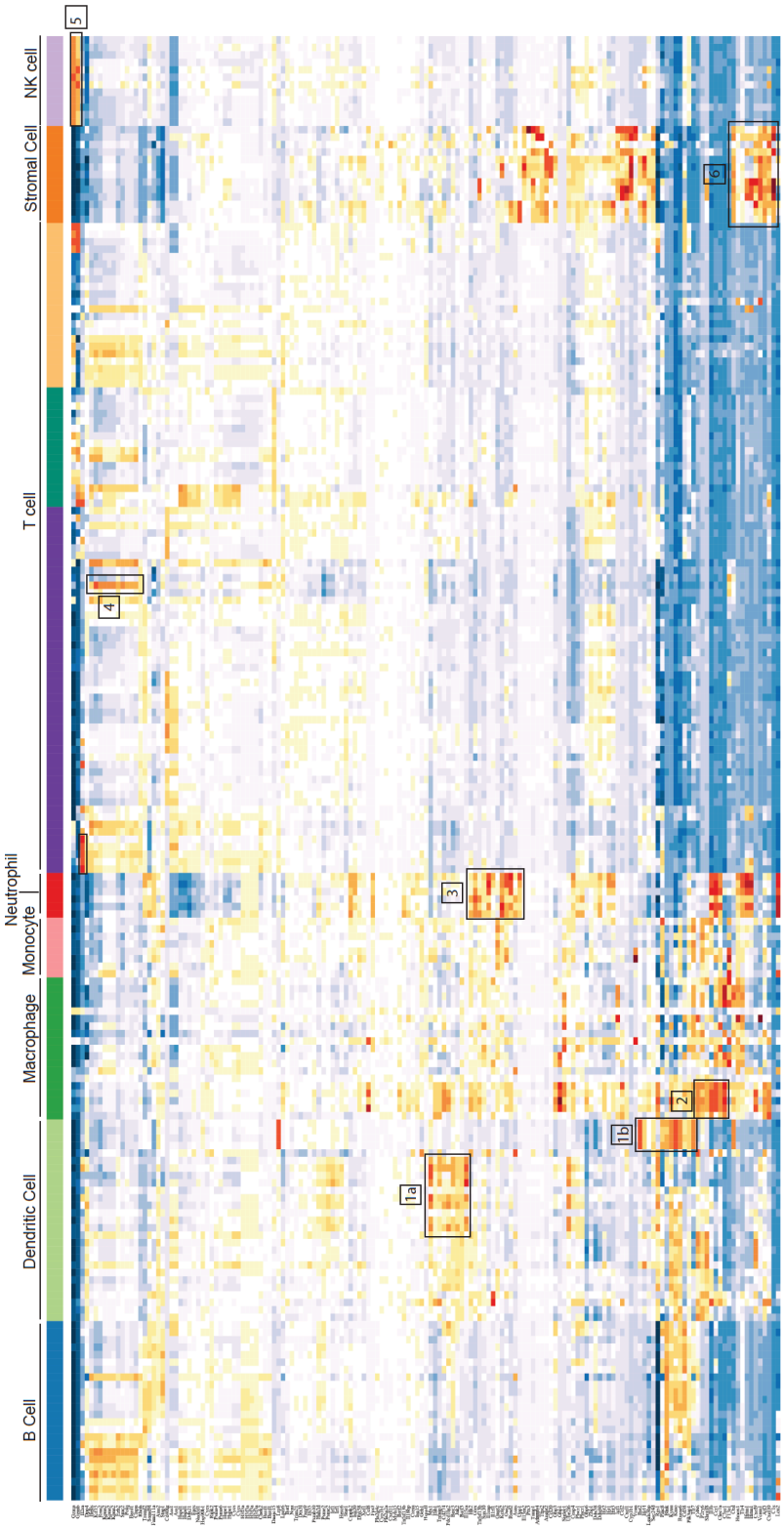
B Cell
Dendritic Cell
Macrophage
Monocyte
Neutrophil
T cell
Stromal Cell
NK cell
1a
1b
2
3
4
5
6

(Previous page) Figure 2.10 ImmGen heatmap showing the expression profile of the up-regulated immune related genes found at day 7 post-infection across different immune cell populations. Each row represents a gene and a corresponding microarray ID and columns represents an immune cell type and study. Colors represent expression levels where red indicates the likelihood that the gene of interest is highly expressed by a specific cell type and blue represents low expression. Gene cluster 1a,b show antiviral genes (*MX1* and *IFIH1*), immune homeostatic genes (*CD274* and *PDCD1LG2*) and genes involved with apoptosis (*TNFAIP3* and *BIRC3*) highly expressed by dendritic cells. Cluster 2 highlights a cluster of genes highly expressed in the macrophages that are involved in the proinflammatory response such as *CD86*, *IL1b* and *CCR1*. Cluster 3 shows antiviral genes (*OAS2* and *RSAD2*) and proinflammatory genes (*TNFSF13B* and *IL1RAP*) primarily expressed in neutrophils. Cluster 4 shows highly expressed shared by B and T cells (*RRM2*, *KPNA1* and *EZH2*). Gene cluster 5 shows *GZMA* and *GZMB* being highly expressed by NK cells. Gene cluster 6 shows genes highly expressed in stromal cells, many of which are also involved in proinflammation (e.g *CXCL9*, *CXCL10* and *IFITM1*)

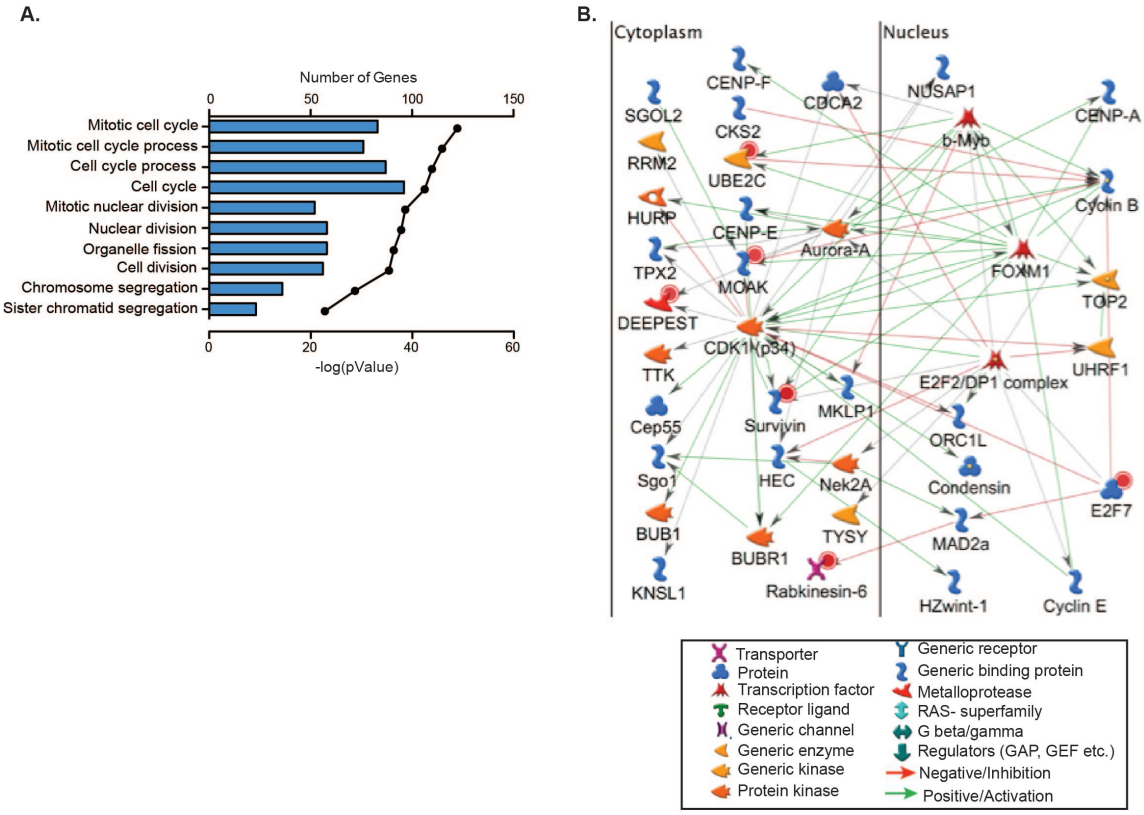
A.
Number of Genes
0
50
100
150
Mitotic cell cycle
Mitotic cell cycle process
Cell cycle process
Cell cycle
Mitotic nuclear division
Nuclear division
Organelle fission
Cell division
Chromosome segregation
Sister chromatid segregation
0
20
40
60
-log(pValue)
B.
Cytoplasm
Nucleus
CENP-F
CDCA2
NUSAP1
SGOL2
CKS2
b-Myb
CENP-A
RRM2
UBE2C
Cyclin B
HURP
CENP-E
Aurora-A
FOXM1
TPX2
MCAK
TOP2
DEEPEST
CDK1(p34)
UHRF1
TTK
E2F2/DP1 complex
MKLP1
Cep55
Survivin
ORC1L
Sgo1
HEC
Nek2A
Condensin
E2F7
BUB1
TYSY
MAD2a
BUBR1
KNSL1
Rabkinesin-6
HZwint-1
Cyclin E
Transporter
Protein
Transcription factor
Receptor ligand
Generic channel
Generic enzyme
Generic kinase
Protein kinase
Generic receptor
Generic binding protein
Metalloprotease
RAS- superfamily
G beta/gamma
Regulators (GAP, GEF etc.)
Negative/Inhibition
Positive/Activation
C.
Number of Genes
0
20
40
60
80
100
System development
Multicellular organismal development
Single-organism developmental process
Movement of cell or subcellular component
Developmental process
Axon development
Anatomical structure development
Appendage morphogenesis
Limb morphogenesis
Axonogenesis
5.0
5.5
6.0
6.5
7.0
-log(pValue)
D.
-1.5
-1.0
-0.5
0.0
0.5
1.0
1.5
2.0
CYS1
PALM
FN3K
PRKCE
TEAD1
CYP26B1
NFIC
NOS1
KCNA2
FZD8
GDPD5
NTN1
FOXJ1
SEMA5A
CX3CL1
HES4
TSKU
DNAH2
COL2A1
KRT5
Controls
10DPI

(Previous page) Figure 2.11 DEGs detected 10 DPI are involved in cell cycle and organ development. (A) Bar graph shows the number of genes mapping to each of the 10 most statistically significant GO terms to which the 300 up-regulated genes enriched. Line represents the –log(p-value) associated with each GO term. (B) Network image of the 50 most up-regulated genes in the GO term "cell cycle". (C) Bar graph shows the number of genes mapping to each of the 10 most statistically significant GO terms to which the 223 down-regulated genes enriched. Line represents the -log(p-value) associated with each GO term. (D) Network image of the 20 genes that mapped to the GO term "system development" and have direct interactions.

(*CDK1*, FC 10, mitosis, G2-M phase transition, apoptosis and genome stability (257)). *CDK1* also interacts with the centrosomal protein 55kDa (*CEP55*, FC 26), involved in cytokinesis (258); budding uninhibited by benzimidazoles 1 homolog (*BUB1*, FC 26), essential for spindle assembly and chromosome alignment (259); and ribonucleotide reductase M2 (*RRM2*, FC 22). As noted earlier, several immune related genes identified 7 DPI remained up-regulated 10 DPI (Fig. 2.9D) including: cytolytic molecules *GZMA* (FC 104), *GZMK* (FC 17), and *GZMB* (FC 8); cytokines/chemokines e.g. interleukin 2 receptor (*IL2RA*, FC 13), *CCR2* (FC 12), and *IL8* (FC 9); and activation markers such as major histocompatibility complex, class II (*HLADQB1*, FC 10) and *IGJ* (FC 12).

The 223 DEGs down-regulated 10 DPI were enriched in GO terms important for organ development (Fig. 2.11C). The most highly down-regulated genes within these GO processes include *KRT5* (FC 66, lung regeneration (252)), collagen II (*COL2*, FC 30, lung structure (260)), and Netrin-1 (*NTN-1*, FC 6, leukocyte transport into alveolar space (261)) (Fig. 2.11D). Other highly down-regulated genes include secretoglobin family 1A member 1 (*SCGB1A1*, FC 15, immunomodulation (262)), and troponin T type 1 (*TNNT1*, FC 11 muscle contraction (263)).

ImmGen analysis revealed a large cluster of genes highly expressed in B cells and T cells that play a role in the cell cycle (e.g. *CCNB1*, *BUB1*, and *CDK1*). This enrichment correlates with the significant increase in T cells at 10 DPI in lung tissue (Fig. 2.12, cluster 1, Fig. 2.2A and Fig. 2.3A,B). We also observed a cluster of genes that are highly expressed in MACs (CCR1, CD86, CD163, IgJ, CCL2, and CXCL9); NK and T cells (GZMA, GZMB, CCR2, and CCL5); and T cells (*CD96*, *CD3D* and *CD2*) (Fig. 2.12, clusters 2-4). As described for 3 and 7 DPI, none of the down-regulated DEGs were highly expressed by immune cells (data not shown).

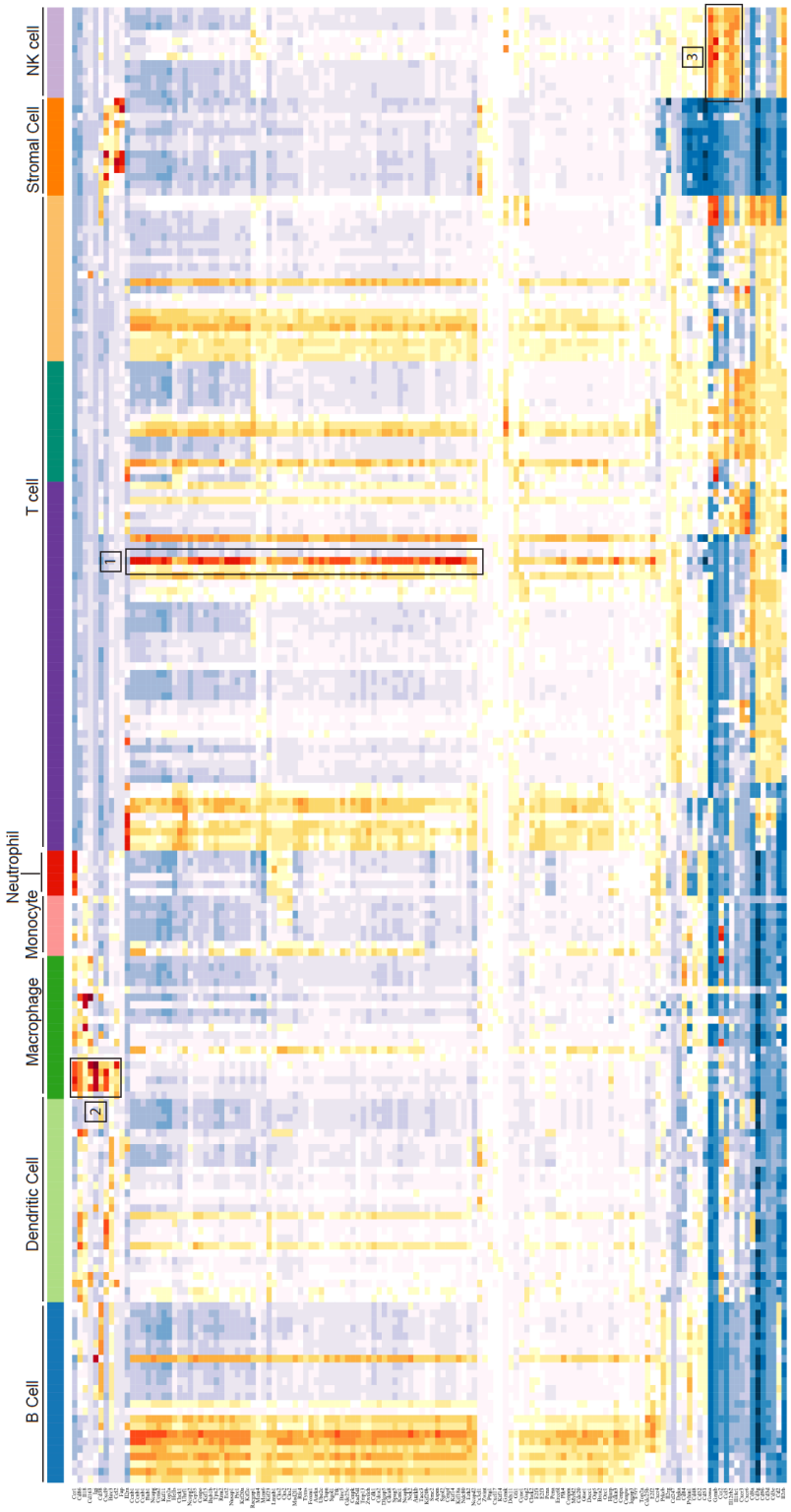
B Cell
Dendritic Cell
Macrophage
Monocyte
Neutrophil
T cell
Stromal Cell
NK cell
1
2
3

(Previous page) Figure 2.12 ImmGen heatmap showing the expression profile of the up-regulated genes at day 10 post-infection across different immune cell populations. Each row represents a gene and a corresponding microarray ID and column represents an immune cell type and study. Colors represent expression levels where red indicates the likelihood that the gene of interest is highlt expressed by a specific cell type and blue represents low expression. Gene cluster 1 shows scavenger receptor CD163 and proinflammatory genes such as *IL-18*, *CCR1* and *CXCL9* highly expressed in macrophages. Cluster 2 shows a large number of genes involved with the cell cycle (e.g. *CCNM1*, *KIF11*, *TOP2a*, *SPAG5* and *CENPF*). Cluster 3 shows genes that were highly expressed in NK cells (*GZMA*, *GZMB*, *CCR2* and *CCL5*).

Gene expression returns to pre-infection levels by 14 DPI

Only 5 DEGs with human homologs were detected 14 DPI. The two up-regulated genes were phospholipase A2 (*PLA2G2A*, FC 37), which is involved in phospholipid metabolism and is overexpressed in lung cancer cells (264), and solute carrier family 38 member 4 (*SLC38A4*, FC16), important for amino acid transport (265). The three down-regulated genes played a role in cellular motility: dynein axonemal, heavy chain 2 (*DNAH2*, FC 21), involved in respiratory cilium motility and microtubule movement (266); protein phosphatase 1 regulatory subunit 1B isoform 1 (*PPP1R1B*, FC 5), which modulates microtubule stability via inhibition of protein-phosphatase 1 (267); and desmin (*DES*, FC 5), a major intermediate filament found in muscle and endothelial cells (268).

DISCUSSION

Although VZV is primarily transmitted via inhalation and replicates in the lungs (229), our understanding of the impact of VZV infection on lung function and the host response to VZV in the respiratory tract remains incomplete. In this study, we leveraged a robust model of VZV infection wherein rhesus macaques are intrabronchially infected with the homologue SVV to carry out the first in depth analysis of the host-pathogen interactions during acute varicella infection in the lungs using a combination of immunohistochemistry, flow cytometry, multiplex ELISA, and RNA sequencing. Our analyses show for the first time that SVV spreads rapidly through the lungs replicating both within the lung parenchyma as well as BAL immune cells. We also report the down-regulation of genes important for lung function, indicative of lung injury during the acute phase of infection. Immune responses and changes in gene expression tightly correlate with viral loads with the up-regulation of pro-inflammatory cytokines, ISGs, chemokines and granzyme genes at peak viral loads. In contrast, genes associated with cell cycle and lung repair were up-regulated after cessation of viral replication.

Immunohistochemistry staining and flow cytometry show that SVV infection results in significant infiltration of lymphocytes and MACs in the lungs as early as 3 DPI and before the appearance of varicella rash, typically detected 10-14 DPI. This is in agreement with previous reports of patients who developed varicella pneumonia before the development of the vesicular rash (231, 232). As previously reported for BAL (221), we saw a higher accumulation of highly differentiated CD8 T cells compared to CD4 T and CD20 B cells within lung biopsies. CD8 T cells were also the most abundant lymphocyte subset in the lungs of mice intra-nasally infected with respiratory syncytial virus (RSV) (269) and rhesus macaques infected with H1N1 influenza (270). Furthermore, CD8 T cells were shown to be essential for recovery in mice infected with

Vaccinia virus (271). In addition to lymphocytes, frequency of MACs within the lung biopsy also increased 3 and 7 DPI, returning to pre-infection levels 10 DPI. Bioinformatic analysis of DEGs detected 3-10 DPI using ImmGen also indicate that transcriptional changes are mediated by T cells, B cells, DCs, MACs, neutrophils and NK cells 3 and 7 DPI, with a bigger contribution of DCs, MACs, and neutrophils 7 DPI. In contrast, gene expression changes 10 DPI seem to be primarily originating from lymphocytes.

Concomitant with the influx of T cells, B cells, MACs and DCs into the BAL and lung tissue, we detected a significant increase in T cell attractants I-TAC and MIG, B cell chemokine BLC and granyulocyte attractant IL-8 and eotaxin in the BAL 3 and 7 DPI. Levels of pro-inflammatory cytokines IL-18, IL-1β, IL-6 and IFNγ also significantly increased in the BAL. These factors have been reported during other lung infections suggesting a common defense response to respiratory pathogens. For instance, IL-18 has been shown to activate NK cells and stimulate IFNγ production during influenza infection in the lungs (272). Increases in IL-6 and IFNγ have also been observed in nasopharyngeal lavage samples taken from influenza patients, BAL samples taken from flu infected rhesus macaques, and BAL samples from rhesus macaques infected with pulmonary nontuberculous mycobacteria (273-275). The sources of these factors could be alveolar macrophages and lung epithelial cells as previously reported during influenza infection and lung injury (276, 277). Indeed, ImmGen analysis also shows IL-18 and IL-1β to be highly expressed by MACs. Interestingly, no chemokines or cytokines were increased in the lung homogenate, suggesting that immune mediators are quickly secreted into the alveolar space and do not remain within the lung parenchyma. In support of this hypothesis, mRNA transcripts of

CXCL9 (*MIG*), *CXCL10*, *CXCL11* (*ITAC*), *IL-1β*, and *IL-8* within lung homogenates were significantly increased. Protein levels of all these chemokines were increased in the BAL at the same time point.

The pDC infiltration 3 DPI correlated with a robust induction of IFNα in the BAL supernatant 3-7 DPI. Another source of IFNα could be epithelial cells, which, like pDCs, express the double stranded DNA sensor TLR9 (278), and could secrete type 1 interferons in a RIG-I dependent manner as described for RSV infection (279). Alternatively, IFNα could also be secreted by alveolar macrophages, which were the primary producers of IFNα in mice infected with Newcastle disease virus (280). Concomitant with the increased IFNα levels in the BAL, we detected a significant up-regulation of the transcription factor *STAT1*, induced by type 1 and 2 interferons 3 DPI (237). *STAT-1* in turn regulates the expression of interferon-stimulated genes (ISGs), which play a critical role in inhibiting viral replication. Indeed, ISGs were among the most highly up-regulated genes in our data set (average FC = 18). The increased expression of ISGs persists until 10 DPI and correlates with decreased viral loads 10 and 14 DPI. Our observations are similar to those described for influenza and RSV where increased expression of *ISG15, RIGI, IRF1, CXCL10, CXCL11, IFIT1* and *STAT1* have been shown to play a role in disease resolution (281-283). Similarly, reduced ISG expression has been associated with severe cases of H5N1 infection in cynomologous macaques (284).

STAT1 also regulates the expression of granzymes (*GRZM*) *A*, *B* and *K* (285), which were amongst the most highly up-regulated DEGs in our dataset. NK cells and CD8 T cells produce these cytolytic molecules during viral infections to kill infected cells (286). Increased expression of GRMZ genes correlated with increased frequency of EM CD8 T cells and was confirmed by

IHC staining. Bioinformatic analysis using ImmGen also confirmed that GZMA and GZMB was highest in NK and T cells 3-10 DPI. We previously reported increased GRMZB levels within BAL-resident CD4 and CD8 T cells during SVV infection (221). Elevated *GRZMA* and *GRZMB* expression have also been reported during RSV and influenza A infection (287, 288). Moreover, increased expression of GRZMK during acute lung inflammation can in turn induce IL-6, IL-8 and CCL2 production (289). Both mRNA and protein levels of IL-6 and IL-8 were increased during acute varicella 3 DPI. Together with previous reports, data reported in this study suggest that the lung generates a similar response to respiratory viral pathogens lead by ISGs, granzymes, similar chemokines and cytokines followed by an infiltration of B and T cells.

Acute varicella is accompanied by lung injury as evidenced by the severe focal hemorrhaging and damaged alveolar walls as well as the down-regulation of genes involved in lung development and function. This damage is likely caused by both the anti-viral immune response as well as viral replication as previously described for influenza (290). Indeed, the damage was most severe at the peak of viral loads and immune response (7 DPI). For instance, expression of *IRX3* (3 DPI), important for lung development and airspace maintenance (238) and *SEC14-like 3* (7 DPI), which plays a critical role in preventing lung collapse (254), were significantly down-regulated by SVV infection. Similarly, down-regulation of *TNNT1* (10 DPI) has been proposed as a cause of acute respiratory distress (291). Moreover, genes that play a role in controlling lung inflammation were down-regulated such as *SCGB3A1* (10 DPI), which regulates airway inflammation and tissue repair (292). Interestingly, type 1 and 2 interferons, which were increased 3 and 7 DPI, have been shown to decrease *SCGB3A1* expression (293). Similarly, *IRS2*, which interacts with IL-4 and acts as an anti-inflammatory agent in the lungs (253), was also down-regulated (7 DPI).

Several tumor suppressor genes were down-regulated, while genes that were involved in the cell cycle were up-regulated, which could have contributed to the increased T cell numbers seen 7-10 DPI. Indeed, analysis using ImmGen indicates that these genes are most highly expressed by T cells. Significant increase in expression of cell cycle genes was also observed in mice recovering from MRSA-induced pneumonia (294). The up-regulated cell cycle genes could also indicate the beginning of the repair process in the lungs since young immune competent rhesus macaques resolve primary varicella infection without complication. In line with that hypothesis, we detected an increase in growth factors VEGF and PDGF-BB, and angiogenic factor VEGF-A 10 and 14 DPI, which have been shown to play a critical role in alveolarization in the lungs and repairing damaged alveolar walls (295, 296). Interestingly, several genes involved with lung function remained down-regulated 10 DPI and 14 DPI, suggesting that repair continues after cessation of viral replication. For instance, KRT5, essential for lung tissue repair (252), remained one of the most significantly down-regulated genes at 10 DPI, and DNAH2, involved with cilium motility in the lungs (266) also remained down-regulated at 14 DPI.

In summary, data from this study provides the first kinetic analysis of host-pathogen interactions within the lungs during acute varicella infection. A robust immune response led by interferon-stimulated genes, granzymes, cytokines and chemokines is critical for the resolution of infection. These data also show that although SVV infection in young macaques is self-limiting, significant lung injury occurs during the acute phase as a result of the immune response and viral replication, a phenomenon that has not previously been described. Our results provide potential insights to both what happens in a self –resolving infection, and by extension, what may be happening when infection results in severe complications. Specifically, our RNA sequencing data show reduced expression of genes important for lung function during peak viral replication. In immune deficient

individuals who lack the vigorous immune response, uncontrolled viral replication could lead to sustained reduction in the expression of these critical genes, which in turn results in severe lung damage and viral pneumonia. Furthermore, immune genes that are significantly up-regulated likely play a critical role in resolving infection; therefore, lack of increased expression of these genes may explain why the immunocompromised develop severe disease. On the other hand, adults may generate too vigorous of an immune response that results in severe inflammation and viral pneumonia. These data help design interventions to mitigate complications associated with VZV pneumonia and other infectious respiratory diseases.

CHAPTER 3: Acute simian varicella infection causes robust and sustained changes in gene expression in the sensory ganglia

Nicole Arnold[1], Thomas Girke[2], Suhas Sureshchandra[3], and Ilhem Messaoudi[1,3,4*]

[1]Graduate Program in Microbiology, University of California-Riverside, CA, USA

[2] Department of Botany and Plant Sciences, University of California-Riverside, CA, USA

[3]Graduate Program in Genetics, Genomics and Bioinformatics, University of California-Riverside, CA, USA

[4]Division of Biomedical Sciences, School of Medicine, University of California-Riverside, Riverside, CA

A version of this chapter is published in the Journal of Virology:
Arnold N, Girke T, Sureshchandra S, Messaoudi I. 2016. Acute simian varicella infection causes robust and sustained changes in gene expression in the sensory ganglia. J Virol doi:10.1128/JVI.01272-16.

ABSTRACT

Primary infection with varicella zoster virus (VZV), a neurotropic alpha herpesvirus, results in varicella. VZV establishes latency in the sensory ganglia and can reactivate later in life to cause herpes zoster. The relationship between VZV and its host during acute infection in the sensory ganglia is not well understood due to limited access to clinical specimens. Intrabronchial inoculation of rhesus macaques with simian varicella virus (SVV), recapitulates the hallmarks of VZV infection in humans. We leveraged this animal model to characterize the host-pathogen interactions in the ganglia during both acute and latent infection by measuring both viral and host transcriptomes on days 3, 7, 10, 14 and 100-post infection (DPI). SVV DNA and transcripts were detected in sensory ganglia 3 DPI, before the appearance of rash. CD4 and CD8 T cells were also detected in the sensory ganglia 3 DPI. Moreover, lung-resident T-cells isolated from the same animals 3 DPI also harbored SVV DNA and transcripts, suggesting that T-cells may be responsible for trafficking SVV to the ganglia. RNA-Seq analysis showed that cessation of viral transcription 7 DPI coincides with a robust antiviral innate immune response in the ganglia. Interestingly, a significant number of genes that play a critical role in nervous system development and function remained down-regulated into latency. These studies provide novel insights into host-pathogen interactions in the sensory ganglia during acute varicella, and demonstrate that SVV infection results in profound and sustained changes in neuronal gene expression.

INTRODUCTION

Varicella zoster virus (VZV) is a neurotropic alpha herpesvirus and the causative agent of varicella (chickenpox) (9). VZV establishes latency in the sensory ganglia and can reactivate later in life to cause herpes zoster (shingles), a painful disease that affects almost one million individuals in the United States alone (297). VZV is transmitted through the inhalation of virus-laden saliva droplets or by direct contact with the infectious fluid from vesicles (9). It is believed that VZV replicates in the upper respiratory tract including the tonsillar lymph nodes, where it infects memory CD4 T cells that disseminate the virus to cutaneous sites where infection of keratinocytes results in varicella exanthem (9).

Two models have been put forth to explain how VZV reaches the ganglia. One model proposes that cell-free virus in varicella lesions infects the nerve terminals and travels to the ganglia via retrograde transport as described for the closely related herpes simplex virus (33). A second model proposes that VZV is transported to the ganglia via the hematogenous route within infected T cells (214, 298). The contribution of retrograde axonal transport versus hematogenous spread to VZV dissemination to the ganglia *in vivo* is poorly understood. Furthermore, whether VZV establishes latency immediately or replicates first in sensory ganglia remains unclear. Experiments using human fetal dorsal root ganglia xenografts directly inoculated with VZV-infected fibroblasts in hu-SCID mice, have shown VZV transcription in the ganglia until 14 DPI (193). However, it is unknown whether viral gene expression is sustained for a similar duration in an immune competent host.

Similarly, the host response that develops in the ganglia during primary VZV infection remains poorly understood. Previous studies report the presence of T cells (primarily non-cytolytic CD8+ T cells), B cells, macrophages, and natural killer cells within ganglia isolated from individuals who suffered from herpes zoster shortly before they died from other causes (148, 149, 299). These studies also showed increased expression of chemokine CXCL10 that binds to CXCR3 to induce migration of memory T cells and natural killer cells (149) as well as increased expression of MHC-I and MHC-II molecules (148). These observations suggest that both innate and adaptive immunity play a critical role in the resolution of VZV reactivation. However, it is uncertain if similar responses occur in the ganglia during acute infection.

Our incomplete understanding of host-pathogen interactions in the ganglia during acute VZV infection is due to the difficulty in obtaining clinical samples and the strict human host specificity of VZV. Intrabronchial infection of rhesus macaques with the closely related Simian Varicella Virus (SVV) recapitulates hallmarks of primary VZV infection, including the appearance of varicella, the development of cellular and humoral immunity, and establishment of latency in sensory ganglia (217). Moreover, as described for VZV, SVV can reactivate during episodes of immune suppression and stress (216, 218, 300) and this reactivation is accompanied by the up-regulation of CXCL10 and T cell infiltration (225). Recent studies using African green monkeys (AGMs) inoculated with SVV-GFEP have shown that SVV infects T cells that infiltrate the ganglia during acute infection 9 DPI (223). However, SVV infection of AGMs, in contrast to human VZV infection, results in significant mortality (301) and SVV-GFEP is attenuated compared to WT (223). Moreover, ganglia samples were only analyzed at time points after the appearance of varicella rash (>9 DPI), therefore the role of T cells versus the axonal route in SVV dissemination to the ganglia remain unclear.

In this study, we leveraged SVV infection of rhesus macaque to interrogate the kinetics by which SVV reaches the ganglia and establishes latency as well as the host response to SVV using ganglia collected from naïve animals 3, 7, 10, 14 and 100 days post-infection (DPI). At every time point, we measured viral loads and characterized both viral and host gene expression. We show that SVV DNA and RNA transcripts are detected in the ganglia as early as 3 DPI at the same time as memory T cells. Peripheral T cells from the same animals 3 DPI harbor viral DNA suggesting a role for these cells in SVV transport to the ganglia. In addition, cessation of viral gene expression in the ganglia coincides with the induction of a robust antiviral innate immune response. Robust changes in expression of genes associated with nervous system development were observed throughout the study, suggesting that SVV infection has a sustained effect on neuronal gene expression long after viral replication ceases.

MATERIALS AND METHODS

Ethics Statement

The study was carried out in strict accordance with the recommendations described in the Guide for the Care and Use of Laboratory Animals of the National Institute of Health, the Office of Animal Welfare and the United States Department of Agriculture. All animal work was approved by the Oregon National Primate Research Center Institutional Animal Care and Use Committee (IACUC protocol # 0779). The ONPRC has been continuously accredited by the American Association for Accreditation of Laboratory Animal Care since 1974 (PHS/OLAW Animal Welfare Assurance # A3304-01). Animals were either housed single or paired in caging that allowed for social interactions in a temperature and humidity controlled environment. Food and water were available ad libitum and enrichment was provided daily. All procedures were carried out under Ketamine anesthesia in the presence of veterinary staff and all efforts were made to minimize animal suffering. Animals were euthanized in accordance with the recommendations of the American Veterinary Medical Association guidelines for euthanasia.

Cells and virus

SVV was propagated in primary rhesus fibroblasts (1° RF) (a generous by Dr. Scott Wong, Oregon National Primate Center) at 37°C in 175 cm^2 flasks with DMEM supplemented with 10% FBS. SVV-infected 1° RF were frozen in FetalPlex with 10% DMSO, stored in LN_2, and assayed by plaque assay.

Animals and sample collection

Fifteen colony-bred Rhesus macaques (*Macaca mulatta,* RM) 3-5 years of age and of Indian origin were used in these studies. Twelve were inoculated intrabronchially with 4×10^5 PFU wild-

type SVV as previously described (217) and subsequently euthanized on 3 (n=3), 7 (n=2), 10 (n=2), 14 (n=3), and 100 (n=2) DPI. An additional 3 animals served as non-infected controls. Animals were housed and handled in accordance with the Oregon National Primate Research Center Institutional Animal Care and Use Committee. These animals were previously used to characterize specificity of the anti-SVV T cell response (222). Blood, bronchial alveolar lavage (BAL), and sensory ganglia were collected from all animals. Blood and BAL were used to measure viral loads, isolate CD20, CD4 and CD8 T cell population for additional viral loads and viral transcription analyses. Trigeminal and dorsal root ganglia (DRG) (cervical, thoracic and lumbar-sacral) were collected from each animal and were divided to carry out multiple assays described in greater detail below: DNA extraction for viral loads, RNA extraction for viral transcription, digestion and isolation of mononuclear cells, and paraffin embedding for IHC analysis. DRG ganglia from naïve animals were used for RNA-Seq analysis. Skin biopsies were collected from the trunk of the animals at 3 DPI.

Isolation of immune cells from ganglia

Ganglia were digested in 150U/ml collagenase for 1 hour at 37°C with shaking then homogenized using a cell strainer to generate single-cell suspensions. Cells were pelleted at 2000rpm for 5 minutes, and then resuspended in 30% percoll gradient and spun for 15 minutes at 2000rpm to isolate mononuclear cells. Cells were then stained with antibodies directed against surface markers: CD4 (Tonbo Biosciences, San Diego, CA), CD8β (Beckman Coulter, Brea, CA), CD28 (Tonbo Biosciences), CD95 (BioLegend, San Diego, CA) and CCR7 (BD Pharmingen, San Diego, CA) to delineate naïve and memory T cell subsets as well as CD20 (Southern Biotech, Birmingham, AL), IgD (Southern Biotech, Birmingham, AL), and CD27 (Biolegend) to delineate B cell subsets as previously described (221). Samples were analyzed

using the LSRII instrument (Becton, Dickinson and Company, San Jose, CA) and Flowjo software (TreeStar, Ashland, OR). Due to the low amount of lymphocytes in the ganglia, half DRG-C, DRG-T and DRG-LS from the same animal were pooled in order to get a sufficient number of events to quantify the frequency of lymphocytes. The same number of DRGs was used for every animal.

Purification of CD4/CD8 T cells

CD4 and CD8 T cells were isolated from BAL and PBMC samples using Magnetic Cell Sorting (MACs). BAL and PBMC cells were first incubated with CD4 microbeads (Miltenyi Biotec, San Diego) for 20 mins at 4°C. Cells were then washed in buffer and the cell suspension was applied to the magnetic column to capture CD4 T cells. CD4 negative fraction was then stained with CD8-PE (Beckman Coulter) and incubated with the cells for 20 mins in the dark at 4°C. Cells were then washed and anti-PE beads (Miltenyi Biotec) were added and incubated for 15 mins in the dark at 4°C. Cells were then washed and the cell suspension was applied to a magnetic column to isolate CD8 T cells. Finally, the CD4 and CD8 negative population was incubated with CD20 microbeads (Miltenyi Biotec) to isolate B cells. Purity of the fractions was determined using flow cytometry. All samples used had a purity of >90%.

DNA/RNA extraction and quantitative PCR

Ganglia and skin tissue was digested in Proteinase K Solution (20mg/ml) overnight and DNA was extracted using the Qiagen genomic DNA extraction kit (Qiagen, Valencia, CA). Viral DNA loads were determined exactly as previously described (217) by real-time PCR using primers and probes specific for ORF21 and the ABI StepOne instruments (Applied Biosystems, Foster City,

CA). 1 ug of DNA was used for ganglia tissue viral loads. For RNA extraction, ganglia tissue in trizol was homogenized using a bead beater and zirconia/silica beads followed by extraction using the Purelink RNA Mini Kit (Ambion, Carlsbad, CA)

Measuring anti SVV T and B cell responses

The ELISpot data was derived from a previous study characterizing the specificity of the T cell response to SVV during acute and latent infection (222). The total spot forming cells (SFC) in PBMCs or BAL was determined by adding up the individual responses to each of the 70 ORFs. SVV-specific IgG titer was determined as previously described (217).

Viral gene expression analysis

10 ng of total RNA from each sample and 10 External RNA Controls Consortium (ERCC, internal positive control used for normalization) were randomly primed for reverse transcription and subsequently amplified with 71 custom viral gene-specific and 10 ERCC-targeted primers for 19 cycles of PCR. Barcoded DNA adapters were ligated to amplicons to allow multiplexing libraries for sequencing. Libraries were amplified onto Ion Sphere Particles (ISPs) using the One Touch 2 (Life Technologies, Carlsbad, CA) and sequenced on the Ion Torrent Proton (Life Technologies, Carlsbad, CA) per manufacturer's protocol for v3 templating and sequencing chemistries. Sequencing reads that were less than 60 base pairs long were removed from further analysis, and remaining reads were stringently aligned to the viral genome and ERCC sequences using TMAP, an Ion Torrent Proton specific sequence aligner.

Host Transcriptome Analysis

RNA was extracted from ganglia using the Ambion Purelink RNA Mini Kit extraction kit (Life Technologies, Carsbad, CA). RNA library preparation was done using the New England Biolab (NEB) Next Ultra Direction RNA Prep kit for Illumina (Ipswich, MA). DNA libraries were then multiplexed and sequenced on the Illumina HiSeq2500 (Illumina, San Diego, CA) platform at single-ends 100bps. All data analysis steps were performed with the RNA-Seq workflow module of the *systemPiperR* package available on Bioconductor (302). NGS quality reports were generated with the *seeFastq* function defined by the same package. RNA-Seq reads were mapped with the splice junction aware short read alignment suite Bowtie2/Tophat2 (303, 304) against the *Macaca mulatta* genome sequence downloaded from Ensembl (305). The default parameters of Tophat2 optimized for mammalian genomes were used for the alignments. Raw expression values in form of gene-level read counts were generated with the *summarizeOverlaps* function(306). Only reads overlapping the exonic regions of genes were counted, while reads mapping to ambiguous regions of exons from overlapping genes were discarded. Given the non-stranded nature of our RNA-Seq libraries, the read counting was performed in a non-strand-specific manner.

Analysis of differentially expressed genes (DEGs) was performed with the GLM method from the *edgeR* package (307, 308). Differentially expressed genes (DEGs) were defined as those with a fold change of ≥3 and a false discovery rate (FDR) of ≤0.01. Enrichment analysis of functional annotations was performed to identify significant gene ontology (GO) processes using MetaCore™ software (GeneGo, Philadelphia, PA).

Gene Validation

RNA was reverse transcribed using random hexamers and SuperScript ® IV RT in the SuperScript ® IV First-Strand Synthesis System (Invitrogen, Lithuania) to generate cDNA. Taqman gene expression assays (Thermo Fisher, Waltham, MA) of candidate genes and housekeeping gene (RPL32) were used with 50ng of cDNA and carried out in duplicate on the ABI StepOne instrument (Applied Biosystems). mRNA expression levels were calculated relative to our housekeeping gene (RPL32) using $2^{-}\Delta Ct$ calculations.

Immunohistochemistry Staining

4µm ganglia sections were deparaffinized and rehydrated before antigen retrieval. Antigen retrieval was done using a pressure cooker in citrate buffer for 20 minutes. The sections were then blocked in 10% bovine serum albumin (BSA) and 1% normal goat serum for 1hr followed by avidin and then biotin for 15 minutes. Tissues were then stained with primary antibodies CD3 (1:200 dilution, Dako M0452), for labeling T lymphocytes, CD68 (1:75 dilution, Dako) for labeling macrophages, CD20 (1:300 dilution, Dako M0755) for labeling B cells, proteoglycan 4 (PRG4) (1:200 dilution, antibodies-online), Glial fibrillary acidic protein (GFAP) (1:500 dilution, Dako), and Complexin 1 (CPLX1) (1:200 dilution, Proteintech Group). Slides were then incubated with the appropriate secondary antibody and treated with 10% peroxidase in methanol for 10 minutes in the dark. Color development of antigen staining was done with ImmPACT™ DAB (Vector labs, Burlingame, CA) and counter stained with Hematoxylin QS (Vector Laboratories, Burlingame, CA). Slides were then covered with coverslips using Omnimount™ (National Diagnostics, Atlanta, Georgia). Images were taken on the Leica DM5500 B (Leica Biosystems, Buffalo Grove, IL) microscope at 40x. Isotype IgG antibody was used as a negative control.

IHC quantification for PRG4 was done using ImageJ software. Optical density values (OD) of DAB (brown) and hemotoxylin staining (blue) were taken from three different sections of each slide then averaged. Ganglia from three different infected animals and the three naïve controls were used for each staining.

Hematoxylin and Eosin (H&E) staining of 4μm ganglia sections were deparaffinized with Histo-Clear™ II (National Diagnostics, Atlanta, Georgia) and rehydrated. Tissue was then stained with Hematoxylin for 2 minutes followed by Eosin for 40 seconds and the hydrated back to Histoclear and then covered with coverslips using Omnimount™ (National Diagnostics, Atlanta, Georgia).

Statistical Analysis

Statistical analysis and graphing were conducted through the GraphPad Prism software (GraphPad, Software, Inc., La Jolla, CA). Significant values were determined using one-way ANOVA.

RESULTS

SVV DNA is detected before the appearance of the rash.

To determine the kinetics of viral replication in the lung and in the blood, we performed qPCR using primers and probes against open reading frame (ORF) 21. SVV replication kinetics and viral loads in the bronchial alveolar lavage (BAL) and whole blood (WB) following intrabronchial infection (Fig. 3.1A) were similar to our previous studies, with higher SVV viral loads detected in the BAL compared to peripheral blood (217). SVV-specific cellular and humoral immune responses were detected 7, 10, 14 and 100 days post-infection (DPI) (Fig. 3.1B). Animals euthanized 10 and 14 DPI showed a characteristic varicella rash (data not shown).

To determine when SVV reached the ganglia, SVV viral loads were measured in trigeminal (TG) and dorsal root (DRG) ganglia (cervical, thoracic and lumbar-sacral) collected from naïve animals and from animals euthanized 3, 7, 10, 14 and 100 DPI. SVV viral DNA was detected in sensory ganglia 3 DPI, before the appearance of varicella rash. Genome copy numbers were initially higher in the TG compared to the DRG (Fig. 3.1C), but comparable 7 DPI (Fig. 3.1C). Since SVV DNA was detected in the ganglia before appearance of skin lesions and SVV viral DNA was not detected in non-lesioned skin, these data suggest that SVV first reaches the ganglia via other means than retrograde transport from skin lesions.

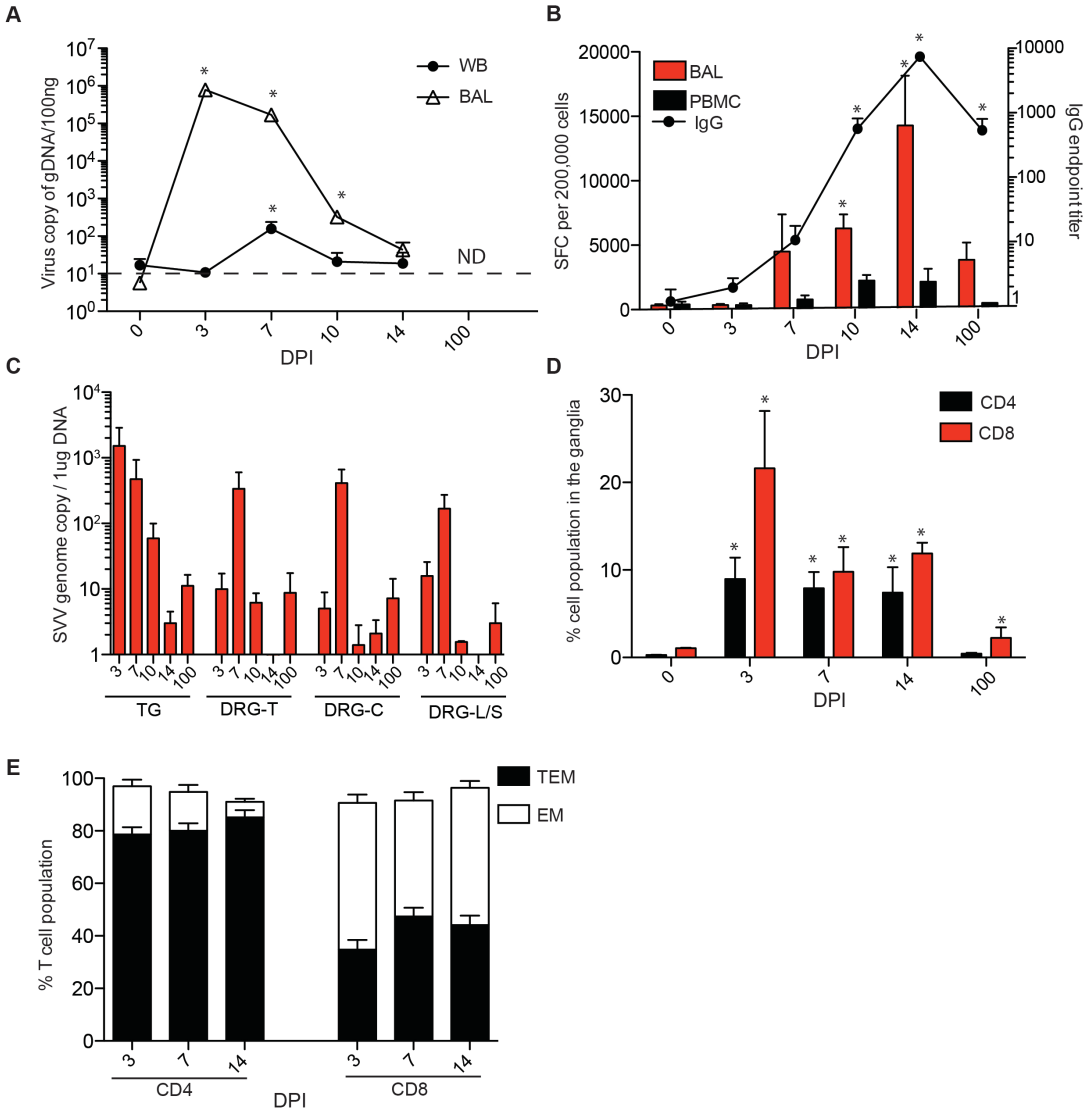
A
Virus copy of gDNA/100ng
WB
BAL
ND
DPI
B
SFC per 200,000 cells
IgG endpoint titer
BAL
PBMC
IgG
DPI
C
SVV genome copy / 1ug DNA
TG
DRG-T
DRG-C
DRG-L/S
D
% cell population in the ganglia
CD4
CD8
DPI
E
% T cell population
TEM
EM
CD4
CD8
DPI

(Previous page) Figure 3.1 SVV viral DNA and immune infiltrates are detected in sensory ganglia as early as 3DPI. (A) SVV DNA levels in the BAL and WB were measured by quantitative real-time PCR (100ng/sample) using primers and probes specific for SVV ORF21 (0 DPI, n=15; 3 DPI, n=11; 7 DPI, n=8; 10 DPI, n=5; 14 DPI, n=4; 100 DPI, n=2) (ND = Not Detected). Line indicates limit of detection. (B) Frequency of SVV-specific T cells in the BAL was measured using IFN gamma ELISpot assay by enumerating the number of spot-forming cells in response to all 69 unique SVV open reading frame as previously described (121) (0 DPI, n=3; 7 DPI, n=3; 10 DPI, n=2; 14 DPI, n=3; 100 DPI, n=2). SVV-specific IgG titers were determined using ELISA (0 DPI, n=15; 3 DPI, n=11; 7 DPI, n=8; 10 DPI, n=5; 14 DPI, n=3; 100 DPI, n=2). (C) SVV viral DNA was detected in the ganglia using quantitative PCR (1 μg/sample); TG= Trigeminal, DRG-T= Dorsal Root Ganglia Thoracic, DRG-C=Dorsal Root Ganglia Cervical, DRG-L/S= Dorsal Root Ganglia Lumbar/Sacral (3 DPI, n=3; 7 DPI, n=2; 14 DPI, n=3). No SVV DNA were detected in ganglia from naïve animals. (D) DRG-C, T and L/S isolated at the indicated times post infection were pooled, digested and mononuclear cells were isolated over a percoll gradient. Frequencies of CD4 and CD8 T cells were then measured using flow cytometry (3 DPI, n=3; 7 DPI, n=2; 14 DPI, n=3). (E) The percentage effector memory (EM) or central memory (CM) T cells were determined also using flow cytometry (3 DPI, n=3; 7 DPI, n=2; 14 DPI, n=3). *$P < 0.05$ compared to day 0

T cells infiltrate the ganglia during acute SVV infection.

Previous studies have shown a role for T cells in VZV and SVV dissemination (84, 223, 224). To determine whether T cells infiltrate the ganglia early after SVV infection in rhesus macaques, we digested DRG-T, DRG-C, DRG-L/S collected 3, 7, 10, 14 and 100 DPI and analyzed the isolated lymphocytes using flow cytometry and antibodies directed against CD4, CD8, CD28, CD95, and CCR7 in order to delineate naïve and memory T cell subsets as well as CD20, CD27 and IgD to delineate naive and memory B cell subsets as recently described (221). Both CD4 and CD8 T cells were detected 3-14 DPI (Fig. 3.1D) and they were highly differentiated into memory ($CD28^{+/-}CD95^{+}CCR7^{-}$) phenotype (Fig. 3.1E). No T cells were detected in the ganglia isolated from naïve animals (day 0) or animals euthanized 100 DPI. No B cells were detected in the ganglia at any time point.

We then carried out immunohistochemistry (IHC) using CD3 antibody to get a better understanding of the spatial distribution of T cells, and CD20 antibody to confirm absence of B cells. Our analysis confirmed the presence of T cells in the ganglia 3 to 14 DPI (Fig. 3.2). CD68+ cells were detected day 3-post infection (Fig. 3.2). In line with the flow cytometry data described above, no CD20+ B cells were detected at any time point (Fig. 3.2).

To determine if T cells support SVV replication and dissemination, we isolated CD4 T, CD8 T and CD20+ cells from BAL and PBMC samples collected from the same animals from which we collected ganglia 3, 7, 10 and 14 DPI. SVV DNA was detected 3-14 DPI in CD4 and CD8 T cells from both BAL and PBMC (Fig. 3.3A and 3.3B). No viral DNA was detected in T cells obtained from naïve animals or 100 DPI or from B cells detected at any time point. To determine whether T cells can support SVV replication, viral transcripts were measured using Ion AmpliSeq

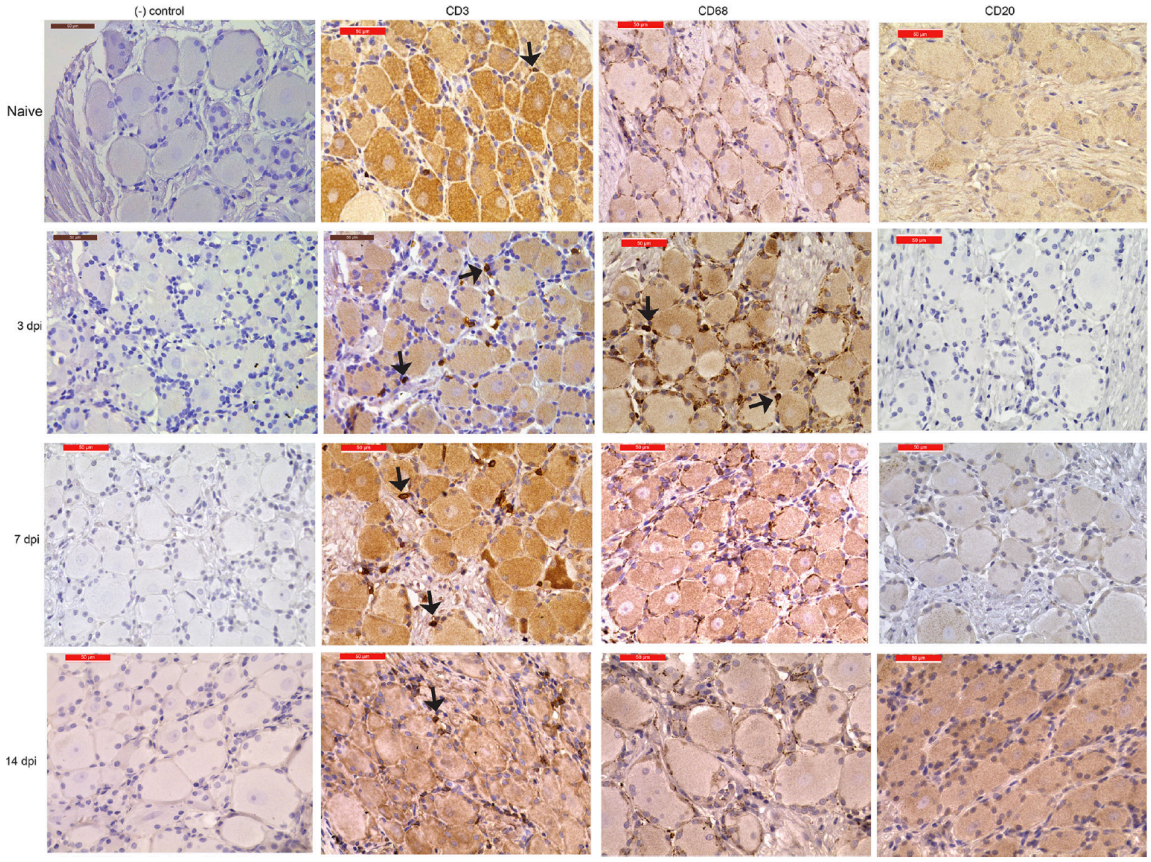

Figure 3.2 Immunohistochemistry staining shows immune infiltration of T cells and macrophages. Representative immunohistochemistry staining for CD3+, CD68+, and CD20+ cells in the dorsal root ganglia cervical (DRG-C) at naïve, 3 and 7 DPI and in the DRG-thoracic 14 DPI. Scale bar corresponds to 50µm (40x magnification). Arrows indicate CD3+ and CD68+ cells. Isotype IgG served as our negative control.

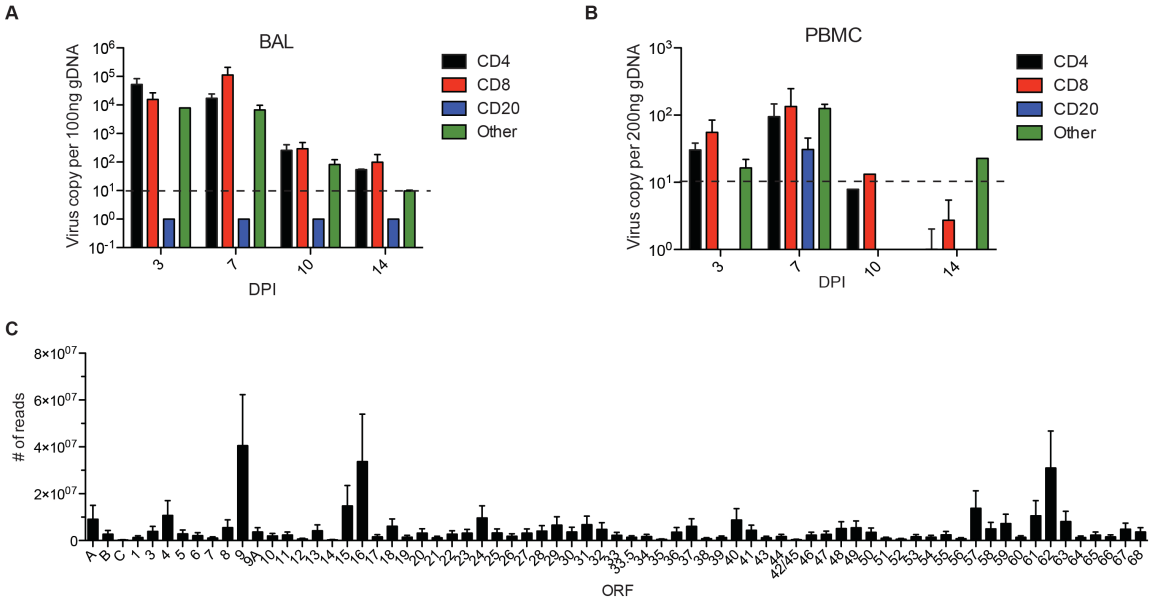

Figure 3.3 SVV trafficking and replication is supported in T cells of the BAL (A, B) SVV viral loads in purified CD4 T, CD8 T, CD20+ and other (remaining cell population) cells from (A) BAL and (B) PBMC were measured by qRT-PCR with primers and probes for ORF21. Dashed line indicates limit of detection. (C) SVV viral transcripts in BAL T cells (n= 5 (n=3, CD4 and n=2, CD8) isolated 3 and 7 DPI using Ion Ampliseq technology.

technology. Due to the limited amount of RNA and because the viral loads were comparable, we pooled RNA from BAL CD4 and CD8 T cells isolated 3 and 7 DPI. Transcripts from immediate early, early and late genes were detected in both CD4 and CD8 T cells albeit at a lower frequency in CD8 T cells (Fig. 3.3C and data not shown). The most abundant transcripts were *ORF9* (tegument protein), *ORF16* (viral DNA polymerase subunit) and *ORF62* (viral transactivator) (1) (Fig. 3.3C).

SVV transcripts are detected during acute infection

We next determined when SVV establishes latency in the ganglia by measuring the abundance of SVV viral transcripts using Ion Torrent AmpliSeq technology (Fig. 3.4). Viral transcripts associated with almost all SVV ORFs were detected 3 DPI in the ganglia (Fig. 3.4A). As previously described for infected BSC-1 and Vero cells (309), transcripts of *ORF9* (tegument protein), were the most abundant 3 DPI. In addition, transcripts of *ORF16*, *ORF15* (membrane protein), *ORF 37* (glycoprotein H) and *ORF62*/*ORF63* (viral transactivators) were also abundant (1). In contrast, only transcripts from *ORF18* (viral ribonucleotide reductase), *ORF34* (viral DNA packaging protein), and *ORF35* (a nuclear matrix protein required for infectivity of skin and T cells (310)) were detected 7 DPI (Fig. 3.4B). No viral transcripts were detected 10 and 14 DPI.

These data suggest that SVV begins to establish latency 7 DPI. Previous studies from our lab have shown *ORF61* transcripts being the most abundant latency-associated transcripts during SVV latency (>70 DPI) (220). Interestingly, *ORF61* transcripts were not detected by AmpliSeq on day 7, 10 and 14-post infection. Since our previous studies looked at later time points (>70 DPI) (311), we hypothesized that *ORF61* transcription may be first turned off, then restart after 14 DPI.

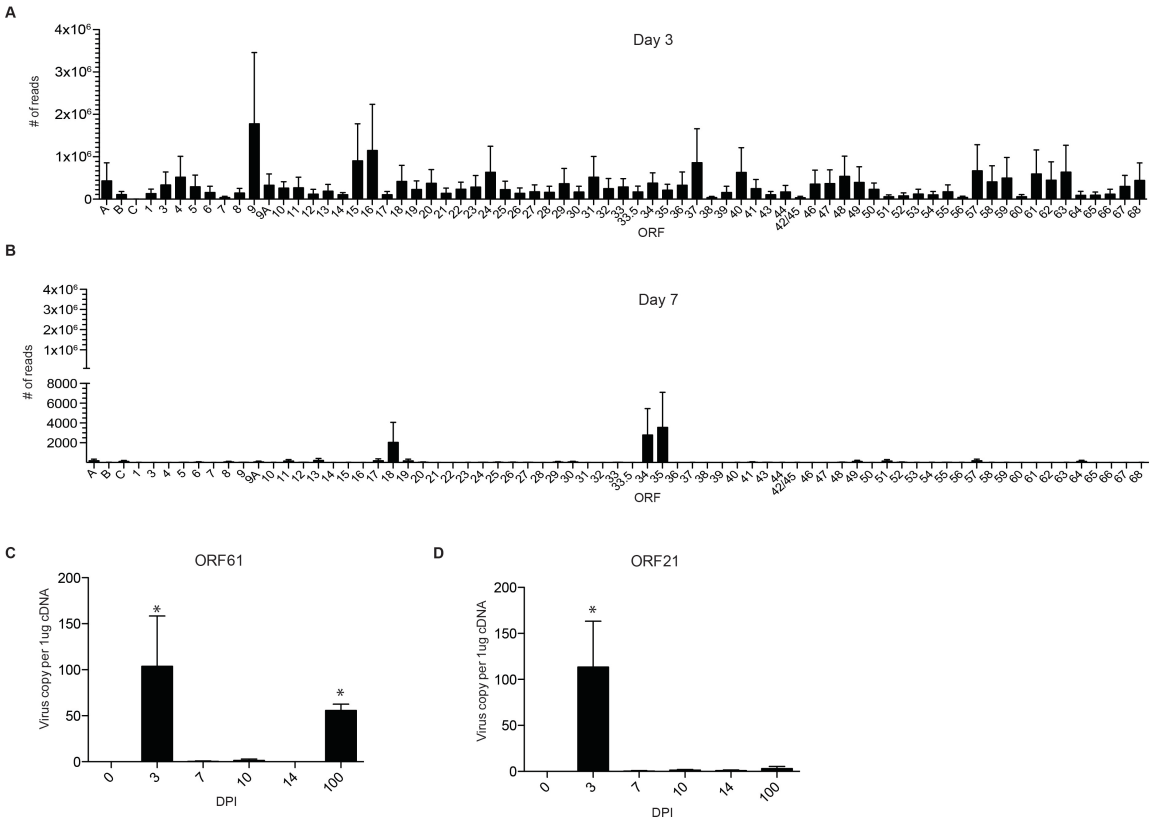

Figure 3.4 SVV replicates in the ganglia before establishing latency at 7DPI.
(A, B) Abundance of SVV viral gene transcripts at day 3 (A) (n=3) and day 7 (B) (n=3) post-infection in the ganglia were measured using Ion Ampliseq technology. (C, D) Viral transcripts of (A) *ORF61* and (B) *ORF21* (control transcript) were measured using qRT-PCR. (0 DPI n=3; 3 DPI n=3; 7 DPI n=2; 10 DPI n=2; 14 DPI n=3; 100 n=2, DPI) **P*< 0.05 compared to day 0.

To test this hypothesis, we measured *ORF61* and *ORF21* transcripts using qRT-PCR using the same RNA samples, including samples from 100 DPI. *ORF21* served as our control transcript. In line with our AmpliSeq data, *ORF61* and *ORF21* transcripts were detected 3 DPI, but not 7, 10 and 14 DPI (Fig. 3.4C and 3.4D). More importantly, *ORF61* but not *ORF21* transcripts were detected on 100 DPI, in agreement with our previous data (220) (Fig. 3.4C).

SVV infection results in large and sustained changes in gene expression in the ganglia

To characterize the host response in the ganglia during acute SVV infection, we used RNA-Seq to determine the transcriptome of sensory ganglia isolated from naïve animals (n=3) and SVV infected animals 3 (n=3), 7 (n=2), 10 (n=2), 14 (n=3) and 100 (n=2) DPI. Type of ganglia and average viral loads of samples used for RNA-Seq are shown in Table 3.1. Given the limited number of animals and available ganglia harboring SVV DNA, it was not possible to use the same type of ganglia at every time point. To address the issue of our small sample size, we used a cut off fold change (FC) ≥ 3 and a false discovery rate (FDR) corrected p-value ≤ 0.01 compared to naïve animals (instead of the traditional cut off FC≥ 2 and FDR corrected p-value ≤ 0.05) to identify differentially expressed genes (DEGs). SVV infection resulted in large changes in gene expression at all time points examined (Table 3.1, Fig. 3.5A). We confirmed changes in the expression of 8 genes by qRT-PCR and 3 genes by IHC analysis (Figs. 3.6 and 3.7). Functional enrichment of the DEGs was carried out using Metacore™ software, which requires the use of human gene identifiers for analysis. On average 83% of rhesus DEGs were successfully mapped to human homologs.

Day	Samples*	Average Viral Load±SEM**	Number of DEGs	Human Homologs***	Up-regulated DEGs	Down-regulated DEGs
3	DRG-L/S, DRG-C, DRG-T	28±6	393	324	137	187
7	DRG-T, DRG-C	26±6	1,118	904	368	536
10	DRG-C, TG	17±5	809	643	164	479
14	TG, DRG-C, TG	17±9	576	512	51	461
100	TG, TG	39±3	1100	839	203	636

Table 3.1 The number of differentially expressed genes (DEGs) found in the ganglia after SVV infection

*Types of ganglia used for RNA-Seq analysis

** Average SVV genome copy number of all ganglia used in the RNASeq experiment/1µg DNA

*** The number of rhesus DEGs with human homologues used for enrichment analysis.

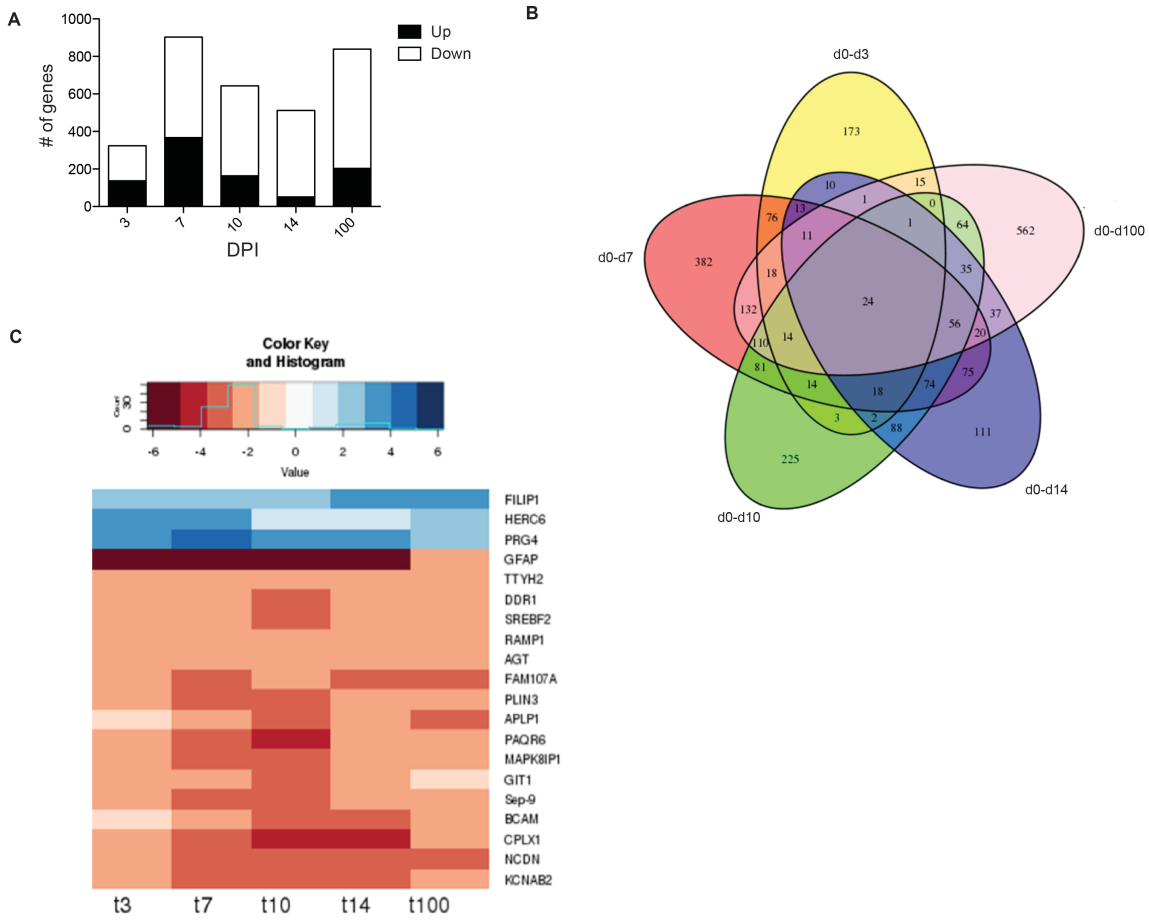

Figure 3.5 SVV infection results in robust changes in gene expression.
(A) Number of up-regulated and down-regulated differentially expressed genes (DEGs) detected at day 3, 7, 10, 14 and 100 post infection (B) 5-way venn diagram of the DEGs detected at each time point with human homologues. (C) Heatmap analysis of the 20 common DEGs.

A total of 24 (20 characterized; 3 up-regulated and 17 down-regulated) were differentially expressed at all time points examined (Fig. 3.5B and 3.5C). The three genes that remained up-regulated throughout infection were proteoglycan 4 (*PRG4*), Filamin A interacting protein 1 (*FILIP1*), and HECT/ RCC1-like domain containing protein 6 (*HERC6*) (Fig. 3.5C). *PRG4* (confirmed by IHC staining; Fig. 3.7A) is a lubricating glycoprotein that can induce schwann cell proliferation (312). *FILIP1* (confirmed by qRT-PCR; Fig. 3.6A) interacts with Filamin A to control neuron migration out of the ventricular zone (313) and it interferes with myosin 2b binding to F-actin in glutamatergic neurons, affecting the neural spine structure (314). The current function of *HERC6* is unknown, however, *HERC5*, with which it shares 50% nucleotide sequence identity, plays a role in innate antiviral responses (315).

Glial fibrillary acidic protein (*GFAP*), an intermediate filament protein that plays a critical role in maintaining astrocyte function (316), was the most down-regulated common gene throughout infection (Fig. 3.5C) (confirmed by IHC and qRT-PCR (Fig. 3.6B and 3.7B)). Other genes that remained down-regulated during infection were Neurochondrin (*NCDN*), involved in neurite outgrowth (317); Complexin 1 (*CPLX1*), expressed by neurons and regulates synaptic vesicle exocytosis (318) (confirmed by IHC and qRT-PCR (Fig. 3.6C and 3.7C)); and Progestin and adipoQ receptor 6 (*PAQR6*) a G-coupled membrane progesterone receptor that exhibits neuroprotective properties (319) (Fig. 3.5C).

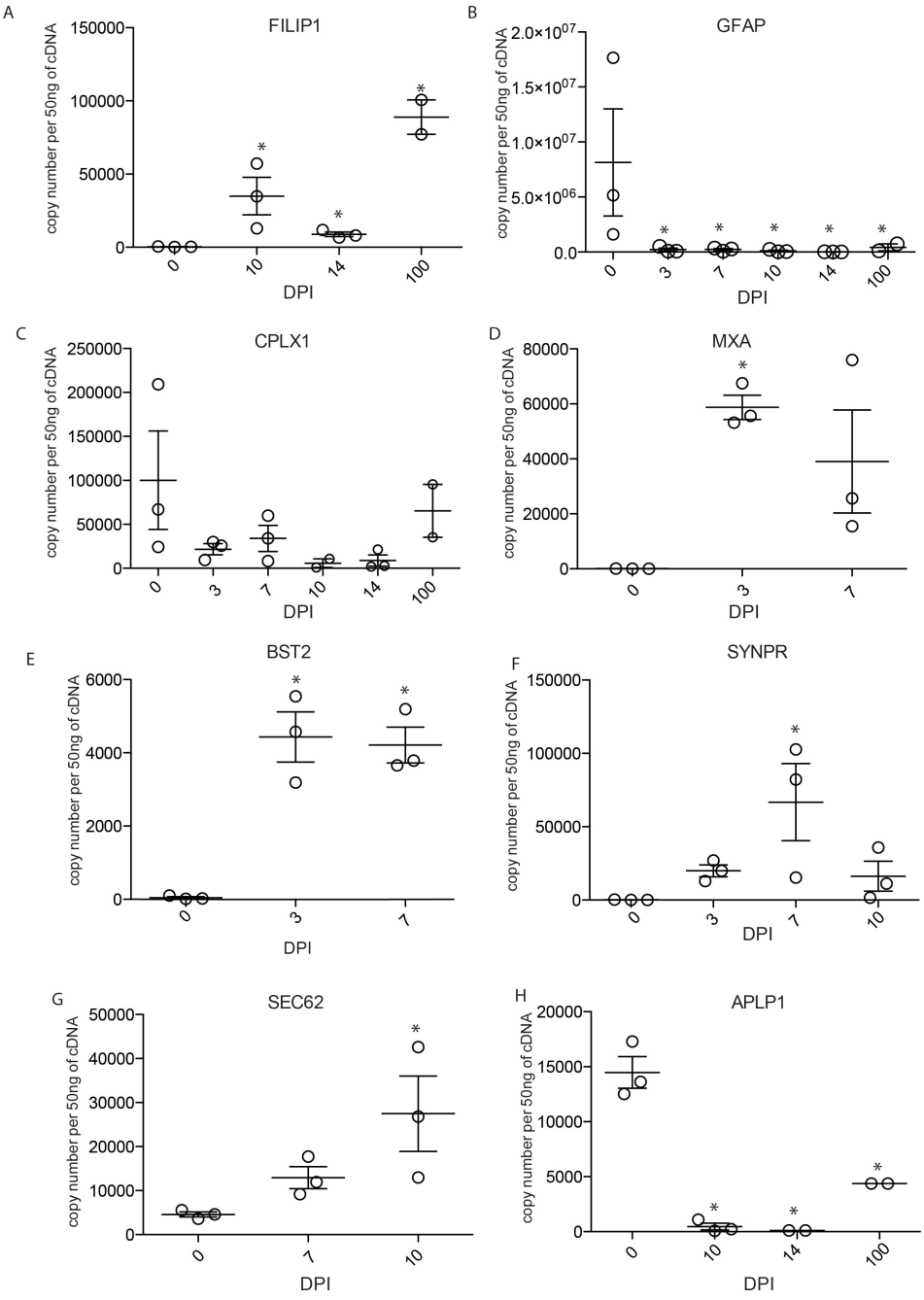

Figure 3.6 Gene Validation. Taqman assays were done on (A) FILIP1; up-regulated 10, 14 and 100 DPI (B) GFAP; down-regulated 3, 7, 10, 14 and 100 DPI (C) CPLX1; down-regulated 3, 7, 10, 14 and 100 DPI (D) MXA; up-regulated 3 and 7 DPI (E) BST2; up-regulated 3 and 7 DPI (F) SYNPR; up-regulated 7 DPI (G) SEC62; up-regulated 10 DPI and (H) APLP1; down-regulated 10, 14 and 100 DPI. (1 additional ganglia tissue from the same animal was used on 7 DPI and 10 DPI). *P< 0.05 compared to day 0.

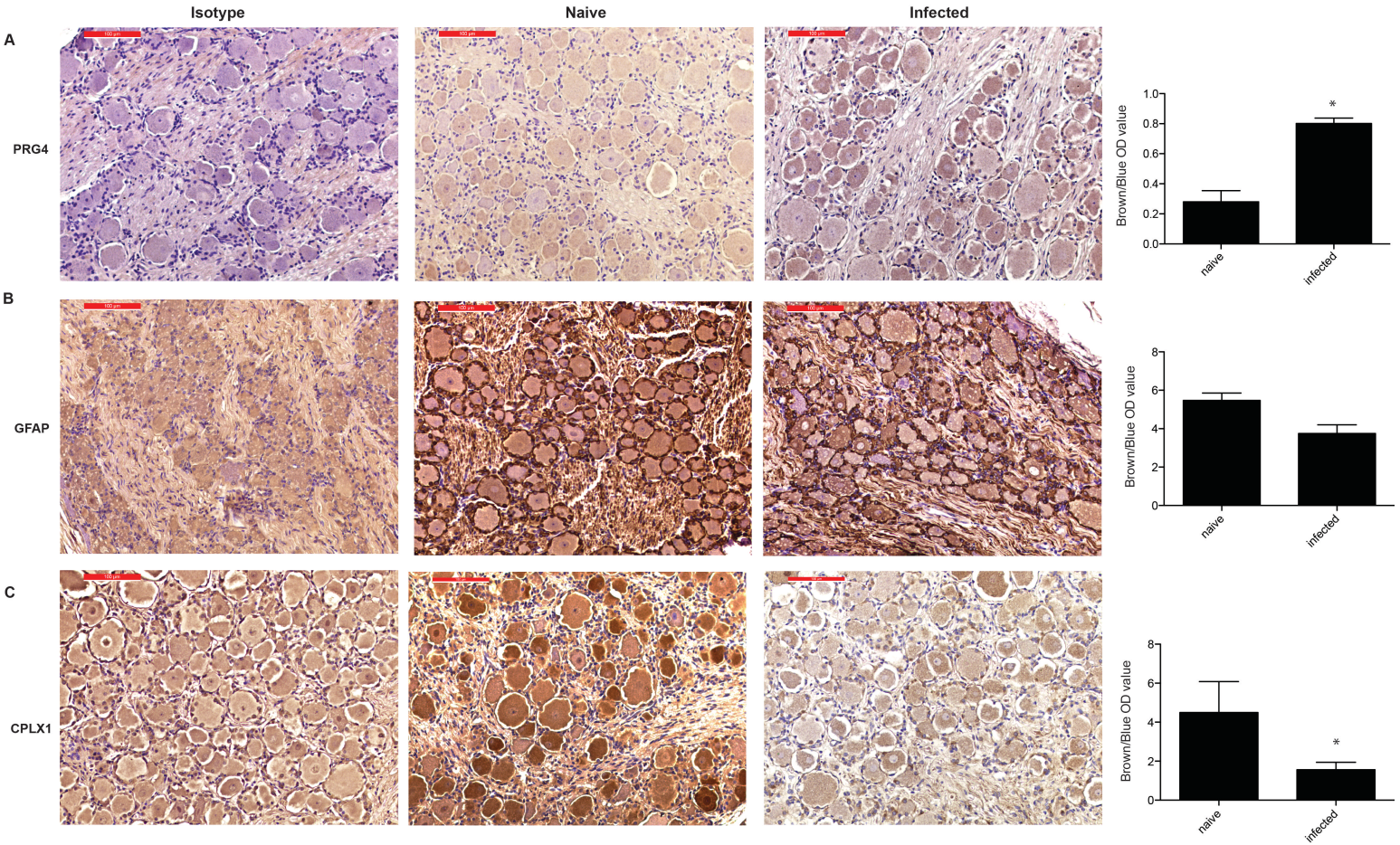
Isotype
Naive
Infected
A
PRG4
B
GFAP
C
CPLX1
Brown/Blue OD value
naive
infected
*

(Previous Page) Figure 3.7 Immunohistochemistry gene validation. IHC staining and IHC quantification of (A) PRG4 (B) GFAP and (C) CPLX1 on isotype controls, naïve and infected ganglia tissue. (n=3, for naïve and infected tissue were used for quantification). Representative images are all from DRG-L/S isolated 10 DPI. Quantification on infected tissue was from 3 DPI (DRG-T), 7 DPI (DRG-T) and 10 DPI (DRG-L/S). Unpaired t-test, *P< 0.05 compared to naïve tissue

DEGs on day 3 play a role in axon transport, immunity and neuronal development

Of the 137 up-regulated DEGs in the ganglia 3 DPI, several mapped to gene ontology (GO) terms associated with filament movement (Table 3.2). The 2 most significantly up-regulated genes were subunits C and T of the troponin complex (*TNNC*, FC=272 and *TNNT*, FC=226), which plays a role in intra-axonal movements in rat dorsal root ganglia (320). Additional genes that were highly up-regulated include myosin essential light chain (*MYL3*, FC 44), which plays a role in synaptic plasticity (321), and Tetranectin (*CLEC3B*, FC 24), a glycoprotein that regulates proteolytic processes in neurons and dendrites (322). In addition, a number of innate immune genes were up-regulated at 3DPI (Fig. 3.8A), most notably, several interferon-induced genes that play a critical role in the antiviral immune response (323) such as *MXA* (FC 7, confirmed by qRT-PCR; Fig. 3.6D) (324); chemokine ligand 1(*CCL1*, FC 6), secreted by activated T cells to recruit monocytes (325)); and bone marrow stromal cell antigen 2 (*BST2*, FC 5), a restriction factor that interferes with the release of enveloped viruses, including HSV2 (confirmed by qRT-PCR; Fig. 3.6E) (326)).

Almost half of the 187 down-regulated DEGs at 3 DPI, mapped to GO terms associated with transport and localization (Table 2). The most down-regulated genes amongst these DEGs were myelin associated oligodendrocyte basic protein (*MOBP*, FC 41, involved in myelin formation (327)), ATP-binding cassette subfamily A member 2 (*ABCA2*, FC 13, regulates transmembrane lipid transport in neural tissues (328)), myelin associated glycoprotein (*MAG*, FC 10, important for myelination and maintaining the axon-Schwann arrangement (329)), and sodium channel voltage-gated type VII alpha subunit (*SCN7A*, FC 7, regulates sodium homeostasis in neural cells (330)).

GO Process	# of Genes	-log pValue
Day 3 Up		
muscle filament sliding	13	14.53
actin-myosin filament sliding	13	14.53
muscle contraction	22	14.5
actin-mediated cell contraction	13	13.38
muscle system process	22	12.79
actin filament-based movement	13	11.69
Striated muscle contraction	12	8.44
heart process	10	7.64
regulation of ATP activity	8	6.07
Regulation of muscle contraction	12	5.98
Day 3 Down		
localization	75	3.21
regulation of synaptic plasticity	11	3.21
transport	64	3.21
establishment of localization	65	3.21
anion transport	18	2.96
ion transport	31	2.92
developmental process	82	2.85
single-organism developmental process	81	2.74
single-organism transport	52	2.47
endocytosis	17	2.46
Day 7 Up		
response to virus	23	5.188
defense response to virus	17	5.188
nucleobase-containing compound metabolic process	125	5.09
nucleic acid metabolic process	107	5.05
smooth muscle metabolic process	11	4.77
skeletal myofibril assembly	6	4.76
cellular nitrogen compound metabolic process	130	4.76
heterocycle metabolic process	125	4.47
RNA metabolic process	92	4.41
cellular aromatic compound metabolic process	125	4.41
Day 7 Down		
nervous system development	155	20.63
neurogenesis	111	14.38
system development	206	12.66
generation of neurons	102	12.16
anatomical structure development	219	10.38
regulation of signaling	149	10.38
ensheathment of neurons	23	10.38
axon ensheathment	23	10.38
regulation of cell communication	149	10.38
multicellular organismal development	216	9.61

GO Process	# of Genes	-log pValue
Day 10 Down		
nervous system development	120	10.49
regulation of cellular component organization	101	10.49
regulation of signaling	134	9.38
regulation of cell communication	133	9.16
system development	176	9.16
negative regulation of cellular process	156	8.27
neurogenesis	87	8.15
multicellular organismal development	190	7.96
negative regulation of cellular component organization	43	7.96
negative regulation of biological process	163	7.32
Day 14 Down		
regulation of signaling	132	9.84
regulation of cell communication	132	9.84
regulation of signal transduction	114	7.32
nervous system development	106	7.08
phosphate-containing compound metabolic process	107	6.48
phosphorylation	63	6.42
phosphorus metabolic process	108	6.42
intracellular signal transduction	79	5.97
epidermal growth factor receptor signalling pathway	22	5.81
ERBB signaling pathway	22	5.79
Day 100 Up		
cellular component organization or biogenesis	82	8.4
cellular component organization or biogenesis	79	7.73
organelle organization	53	7.44
cell division	22	6.36
cell cycle	32	5.97
microtubule-based process	18	5.94
RNA spicing	14	5.53
nucleic acid metabolic process	63	5.4
RNA metabolic process	55	5.02
mitotic nuclear division	13	4.92
Day 100 Down		
nervous system development	194	30.15
localization	293	26.92
regulation of cellular component organization	150	22.31
establishment of localization	246	22.13
neurogenesis	138	21.55
single-organism metabolic process	281	21.16
transport	239	21.05
protein localization	135	20.14
cellular localization	157	20
system development	259	19.85

Table 3.2 Ten most statistically significant GO terms to which DEGs enriched at each time point.

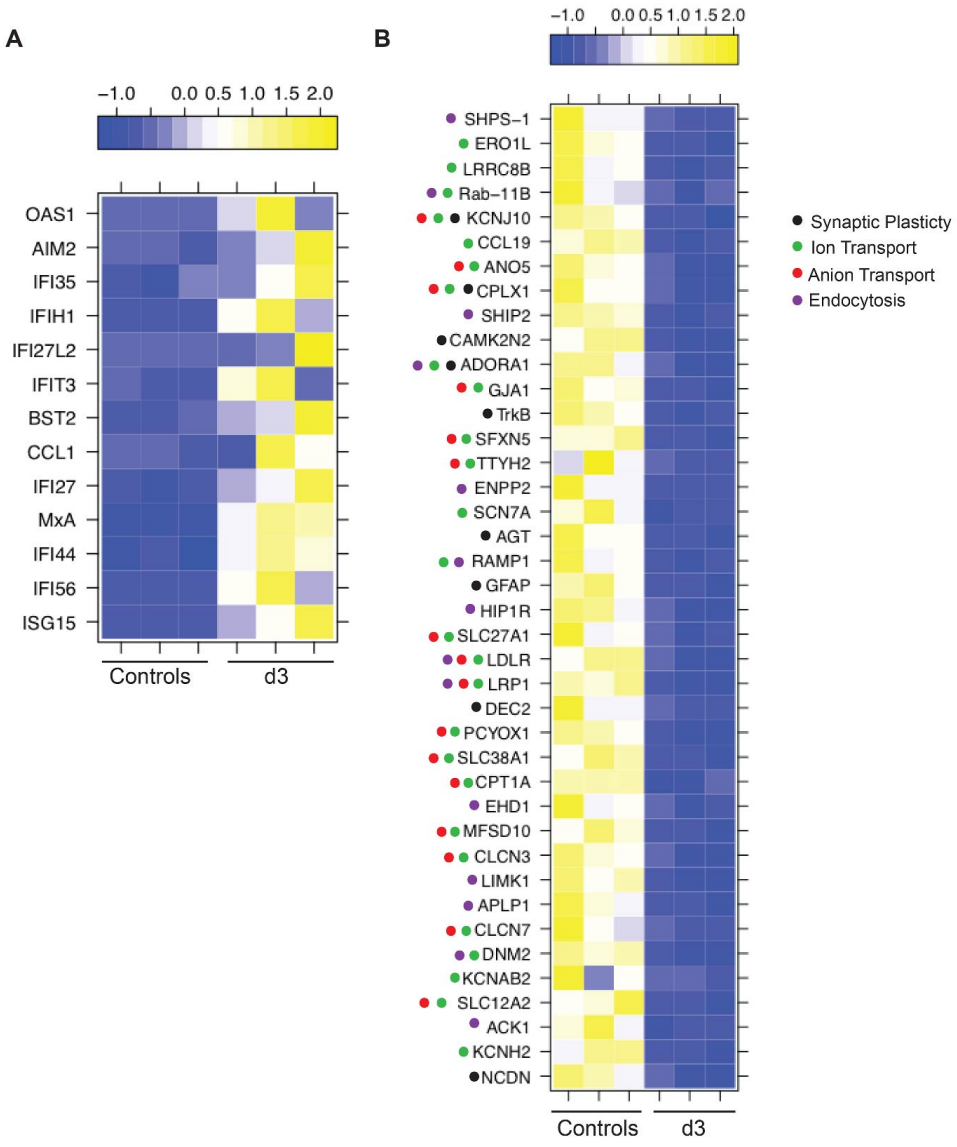

Figure 3.8 DEGs at 3 DPI play a role in axon transport, immunity and neuronal development. (A) Heat map of the immune genes up-regulated 3 DPI. (B) Heat map of the down-regulated DEGs that mapped to the GO processes "regulation of synaptic plasticity", "ion transport", "anion transport" and "endocytosis".

The most down-regulated gene amongst the 9 DEGs that mapped to the GO term "regulation of synaptic plasticity" (Fig. 3.8B) was *GFAP* (FC 43), one of the 17 genes that remained down-regulated throughout infection. Other notable DEGs that mapped to this GO term are Calcium/calmodulin independent protein kinase II inhibitor 2 (*CAMK2N2*, FC 6, regulates neuronal synaptic plasticity through phosphorylation of glutamate receptors (331)), helix-loop-helix member e41 (*BHLHE41*, FC 6, a transcriptional repressor suppressed by axonal injury (332)), Synaptoporin (*SYNPR*, FC4, synaptic vesicle component (333), confirmed by qRT PCR (Fig. 3.6F)), and angiotensinogen (*AGT*, FC 4, regulates salt uptake by astrocytes and neurons (334)). DEGs that mapped to both GO terms "ion transport" and "anion transport" (Fig. 3.8B), include fatty acid transport protein (*SLC27A1*, FC 5) (335); solute carrier family 38 member 1 (*SLC38A1*, FC 4, a glutamine transporter in the CNS (336)); Complexin 1 (*CPLX1*, FC 4, a regulator of synaptic vesicle exocytosis); and sideroflexin-5 (*SFXN5*, FC 4, involved in iron transport in the brain (337)). DEGs that mapped to "endocytosis" (Fig. 3.8B) are known to regulate phagocytosis (e.g. *DNM2*, FC 7; and signal-regulatory protein alpha (*SHPS-1*), FC 5) and chemotaxis (e.g. ectonucleotide pyrophosphatase/ phosphodiesterase 2 (*ENPP2*, FC 6)) by macrophages (338-340).

DEGs on 7 DPI play a role in antiviral immunity and neuron development

"Response to virus" and "defense response to virus" were the most significant GO terms to which DEGs up-regulated 7 DPI mapped (Table 3.2 and Fig. 3.9A). Five of these genes were also up-regulated at 3 DPI: *ISG15*, *IFI44*, *MxA*, *RIG-G*, and *MDA-5*. The 5 most up-regulated genes at 7DPI were: *ISG15* (FC 16), *IFI56* (FC 12), *IFI44-like* (IF44L, FC 9), guanylate binding protein 1 and 3 (*GBP1* and *GBP3*, FC 8), and *IFI44* (FC 7). These genes are induced by a type 1 IFN response and block viral replication (323). Other immune genes that were up-regulated but did

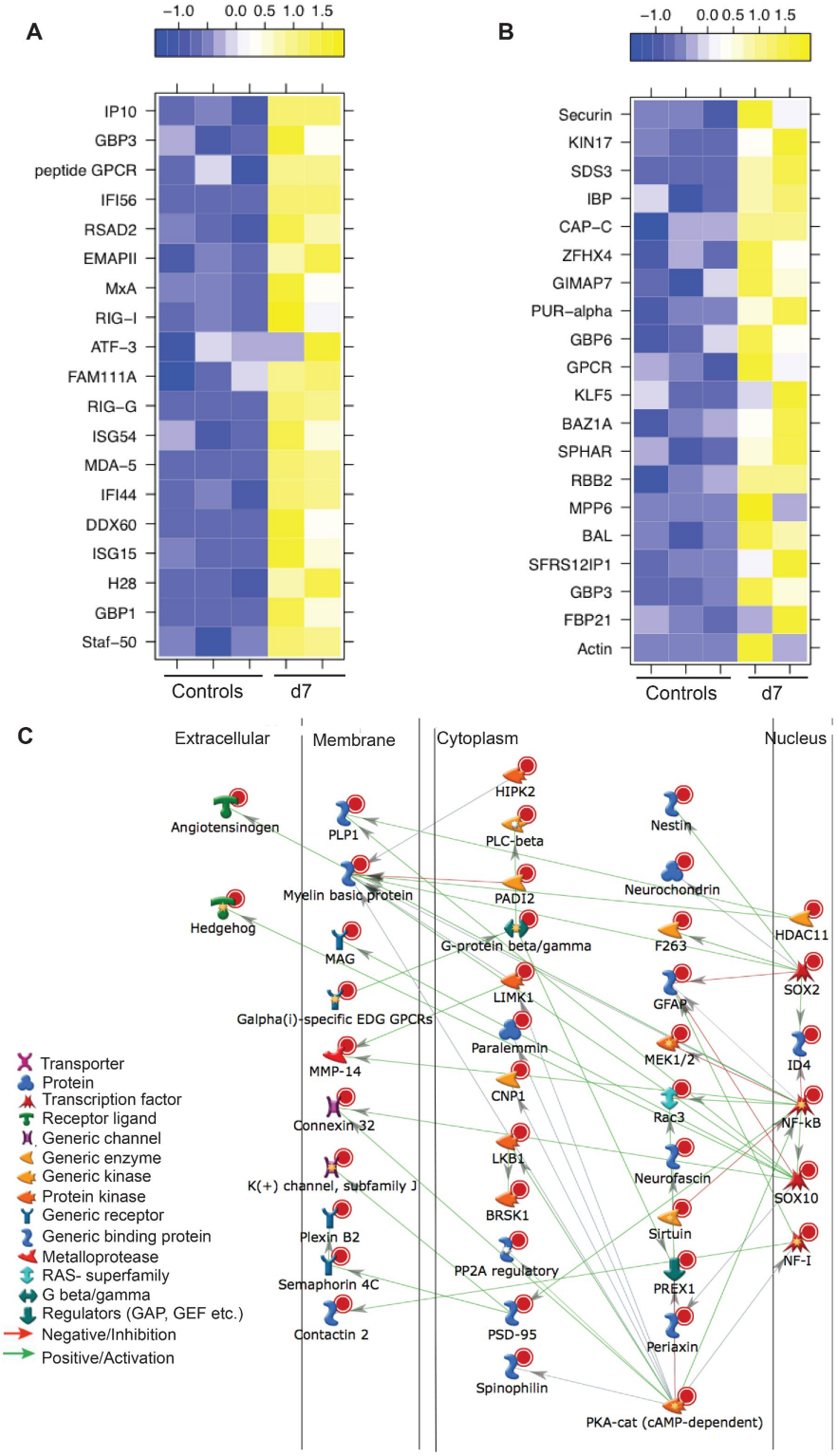
A
−1.0 0.0 0.5 1.0 1.5
IP10
GBP3
peptide GPCR
IFI56
RSAD2
EMAPII
MxA
RIG−I
ATF−3
FAM111A
RIG−G
ISG54
MDA−5
IFI44
DDX60
ISG15
H28
GBP1
Staf−50
Controls
d7
B
−1.0 0.0 0.5 1.0 1.5
Securin
KIN17
SDS3
IBP
CAP−C
ZFHX4
GIMAP7
PUR−alpha
GBP6
GPCR
KLF5
BAZ1A
SPHAR
RBB2
MPP6
BAL
SFRS12IP1
GBP3
FBP21
Actin
Controls
d7
C
Extracellular
Membrane
Cytoplasm
Nucleus
Angiotensinogen
Hedgehog
PLP1
Myelin basic protein
MAG
Galpha(i)-specific EDG GPCRs
MMP-14
Connexin 32
K(+) channel, subfamily J
Plexin B2
Semaphorin 4C
Contactin 2
HIPK2
PLC-beta
PAD12
G-protein beta/gamma
LIMK1
Paralemmin
CNP1
LKB1
BRSK1
PP2A regulatory
PSD-95
Spinophilin
Nestin
Neurochondrin
F263
GFAP
MEK1/2
Rac3
Neurofascin
Sirtuin
PREX1
Periaxin
PKA-cat (cAMP-dependent)
HDAC11
SOX2
ID4
NF-kB
SOX10
NF-I
Transporter
Protein
Transcription factor
Receptor ligand
Generic channel
Generic enzyme
Generic kinase
Protein kinase
Generic receptor
Generic binding protein
Metalloprotease
RAS- superfamily
G beta/gamma
Regulators (GAP, GEF etc.)
Negative/Inhibition
Positive/Activation

(Previous Page) Figure 3.9 DEGs at 7 DPI play a role in antiviral immunity and neuronal development. (A) Heat map of the up-regulated DEGs that mapped to the GO process "response to virus" and (B) the 20 most up-regulated DEGs that mapped to GO processes involved with nucleic acid metabolism. (C) Network image showing direct interaction between the down-regulated DEGs that mapped to the GO process "nervous system development".

not map to these GO terms were C-X-C motif chemokine 10 (*CXCL10*, FC 7), a chemokine that binds to CXCR3 to induce monocyte, NK, and activates T cell migration to sites of infection (341)); chemokine ligand 8 (*CCL8*, FC 6), primarily produced by monocytes and may be involved in neurodegeneration (342); tumor necrosis factor ligand superfamily member 10 (*TNSF10*, FC 4), *AIM2* (FC 4) and *IFI27* (FC 4), which induce apoptosis of viral infected cells (343-345); and monocyte to macrophage differentiation protein (*MMD*; FC 3) (345). Up-regulated DEGs that mapped to the remaining 8 GO terms were associated with nucleic acid metabolism (Fig. 3.9B) and play a role in splicing (e.g. splicing factor arginine/serine rich 12 (*SFRS12*, FC 6) and formin binding protein 21 (*FBP21*, FC 9) (346, 347); or anti-viral defense (e.g. guanylate binding protein 3 and 6 (*GBP3* and *GBP6*, FC 3 and 5), which repress viral polymerases (348).

DEGs down-regulated 7 DPI mapped to GO terms associated with neuron development and function (Table 3.2). Network analysis of 155 DEGs that mapped to the GO term "nervous system development showed that 41 are regulated by transcription factors important for nervous system function: nuclear factor I/X (*NF1*, FC 4), sex determining region Y-box 2 and 10 (*SOX 2* and *SOX10*, FC 3), and nuclear factor kappa-light-chain-enhancer of activated B cells (*NFkb*, FC 4) (349-351) (Fig. 3.9C). The most down-regulated gene in this group was *GFAP* (FC 41), while other DEGs play an important role in myelination such as *MAG* (FC 38), *MOBP* (FC 24), plasmolipin (*PLLP*, FC 23), claudin-11 (*CLDN11*, FC 14), *PAQR6* (FC 13), myelin basic protein (*MBP*, FC 12), fatty acid 2 –hydroxylase (*FA2H*, FC 10), and gap junction protein beta 1 (*GJP1*, FC 8) (329, 352-355). Other highly down-regulated genes include *ABCA2* (FC 16), which was also significantly down-regulated at 3 DPI and the lipid-anchored membrane paralemmin (*PALM*, FC 8), which regulates neuron cell shape and motility (356). Some of the most down-regulated

DEGs that mapped to these GO terms were also detected at 3 DPI, notably *GFAP*, *MAG*, *MOBP* and *CLDN11*. Other down-regulated DEGs play a role in the maintenance of the blood-brain barrier such as matrix-remodeling associated 8 (*Mxra8*; FC 10), and Vasohibin (*VASH1*, FC 9) (357, 358). Interestingly, T-cell differentiation protein (*MAL*, FC 10), which is involved in T cell signal transduction was also down-regulated (359).

DEGS at 10 DPI play a role in neuronal development

The 5 most up-regulated DEGs at 10 DPI were proteoglycan 4 (*PRG4*, FC 15), coiled-coil domain containing 80 (*CCDC8*, FC 8), small nucleolar RNA c/d box 112 (*SNORD112*, FC 8), s-phase response (*SPHAR*, FC 8), actin (FC 7) and translocation protein 1 (*SEC62*, FC3) (confirmed by qRT-PCR) (Fig. 3.6G). *PRG4* is one of the genes that remained up-regulated throughout acute infection while the other genes play a role in DNA replication (*CCDC80* (360) and *SPHAR* (361)), translation (*SNORD112* (362)), axon elongation (Actin (363)) and protein transport (*SEC62* (364)).

Amongst the 479 DEGs down-regulated 10 DPI, 120 DEGs mapped to "nervous system development" and "neurogenesis" (Table 3.2). In addition to *GFAP*, which was the most down regulated gene (FC 75), other notable DEGs mapping to these GO terms include Periaxin (*PRX*, FC 20, important for the ensheathment of neurons and axons (365)); *CPLX1* (FC 16, regulates synaptic vesicle exocytosis); and proprotein convertase subtilisin/kexin type 1 inhibitor (*ProSAAS*;FC 17, neural tissue inhibitor of prohormone convertase 1, which is involved in insulin synthesis (366)).

Of 176 DEGs that mapped to GO term "system development", 60 directly interact with each other through transcription factors *SOX2* (FC 8), *SOX10* (FC 6) and transcription intermediate factor 1 beta (*TIF1-beta*; FC 6) (Fig. 3.10A). Interestingly, TIF1-beta, which associates with the KRAB domain of zinc finger proteins, has been reported to play a critical role in the latency of another herpesvirus, human cytomegalovirus (367). Several of the DEGs that enriched to the GO term "regulation of cellular processes" (Fig. 3.10B) play an important role in neuron survival such as hepatic and glial cell adhesion molecule (*HEPACAM*, FC 11, an axon protein that plays a role in neuron motility (368)); mitogen activated protein kinase 8 interacting protein 1 (*JIP1*, FC 10, part of the MAP-kinase signal transduction pathway in neurons (369)); FK056-binding protein 8 (*FKBP8*, FC 9, inhibits programmed cell death in neurons (370)); and *BM88* antigen (FC 10, involved in neuron differentiation (371)).

DEGs down-regulated at 14 DPI play a role in neuron signaling and development

The most up-regulated DEGs 14 DPI are *PRG4* (FC 10) and *FILIP1* (FC 7), important for myelination and neuron migration; fibroblast growth factor 7 (*FGF7*, FC 7), which regulates balance between excitatory and inhibitory synapse signaling in neurons (372), and NIMA-related kinase 1 (*NEK1*, FC 5), which plays a role in axon development (373). The 509 DEGs down-regulated 14 DPI, enriched to GO terms associated with signaling and nervous system development (Table 3.2). Thirty of the DEGs enriching to the GO term "phosphorus metabolic process" have direct interactions (Fig. 3.10C) and are regulated by transcription factors *AP-1* (FC 3), heat shock factor protein 1 (*HSF1*, FC 4) and binding protein *TIF1-beta* (FC 5). Casein kinase 1 gamma 2 (*CSNK1G2*, FC 11) was among the most down-regulated genes in these GO terms and is critical in the regulation of glutamatergic synaptic transmission in the brain (374) as well as neuronal gene expression through its interaction with eukaryotic elongation factor 2 kinase

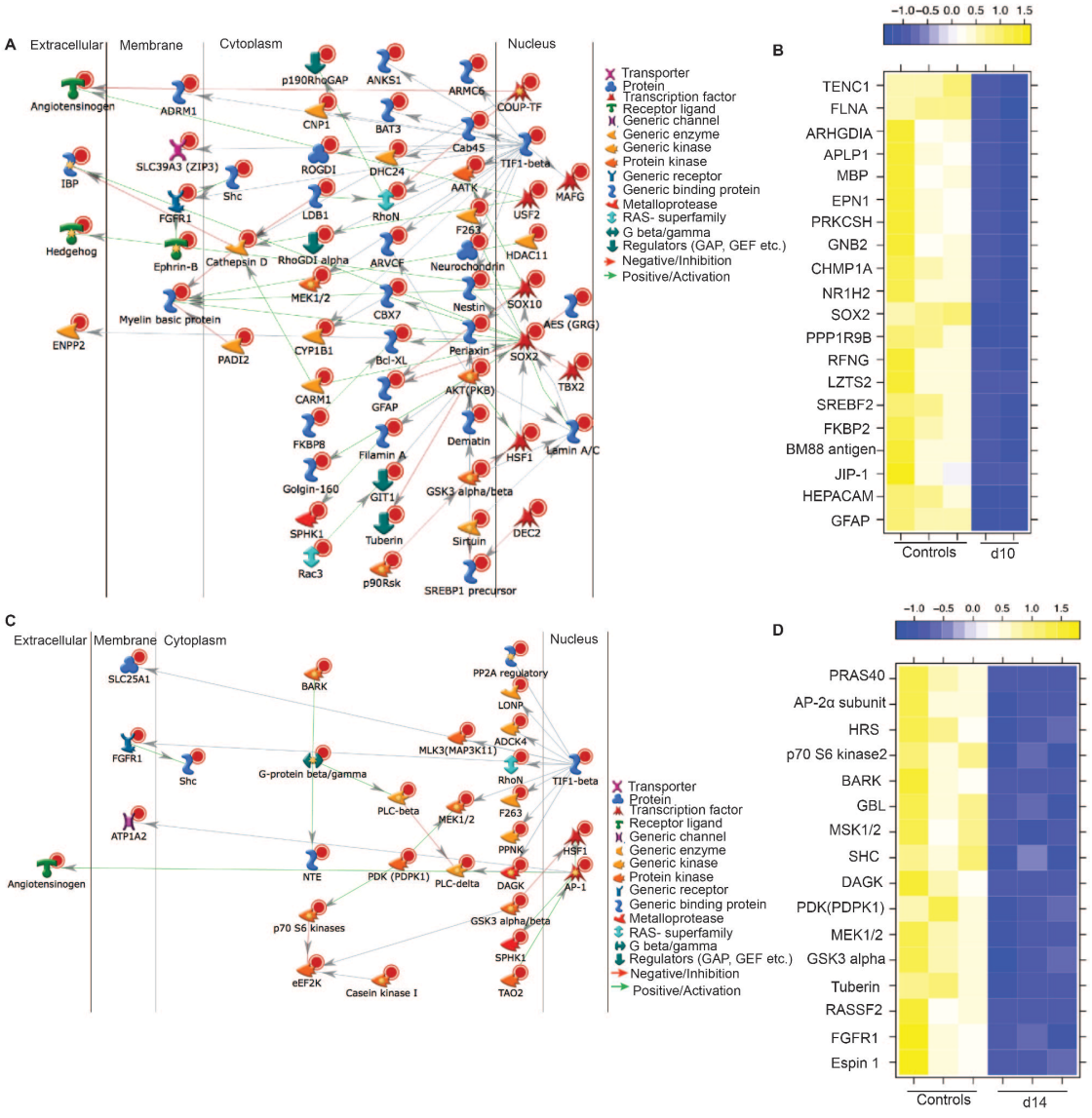

Figure 3.10 DEGs at 10 DPI and 14 DPI are associated with neuronal development.
(A) Network image of DEGs down-regulated 10 DPI that mapped to the GO process "multicellular organismal development" and directly interact. (B) Heat map of the 20 most down-regulated genes 10 DPI mapping to the GO process "negative regulation of biological process". (C) Network image of DEGs down-regulated 14 DPI that mapped to the GO process "phosphorus metabolic process" and directly interact. (D) Heat map of DEGs down-regulated 14 DPI mapping to the GO process "ERBB signaling pathway".

(*eEF2K*, FC 3) (375). Other interesting DEGs that were associated with nervous system development include secreted frizzled-related protein 2 (*SFRP2*; FC 35, important in neuron development (376) C-C motif chemokine ligand 19 (*CCL19*; FC 29, important for lymphocyte recirculation and homing to lymphoid tissue (377)), and aquaporin 4 (*AQP4*, FC 13, a water channel expressed in astrocytes (378). The most down-regulated DEGs that mapped to GO term "nervous system development" include *GFAP* (FC 59) *SFRP2*, (FC 35), *MOBP* (FC 26), *CPLX1* (FC 18) and patatin-like phospholipase domain containing 2 (*PNPLA2*, FC 14). *PNPLA2* plays a role in the interactions between neurons and glial cells (379).

In addition, we also saw several down-regulated DEGs known to regulate apoptotic process in neurons; notably *NRBP2* (FC 11) (380), proline rich Akt substrate 40 (*PRAS40*, FC 8) (381), mitogen-activated protein kinase 11 (*MAP3K11*, FC 5) (382), homeodomain interacting protein kinase 2 (HIPK2, FC 6) (383), and mannosylinositol phosphorylceramide (*BCL21*; FC 3) (384). Finally, 16 down-regulated DEGs mapped to the GO terms "ERBB (Erythroblastic Leukemia Viral Oncogene Homolog) signaling pathway" (Fig. 3.10D). Insufficient ERBB signaling is associated with the development of neurodegenerative diseases (385, 386). Some of the most significantly down-regulated genes found in these two GO terms include diacylglycerol kinase1 (*DAGK1*, FC 6, plays a role in myelination and neuronal plasticity (387)), Epsin1 (*EPN1*, FC 6, contributes to clathrin-coated pit formation and endocytosis (388)), and RAS association domain-containing protein 2 (*RASSF2*; FC 5, a tumor suppressor in gliomas (389)).

SVV infection results in a sustained down-regulation of genes important for nervous system development

Up-regulated DEGs at 100 DPI played a role in cell cycle progression (Table 3.2). The 20 most up-regulated DEGs enriched to cellular component organization: intraflagellar transport 74 (*IFT74*, FC 8), important for survival and differentiation of sensory neurons (390); thyroid hormone receptor interactor 11 (*TRIP11*, FC 7), important for maintenance of Golgi structure and proteins transport (391) and chromodomain helicase DNA binding protein 9 (*PRIC320*, FC 6), controls the expression of genes involved in energy homeostasis and cell cycle (392) (Fig. 3.11A). Interestingly, *MBP* (FC 4), which was significantly down-regulated during acute infection, is up-regulated at latency (Fig. 3.11A). DEGs that mapped to GO terms "nucleic acid metabolism" are involved in the regulation of gene expression, such as bromodomain adjacent to zinc finger domain protein 2B (*BAZ2B*; FC 6), zinc finger homeobox 4 (*ZFHX4*; FC 4), zinc finger protein 292 (*ZNF292*; FC 4), polymerase RNA III polypeptide G (*POLR3G*; FC 4), and TWIST neighbor protein (*TWISTNB*; FC 4)(393) (Table 3.2).

Interestingly, 636 DEGs remained down-regulated genes 100 DPI, with the majority (456 DEGs) enriching to GO terms associated with the nervous system and cellular localization (Table 3.2). The most significantly down-regulated DEGs in these GO terms play a role in immunity (myeloid differentiation marker gene, *MYADM*, FC 6)(394) and serpin peptidase inhibitor (*SERPIN*, FC 9, an inhibitor of the complement classical pathway(395)); pain (purinergic receptor, *P2X3*, FC 7)(396); and cell division (sushi domain containing 2, *SUSD2*, FC 9)(397) (Fig. 3.11B). Several of the 20 most down-regulated genes enriched to "nervous system development" and play a role in astrocyte function e.g. chitinase 3 like protein 1 (*CHI3L*, FC 17) and *GFAP* (FC 6) (398);

inflammation e.g. hemoglobulin alpha 2 (*HBA2*, FC 13) (399); neurite growth e.g. amyloid beta (A4) precursor-like protein 1 (*APLP1*, FC 10) (confirmed by qRT-PCR; Fig. 3.6H) and neurochondrin (*NCDN*, FC 8) (400, 401); synaptic plasticity e.g. copine 6 (*CPNE6*, FC 7) (402); and myelination, e.g. *MAG* (FC 7) and *CLDN11* (FC 6) (Fig. 3.11C). Interestingly, a secondary functional enrichment analysis for diseases by biomarkers using the down regulated genes at 100 DPI showed enrichment for processes involved with neurodegeneration and mental health disease (Fig. 3.11D).

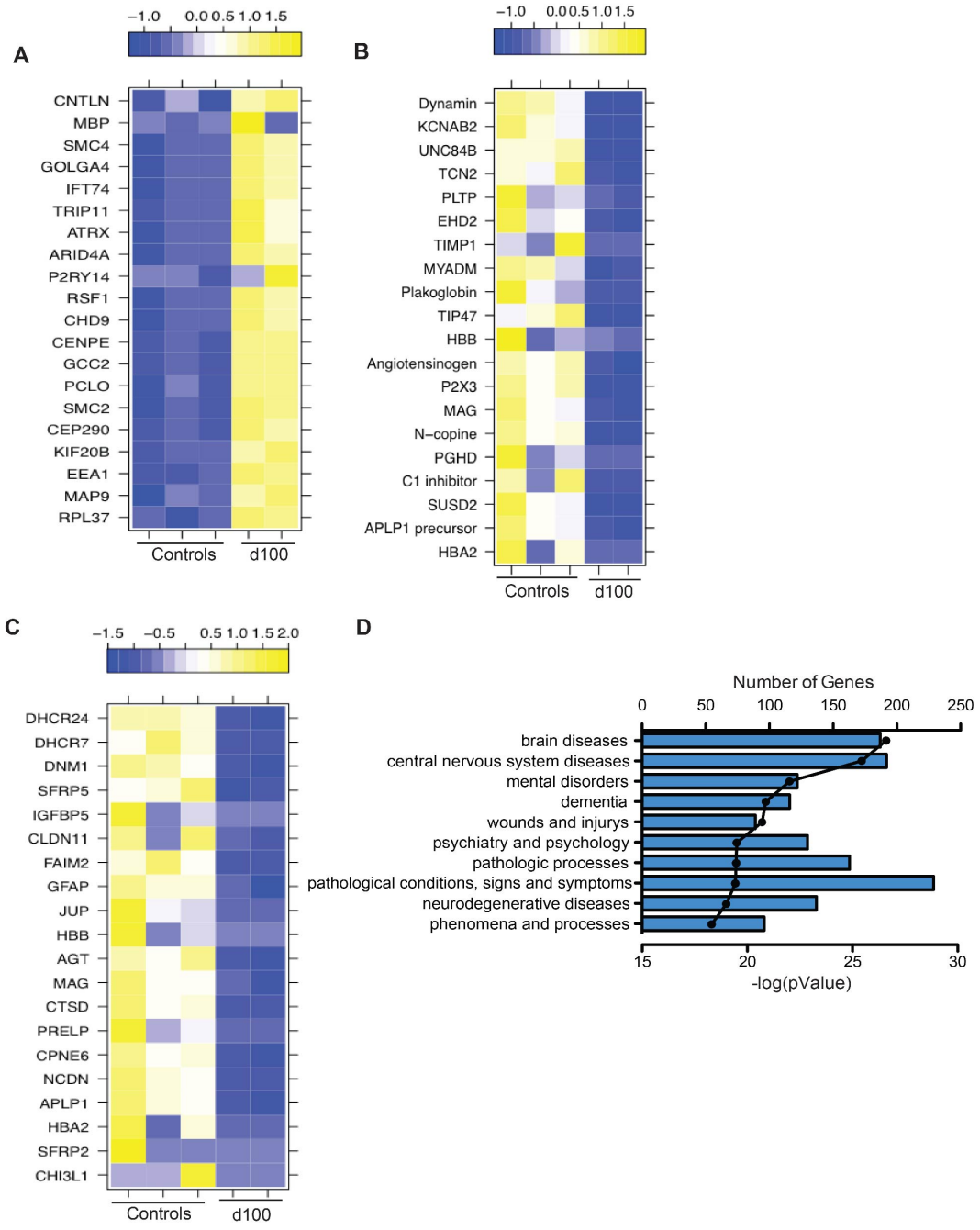

Figure 3.11 DEGS in latently infected ganglia tissue (100 DPI) play a role in the development of the nervous system and are associated with neurological diseases.
(A) Heat map of the 20 most up-regulated genes that mapped to the GO process "cellular component organization or biogenesis". (B) Heat map of the 20 most down-regulated genes that mapped to the GO process "localization" and (C) "system development". (D) The 10 most statistically significant diseases (by biomarkers) to which down-regulated DEGs mapped.

DISCUSSION

In this study, we leveraged a rhesus macaque model of intrabronchial SVV infection to gain a better insight into host-viral interactions during acute and latent VZV infection in the ganglia. We analyzed viral loads, viral transcriptome, and host transcriptome in sensory ganglia collected from naïve animals and on days 3, 7, 10, 14 and 100 post-SVV infection. Our analysis shows that SVV DNA is detected in the trigeminal ganglia as early as 3 DPI before the appearance of the rash (typically seen 7-10 DPI). These results are in agreement with previous studies that reported the presence of SVV DNA in the ganglia before the appearance of rash in intratracheally infected AGMs, the detection of VZV DNA in the ganglia of immunocompromised children who died from varicella before the appearance of the rash (193, 214), and the ability of the Oka vaccine strain to establish latency in sensory ganglia in the absence of varicella rash (115). Given that SVV rapidly reaches the ganglia before the appearance of vesicular rash and that we cannot detect SVV DNA in non-lesioned skin, we believe that SVV is most likely transported to the ganglia via the hematogenous route as has been previously suggested for VZV (35). DNA viral loads in the DRG were higher 7 DPI compared to 3 DPI, suggesting additional seeding via axonal transport (rash is observed 7 DPI) and/or as a result of viral replication detected 3 DPI in the ganglia.

In addition, our data suggest that T cells play a role in varicella virus dissemination since memory T cells are detected in the ganglia 3 DPI at the same time as viral DNA. Our data also suggest that this is a selective recruiting of T cells since no B cells were detected at any time point. It is highly unlikely that these T cells are SVV-specific given that SVV-specific T cell responses are not detected in the blood or BAL until 7 DPI in this animal model (217, 221, 222). Similarly, VZV-specific T cells are also not detected in the blood until 3 days post rash (approximately 14 days

after exposure) in children during primary infection (70). Rather, we hypothesize that these T cells are transporting SVV to the ganglia. This hypothesis is in line with data from previous studies that have suggested an initial role for T cells in VZV dissemination. In vitro experiments showed an increased propensity of VZV to infect tonsillar memory CD4 T cells (37, 194) and intravenous injection of VZV-infected CD4 T cells and not fibroblasts results in a rash on human skin explant in SCID-hu mice (84). In this study, we examined ganglia at earlier time points than previous similar studies (223, 224) and were able to show T cell infiltration as early as 3 DPI and before the onset of varicella. Although we were not able to determine whether T cells isolated 3 DPI from the ganglia were infected with SVV, we were able to show that BAL CD4 and CD8 T cells isolated 3 DPI from the same animals harbor SVV DNA and viral transcripts. Collectively, these data suggest that T cells play a critical role in SVV dissemination and may potentially support viral replication.

Additionally, given the intrabronchial challenge route we used, SVV may be reaching the ganglia at this early time point post infection by traveling directly from the lung (site of infection) to the ganglia through the vagus nerve as observed in mice infected intranasally with influenza (403) and intraperitoneally with HSV (404). We also report for the first time that SVV transcripts are detected 3 DPI in the ganglia. Since we did not measure infectious virus, these transcripts could be the result of abortive replication either in neurons or the surrounding T cells. This issue will have to be clarified in future studies using ganglionic explants. SVV transcription in the ganglia ceased 7 DPI, at in which point we observed low level gene expression from *ORF18*, *ORF34* and *ORF35*. This is followed by a quiescent period before re-expression of SVV *ORF61* (viral transactivator) 100 DPI, which suggests additional regulatory mechanisms controlling the transcription of *ORF61*. This hypothesis is supported by the fact that *ORF61* transcripts detected

during latency are anti-sense whereas those detected during acute/lytic infection are sense (311). Similar to our observations, HSV-1 replication was also only seen at 4 DPI in the ganglia of mice inoculated through the snout or the cornea (405). Our results differ from previous studies that showed that VZV replication of directly inoculated fetal xenografts in SCID mice is sustained until 14 DPI (193). This discrepancy could be due to the lack of adaptive immunity in the SCID mouse, the immature nature of fetal DRG, and/or the direct inoculation of the virus into xenografts that bypasses host restriction factors.

Viral gene expression at 3 DPI was accompanied by several significant changes in host gene expression. The most highly up-regulated genes were involved in the troponin complex. It is believed that the troponin complex may control intra-axonal movement in neurons and SVV might be using this mechanism for neuronal spread as previously described for HSV (320). Elevated troponin levels in the blood are also often seen in patients during an acute stroke (406, 407). Interestingly, both primary VZV infection and reactivation have been associated with an increased risk of stroke after infection (408, 409). In addition, genes associated with synaptic plasticity and ion transport were down-regulated 3 DPI, indicative of potentially impaired neuronal signal transduction.

Several, IFN stimulated genes (ISG) were also highly up-regulated 3 DPI (*OAS1*, I*SG15*, *MXA*). This innate immune response is likely mediated by the satellite glial cells (SGCs), which share phenotypic and functional characteristics with dendritic cells and macrophages (410). Importantly, SGC express toll-like receptor (TLR) 9 (411), an intracellular sensor of double stranded DNA viruses such as SVV and VZV (412). Therefore, recognition of SVV viral DNA by TLR-9 may result in the induction of a type 1 interferon response. Type 1 interferons play a

critical role in the host defense against VZV since treatment of immunocompromised patients with IFNα within the first 72 hours after the appearance of the rash reduced the number of lesions in children with cancer (69). Moreover, IFNα plays an important role in controlling VZV spread in the skin of the SCID mouse model (84). Interestingly, we did not detect interferon α/β transcripts. This may be due to the small number of infected cells and the ability for SVV to suppress interferon expression within those infected cells (227, 228), which could have diluted the strength of the IFN signal, especially since we are using total ganglia RNA. IFN stimulated genes could potentially be up-regulated within infiltrating innate immune cells. Although we detected increased expression of CD68 in ganglia at 3 DPI, it should be noted that CD68 can also be expressed by SGCs (410). Unfortunately, due to limited number of cells recovered after ganglia digestion, we were unable to quantify other immune cells that may have infiltrated the ganglia during acute infection using flow cytometry. Expression of ISG and other innate immune genes remained increased at 7 DPI and coincided with the establishment of latency.

As previously reported for ganglia explants experimentally infected with VZV (193) and ganglia collected from acutely infected AGMs (225), we saw an up-regulation of *CXCL10* in the ganglia at 7 DPI. CXCL10 is a chemokine that can be produced by neurons, astrocytes and oligodendrocytes (413), binds the receptor CXCR3 on memory T cells and NK cells to induce their migration to the site of infection (414). Indeed the NK specific transcript, natural killer cell triggering receptor (*NKTR*), was up-regulated 7 and 10 DPI (FC = 3 and 4 respectively). NK cells have also been shown to infiltrate the ganglia in patients who have had herpes zoster a few months prior to death (299). Increased expression of *CXCL10* may contribute to the infiltration of antigen-specific T cells in the ganglia after 7 DPI. However, DEGs associated with T cell effector function (such as IFNγ, granzyme B or CD69) were not detected, possibly due to the low

frequency of SVV-specific T cells in the ganglia. These data differ from a recent study that reported an increase in granzyme B 9 and 21 DPI in the ganglia of SVV-infected AGMs (224). This discrepancy could be due to the fact that in contrast to rhesus macaques, SVV infection in AGMs is often fatal (301). Expression of genes important for macrophage mediated phagocytosis (*DNM2*, *SHIPS*, and *ENPP2*) was reduced 3 and 7 DPI. The reduced expression of genes involved in endocytosis may be due to increased expression of ISGs, several of which inhibit viral uptake through endocytosis as a strategy to stop viral spread (415, 416).

Many of the down-regulated DEGs 7, 10, 14 and 100 DPI, mapped to the GO terms associated with nervous system development. Interestingly, these DEGs remained down-regulated long after virus replication has ended, suggesting that SVV infection of the ganglia results in long-term changes in ganglia transcriptome. Several of these genes were involved in myelination (*MOBP*, *MAG*, *MBP* and *PRG4),* which suggest that SVV may lead to demyelination as has been described for HSV-1 and 2 (417, 418). Genes down-regulated 14 DPI were involved in neuronal apoptosis which may be another strategy SVV utilizes to establish latency in the ganglia. VZV *ORF63* has indeed been shown to inhibit apoptosis in neurons (52). We also report a down-regulation of genes involved in ERBB signaling, a critical pathway for DRG development (419), 14 DPI. As previously reported for VZV-infected human astrocytes (420), expression *GFAP*, which plays a critical role in astrocyte function, remained down-regulated in sensory ganglia of SVV infected macaques until 100 DPI.

A recent study examined gene expression changes in keratinocyte cell lines infected *in vitro* with VZV using RNA-Seq (421), however this study only reported changes in epidermal genes (cytokeratins and desmosomal) and did not discuss changes in the innate immune response to

VZV. An earlier study using microarray studies showed altered gene expression in T cells infected with VZV in vitro and in skin xenografts harvested from VZV infected SCIDhu mice (422). Only 5 DEGs in the skin xenografts were detected in our study. These include *RGS* (G-coupled protein signaling, 3 and 7 DPI), RPS (ribosomal protein, 7 DPI), GAS (apoptosis, 3 and 10 DPI) GADD (growth arrest and DNA damage, 100 DPI) and CHI3L (angiogenesis, 100 DPI). Together with the recent study using keratinocytes (421), these observations strongly suggest that skin cells generate a different response than neuronal cells to varicella virus infection. In contrast, and in line with the fact that T cells infiltrate the ganglia after SVV infection, 31 DEGs were detected in VZV infected T cells and SVV infected ganglia. These include genes such as *TRIP11* (protein transport, up-regulated 7 DPI), S100A11 (cell cycle, down-regulated 3 DPI), *BAZ2B* (transcriptional regulation, up-regulated 7 and 10 DPI) and *APOB* (lipid transport, up-regulated 3 DPI).

In summary, this study is the first to use next generation sequencing of ganglia collected during both acute and latent infection following experimental inoculation of a robust nonhuman primate model of VZV infection to study both host and viral transcriptomes. Although a small number of animals were used in these studies, the outbred nature of rhesus macaques coupled with the stringent bioinformatics approaches provide novel insight into host-pathogen interactions during acute varicella and latent infection. Our data show that SVV reaches the ganglia very quickly after infection, most likely via hematogenous spread within infected T cells. SVV transcription is detected briefly before establishing latency. Cessation of viral transcription correlates with a robust up-regulation of IFN stimulated genes and antiviral innate immune response. Importantly, SVV infection results in significant changes in the expression of genes involved in neurogenesis and nervous system development that persist long after cessation of viral replication. It is possible

that some of these gene changes could in part be mediated by the robust immune response that develops during acute infection. Given the similarities between SVV and VZV, these data enhance our current understanding of the neurological consequences of VZV infection.

CHAPTER 4: Simian Varicella Virus causes robust transcriptional changes in T cells that support viral replication

Nicole Arnold[1] and Ilhem Messaoudi[2*]

[1]Graduate Program in Microbiology, University of California-Riverside, CA, USA

[2]Division of Biomedical Sciences, School of Medicine, University of California-Riverside, Riverside, CA

ABSTRACT

Varicella zoster virus (VZV) causes varicella (chickenpox) during acute infection. Several studies have shown that T cells are early and preferential targets of VZV infection that play a critical role in disseminating VZV in to the skin and ganglia. However, the transcriptional changes that occur in VZV infected T cells remain unclear due to limited access to clinical samples and robust translational animal models. In this study, we used a nonhuman primate model of VZV infection where rhesus macaques are infected with the closely related Simian Varicella Virus (SVV) to provide novel insights into VZV-T cell interactions. RNA sequencing of T cells isolated from lungs of infected rhesus macaques show that SVV alters several cellular processes that may support viral replication and facilitate SVV dissemination. Moreover, our data provides further insight into mechanisms by which SVV is able to evade the host immune system.

INTRODUCTION

Varicella Zoster Virus (VZV) is a highly contagious neurotropic alpha herpes virus that causes varicella (chickenpox) during acute infection. VZV is spread through the inhalation of virus particles or through direct contact with infectious fluid from skin lesions (10, 11). VZV establishes latency in sensory ganglia, from which it can reactivate causing herpes zoster (shingles), a painful disease most commonly affecting the elderly and immunocompromised individuals. Previous studies have shown that T cells are highly susceptible to VZV infection and may play a critical role in its dissemination to the skin and ganglia. Specifically, direct inoculation of fetal thymus/liver implanted under the kidney capsule of SCID-hu mice with VZV-infected fibroblasts results in the infection of CD4+ and CD8+ thymocytes (194). In addition, *in vitro* experiments have shown that VZV has an increased propensity to infect tonsillar CD4 T cells compared to tonsillar CD8 T cells (37). Moreover, co-culture experiments showed that activated tonsillar CD4 T cells with skin homing markers were more likely to be infected with VZV (37). Importantly, human tonsillar CD4 T cells infected *in vitro* with VZV, but not fibroblasts, intravenously injected into SCID-hu mice were able to transport the virus to fetal human skin explant resulting in development of varicella rash (84) and fetal dorsal root ganglia xenografts (193).

Although these studies suggest that T cells play a critical role in VZV pathogenesis, none of these findings have been confirmed using T cells isolated from varicella patients. The strict host tropism of VZV has precluded the development of animal models. An alternative is to use rhesus macaques intra-bronchially infected with the homologous simian varicella virus (SVV), a model that mimics the key characteristics of VZV infection including the development of varicella, a cellular and humoral immune response, the establishment of latency in the sensory ganglia, and

reactivation (216, 217, 300, 423). As described for VZV, we and others have demonstrated that SVV like VZV, primarily infects T cells, which can traffic to the ganglia as early as 3 days post-infection (223, 424). Moreover, we showed that T cells isolated from the broncho-alveolar lavage (BAL) during acute infection supported SVV replication (424). These data firmly established the importance of T cells in SVV pathogenesis making this model ideal for investigating how VZV infection alters T cell behavior and function. In this study, we used this animal model to investigate the transcriptional changes that SVV infection induces within CD4 and CD8 T cells isolated from the BAL during acute infection. Our results show that SVV induces robust transcriptional changes involved with chromatin assembly, translation, the cell cycle and metabolism. In addition, several gene expression changes reveal possible mechanisms by which SVV may evade the host response as well as the T cell response to SVV infection.

METHODS AND MATERIALS

Animals and samples

Samples from seven colony-bred Indian origin Rhesus macaques (*Macaca mulatta,* RM) 3-5 years of age were used in these studies. These animals were previously described in (222). Three of these animals were inoculated intrabronchially with 4×10^5 PFU wild-type SVV as previously described and were euthanized 3, 7 and 10 days post infection (DPI, n=1/time point) (222). Bronchial alveolar lavage (BAL) was collected from all animals to measure viral loads, isolate CD4 and CD8 T cell population for viral loads and transcriptional analyses

Purification of T cells

CD4 and CD8 T cells were isolated from BAL samples using Magnetic Cell Sorting (MACs). BAL cells were first incubated with CD4 microbeads (Miltenyi Biotec, San Diego) for 20 mins at 4°C. Cells were then washed and the cell suspension was applied to the magnetic column to capture CD4 T cells. CD4 negative fraction was then stained with CD8-PE (Beckman Coulter) and incubated with the cells for 20 mins in the dark at 4°C. Cells were then washed and anti-PE beads (Miltenyi Biotec) were added and incubated for 15 mins in the dark at 4°C. Cells were then washed and the cell suspension was applied to a magnetic column to isolate CD8 T cells Cells were then stained with antibodies directed against surface markers: CD4 (Tonbo Biosciences, San Diego, CA) and CD8β (Beckman Coulter, Brea, CA) and then analyzed on the LSRII instrument (Becton, Dickinson and Company, San Jose, CA) and Flowjo software (TreeStar, Ashland, OR) to access purity. All samples used had a purity of >90%.

RNASeq and bioinformatics

RNA was extracted from T cells using the Ambion Purelink RNA Mini Kit extraction kit (Life Technologies, Carsbad, CA). RNA library preparation was done using the New England Biolab (NEB) Next Ultra Direction RNA Prep kit for Illumina (Ipswich, MA). We were unable to generate a library of the CD4 T cells isolated from 7DPI animal. Therefore we have paired CD4/CD8 libraries from the animals euthanized 3 and 10 DPI and only CD8 T cell library from the animal euthanized 7 DPI. DNA libraries were next multiplexed and sequenced on the Illumina NextSeq (Illumina, San Diego, CA) platform at single-ends 75bps. All data analysis steps were performed with the RNA-Seq workflow module of the *systemPiperR* package available on Bioconductor (302, 425). NGS quality reports were generated with the *seeFastq* function defined by the same package. NextSeq reads were mapped with the splice junction aware short read alignment suite Bowtie2/Tophat2 (303, 304) against the *Macaca mulatta* genome sequence downloaded from Ensembl (305). The default parameters of Tophat2 optimized for mammalian genomes were used for the alignments. Raw expression values in form of gene-level read counts were generated with the *summarizeOverlaps* function(306). Only reads that overlapped with exonic regions of genes were counted, reads that mapped to ambiguous regions of exons from overlapping genes were discarded.

Analysis of differentially expressed genes (DEGs) was performed with the GLM method from the *edgeR* package (307, 308). Differentially expressed genes (DEGs) were defined as those with a fold change of ≥2, a false discovery rate (FDR) of ≤0.05 and an average reads per kilobase per million (RPKM) value ≥5. Enrichment analysis of functional annotations was performed to identify significant gene ontology (GO) and Network Processes using MetaCore™ software (GeneGo, Philadelphia, PA).

RESULTS

T cells isolated from SVV infected animals show robust transcriptional changes

We recently reported that SVV primarily infects both CD4 and CD8 T cells in the BAL, which can support viral replication (424). To determine SVV-induced transcriptional changes within T cells, we performed RNA-Seq on infected BAL T cells shown to express viral transcripts (measured through AmpliSeq technology (424)) and uninfected BAL T cells (4 paired CD4/CD8 T cell samples isolated from 4 control animals). A principle performance assay (PCA) indicated that infected and uninfected T cells have distinct transcriptional profiles (Fig. 4.1A). Overall, a total of 1463 (739 up-regulated and 724 down-regulated) differentially expressed genes (DEGs) were detected, 1130 of which (586 up-regulated and 544 down-regulated) were characterized (Fig. 4.1B, Supplemental Dataset 4.1).

Enrichment analysis on the up-regulated and down-regulated genes was performed using Metacore software. Up-regulated DEGs enriched to network processes related to inflammation and cell cycle (Fig. 4.1C) and GO processes related to immunity, metabolism and gene expression (Fig. 4.1D). Down-regulated DEGs enriched to process networks involved with phagocytosis and signaling (Fig. 4.1C) and GO processes involved with intercellular transport and metabolism (Fig. 4.1D).

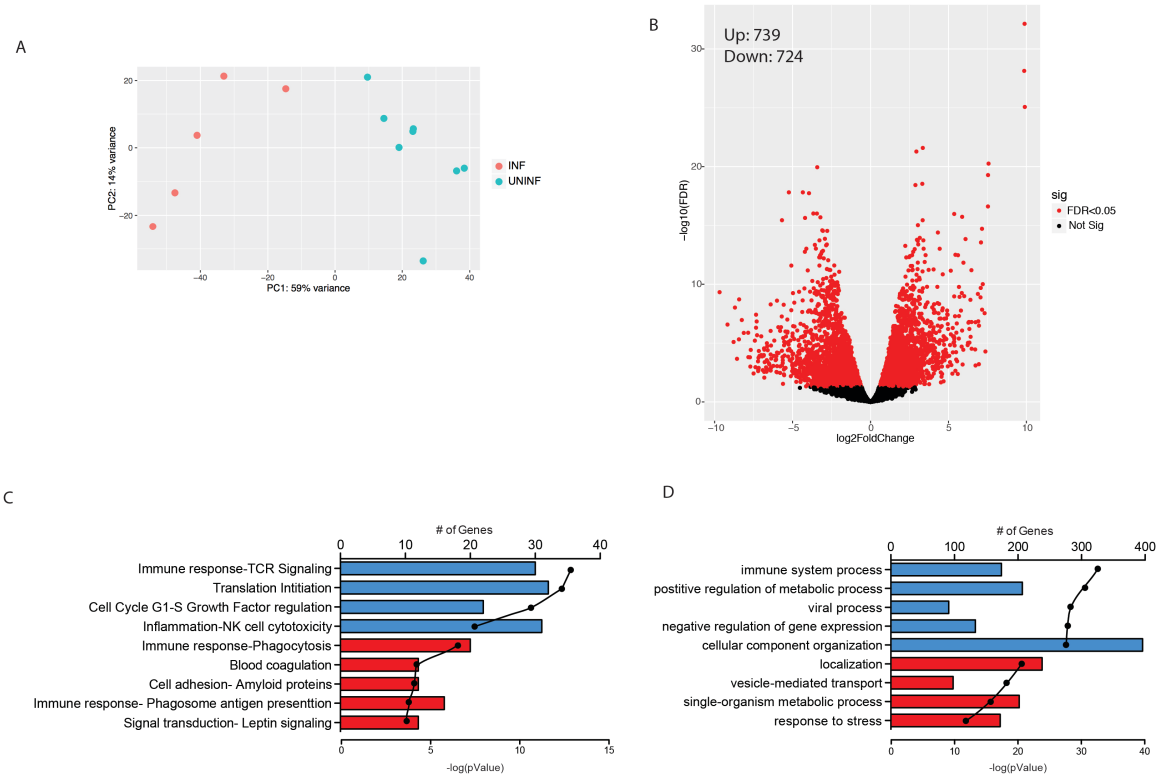

Figure 4.1 SVV causes robust gene expression changes in T cells. (A) PCA plot of samples used for RNA sequencing. (B) Volcano plot representing overall gene expression changes observed in infected T cells. Enrichment analysis of the most statistically significant up-regulated (in blue) and down-regulated (in red) genes by (C) Process Network and (D) GO process. Line represents the –log(p-value) associated with each process.

SVV infection up-regulates cell cycle processes and immune responses

Many of the up-regulated genes were involved with gene regulation, notably chromatin assembly (Fig. 4.2A), such as histone genes: *HIST1H2AJ* (FC13), *HIST1H1B* (FC 11), *HIST2H2AA4* (FC 11), *HIST1H3A* (FC 10) and *H2AFX* (FC 9). These histones play a critical role in DNA packaging into chromatin, and have been shown to support replication of several viruses such as adenoviruses and HSV-1 (426-428). Other DEGs that play a role in chromatin assembly include transcription factors *C-FOS* (FC 4), *JUNB* (FC 6) and *JUND* (FC 5) (429) (Fig. 4.2A).

Thirty-two genes mapped to the network process "translation initiation" (Fig. 4.1C), including several ribosomal protein L (RPL) and ribosomal protein S (RPS) genes, which are important for 60S and 40S ribosomal assembly respectively (Fig. 4.2B) (430). Other genes that mapped to this network process include gene encoding eukaryotic translation initiation factor (EIF) subunits, which play critical roles in ribosome stabilization and the initiation of translation (431) (Fig. 4.2B). Twenty-three genes that play a role in cell cycle regulation mapped to "cell cycle G1-S growth factor regulation" (Fig. 4.1C) such as *E2F4* (FC 2), *CDKN1B* (FC 2) *CFL1* (FC 3), *CALM1* (FC 2) and *PLCG1* (FC 4). Interestingly, several of the genes that mapped to the GO process "negative regulation of gene expression" (Fig. 4.1D), suppress/inhibit different cellular processes such as NFkB signaling (*AES*, FC 5) (432), cell cycle progression (*CHMP1* (FC 4)) (433), RNA polymerase III transcription (*MAF1*, FC 2) (434) and gene expression (*MBD3* FC 4, and *TRIM28*, FC 3) (435, 436). Up–regulated DEGs were also involved

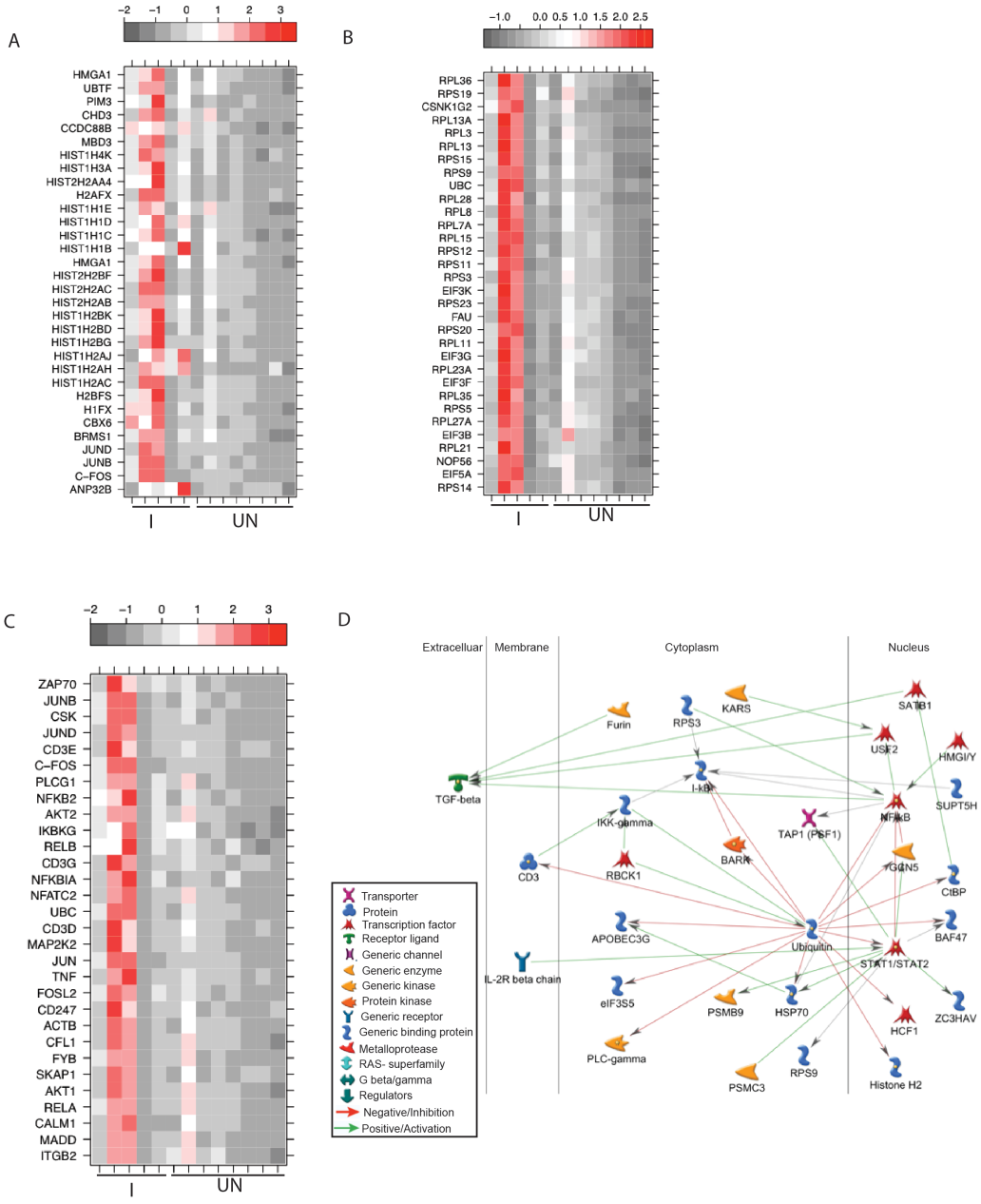

Figure 4.2 Enrichment analysis revealed an up-regulation in gene regulation. (A) Heatmap analysis of the up-regulated gense involved with (A) chromatin assembly (B) translation initiation and (C) TCR Signaling. (D) Network image of the genes that mapped to the GO process "viral process" and have direct interactions

in various metabolic processes (Fig. 4.1D), such as calcium dependent signaling (*CAMK4* FC 3) (437), oxygen homeostasis (*EGLN2*, FC) (438), and nitric oxide synthases regulation (*EDF1*, FC 3) (439).

Enrichment analysis on the up-regulated genes revealed that several play a role in immunity and inflammation (Fig. 4.1C,D), such as cytolytic molecule granzyme B (*GZMB*, FC 20) (440); interferon stimulated genes *IFI17* (FC 4), *ISG20* (FC 10), *MxA* (FC 6) and *OAS2* (FC 6) (441); and transcription factors *IRF1* (FC 5) and *IRF8* (FC 5) which promote TH1 cell responses (442). Moreover, several up-regulated DEGs play a critical role in "TCR signaling" (Fig. 4.1C), notably *ZAP70* (FC 8), *AKT* (FC 4), *ITGB2* (FC) CD3ε (FC 4), *CD3δ* (FC 3), and *CD3γ* (FC 3) (443-447) (Fig. 4.2C).

Several of the 91 genes that mapped to the "viral process" directly interact with each other (Fig. 4.2D). Most of the genes in this network interacted with ubiquitin (*UBC*, FC 3), which regulates protein function and transcription (448) (Fig. 4.2D), including several key transcription factors that regulate antiviral immune processes such as *NFκB* (FC 3), *STAT1* (FC 2) and *STAT2* (FC2). Other genes that mapped to "viral process" have been shown play a role in supporting viral replication such as *HCF1* (FC 3, alpha herpesviruses (449)), *SMARCB1* (FC 2, HIV-1(450)), PLC-gamma (*PLCG1*, FC 4, simian virus 40 (451)) and TGF-beta (*TGFβ*, FC 3, Epstein-barr virus (452).

SVV infection down-regulates genes involved in antigen presentation and metabolic processes

Most of the down-regulated genes mapped to the GO terms "localization" and "vesicle-mediated transport" (Fig. 4.1D). Fifty-four of these genes are part of a network (Fig. 4.3A) including chemokine *IL-8* (FC 29), *CCL23* (FC 5) and *CXCL16* (FC 3) (Fig. 4.3A). Most genes were regulated by transcription factors *PPARγ* (FC 8) and *TCF/LEF* (FC 10) (Fig. 4.3A). Another 12 down-regulated genes were involved in cell adhesion (Fig. 4.1C) such as *APP* (FC 4) (453), *TCF7L2* (FC 10) (454) and *CDH1* (FC 6) (455).

Enrichment analysis using network processes showed that several down-regulated genes play a role in phagocytosis and antigen presentation (Fig. 4.1C). These genes included pathogen recognition receptors (PRRs) *CLEC7A* (FC 4) (456), *MSR1* (FC 5) (457), *TLR4* (FC 3) (458); genes involved in vesicle transport such as *SPIRE1* (FC 8) (459), *EXOC5* (FC 2) and *EXOC6B* (FC 3) (460); and receptors that mediate viral entry such as *SCARB1* (hepatitis C, FC 2) (461) , *MRC1L1* (dengue virus, FC 6) (462), and *ITGAV* (HSV-1 , FC 4) (463) (Fig. 4.3B). Interestingly, 12 down-regulated genes mapped to "blood coagulation" (Fig. 4.1C), including those involved with plasminogen activation (*PLAU,* FC 3) (464), *THBS1* (FC 3) (465), and *ANXA5* (FC 2) (466)), and fibrinolysis inhibition (*A2M*, FC 3 (467) and *SERPINE1*, FC 5 (468)).

Two hundred and two down-regulated DEGs were involved with metabolic processes such as glycerolipid biosynthesis (*GPAM,* FC 11), lipoprotein metabolism (*APOC2*, FC 12) (469), insulin signaling (*ENPP1*, FC 14) (470) and calcium signaling (CACNB4, FC 6) (Fig. 4.3C). Several other genes were involved with NADH oxidation such as *CYBB* (FC 4) (471), *NCF1* (FC

2) , *NCF2* (FC 3) (472) and *GPD1*, (FC2) (473). Finally, genes that enriched only to the GO term "response to stress", play a role in apoptosis and oxidative stress such as TNFRSF10B (FC 7) (474), SOD2 (FC 4) (475), and TGM2 (FC 7) (476).

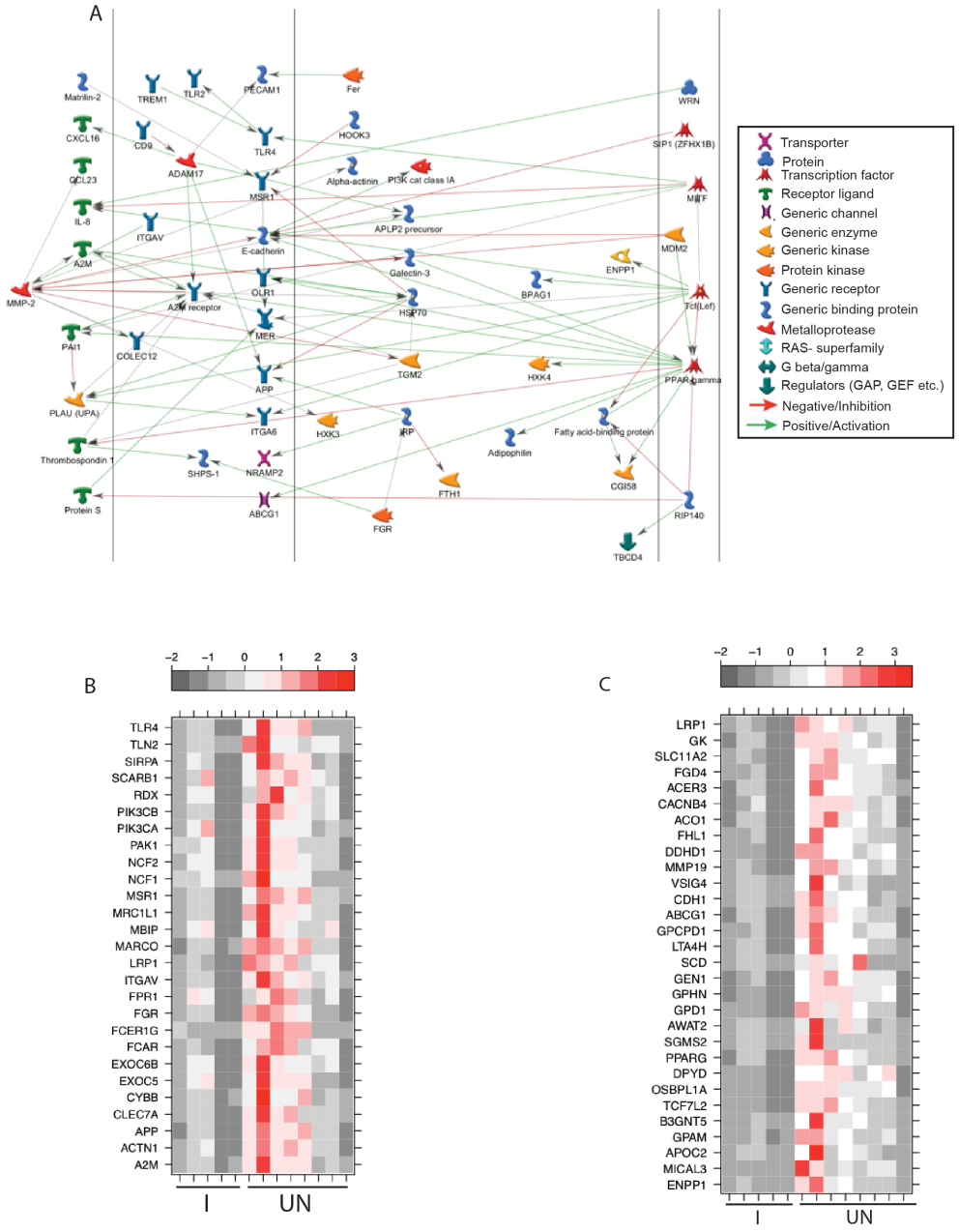

Figure 4.3 Enrichment analysis of down-regulated gene are involve with the immune system and antigen presentation (A) Network image of the genes that mapped to the GO process "localization and have direct interactions. Heatmap analysis of the genes that mapped to (B) phagocytosis/phagosome antigen presentation and (C) top 30 genes that mapped to "single organism metabolic process".

DISCUSSION

Although many studies have demonstrated a role for T cells in varicella pathogenesis (37, 86, 194, 223), the impact of VZV infection on T cell function remains poorly understood due to limited access to T cells infected in vivo. In this study, we leveraged a robust animal model where rhesus macaques are intrabronchially infected with the closely related SVV to address this question. We characterized SVV-induced changes in trancriptome of T cells isolated from the BAL that were previously shown to harbor SVV transcripts (424). Our RNASeq analysis revealed large gene expression changes between T cells isolated from infected and naïve animals.

Several of the up-regulated genes were involved with regulation of gene expression. Several of these genes encode ribosomal components. Ribosomes play a critical role in protein synthesis and have indeed been found to support viral protein synthesis (477). Specifically, RPL40 supports vesicular stomatitis virus translation (478) and EIF4 supports translation of herpes simplex 1 (HSV-1) (479) and human cytomegalovirus (HCMV) (480). Many histone genes, which regulate chromatin assembly, were also up-regulated after SVV infection. Histones have been shown to regulate viral gene expression. For instance, the inhibition of histone demethylase has been shown to block HSV and VZV replication (481). Moreover, VZV ORF 63 has been shown to regulate histone levels in infected cells (482). Several of the other up-regulated genes that were involved with chromatin assembly such as *CFOS*, *JUNB* and *JUND* were reported to be up-regulated with other viral infections such as measles (483), JC virus (484) and echoviruses (485).

Expression of genes that regulate the cell cycle was also altered with SVV infection in T cells. Viruses have been shown to promote infected cells to enter the cell cycle in order to produce nucleotides that are used for viral replication (486), while inhibiting progression into the next

phase of the cell cycle in order to maintain the cell in a state that supports viral replication and prevents apoptosis. For example, influenza A and severe acute respiratory syndrome coronavirus (SARS-CoV) have been found to induce GO/G1 arrest (487, 488) and HIV- 1 has been found to induce G2/M arrest (489). Furthermore, genes that mapped to "viral process" have been shown to support replication of other viruses, such as HIV-1 (450) and Epstein-barr virus (452). These data demonstrate that viruses manipulate similar cellular processes to support viral replication.

Functional enrichment revealed that a large portion of DEGs were involved with metabolic processes. This implies that SVV, like other viruses, may dysregulate T cell metabolism in order to support successful viral replication. Calcium signaling has been shown to increase viral protein expression and T cell activation in viruses such as HIV-1 and HSV-1/2 (490). Furthermore, fatty acid synthesis has been shown to support the formation of VZV virions by facilitating production of VZV glycoproteins (491). Hepatitis C has been shown to reduce insulin signaling (492) in infected cells; moreover, lipid metabolism has also been shown to be down-regulated in T cells infected with HIV (493) in order to support viral replication. However, several of the changes in metabolic processes could be part of the host defense response to SVV. For instance, genes involved with nitric oxide synthase, known to inhibit viral replication, were up-regulated in our dataset (494).

SVV infection also resulted in the dysregulation of several immune genes. Most of the up-regulated immune genes were involved in the antiviral innate immune response. For instance, several interferon stimulated genes (ISGs), which play a critical role in inhibiting various steps of the virus life cycle (441), were up-regulated in our infected T cell population. This up-regulation could be in response to a robust up-regulation of IFNα in BAL of SVV infected macaques, which

we previously reported (228). Other immune genes that were up-regulated include cytolytic molecules and components of the TCR signaling complex. These results are in line with those from previous in vitro studies that investigated how VZV infection affects the phenotype of human tonsil T cells using mass cytometry (CyTOF), which also reported increased expression of ZAP70, AKT, and CD3 (495). SVV-induced T cell activation may increase viral gene expression and enhance T cell trafficking to the ganglia/skin as previously reported for VZV (37, 84, 193).

Down-regulated immune genes were involved with phagocytosis and antigen presentation. These included several pathogen recognition receptors (PRR) which play a critical role in detecting pathogens and mediating proinflammatory responses (496). As previously reported for influenza, PRRs *CLEC7a* and *MSR1* were down-regulated (497). The down-regulation of these genes may be indicative of viral immune evasion. Indeed, down-regulation of antigen presentation has been reported in VZV infected T cells (92, 94). Some of the down-regulated genes can act as receptors for viral entry (e.g. *SCARB1*, *MRC1L1* and *ITGAV*), which may be a host mechanism to block viral entry. Expression of chemokines IL-8, CCL23, and CXCL16 was reduced in our infected T cell population, which may be a strategy for SVV to inhibit the recruitment of other immune cells to the site of infection. Similar results have also been observed in cells infected with human herpesvirus-6A (HHV6A) (498), cytomegalovirus (CMV) and vaccinia virus (499).

Our data set was somewhat similar to a previous in vitro gene expression study that investigated the impact of *in vitro* VZV infection on human T cells using microarray analysis (422). This study also reported an increase in genes involved with antiviral immunity, cell cycle, transcription and translation.e.g. *MXA*, *JUNB* and *NRP2* were observed. The limited similarities of our study

with this earlier study could be due to the use of the attenuated Oka vaccine strain and the *in vitro* infection of the earlier study, which excludes other environmental factors that that our T cells were exposed to *in vivo*.

The major limitation of our study is that we were not able to isolate the SVV infected T cells from the bystander T cells from our BAL samples. Due to this limitation, we are unable to determine whether some of the gene changes we reported are originating from the infected T cells or from non-infected T cells responding to SVV infection. Future studies will utilize single cell RNASeq analysis to address this crucial question. In summary, this study provides the first *in vivo* analysis of SVV-infection induced changes in the T cell gene expression profile. Our data provides novel insight into how SVV may use the host cell machinery to support its replication while evading host defense responses. Increased expression of T cell activation genes may enhance the ability of SVV infected T cells to travel to the skin and ganglia. Given the fact T cells may play a critical role in transporting VZV into the ganglia, our RNA-Seq analysis may guide future studies in the development of more efficacious antivirals.

CHAPTER 5: Robust gene expression changes in the ganglia following subclinical reactivation in rhesus macaques infected with Simian Varicella Virus

Nicole Arnold[1], Christine Meyer[2], Flora Engelmann[3] and Ilhem Messaoudi[2,3]

[1]Graduate Program in Microbiology, University of California-Riverside, CA, USA

[2]Division of Pathobiology and Immunology, Oregon National Primate Research Center, Beaverton, Oregon, USA

[3]Division of Biomedical Sciences, School of Medicine, University of California-Riverside, Riverside, CA

A version of this chapter is under review at the Journal of NeuroVirology

ABSTRACT

Varicella zoster virus (VZV) causes varicella during acute infection and establishes latency in the sensory ganglia. Reactivation of VZV results in herpes zoster, a debilitating and painful disease. It is believed that VZV reactivates due to a decline in cell-mediated immunity; however, the role that CD4 versus CD8 T cells play in the prevention of herpes zoster remain poorly understood. To address this question, we used a well-characterized model of VZV infection where rhesus macaques are intrabronchially infected with the homologous simian varicella virus (SVV). Latently infected rhesus macaques were thymectomized and depleted of either CD4 or CD8 T cells to mimic selective senescence of each T cell subset. After T cell depletion, the animals were transferred to a new housing room to induce stress. Reactivations (viremia in the absence of rash) were detected in 3 out of 6 CD8-depleted and 2 out of 6 CD4-depleted animals suggesting that both CD4 and CD8 T cells play a critical role in preventing SVV reactivation. Viral loads in multiple ganglia were higher in reactivated animals compared to non-reactivated animals. In addition, reactivation results in sustained transcriptional changes in the ganglia that enriched to Gene Ontology terms and diseases associated with neuronal function. These studies support the critical role of cellular immunity in preventing varicella virus reactivation and indicate that reactivation results in long-lasting remodeling of the ganglia transcriptome.

INTRODUCTION

Varicella Zoster Virus (VZV) is a human neurotropic alpha herpesvirus that causes varicella (chickenpox) during primary infection. VZV establishes latency in the sensory ganglia where it can reactivate to cause herpes zoster (HZ, shingles). The risk of getting HZ significantly increases with age, from an average of 3 cases per 1000 adults 40-50 years old, to 10 cases of HZ per 1000 adults aged 80 years or above (121). In addition, the incidence of HZ in individuals receiving immunosuppressive drugs such as those with autoimmune diseases, cancer, and organ transplant recipients is higher (66, 500-502). VZV has also been shown to reactivate with high stress (503), such as during and after spaceflight (504) and in medical students (505).

It is generally believed that VZV reactivation is due to the loss of VZV-specific cell mediated immunity (506), since antibody titers remain relatively stable with increasing age (118, 155, 507). Similarly, VZV reactivation in hematopoietic stem cell transplants was associated with low CD4 T cell counts in the absence of significant changes in antibody titers (508). Finally, T cell responses but not antibody titers, negatively correlate with HZ disease severity (509, 510). However, the role of CD4 versus CD8 T cell immunity in preventing VZV reactivation is not well understood. Previous studies showed that the frequency of VZV-specific CD4 T cells declines more dramatically with age compared to VZV-specific CD8 T cells, suggesting a greater role for CD4 T cells in reactivation, but this hypothesis has yet to be formally tested (118, 146).

In this study, we investigated the role of CD4 and CD8 T cell immunity in preventing herpes zoster using a nonhuman primate model of VZV infection. In this model, rhesus macaques are inoculated intrabronchially with simian varicella virus (SVV), a homologue of VZV. We previously showed that this model recapitulates the essential features of VZV infection in humans including varicella and establishment of latency in sensory ganglia (217). Moreover, as described

for VZV, SVV reactivates under conditions of immune suppression (218, 225, 511, 512). To investigate the role that T cell senescence plays in SVV reactivation, rhesus macaques latently infected with SVV were thymectomized and then depleted of either CD4 or CD8 T cells. The animals were then moved to a new room to induce stress.

SVV reactivation was detected in 42% of depleted animals (2 CD4 depleted and 3 CD8 depleted animals). Moreover, average viral loads in the sensory ganglia from the animals that experienced subclinical reactivation were significantly higher. Finally, large gene expression changes were detected in ganglia collected from animals that underwent reactivation compared to ganglia from animals that did not. These data support the hypothesis that both CD4 and CD8 T cells play a critical role in preventing SVV reactivation and that SVV reactivation remodels the ganglia transcriptome.

MATERIALS AND METHODS

Animals and sample collection

Sixteen colony-bred Rhesus macaques (Macaca mulatta, RM) 3-4 years of age and of Indian origin were used in these studies. All animals were house and handled in accordance with the Oregon National Primate Research Center Institutional Animal Care and Use Committee (protocol #0779). 16 RM were intrabronchially inoculated with 4×10^5 PFU SVV as previously described (221). At 148 days post infection all animals were thymectomized. At 29, 32 and 37 DPT 6 animals were depleted of CD4 T cells using the humanized monoclonal antibody OKT4-HulgG at a dose of 50mg/Kg. Another 6 animals were depleted of CD8 T cells using a mouse-human chimeric monoclonal antibody cM-T807 at a dose of 5mg/Kg on days 29, 32 and 37 post-thymectomy. The remaining 4 animals served as controls. All animals were moved to a different room 364 DPT and were then euthanized ~646 DPT. All procedures were done under Ketamine anesthesia to minimize pain. Necropsy was carried out in accordance with the recommendation of the American Veterinary Association guidelines for euthanasia. Sensory ganglia tissue (trigeminal, dorsal root ganglia (DRG) cervical, DRG-thoracic and DRG-lumbar sacral were collected at necropsy. Tissues were then flash frozen or stored in trizol at -80°. Peripheral blood mononuclear cells (PBMC) were isolated over a density gradient cell separation medium (Corning, Manassas, VA) and resuspended in RPMI with 10% FBS and PSG.

DNA extraction and viral loads

DNA was extracted from whole blood using the Qiagen genomic DNA extraction kit (Qiagen, Valencia, CA). Ganglia tissue was digested in Proteinase K Solution (20mg/ml) overnight and DNA was extracted using the Qiagen genomic DNA extraction kit (Qiagen, Valencia, CA). Viral

loads were determined as previously described by real-time PCR using primers and probes specific for ORF21 and measured on the ABI StepOne instrument (Applied Biosystems, Foster City, CA).

Identification of immune cell populations

PBMC cells were stained with antibodies against CD8β (Beckman Coulter), CD4 (eBioscience, San Diego, CA), CD28 (BioLegend), CD95 (BioLegend), and CCR7 (BD Pharmingen), which allowed the delineation of central memory (CM; $CD28^+$ $CD95^+$ $CCR7^+$), transitional effector memory (TEM; $CD28^+$ $CD95^+$ $CCR7^-$), and effector memory (EM; $CD28^-$ $CD95^+$ $CCR7^-$) CD4 and CD8 T cells. PBMC cells were also surface stained with antibodies against CD20, IgD (Southern Biotech, Birmingham AL) and CD27 (Biolegend) to delineate IgM (IgD+ CD27+), class-switched memory (IgD- CD27+), exhausted memory (IgD- CD27-), and naïve (IgD+ CD27-) B cell subsets. Cells were fixed and permeabilized according to manufacturer recommendations (BioLegend) before the addition of a Ki67-specific antibody (BD Pharmingen). The samples were analyzed using the LSRII instrument (Becton, Dickinson and Company, San Jose, CA) and FlowJo software (TreeStar, Ashland, OR).

Intracellular Cytokine Staining

PBMC were stimulated ex vivo with SVV lysate (1ug) in the presence of brefeldin A (Sigma, St. Louis, MO) for 14 hr. Cells were then stained with antibodies against CD4 and CD8β. Cells were then fixed, permeablilzed (BioLegend) and stained for IFN-γ (eBioscience) and TNF-α (eBioscience). Samples were then acquired on the LSRII instrument and data was analyzed using FlowJo software.

RNA-Sequencing analysis

RNA was extracted from ganglia tissue homogenized in trizol using a bead beater and zirconia/silica beads followed by extraction using the Ambion Purelink RNA Mini Kit (Life Technologies, Carlsbad, CA). RNA library preparation was done using the NEXTflex® Rapid Directional RNA-Seq kit (BIOO Scientific, Austin, TX). DNA libraries were then multiplexed and sequenced on the Illumina HiSeq2500 (Illumina, San Diego, CA) platform. All data analysis steps were performed with the RNA-Seq workflow module of the *systemPiperR* package available on Bioconductor (302, 425). Next generation sequencing (NGS) quality reports were generated with the *seeFastq* function defined by the same package. RNA-Seq reads were mapped with the splice junction aware short read alignment suite Bowtie2/Tophat2 (303, 304) against the *Macaca mulatta* genome sequence downloaded from Ensembl (305). The default parameters of Tophat2 optimized for mammalian genomes were used for the alignments. Raw expression values in form of gene-level read counts were generated with the *summarizeOverlaps* function (306). Only reads overlapping the exonic regions of genes were counted, while reads mapping to ambiguous regions of exons from overlapping genes were discarded. Analysis of differentially expressed genes (DEGs) was performed with the GLM method from the *edgeR* package (307, 308). Differentially expressed genes (DEGs) were defined as those with a fold change ≥2, a false discovery rate (FDR) ≤0.05 and a median RPKM value ≥5. Enrichment analysis was performed using MetaCore software (GeneGo, Philadelphia, PA).

Gene Expression Change Validation

RNA was reverse transcribed using random hexamers and SuperScript ® IV RT using the SuperScript ® IV First-Strand Synthesis System (Invitrogen, Lithuania) to generate cDNA. Taqman gene expression assays (Thermo Fisher, Waltham, MA) of selected genes and

housekeeping gene (RPL32) were carried out using 100ng of cDNA in duplicate on the ABI StepOne instrument (Applied Biosystems). mRNA expression levels were calculated relative to our housekeeping gene (RPL32) using $2^{-\Delta Ct}$ calculations.

Statistical Analysis

Graphing was performed with GraphPad Prism software (GraphPad Software Inc., La Jolla, CA). One-way repeated-measures analysis of variance (ANOVA) with Dunnett's multiple comparison posttest was used to explore differences relative to and pre-thymectomy (-6 DPT) values. Unpaired t test was used to determine significance of ganglia viral loads and gene validation.

RESULTS

T cell depletion after thymectomy results in permanent loss of naïve T cells

Analysis of SVV replication kinetics and host responses in the 16 animals used in this study were previously published (221). All animals generated robust T and B cell responses as evidenced by the detection of antigen-specific T cells and antibodies (221). At 148 days post infection (DPI) all 16 animals we thymectomized, and 29 days post thymectomy (DPT), 12 animals were depleted of either CD4 T or CD8 T cells (n= 6/group) while the remaining 4 animals served as thymectomized controls. At 364 DPT all animals were moved to a different room to induce environmental stress (Fig. 5.1A).

Thymectomy alone (control animals) had minimal impact on the frequency of circulating white blood cells (WBC) including lymphocytes and neutrophils (Fig 5.1B-D). Similarly, thymectomy alone did not impact frequency of circulating CD4 T, CD8 T and CD20 B cells (Fig. 5.2A). Furthermore, very few changes were noted in the frequency of naïve and memory CD4 T, CD8 T and B cell subsets (Fig. 5.2D,G, and J). In contrast, CD4 depletion resulted in a significant decrease in the number of circulating lymphocytes (Fig. 5.1C) due to the loss of CD4 T cells (Fig. 5.2B), and more specifically, naïve CD4 T cells (Fig. 5.2E), which remained significantly decreased for the remainder of the study. This change was accompanied by an increase in the frequency of terminally differentiated CD4 EM T cells (Fig. 5.2E). Initially, frequency of CD8 T cells significantly increased at 153 DPT in CD4 depleted animals but then decreased as CD4 numbers partially recovered in the CD4 depleted animals (Fig. 5.2B). We also saw a significant increase in CD8 EM T cells and a decrease in naïve and TEM CD8 T cells in the CD4 depleted animals (Fig. 5.2H). No changes in B cell subsets were noted in the CD4 depleted animals (Fig. 5.2K).

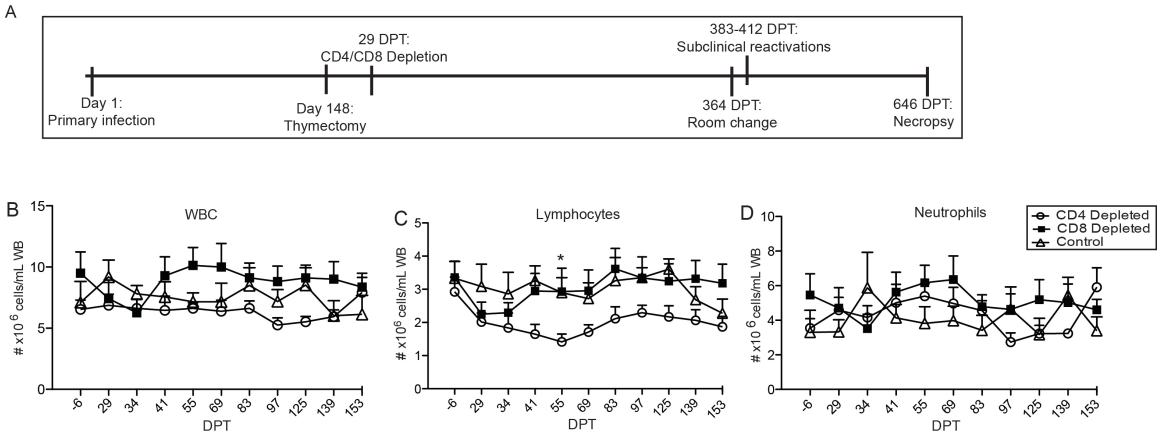

Figure 5.1 Animal treatments and whole blood cell counts. (A) Experimental timeline. Absolute numbers of (B) white blood cells (WBC) (C) lymphocytes and (D) neutrophils were measured in controls (n=4), CD4 depleted (n=6) and CD8 depleted animals (n=6) using a Hemavet. *P< 0.05 for CD4 depleted animals compared to day -6 post-thymectomy

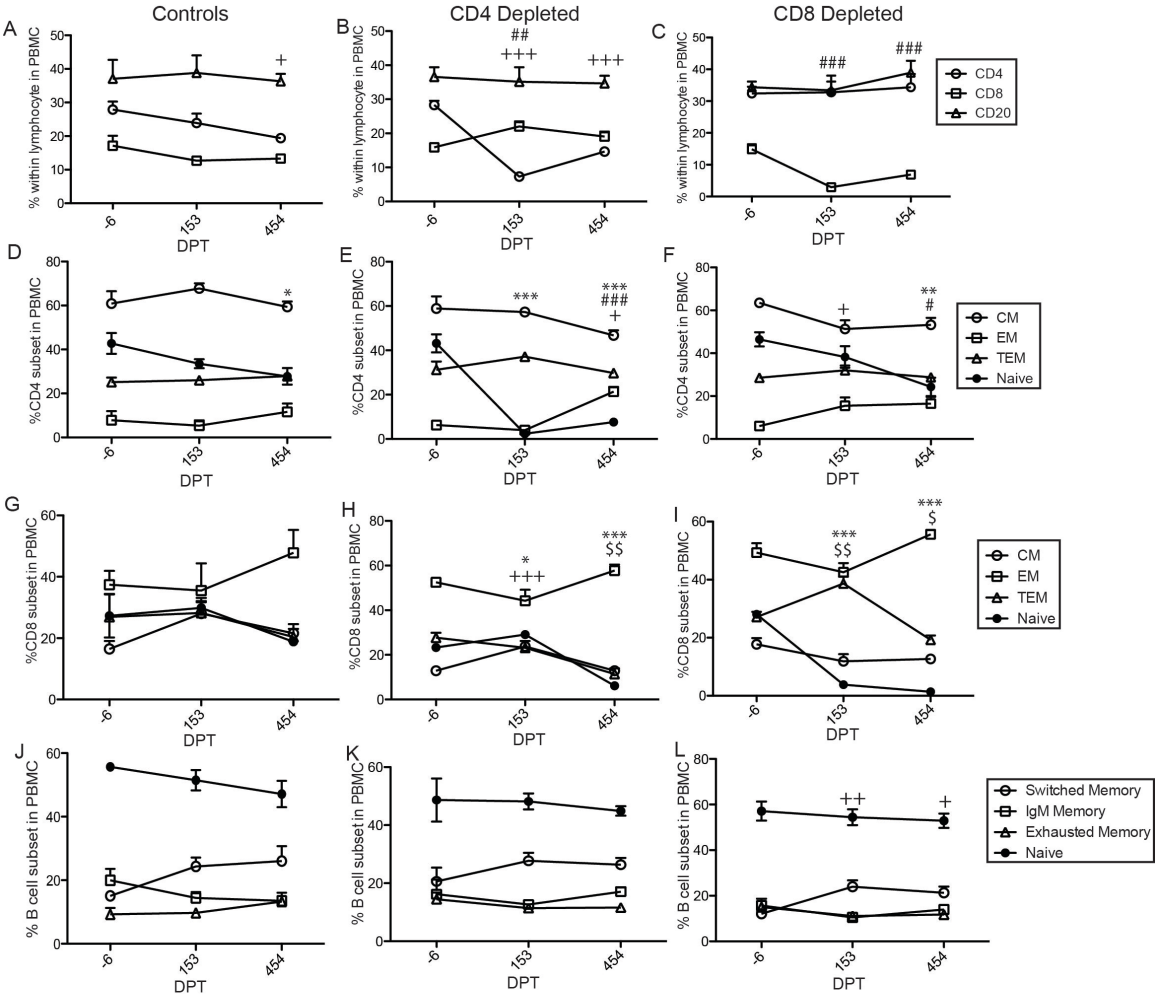

Figure 5.2 Thymectomy followed by depletion results in the loss of naïve T cells. The frequencies of (A) CD4 T, (B) CD8 T and (C) CD20 B cells (means ± SEM) were determined in the PBMC by flow cytometry (+++, P< 0.001 for CD4 T cells; ##, P<0.01; ### P< 0.001 for CD8 T cells). The frequencies of CM, EM, TEM and naïve CD4 T cells in (D) controls (E) CD4 depleted and (F) CD8 depleted animals and CD8 T cells in the (G) controls (H) CD4 depleted (I) CD8 depleted animals determined by flow cytometry. (+, P< 0.05; ++ P< 0.01; +++, P< 0.001 for CM; #, P< 0.05; ## P< 0.01; ###, P< 0.001 for EM; $, P< 0.05, $$, P< 0.01 for TEM; *, P< 0.05; **, P< 0.01; ***, P< 0.001 for naïve). The frequency (mean ± SEM) of class-switched memory, IgM memory, exhausted memory, and naïve B cells in the (j) controls (k) CD4 depleted (l) CD8 depleted animals was determined by flow cytometry in PBMC. (+, P< 0.05; ++ P< 0.01, for switched memory). (Controls, n=4; CD4 Depleted, n=6; CD8 Depleted, n=6)

As described for CD4 T cells, CD8 depletion resulted in a profound and sustained loss of CD8 T cells while frequency of CD4 T cells and CD20 B cells remained relatively stable (Fig. 5.2C). This loss was also primarily driven by a significant reduction in the number of naïve CD8 T cells (Fig. 5.2I), which was accompanied by a transient increase in TEM CD8 T cells and an increase in the EM frequency (Fig. 5.2I). Interestingly, following CD8 depletion, frequency of CD4 EM T cells increased while that of naïve and CM CD4 T cells decreased (Fig. 5.2F). The CD8 depleted animals had a significant increase in their switched memory B cell population after depletion (Fig. 5.2L).

T cells undergo robust homeostatic proliferation following depletion

The changes in relative frequency of naïve and memory T cells in the depleted animals prompted us to investigate the role of homeostatic proliferation. In the thymectomized non-depleted group we observed a transient increase in proliferation in CD4 T cells and B cells, but not CD8 T cells 55-83 DPT (Fig. 5.3A, D, G). Following CD4 and CD8 T cell depletion, we observed robust proliferation in both CD4 T, CD8 T cells and B cells as early as 29 DPT (Fig. 5.3). In the CD4 depleted animals, the magnitude of CD4 T cell proliferation was much more robust than that of CD8 T cells and B cells (Fig. 5.3B, E, H). Interestingly, in the CD8 depleted animals, CD4 T cell proliferation occurred earlier than CD8 T cell proliferation and reached similar magnitude (Fig. 3C,F). Although proliferation of naïve T cells was observed in both CD4 depleted and CD8 depleted groups, the naïve T cell numbers remained significantly reduced due to lack of thymic output and rapid conversion to memory phenotype cells.

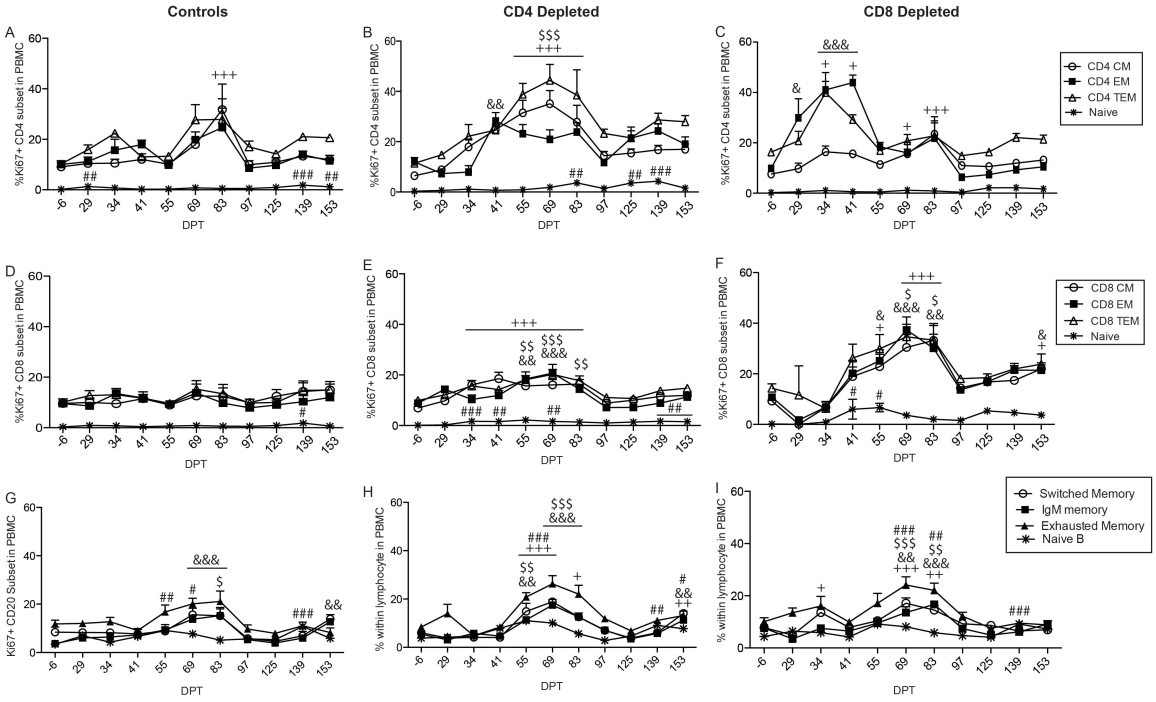

Figure 5.3 Depletion results in robust homeostatic proliferation. Magnitude and kinetics of proliferation (means ± SEM) of CD4 T cell subsets was measured in (A) controls (B) CD4 depleted (C) CD8 depleted animals; CD8 T cell subsets in (D) controls (E) CD4 depleted (f) CD8 depleted animals; and B cell subsets in (G) controls (H) CD4 depleted (I) CD8 depleted animals was determined by measuring Ki67 expression within specific lymphocyte subsets by flow cytometry. (+, P< 0.05; ++ P< 0.01; +++, P< 0.001 for CM; (&, P< 0.05; &&, P< 0.01; &&&, P< 0.001 for EM; $, P< 0.05, $$, P< 0.01; $$$, P< 0.001 for TEM; #, P< 0.05; ## P< 0.01; ###, P< 0.001 for naïve T cells; +, P< 0.05; ++ P< 0.01; +++, P< 0.001 for switched memory; &&, P< 0.01; &&&, P< 0.001 for IgM memory; $, P< 0.05, $$, P< 0.01; $$$, P< 0.001 for exhausted memory; #, P< 0.05; ## P< 0.01; ###, P< 0.001 for naïve B cells).

T cell depletion followed by environmental stress results in subclinical reactivations

SVV reactivation was monitored by measuring SVV viral loads in the whole blood using quantitative real-time PCR (qPCR) as well as visual inspection for zoster lesions. After almost a year with no signs of reactivation, all of the animals were moved to a different room in the facility to induce stress (Fig. 5.1). No obvious rash was detected in the animals; however, SVV DNA was detected in whole blood (WB) from 5 animals (2 CD4 depleted and 3 CD8 depleted) approximately 20-48 days after the move (383-412 DPT) (Fig. 5.4A). To characterize the immune response during SVV reactivation, we measured changes in SVV specific IgG titers and frequency of antigen-specific T cells. We observed no significant increases in IgG titers or CD4 T cell responses in the animals that experienced SVV reactivation (Fig. 5.4B-E). Increased CD8 T cell responses were detected in some of the depleted animals 412- 454 DPT regardless of whether they experienced renewed viremia (Fig. 5.4F).

SVV reactivation results in increased viral loads and long-lasting transcriptional changes in the ganglia

No additional reactivation events were detected during the next several months. We therefore elected to euthanize the animals at 646 DPT and investigate changes in SVV viral loads and transcriptional profiles in the sensory ganglia from animals that experienced a reactivation event. Significantly higher viral loads were observed from the trigeminal (TG) and dorsal root ganglia thoracic (DRG-T) of animals that showed signs of subclinical reactivation compared to the animals that did not (Fig. 5.5A). No viral loads were detected in lumbar sacral dorsal root ganglia (data not shown).

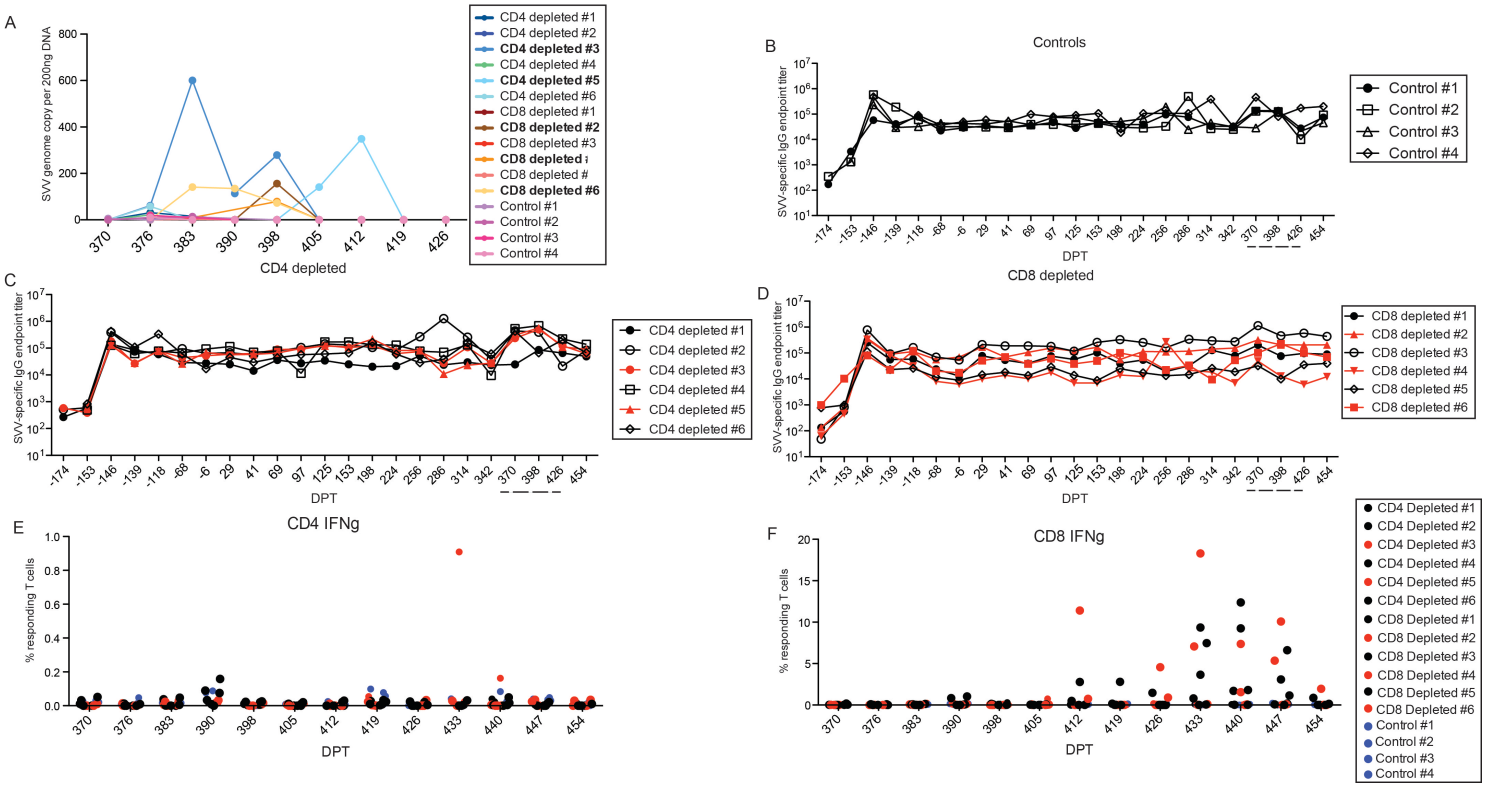
A
SVV genome copy per 200ng DNA
CD4 depleted
CD4 depleted #1
CD4 depleted #2
CD4 depleted #3
CD4 depleted #4
CD4 depleted #5
CD4 depleted #6
CD8 depleted #1
CD8 depleted #2
CD8 depleted #3
CD8 depleted i
CD8 depleted #
CD8 depleted #6
Control #1
Control #2
Control #3
Control #4
B
Controls
SVV-specific IgG endpoint titer
DPT
C
CD4 depleted
D
CD8 depleted
CD8 depleted #1
CD8 depleted #2
CD8 depleted #3
CD8 depleted #4
CD8 depleted #5
CD8 depleted #6
E
CD4 IFNg
% responding T cells
F
CD8 IFNg
CD4 Depleted #1
CD4 Depleted #2
CD4 Depleted #3
CD4 Depleted #4
CD4 Depleted #5
CD4 Depleted #6
CD8 Depleted #1
CD8 Depleted #2
CD8 Depleted #3
CD8 Depleted #4
CD8 Depleted #5
CD8 Depleted #6

(previous page) Figure 5.4 SVV reactivation is detected in depleted animals in the absence of robust changes in immunity. (A) SVV DNA viral loads were assessed in PBMC (200ng/sample). SVV-specific IgG titers were determined in (B) Controls (C) CD4 depleted and (D) CD8 depleted animals. Frequencies of PBMC SVV-specific (E) CD4 and (F) CD8 T cells producing IFNγ in animals that experienced SVV reactivation (red), depleted animals that did not experience a reactivation (black), and controls (blue). Dashed line represents the reactivation period

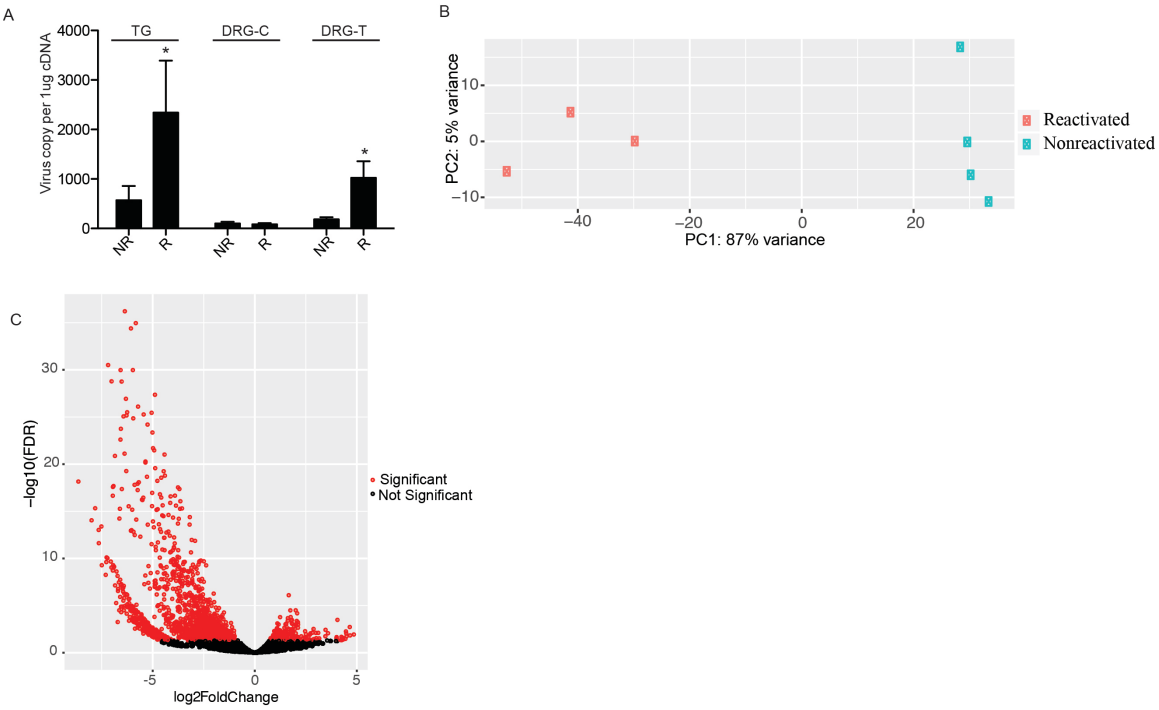

Figure 5.5 SVV reactivation results in substantial host transcriptional changes in the ganglia (A) SVV DNA viral loads were assessed in sensory ganglia (1ug/sample) by quantitative real-time PCR using primers and probes specific for SVV ORF21. (TG= Trigeminal, DRG-C= dorsal root ganglia cervical, DRG-T= thoracic) (TG; n=6 for animals that did not experience reactivation (NR), n=3 for those that experienced reactivation (R); DRG-T; n=6 for NR, n=5 for R; DRG-C; n=6 for NR and n=5 for R). (B) PCA plot of the ganglia transcriptomes (n=3 for R and n=4 NR). (C) Volcano plot representing overall gene expression changes observed in animals that experienced renewed SVV viremia.

In order to determine the host transcriptome changes that occur following reactivation, we performed RNA-Seq on the DRG-T collected from 3 animals that experienced a reactivation event (2 CD4 depleted, 1 CD8 Depleted) and 4 animals that showed no signs of reactivation (2 controls, 1 CD4 depleted and 1 CD8 depleted) (Table 5.1). A principle performance analysis (PCA) showed a clear distinction between the reactivated and the control groups (Fig. 5.5B). Overall, we observed 1202 differentially expressed genes (DEGs) defined as having a fold change (FC) ≥2, a false discovery rate (FDR) of ≤0.05, and a median RPKM value of ≥5 (199 up-regulated, 1003 down-regulated) (Fig. 5.5C). To understand the biological implication of these transcriptional changes, we carried out a functional enrichment using Metacore, which requires the use of human homologues. Conversion of rhesus macaque genes into human homologues resulted in 641 DEGs (120 up-regulated and 521 down-regulated) (Supplemental Dataset 5.1). Changes in expression of 4 DEGs were confirmed by RT-PCR (Fig. 5.6).

Up-regulated genes post reactivation in the ganglia suggest ongoing tissue repair

Only 120 characterized DEGs were found to be up-regulated in ganglia of animals that experienced SVV reactivation. Several of the 30 most up-regulated genes regulate cell cycle progression (Fig. 5.7A) such as *AMD1* (FC 4) which regulates Myc expression (513), *POC1B* (FC 3) involved with centriole assembly (514), and the transcriptional regulator *TAF1D* (FC 4, confirmed by RT-PCR, Fig. 5.6A) (515). Additional genes were involved with apoptosis such as *HIF1A* (FC 3)(516) and *MAP4K5* (FC 3) (517); and protein degradation such as *UFD1L* (FC 3) (518) and *CLPX* (FC 3) (519). Other highly up-regulated genes play a role in neuronal development such as *SNAPC3* (FC 3) (520), *OLIG3* (FC 3) (521), and *ACVR2A* (FC 3) (522)

Sample	Reactivated	Viral Load
CD4 Depleted #3	Y	555
CD4 Depleted #5	Y	189
CD8 Depleted #6	Y	2091
Control #2	N	64
Control #3	N	236
CD4 Depleted #6	N	152
CD8 Depleted #5	N	21

Table 5.1 DRG-T Viral loads of the samples used for RNA-Seq analysis

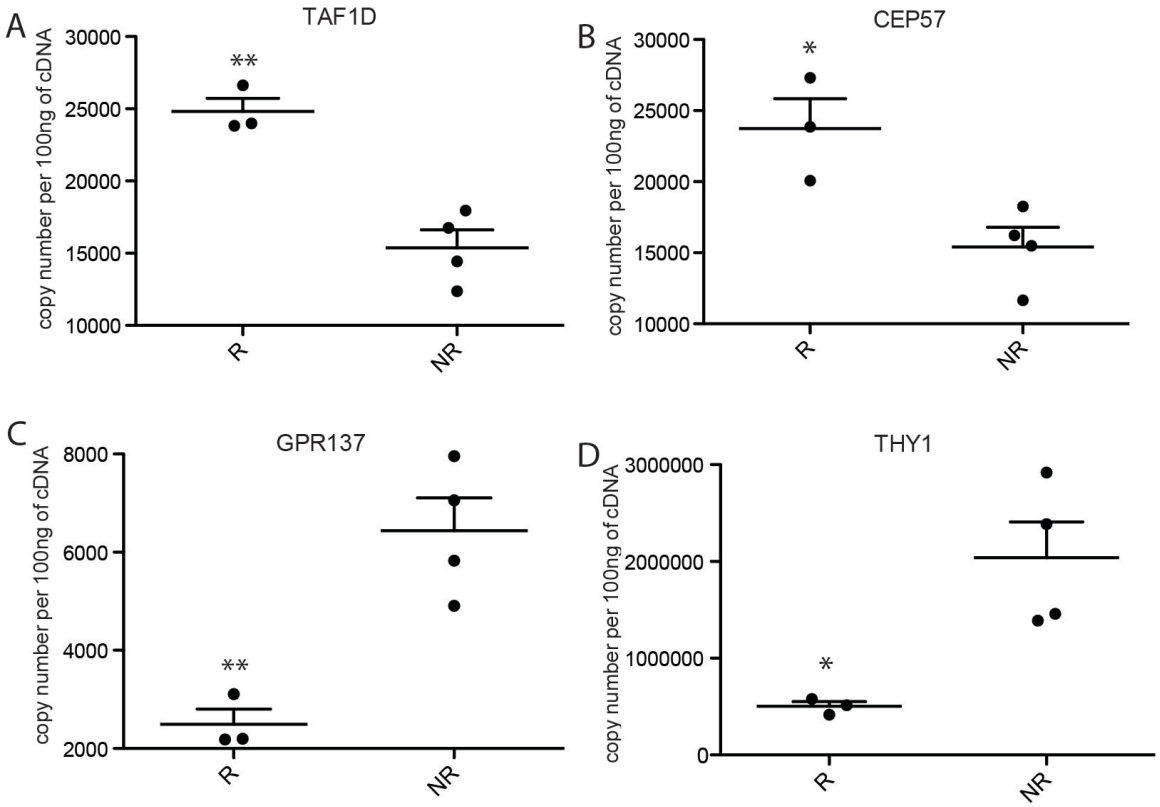

Figure 5.6 Gene validation. Taqman assays were done on (A) TAF1D (up-regulated) (B) GPR137 (down-regulated) (C) THY1 (down-regulated) and (D) CEP57 (up-regulated). n= 3 for reactivated (R) and n= 4 for nonreactivation (NR). *P< 0.05, **P< 0.01 compared to NR

(Fig. 5.7A). Two antiviral genes were also amongst the 30 most up-regulated DEGs: *TRIM23* (FC 3) which enhances antiviral innate responses through the RIG-I/MDA5 mediated pathway (523), and *UFL1* (FC 4), which inhibits NF-kappaB signaling pathway (524).

Functional enrichment showed that most of the up-regulated DEGs mapped to "cellular metabolic process" (Table 5.2), which also included the genes found in "response to glucose". Examples of genes that mapped to these two GO processes include those involved with double-stranded DNA damage repair (*BAZ1A*, FC 3) (525); transcriptional regulation (*MIER1*, FC 3) (526); mRNA degradation (*CNOT7*, FC 2) (527); and regulation of circadian calcium rhythms in neurons (*ARNT*, FC 2) (528). An additional 17 genes that mapped to "multicellular organismal reproductive process" played a role in microtubule stabilization (529) (*CEP57*, FC3, confirmed by RT-PCR, Fig. 5.6B); anion transport (*SLC26A8*, FC 3 (530)); and neuron development (*RARB* FC 2 (531)) (Fig. 5.7B).

Down-regulated DEGs play a role in neuronal damage

Several of the down-regulated genes play a role neuronal development. The most down-regulated gene in our data set was *GPR137* (FC 400, confirmed by RT-PCR, Fig. 5.6C), a G protein coupled receptor essential for controlling pain transmission in the trigeminal ganglia (532) (Fig. 5.8A). Several of the down-regulated DEGs were involved with axon regeneration such as *NDEL1* (FC 123) (533), *AMIGO3* (FC 200) (534), *THY-1* (FC 110) (confirmed by RT-PCR, Fig. 5.6D) (535), and *INA* (FC 89) (536). Additional down-regulated genes were involved in neuron differentiation and stabilization such as *FERD3L* (FC 104) (537), *BASP1* (FC 200) (538), *ATF5* (FC 158) (539)

Up-regulated		
GO Process	**# Genes**	**FDR**
cAMP catabolic process	2	4.951E-03
Multicellular organismal reproductive process	17	5.523E-03
Response to glucose	8	1.360E-02
Cellular metabolic process	72	1.819E-02
Process Networks		
Cell cycle_Chromosome condensation in prometaphase	3	1.730E-02
Signal transduction_Soluble CXCL16 signaling	3	1.104E-01
Translation_Role of Retinoic acid signaling in the initiation of translation	2	2.488E-01
Cell cycle_Role of Nek in cell cycle regulation	2	2.508E-01
Down-regulated		
GO Process	**# Genes**	**FDR**
Axo-dendritic transport	14	4.396E-07
Cellular component organization	244	4.396E-07
Metabolic Process	378	7.202E-07
Chaperone-mediated Autophagy	6	1.740E-06
Cytoskeleton-dependent Intracellular transport	21	1.818E-06
Regulation of intracellular transport	51	2.803E-06
Response to stress	177	9.804E-06
Regulation of protein complex stability	6	1.114E-05
Process Networks		
Protein folding_Response to unfolded proteins	11	1.305E-03
Cytoskeleton_Intermediate filaments	10	1.890E-02
Cell cycle_Meiosis	10	8.081E-02
Cytoskeleton_Regulation of cytoskeleton rearrangement	14	8.081E-02
Transcription_Chromatin modification	11	8.081E-02
Proteolysis in cell cycle and apoptosis	10	1.626E-01
Muscle contraction	12	2.158E-01
Cell cycle_G2-M	12	5.592E-01
Cell adhesion_Cell junctions	10	5.592E-01
Immune response_Antigen presentation	11	5.694E-01
DNA damage_Core	3	5.694E-01
Transcription_Nuclear receptors transcriptional regulation	10	7.890E-01
Protein folding_Protein folding nucleus	4	8.017E-01
Diseases		
Amyloid Neuropathies	9	1.700E-10
Alzheimer disease, early onset	11	2.220E-06
Parkinsonian Disorders	32	4.676E-06
Spinal Cord Diseases	28	1.109E-05
Movement Disorders	49	1.109E-05
Polyneuropathies	18	1.646E-05
Gliosis	9	2.181E-05
Memory Disorders	9	2.181E-05
Basal Ganglia Diseases	45	2.343E-05
Myositis	17	3.364E-05
Motor Neuron Disease	22	3.493E-05
Cerebral Arterial Diseases	10	5.023E-05

Table 5.2 Gene enrichment analysis of up-regulated and down-regulated genes

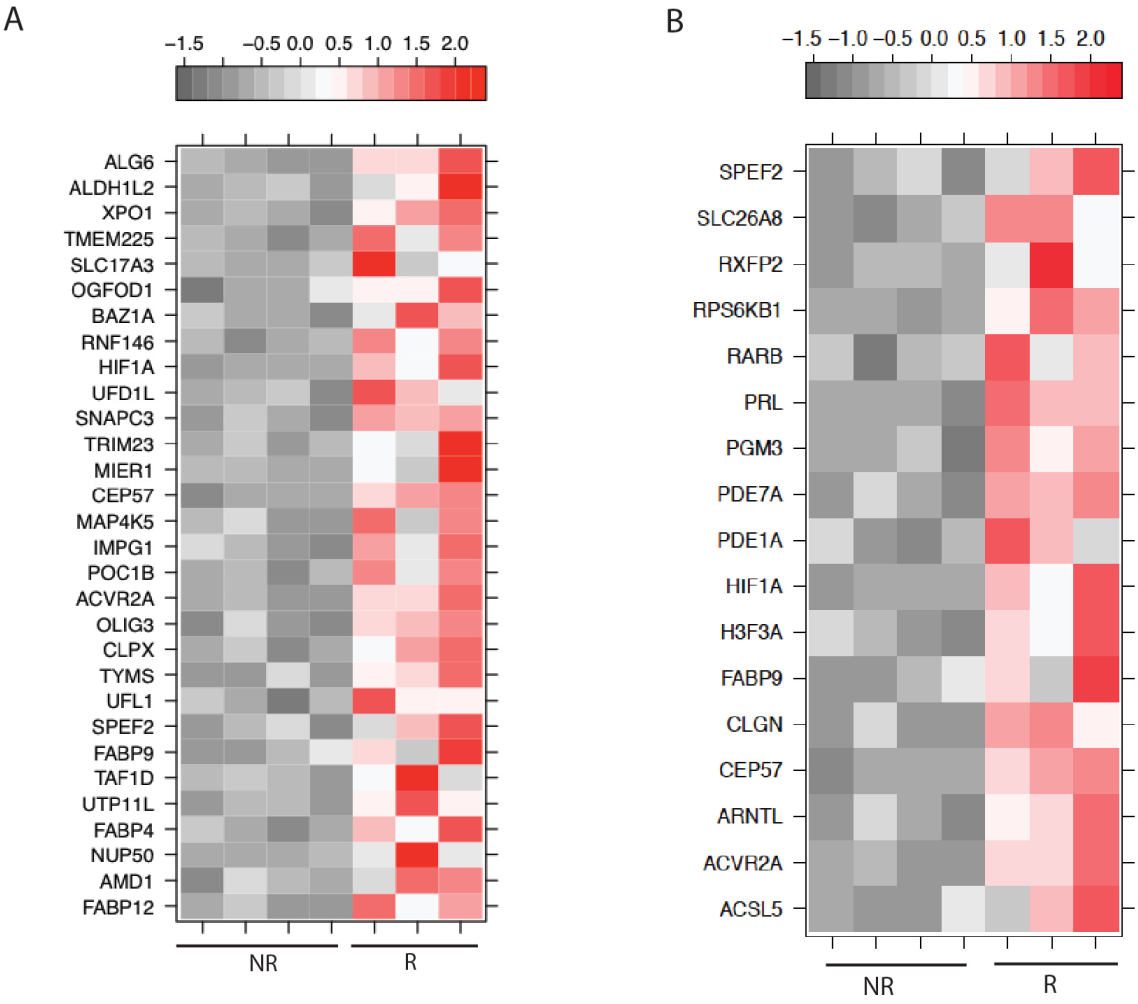

Figure 5.7 Gene enrichment analysis of the up-regulated genes in reactivated animals
Heat map analysis of the (A) 30 most up-regulated and (B) up-regulated genes mapping to "reproductive process". NR=nonreactivated, R= reactivated

and *HSPA12B* (FC 119) (537). Furthermore, some of the most down-regulated genes played a role in cell proliferation (*MZF1*, FC 124) (540); DNA damage repair (*XRCC3*, FC 121) (541); and protein transport (*SSR4*, FC 183) (542) (Fig. 5.8A).

Functional enrichment showed that the most statistically significant GO process to which down-regulated DEGs mapped is "axo-dendritic-transport" which includes genes encoding neurofilaments *NEFL* (FC 7) and *NEFM* (FC 4), and the neurodevelopment protein *NDEL1* (FC 123) (Table 5.2). Several of the 215 down-regulated genes that mapped to "cellular component organization" (Table 5.2) play important roles in the regulation of gene expression within neurons including several histone genes (*HIST1H2AC* (FC 28), *HIST2H2AA4* (FC 70), *HIST2H3D* (FC 47) and *HIST3H2BB* (FC22)) (543), as well as transcription factors such as *ATF5* (FC 158) (544) and *BAIAP2* (FC 155) (545). In addition, several highly down-regulated genes mapped to "metabolic process" (Table 5.2) such as *PGAM2* (FC 149) (546), *CBR3* (FC 130) (547)), and *HEXIM2* (FC 54) (548)). Of the 177 genes that mapped to the GO process "response to stress", 43 directly interact with each other (Fig. 5.8B) including several that interact with *APP* (FC 7), which regulates neurite outgrowth (549), and histone deacetylase class II (*HDAC*, FC 5).

Additional bioinformatics analysis of the down-regulated DEGs revealed enrichment to Process Networks associated with the cell cycle (Table 5.2) including: DNA repair (*HSH5* (FC 4), *RAD1* (FC 3), *RAD9*, (FC 44) and *RAD17* (FC 5)) (550-552); microtubule assembly *TUBA1B* (FC 7) (553); and cell cycle progression, *ANAPC13* (FC 9) (554). Several down-regulated genes also enriched to the process network "immune response-antigen presentation" (Table 5.2) such as *ICAM* (FC 37), *NFKBIB* (FC 12), and several heat shock proteins (*HSPA1L* (FC 95), *HSPA8* (FC

8), *HSPCA* (FC 5) and *HSP90* (FC 2)) (Fig. 5.8C). Finally, analysis of the down-regulated genes using a Diseases Biomarker database revealed enrichment to several diseases related to the neuronal damage and mental health diseases (Table 5.2). The DEGs that enriched to "basal ganglia diseases" played a role in axon regeneration such as *NGF* (FC10) (555) and *SNCG* (FC 59) (556); neuron differentiation e.g. *SUZ12* (FC6) (557); and CNS inflammation such as *CCR7* (FC 8) (558) (Fig. 5.8D).

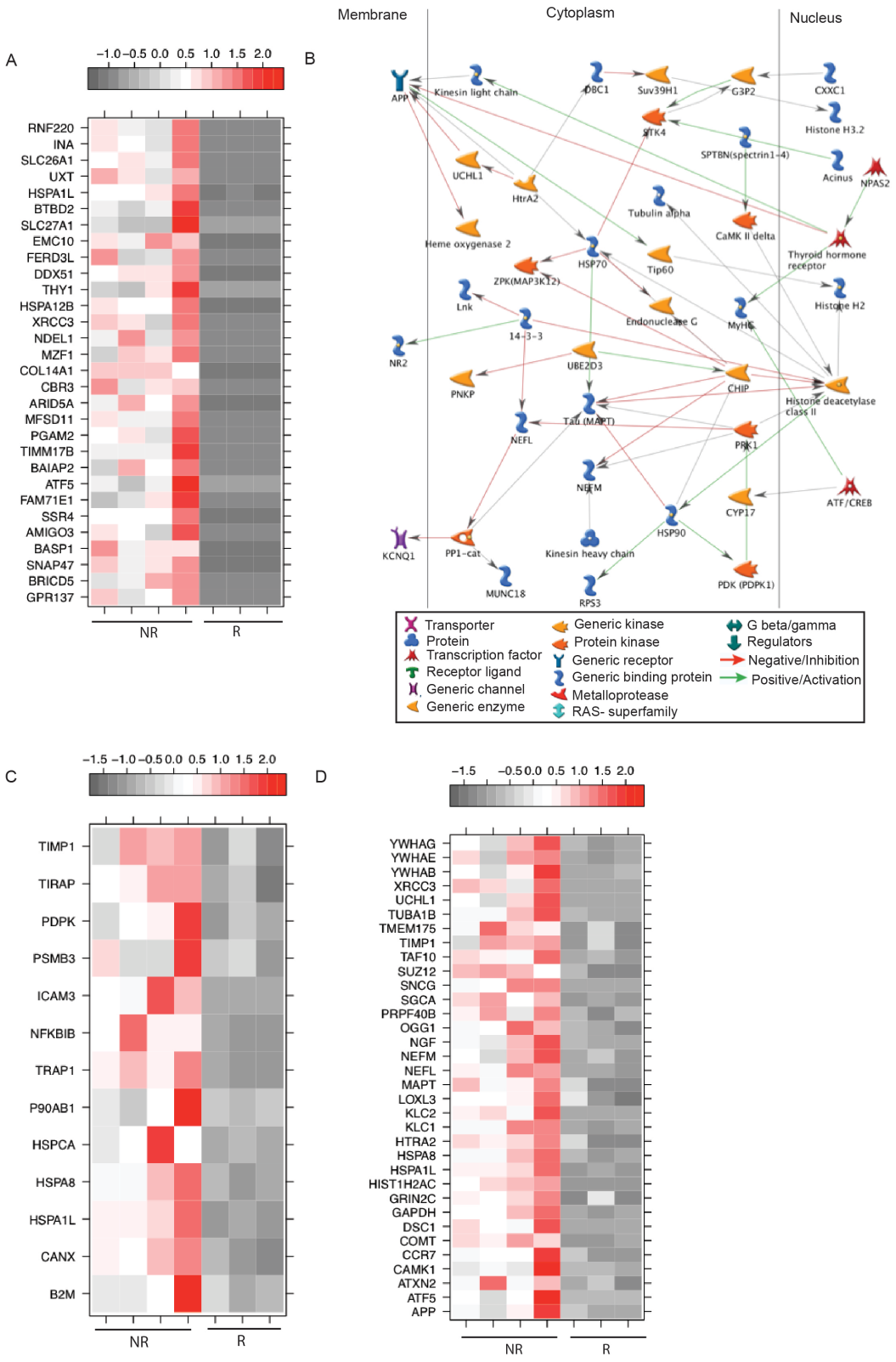
A
−1.0 −0.5 0.0 0.5 1.0 1.5 2.0
RNF220
INA
SLC26A1
UXT
HSPA1L
BTBD2
SLC27A1
EMC10
FERD3L
DDX51
THY1
HSPA12B
XRCC3
NDEL1
MZF1
COL14A1
CBR3
ARID5A
MFSD11
PGAM2
TIMM17B
BAIAP2
ATF5
FAM71E1
SSR4
AMIGO3
BASP1
SNAP47
BRICD5
GPR137
NR
R
B
Membrane
Cytoplasm
Nucleus
APP
Kinesin light chain
DBC1
Suv39H1
G3P2
CXXC1
Histone H3.2
STK4
SPTBN(spectrin1-4)
Acinus
NPAS2
UCHL1
HtrA2
Tubulin alpha
CaMK II delta
Heme oxygenase 2
HSP70
Tip60
Thyroid hormone receptor
ZPK(MAP3K12)
Lnk
Endonuclease G
MyHC
Histone H2
14-3-3
NR2
UBE2D3
PNKP
CHIP
Histone deacetylase class II
Tau (MAPT)
NEFL
PRK1
NEFM
CYP17
ATF/CREB
KCNQ1
PP1-cat
Kinesin heavy chain
HSP90
MUNC18
RPS3
PDK (PDPK1)
Transporter
Protein
Transcription factor
Receptor ligand
Generic channel
Generic enzyme
Generic kinase
Protein kinase
Generic receptor
Generic binding protein
Metalloprotease
RAS- superfamily
G beta/gamma
Regulators
Negative/Inhibition
Positive/Activation
C
−1.5 −1.0 −0.5 0.0 0.5 1.0 1.5 2.0
TIMP1
TIRAP
PDPK
PSMB3
ICAM3
NFKBIB
TRAP1
P90AB1
HSPCA
HSPA8
HSPA1L
CANX
B2M
NR
R
D
−1.5 −0.5 0.0 0.5 1.0 1.5 2.0
YWHAG
YWHAE
YWHAB
XRCC3
UCHL1
TUBA1B
TMEM175
TIMP1
TAF10
SUZ12
SNCG
SGCA
PRPF40B
OGG1
NGF
NEFM
NEFL
MAPT
LOXL3
KLC2
KLC1
HTRA2
HSPA8
HSPA1L
HIST1H2AC
GRIN2C
GAPDH
DSC1
COMT
CCR7
CAMK1
ATXN2
ATF5
APP
NR
R

Figure 5.8 Gene enrichment analysis of the down-regulated genes in reactivated animals. (A) Heatmap analysis of the 30 most down-regulated genes (B) Network image showing the genes that directly interact in the down-regulated genes found in the GO process "response to stress". (C) Heat map analysis of the down-regulated immune genes. (D) Heat map analysis of the genes that mapped to GO process "basal ganglia diseases" NR=nonreactivated, R= reactivated

DISCUSSION

Age and immune status are the primary risk factors for getting herpes zoster. The goal of this study was to investigate the role of CD4 and CD8 T cell immunity in preventing herpes zoster. Using the rhesus macaque animal model of SVV infection, we were able to artificially age either the CD4 or CD8 T cell population in latently infected animals by performing a thymectomy followed by CD4 or CD8 T cell depletion. In the absence of naïve T cell output from the thymus, T cells within the subset that was depleted undergo robust homeostatic proliferation in order to repopulate the T cell compartment, which results in accelerated T cell senescence. Our data showed that T cell numbers of the depleted subset don't recover to baseline levels no matter how robust the homeostatic proliferation. Similar findings have been reported in mice depleted of their lymphocytes (559). Interestingly, we observed increased proliferation in the non-depleted T cell subset and B cells, suggesting all lymphocytes are able to sense and respond to the available space created by the depletion.

Thymectomy and accelerated aging of the T cell compartment alone were not sufficient to cause reactivation. We therefore induced stress by moving the animals to a different room in the facility. SVV reactivation was observed in 2 CD4 depleted and 3 CD8 depleted animals as evidenced by the presence of SVV DNA in blood, increased viral loads in the ganglia, and further confirmed through host transcriptome analysis. VZV reactivation in the absence of rash is referred to as zoster sine herpete (560) and has been reported in HIV positive patients, bone marrow transplant recipients, patients with leukemia, and cynomolgus macaques subjected to stress from travel and isolation (216, 561, 562).

SVV reactivations were observed in both CD4 and CD8 depleted animals, which suggest a role for CD4 and CD8 T cells in the prevention of reactivation. Viral loads in the blood seemed to be slightly higher in the CD4 depleted animals; however, since only 2 CD4 depleted animals experienced reactivations, we could not determine whether this increase was significant. These observations are in line with clinical studies that have indicated a critical role for CD4 T cells in prevention of VZV reactivation. Specifically, HZ is more prevalent in HIV+ patients (563). Furthermore, rapid recovery of CD4 T cells, but not CD8 T cells, after stem cell transplants have also been shown to play a role in preventing reactivation of cytomegalovirus (564). Previous studies from our lab have also shown a greater role for CD4 T cells in the resolution of SVV infection during acute infection where CD4 depleted animals had higher viral loads, prolonged disease and are unable to establish latency in the ganglia (219, 565). On the other hand CD8+ cells in the trigeminal ganglia play a role in the prevention of HSV-1 reactivation in mice (566), which indicates that immunological control of reactivation may differ between these two closely related viruses.

In contrast to what has been previously reported for VZV, no significant changes in antibody titers were detected during SVV reactivation. Similarly, no increase in SVV-specific CD4 T cell responses were detected in reactivated animals. On the other hand, CD8 T cell responses were increased in several depleted animals regardless of the renewed SVV viremia, but in none of the non-depleted controls. This observation suggests that depleted animals were more susceptible to the stress induced by the room change, but only some of the animals experienced a reactivation. Our data differs from previous reports where increased T cell responses have been observed in transplant recipients following subclinical reactivations (561). Although we were unable to detect

a robust immune response in the peripheral blood, SVV reactivations could have triggered a local immune response within the ganglia. Unfortunately, we were unable to address this question since the ganglia tissue was collected nearly 1 year after viremia was detected.

Viral loads were higher in the ganglia collected from animals that experienced a reactivation compared to those collected from non-reactivated animals. The increased SVV viral loads could have been due to viral replication during reactivation as previously reported for VZV and SVV (195, 225). However, it is also possible that the viral loads in the ganglia of the reactivated animals were higher to begin with, which made them more susceptible to reactivation. In addition to increased viral loads, RNA-Seq analysis revealed distinct transcriptional profiles between the DRG-T of the reactivated and non-reactivated animals despite the fact that our analysis was carried out 1 year after SVV viremia was detected. This suggests that SVV reactivations can cause long-lasting gene expression changes in the ganglia. Genes that were down-regulated after reactivation play a critical role in neuron differentiation and axon regeneration as well as DNA repair indicative of significant damage to the ganglia. While genes that were up-regulated after SVV reactivation play a role in cell proliferation and neuronal development, suggesting tissue repair. Although we were not able to examine the ganglia tissue at the time of their subclinical reactivation, our gene expression data are supportive of previous studies reported severe necrosis and inflammation of the ganglia recovered from patients with HZ at the time of death (42, 299).

Recent studies from our lab have shown a down-regulation of neuronal genes during acute infection (424), therefore we compared the DEGs detected after acute SVV infection (100 dpi) and those detected after SVV reactivation. Only 48 common DEGs were identified, most of which were down-regulated after both acute infection and reactivation. Several of these DEGs

play a role in synaptic plasticity (*THRA*, *KIRREL* and *IGFS8*) (567-569) and neuronal growth (*MBP*, *STMN2*, *PRPH* and *RHOG*) (570-572). Other common genes play a role in cell cycle such as *ARF1, HDLBP,* and *BOP1* (573-575). Although a limited number of DEGs were shared between these studies, both revealed a robust number of down-regulated genes that were involved in neuronal function, which suggests that both viral entry and viral reactivation cause neuronal damage but may affect different neuronal functions.

In summary, this study provides additional evidence that supports a critical role of T cells in the prevention of herpes zoster. However, this study showed that T cell senescence by itself is not sufficient, as stress was required to induce reactivation and renewed viremia. This study is also the first to characterize the gene expression changes that occur after SVV reactivation. Remarkably, neuronal genes were altered nearly a year since reactivation, suggesting that SVV reactivations results in sustained remodeling of the ganglia transcriptome. These results provide potential insight into the development of post-herpetic neuralgia caused by neuronal damage that can last for years (576).

CHAPTER 6: Discussion and Future Directions

VZV is a neurotropic alpha herpes virus and the causative agent of varicella during primary infection. Like other herpes viruses, VZV establishes latency in the sensory ganglia and can reactive to cause herpes zoster. Although varicella and herpes zoster are not life threatening in an immune competent host, they can cause significant morbidities and sometimes mortality in the elderly and immune compromised. Due to its strict host specificity, VZV infection in laboratory animals does recapitulate the hallmarks of disease seen in humans. This has resulted in a limited understanding of host pathogen interactions that occur during acute infection and reactivation and hindered the development of better vaccines. The currently approved vaccine for varicella requires two doses and the vaccine against HZ is only 51% efficacious. Moreover, both vaccines are contradicted for people who are immunosuppressed. In contrast, intrabronchial infection of rhesus macaques with the homologous SVV provides a robust animal model of VZV because it mimics the disease hallmarks seen in humans. Using this animal model, the goals of this dissertation were to characterize the kinetics of the host response to SVV during acute infection, uncover mechanisms of virus dissemination, and finally to determine the role that cellular immunity plays in preventing reactivation.

6.1.1 SVV infection causes significant lung inflammation and lung injury

In Chapter 2, we characterized the host response during acute infection in the lungs using immunohistochemistry, flow cytometry, multiplex ELISA and RNA-Sequencing. We report that: 1) SVV replicates in both the lung tissue and the BAL quickly spreading from the infected to the uninfected lobe; 2) SVV elicits a robust immune response characterized by immune infiltrates most notably cytolytic CD8 T cells which play a critical role in killing virally infected cells, as well as the production of cytokines, chemokines and growth factors; and 3) large gene expression

changes in interferon stimulated genes, granzymes and cytokines. Acute varicella also results in severe lung damage, which was evident through severe focal hemorrhaging and broken alveolar walls; and further confirmed by the down-regulation of genes important for lung development. The peak immune responses correlated with decreased SVV viral loads and increased expression of cell cycle genes and growth factors, indicative of tissue repair. In summary, data presented in chapter 2 provide novel insight into the mechanisms by which acute VZV infection can result in pneumonia. These data show for the first time although acute varicella usually results in a self-limiting disease, significant lung injury occurs as a result of both the immune response and viral replication. These results may guide efforts to the development of better therapeutics against respiratory viral infections. An example of new strategies that can be developed using our data include generating antibodies against highly up-regulated gene products in order to dampen the robust immune response without interfering with viral clearance thereby reducing lung damage. Future studies will include characterizing the gene expression changes in the lung of immune-compromised RM in order to determine the specific genes that are responsible for causing severe pneumonia.

6.1.2 SVV reaches the site of latency before the appearance of rash

In Chapter 3, we characterized the kinetics by which SVV reaches the ganglia (site of latency) as well as host response to SVV infection in the sensory ganglia during acute and latent infection. Ganglia tissue was collected from naïve animals and infected animals on days 3, 7, 10, 14 and 100-post infection. In order to determine when SVV reaches the ganglia and establishes latency, we measured SVV DNA viral loads and viral transcription. Our analysis revealed that SVV DNA could be detected as early as 3 DPI, before the appearance of the rash (typically seen on 7-10 DPI). These data supported a hematogenous spread of SVV to the ganglia. Furthermore, viral

transcript analysis revealed that SVV replicates in the ganglia before establishing latency at 7 DPI. We also detected an infiltration of T cells into the ganglia at 3 DPI, suggesting that T cells may be responsible for disseminating SVV into the ganglia. Indeed, BAL CD4 and CD8 T cells isolated from the same animals 3 DPI were shown to harbor SVV DNA and transcripts. In the ganglia, SVV induced a local immune response that was characterized by increased expression of ISGs, chemokines and an infiltration of T cells. We also report significant changes in the expression of genes that play an important role in neuronal function. Importantly, these changes persist long after viral replication ceases. Future studies will determine if any innate immune cells also infiltrate the ganglia during acute infection.

This was the first study to characterize the gene expression changes that occur in the ganglia during acute infection and latency. Given the homology between SVV and VZV, and the genetic and physiological similarities between rhesus macaques and humans, our results provide novel insight into VZV tropism into the ganglia, and how the immune response in the sensory ganglia may initiate latency. Furthermore, the down-regulation of neuronal genes may explain some of the neurological consequences of VZV infection. Future studies will be aimed at confirming whether T cells that infiltrate the ganglia are infected with SVV and whether the origin of these gene expression changes that we saw in the ganglia are from the infiltrating T cells or from the sensory ganglia cells. We will utilize single cell RNA sequencing to determine frequency of infected T cells that infiltrate the ganglia 3 DPI and the transcriptional changes within these cells induced by SVV infection.

Moreover, studies described in this chapter identified a number of viral transcripts highly expressed during acute infection and latency in the ganglia (Fig. 3.4). One of the main limitations of the currently approved vaccine for varicella is that it still establishes latency in the ganglia and can reactivate in immune compromised individuals to cause zoster albeit at a much reduced frequency. Future studies will use these data to develop subunit vaccines or attenuated vaccine strains that may not be able to establish latency or reactivate. We can test the immunogenicity and efficacy of SVV knockout viruses as well as their ability to reactivate under conditions of immune suppression *in vivo*.

6.1.3 SVV induces transcriptional changes T cells in order to support viral replication

Studies described in chapter 3 of this dissertation and earlier in vitro studies using VZV and tonsillar T cells have shown that T cells are the preferential targets for SVV/VZV and play a crucial role in disseminating them to the skin and ganglia (37, 86, 194, 223). In chapter 4, our goal was to characterize the transcriptional changes that SVV produces in T cells. We performed RNA-Seq on CD4 and CD8 T cells isolated from the BAL of animals acutely infected with SVV and controls. Our results show that SVV up-regulates genes that enriched to chromatin assembly, translation, and T cell activation processes. Down-regulated genes enriched to antigen presentation, inflammatory and metabolic processes. These gene expression changes may create advantageous conditions that support replication and possibly dissemination of SVV. Other gene expression changes were indicative of viral immune evasion strategies as well as host defense. However, we were not able to confirm whether the transcriptional changes in the infected T cell population were originating from SVV-infected T cells or by bystander T cells responding to infection. Therefore, future studies will utilize single cell RNA-Sequencing to decipher SVV induced changes in the infected T cells from bystander T cells. Results from these additional

studies could reveal how VZV is able to successfully infect T cells and alter their behavior to facilitate their migration to the skin and ganglia. This could ultimately lead to the design of targeted therapeutics such as antibodies or siRNA that block a specific receptor or expression of genes critical for T cell dissemination.

6.1.4 Both CD4 and CD8 T cells play a critical role in preventing reactivation

In Chapter 5, we investigated the role of T cells in the prevention of SVV reactivation. Latently infected RMs were thymectomized and then depleted of either their CD4 or CD8 T cells to determine the role that each subset plays in preventing reactivation. Shortly after inducing environmental stress, SVV reactivation (viremia without rash) was observed in both CD4 and CD8 depleted animals. This suggested that both subsets played a critical role in prevention of SVV reactivation. After a year since the subclinical reactivations, we performed RNA sequencing on the ganglia from the animals that experienced SVV reactivations and compared that to animals that didn't experience reactivation. Transcriptional profiles of ganglia from animals that experienced a reactivation were distinct from those obtained from animals that did not experience reactivation. Most differentially expressed genes were down-regulated and found to be important for neuronal function. These data suggest that reactivation leads to long-term changes in neuronal function in the sensory ganglia. These results provide potential insight into the reasons why VZV reactivation can result in long lasting nerve pain after reactivation, often referred to as post herpetic neuralgia (PHN). Future studies will include analyzing the gene expression changes in the ganglia immediately after reactivation and utilizing more aggressive immunosuppressive treatments that may result in reactivation with zoster rash so that we can better determine the changes in immune response surrounding SVV/VZV reactivation.

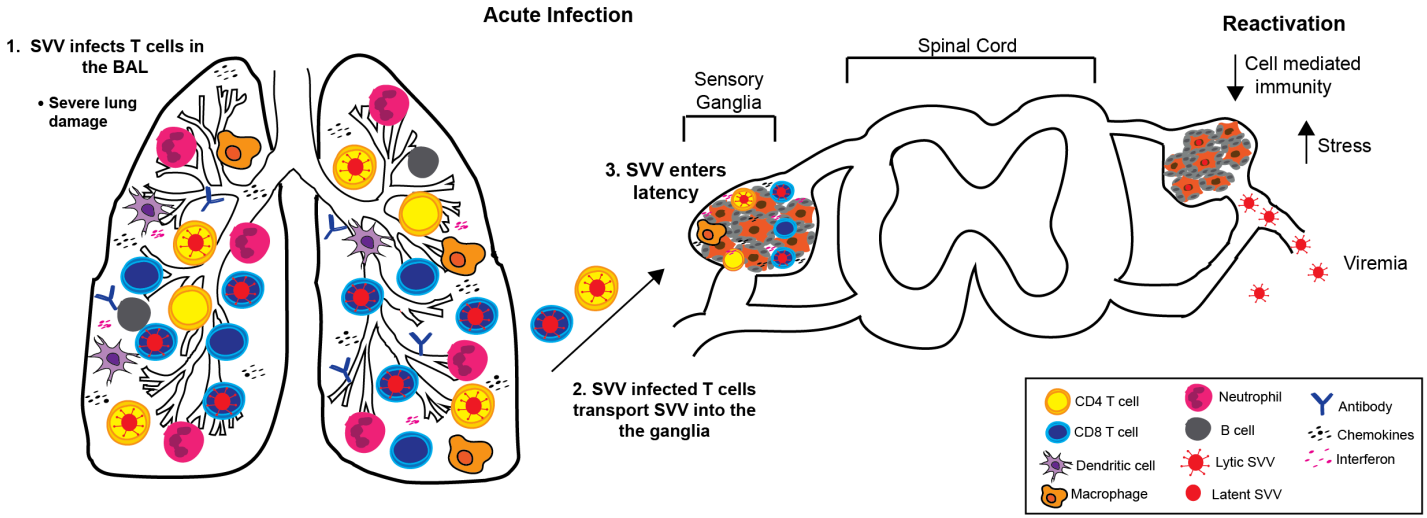
Acute Infection
1. SVV infects T cells in the BAL
• Severe lung damage
2. SVV infected T cells transport SVV into the the ganglia
3. SVV enters latency
Sensory Ganglia
Spinal Cord
Reactivation
Cell mediated immunity
Stress
Viremia
CD4 T cell
CD8 T cell
Dendritic cell
Macrophage
Neutrophil
B cell
Lytic SVV
Latent SVV
Antibody
Chemokines
Interferon

(Previous page) Figure 6.1 SVV pathogenesis in a rhesus macaque. Intrabronchial infection of SVV results in severe lung damage due to viral replication and mass infiltration of immune cells, along with the secretion of interferon's and cytokines. Soon after intrabronchial infection, SVV is carried into the ganglia via T cells from the lungs. SVV entry into the ganglia elicits a robust innate immune response mediated by satellite glial cells and SVV enters latency soon after. With the decline in cell mediated immunity and increase in stress, SVV can reactivate and cause viremia.

6.2 Final thoughts

The data presented in this dissertation provides novel insights into SVV-host interactions in the lungs and ganglia. These crucial sites of infections have not been extensively studied because of the difficulties in accessing them in humans infected with VZV. Therefore, this body of data significantly adds to our understanding of VZV pathogenesis and will guide future studies that can aid in the design of targeted therapeutics and vaccines.

REFERENCES

1. **Cohen JI.** 2010. The varicella-zoster virus genome. Curr Top Microbiol Immunol **342:**1-14.

2. **Zhang Z, Selariu A, Warden C, Huang G, Huang Y, Zaccheus O, Cheng T, Xia N, Zhu H.** 2010. Genome-wide mutagenesis reveals that ORF7 is a novel VZV skin-tropic factor. PLoS Pathog **6:**e1000971.

3. **Visalli MA, House BL, Selariu A, Zhu H, Visalli RJ.** 2014. The Varicella-Zoster Virus Portal Protein is Essential for Cleavage and Packaging of Viral DNA. J Virol doi:10.1128/JVI.00376-14.

4. **Campadelli-Fiume G, Menotti L.** 2007. Entry of alphaherpesviruses into the cell. *In* Arvin A, Campadelli-Fiume G, Mocarski E, Moore PS, Roizman B, Whitley R, Yamanishi K (ed), Human Herpesviruses: Biology, Therapy, and Immunoprophylaxis, Cambridge.

5. **Zhu Z, Gershon MD, Ambron R, Gabel C, Gershon AA.** 1995. Infection of cells by varicella zoster virus: inhibition of viral entry by mannose 6-phosphate and heparin. Proc Natl Acad Sci U S A **92:**3546-3550.

6. **Yang M, Hay J, Ruyechan WT.** 2008. Varicella-zoster virus IE62 protein utilizes the human mediator complex in promoter activation. J Virol **82:**12154-12163.

7. **Reichelt M, Brady J, Arvin AM.** 2009. The replication cycle of varicella-zoster virus: analysis of the kinetics of viral protein expression, genome synthesis, and virion assembly at the single-cell level. J Virol **83:**3904-3918.

8. **Schmader K.** 2001. Herpes zoster in older adults. Clin Infect Dis **32:**1481-1486.

9. **Zerboni L, Sen N, Oliver SL, Arvin AM.** 2014. Molecular mechanisms of varicella zoster virus pathogenesis. Nat Rev Microbiol **12:**197-210.

10. **Arvin AM.** 2001. Varicella-zoster virus: molecular virology and virus-host interactions. Curr Opin Microbiol **4:**442-449.

11. **Grose C.** 1981. Immunization of inbred guinea pigs with varicella-zoster virus grown in a syngeneic transformed embryo cell line. J Clin Microbiol **14:**229-231.

12. **Cohen JI.** 2001. Mutagenesis of the varicella-zoster virus genome: lessons learned. Arch Virol Suppl**:**91-97.

13. **Grose C.** 1981. Variation on a theme by Fenner: the pathogenesis of chickenpox. Pediatrics **68:**735-737.

14. **Leonid I, Evelyn L.** 2009. Primary varicella in an immunocompetent adult. J Clin Aesthet Dermatol **2:**36-38.

15. **Mueller NH, Gilden DH, Cohrs RJ, Mahalingam R, Nagel MA.** 2008. Varicella zoster virus infection: clinical features, molecular pathogenesis of disease, and latency. Neurol Clin **26:**675-697, viii.

16. **Gnann JW, Jr.** 2002. Varicella-zoster virus: atypical presentations and unusual complications. J Infect Dis **186 Suppl 1:**S91-98.

17. **Wiegering V, Schick J, Beer M, Weissbrich B, Gattenlohner S, Girschick HJ, Liese J, Schlegel PG, Eyrich M.** 2011. Varicella-zoster virus infections in immunocompromised patients - a single centre 6-years analysis. BMC Pediatr **11:**31.

18. **Marin M, Watson TL, Chaves SS, Civen R, Watson BM, Zhang JX, Perella D, Mascola L, Seward JF.** 2008. Varicella among adults: data from an active surveillance project, 1995-2005. J Infect Dis **197 Suppl 2:**S94-S100.

19. **Paul R, Singhania P, Hashmi M, Bandyopadhyay R, Banerjee AK.** 2010. Post chicken pox neurological sequelae: Three distinct presentations. J Neurosci Rural Pract **1:**92-96.

20. **Guess HA, Broughton DD, Melton LJ, 3rd, Kurland LT.** 1986. Population-based studies of varicella complications. Pediatrics **78:**723-727.

21. **Bozzola E, Bozzola M, Tozzi AE, Calcaterra V, Longo D, Krzystofiak A, Villani A.** 2014. Acute cerebellitis in varicella: a ten year case series and systematic review of the literature. Ital J Pediatr **40:**57.

22. **van der Maas NA, Bondt PE, de Melker H, Kemmeren JM.** 2009. Acute cerebellar ataxia in the Netherlands: a study on the association with vaccinations and varicella zoster infection. Vaccine **27:**1970-1973.

23. **Askalan R, Laughlin S, Mayank S, Chan A, MacGregor D, Andrew M, Curtis R, Meaney B, deVeber G.** 2001. Chickenpox and stroke in childhood: a study of frequency and causation. Stroke **32:**1257-1262.

24. **Gershon AA.** 2013. Strokes and Infection With Varicella Zoster Virus. Clin Infect Dis doi:10.1093/cid/cit663.

25. **Ramachandra S, Metta AK, Haneef NS, Kodali S.** 2010. Fetal varicella syndrome. Indian J Dermatol Venereol Leprol **76:**724.

26. **Bruder E, Ersch J, Hebisch G, Ehrbar T, Klimkait T, Stallmach T.** 2000. Fetal varicella syndrome: disruption of neural development and persistent inflammation of non-neural tissues. Virchows Arch **437:**440-444.

27. **Cohen J, Breuer J.** 2015. Chickenpox: treatment. BMJ Clin Evid **2015**.

28. **Gilden DH, Vafai A, Shtram Y, Becker Y, Devlin M, Wellish M.** 1983. Varicella-zoster virus DNA in human sensory ganglia. Nature **306:**478-480.

29. **Sloutskin A, Yee MB, Kinchington PR, Goldstein RS.** 2014. Varicella zoster virus and herpes simplex virus type 1 can infect and replicate in the same neurons whether co- or superinfected. J Virol doi:10.1128/JVI.00252-14.

30. **Hanani M.** 2005. Satellite glial cells in sensory ganglia: from form to function. Brain Res Brain Res Rev **48:**457-476.

31. **Chen JJ, Gershon AA, Li Z, Cowles RA, Gershon MD.** 2011. Varicella zoster virus (VZV) infects and establishes latency in enteric neurons. J Neurovirol **17:**578-589.

32. **Rao M, Gershon MD.** 2016. The bowel and beyond: the enteric nervous system in neurological disorders. Nat Rev Gastroenterol Hepatol **13:**517-528.

33. **Bearer EL, Breakefield XO, Schuback D, Reese TS, LaVail JH.** 2000. Retrograde axonal transport of herpes simplex virus: evidence for a single mechanism and a role for tegument. Proc Natl Acad Sci U S A **97:**8146-8150.

34. **Eshleman E, Shahzad A, Cohrs RJ.** 2011. Varicella zoster virus latency. Future Virol **6:**341-355.

35. **Arvin AM, Moffat JF, Sommer M, Oliver S, Che X, Vleck S, Zerboni L, Ku CC.** 2010. Varicella-zoster virus T cell tropism and the pathogenesis of skin infection. Curr Top Microbiol Immunol **342:**189-209.

36. **Moffat JF, Zerboni L, Sommer MH, Heineman TC, Cohen JI, Kaneshima H, Arvin AM.** 1998. The ORF47 and ORF66 putative protein kinases of varicella-zoster virus determine tropism for human T cells and skin in the SCID-hu mouse. Proc Natl Acad Sci U S A **95:**11969-11974.

37. **Ku CC, Padilla JA, Grose C, Butcher EC, Arvin AM.** 2002. Tropism of varicella-zoster virus for human tonsillar CD4(+) T lymphocytes that express activation, memory, and skin homing markers. J Virol **76:**11425-11433.

38. **Ku CC, Zerboni L, Ito H, Graham BS, Wallace M, Arvin AM.** 2004. Varicella-zoster virus transfer to skin by T Cells and modulation of viral replication by epidermal cell interferon-alpha. J Exp Med **200:**917-925.

39. **Abendroth A, Morrow G, Cunningham AL, Slobedman B.** 2001. Varicella-zoster virus infection of human dendritic cells and transmission to T cells: implications for virus dissemination in the host. J Virol **75:**6183-6192.

40. **Sen N, Mukherjee G, Sen A, Bendall SC, Sung P, Nolan GP, Arvin AM.** 2014. Single-cell mass cytometry analysis of human tonsil T cell remodeling by varicella zoster virus. Cell Rep **8:**633-645.

41. **Sen N, Arvin AM.** 2016. Dissecting the Molecular Mechanisms of the Tropism of Varicella-Zoster Virus for Human T Cells. J Virol **90:**3284-3287.

42. **Lungu O, Annunziato PW, Gershon A, Staugaitis SM, Josefson D, LaRussa P, Silverstein SJ.** 1995. Reactivated and latent varicella-zoster virus in human dorsal root ganglia. Proc Natl Acad Sci U S A **92:**10980-10984.

43. **Clarke P, Beer T, Cohrs R, Gilden DH.** 1995. Configuration of latent varicella-zoster virus DNA. J Virol **69:**8151-8154.

44. **Cohrs R, Mahalingam R, Dueland AN, Wolf W, Wellish M, Gilden DH.** 1992. Restricted transcription of varicella-zoster virus in latently infected human trigeminal and thoracic ganglia. J Infect Dis **166 Suppl 1:**S24-29.

45. **Cohrs RJ, Barbour M, Gilden DH.** 1996. Varicella-zoster virus (VZV) transcription during latency in human ganglia: detection of transcripts mapping to genes 21, 29, 62, and 63 in a cDNA library enriched for VZV RNA. J Virol **70:**2789-2796.

46. **Kennedy PG, Grinfeld E, Gow JW.** 1999. Latent Varicella-zoster virus in human dorsal root ganglia. Virology **258:**451-454.

47. **Cohrs RJ, Gilden DH, Kinchington PR, Grinfeld E, Kennedy PG.** 2003. Varicella-zoster virus gene 66 transcription and translation in latently infected human Ganglia. J Virol **77:**6660-6665.

48. **Lungu O, Panagiotidis CA, Annunziato PW, Gershon AA, Silverstein SJ.** 1998. Aberrant intracellular localization of Varicella-Zoster virus regulatory proteins during latency. Proc Natl Acad Sci U S A **95:**7080-7085.

49. **Kennedy PG, Grinfeld E, Traina-Dorge V, Gilden DH, Mahalingam R.** 2004. Neuronal localization of simian varicella virus DNA in ganglia of naturally infected African green monkeys. Virus Genes **28:**273-276.

50. **Cohen JI, Cox E, Pesnicak L, Srinivas S, Krogmann T.** 2004. The varicella-zoster virus open reading frame 63 latency-associated protein is critical for establishment of latency. J Virol **78:**11833-11840.

51. **Cohen JI, Krogmann T, Ross JP, Pesnicak L, Prikhod'ko EA.** 2005. Varicella-zoster virus ORF4 latency-associated protein is important for establishment of latency. J Virol **79:**6969-6975.

52. **Hood C, Cunningham AL, Slobedman B, Arvin AM, Sommer MH, Kinchington PR, Abendroth A.** 2006. Varicella-zoster virus ORF63 inhibits apoptosis of primary human neurons. J Virol **80:**1025-1031.

53. **Kruger P, Saffarzadeh M, Weber AN, Rieber N, Radsak M, von Bernuth H, Benarafa C, Roos D, Skokowa J, Hartl D.** 2015. Neutrophils: Between host defence, immune modulation, and tissue injury. PLoS Pathog **11:**e1004651.

54. **Hogan SP, Rosenberg HF, Moqbel R, Phipps S, Foster PS, Lacy P, Kay AB, Rothenberg ME.** 2008. Eosinophils: biological properties and role in health and disease. Clin Exp Allergy **38:**709-750.

55. **Banchereau J, Steinman RM.** 1998. Dendritic cells and the control of immunity. Nature **392:**245-252.

56. **Pyzik M, Vidal SM.** 2009. Natural killer cells: NK cells stroll down the memory lane. Immunol Cell Biol **87:**261-263.

57. **Chaplin DD.** 2010. Overview of the immune response. J Allergy Clin Immunol **125:**S3-23.

58. **Mosmann TR, Sad S.** 1996. The expanding universe of T-cell subsets: Th1, Th2 and more. Immunol Today **17:**138-146.

59. **Del Prete G, Maggi E, Romagnani S.** 1994. Human Th1 and Th2 cells: functional properties, mechanisms of regulation, and role in disease. Lab Invest **70:**299-306.

60. **Gagliani N, Amezcua Vesely MC, Iseppon A, Brockmann L, Xu H, Palm NW, de Zoete MR, Licona-Limon P, Paiva RS, Ching T, Weaver C, Zi X, Pan X, Fan R, Garmire LX, Cotton MJ, Drier Y, Bernstein B, Geginat J, Stockinger B, Esplugues E, Huber S, Flavell RA.** 2015. Th17 cells transdifferentiate into regulatory T cells during resolution of inflammation. Nature **523:**221-225.

61. **Hale JS, Ahmed R.** 2015. Memory T follicular helper CD4 T cells. Front Immunol **6:**16.

62. **Milstein O, Hagin D, Lask A, Reich-Zeliger S, Shezen E, Ophir E, Eidelstein Y, Afik R, Antebi YE, Dustin ML, Reisner Y.** 2011. CTLs respond with activation and granule secretion when serving as targets for T-cell recognition. Blood **117:**1042-1052.

63. **Harty JT, Tvinnereim AR, White DW.** 2000. CD8+ T cell effector mechanisms in resistance to infection. Annu Rev Immunol **18:**275-308.

64. **Biron CA, Byron KS, Sullivan JL.** 1989. Severe herpesvirus infections in an adolescent without natural killer cells. N Engl J Med **320:**1731-1735.

65. **Etzioni A, Eidenschenk C, Katz R, Beck R, Casanova JL, Pollack S.** 2005. Fatal varicella associated with selective natural killer cell deficiency. J Pediatr **146:**423-425.

66. **Yawn BP, Wollan PC, Kurland MJ, St Sauver JL, Saddier P.** 2011. Herpes zoster recurrences more frequent than previously reported. Mayo Clin Proc **86:**88-93.

67. **Vossen MT, Biezeveld MH, de Jong MD, Gent MR, Baars PA, von Rosenstiel IA, van Lier RA, Kuijpers TW.** 2005. Absence of circulating natural killer and primed CD8+ cells in life-threatening varicella. J Infect Dis **191:**198-206.

68. **Levy O, Orange JS, Hibberd P, Steinberg S, LaRussa P, Weinberg A, Wilson SB, Shaulov A, Fleisher G, Geha RS, Bonilla FA, Exley M.** 2003. Disseminated varicella

infection due to the vaccine strain of varicella-zoster virus, in a patient with a novel deficiency in natural killer T cells. J Infect Dis **188:**948-953.

69. **Arvin AM, Kushner JH, Feldman S, Baehner RL, Hammond D, Merigan TC.** 1982. Human leukocyte interferon for the treatment of varicella in children with cancer. N Engl J Med **306:**761-765.

70. **Arvin AM, Koropchak CM, Williams BR, Grumet FC, Foung SK.** 1986. Early immune response in healthy and immunocompromised subjects with primary varicella-zoster virus infection. J Infect Dis **154:**422-429.

71. **Buchbinder SP, Katz MH, Hessol NA, Liu JY, O'Malley PM, Underwood R, Holmberg SD.** 1992. Herpes zoster and human immunodeficiency virus infection. J Infect Dis **166:**1153-1156.

72. **Jura E, Chadwick EG, Josephs SH, Steinberg SP, Yogev R, Gershon AA, Krasinski KM, Borkowsky W.** 1989. Varicella-zoster virus infections in children infected with human immunodeficiency virus. Pediatr Infect Dis J **8:**586-590.

73. **Weinberg A, Lazar AA, Zerbe GO, Hayward AR, Chan IS, Vessey R, Silber JL, MacGregor RR, Chan K, Gershon AA, Levin MJ.** 2010. Influence of age and nature of primary infection on varicella-zoster virus-specific cell-mediated immune responses. J Infect Dis **201:**1024-1030.

74. **Torigoe S, Ihara T, Kamiya H.** 2000. IL-12, IFN-gamma and TNF-alpha released from mononuclear cells inhibit the spread of varicella-zoster virus at an early stage of varicella. Microbiology and Immunology **44:**1027-1031.

75. **Wallace MR, Woelfl I, Bowler WA, Olson PE, Murray NB, Brodine SK, Oldfield EC, 3rd, Arvin AM.** 1994. Tumor necrosis factor, interleukin-2, and interferon-gamma in adult varicella. J Med Virol **43:**69-71.

76. **Sadzot-Delvaux C, Kinchington PR, Debrus S, Rentier B, Arvin AM.** 1997. Recognition of the latency-associated immediate early protein IE63 of varicella-zoster virus by human memory T lymphocytes. J Immunol **159:**2802-2806.

77. **Arvin AM, Sharp M, Moir M, Kinchington PR, Sadeghi-Zadeh M, Ruyechan WT, Hay J.** 2002. Memory cytotoxic T cell responses to viral tegument and regulatory proteins encoded by open reading frames 4, 10, 29, and 62 of varicella-zoster virus. Viral Immunol **15:**507-516.

78. **Malavige GN, Jones L, Black AP, Ogg GS.** 2007. Rapid effector function of varicella-zoster virus glycoprotein I-specific CD4+ T cells many decades after primary infection. J Infect Dis **195:**660-664.

79. **Malavige GN, Jones L, Black AP, Ogg GS.** 2008. Varicella zoster virus glycoprotein E-specific CD4+ T cells show evidence of recent activation and effector differentiation,

consistent with frequent exposure to replicative cycle antigens in healthy immune donors. Clin Exp Immunol **152:**522-531.

80. **Arvin AM.** 1996. Varicella-zoster virus. Clin Microbiol Rev **9:**361-381.

81. **Ceroni A, Sibani S, Baiker A, Pothineni VR, Bailer SM, LaBaer J, Haas J, Campbell CJ.** 2010. Systematic analysis of the IgG antibody immune response against varicella zoster virus (VZV) using a self-assembled protein microarray. Mol Biosyst **6:**1604-1610.

82. **Good RA, Zak SJ.** 1956. Disturbances in gamma globulin synthesis as experiments of nature. Pediatrics **18:**109-149.

83. **Centers for Disease C, Prevention.** 2013. Updated recommendations for use of VariZIG--United States, 2013. MMWR Morb Mortal Wkly Rep **62:**574-576.

84. **Ku C-C, Zerboni L, Ito H, Graham BS, Wallace M, Arvin AM.** 2004. Varicella-Zoster Virus Transfer to Skin by T Cells and Modulation of Viral Replication by Epidermal Cell Interferon-{alpha}. J Exp Med **200:**917-925.

85. **Ambagala AP, Cohen JI.** 2007. Varicella-Zoster virus IE63, a major viral latency protein, is required to inhibit the alpha interferon-induced antiviral response. J Virol **81:**7844-7851.

86. **Schaap A, Fortin JF, Sommer M, Zerboni L, Stamatis S, Ku CC, Nolan GP, Arvin AM.** 2005. T-cell tropism and the role of ORF66 protein in pathogenesis of varicella-zoster virus infection. J Virol **79:**12921-12933.

87. **Zhu H, Zheng C, Xing J, Wang S, Li S, Lin R, Mossman KL.** 2011. Varicella-zoster virus immediate-early protein ORF61 abrogates the IRF3-mediated innate immune response through degradation of activated IRF3. J Virol **85:**11079-11089.

88. **Sloan E, Henriquez R, Kinchington PR, Slobedman B, Abendroth A.** 2012. Varicella-zoster virus inhibition of the NF-kappaB pathway during infection of human dendritic cells: role for open reading frame 61 as a modulator of NF-kappaB activity. J Virol **86:**1193-1202.

89. **Jones JO, Arvin AM.** 2006. Inhibition of the NF-kappaB pathway by varicella-zoster virus in vitro and in human epidermal cells in vivo. J Virol **80:**5113-5124.

90. **Nikkels AF, Sadzot-Delvaux C, Pierard GE.** 2004. Absence of intercellular adhesion molecule 1 expression in varicella zoster virus-infected keratinocytes during herpes zoster: another immune evasion strategy? Am J Dermatopathol **26:**27-32.

91. **Wang W, Wang X, Yang L, Fu W, Pan D, Liu J, Ye J, Zhao Q, Zhu H, Cheng T, Xia N.** 2016. Modulation of host CD59 expression by varicella-zoster virus in human xenografts in vivo. Virology **491:**96-105.

92. **Abendroth A, Lin I, Slobedman B, Ploegh H, Arvin AM.** 2001. Varicella-zoster virus retains major histocompatibility complex class I proteins in the Golgi compartment of infected cells. J Virol **75:**4878-4888.

93. **Eisfeld AJ, Yee MB, Erazo A, Abendroth A, Kinchington PR.** 2007. Downregulation of Class I Major Histocompatibility Complex Surface Expression by Varicella-Zoster Virus Involves Open Reading Frame 66 Protein Kinase-Dependent and -Independent Mechanisms. J Virol **81:**9034-9049.

94. **Abendroth A, Slobedman B, Lee E, Mellins E, Wallace M, Arvin AM.** 2000. Modulation of major histocompatibility class II protein expression by varicella-zoster virus. J Virol **74:**1900-1907.

95. **Black AP, Jones L, Malavige GN, Ogg GS.** 2009. Immune evasion during varicella zoster virus infection of keratinocytes. Clin Exp Dermatol **34:**e941-944.

96. **Morrow G, Slobedman B, Cunningham AL, Abendroth A.** 2003. Varicella-zoster virus productively infects mature dendritic cells and alters their immune function. J Virol **77:**4950-4959.

97. **Hu H, Cohen JI.** 2005. Varicella-zoster virus open reading frame 47 (ORF47) protein is critical for virus replication in dendritic cells and for spread to other cells. Virology **337:**304-311.

98. **Takahashi M, Otsuka T, Okuno Y, Asano Y, Yazaki T.** 1974. Live vaccine used to prevent the spread of varicella in children in hospital. Lancet **2:**1288-1290.

99. **Gomi Y, Sunamachi H, Mori Y, Nagaike K, Takahashi M, Yamanishi K.** 2002. Comparison of the complete DNA sequences of the Oka varicella vaccine and its parental virus. J Virol **76:**11447-11459.

100. **Davis MM, Patel MS, Gebremariam A.** 2004. Decline in varicella-related hospitalizations and expenditures for children and adults after introduction of varicella vaccine in the United States. Pediatrics **114:**786-792.

101. **Zhou F, Harpaz R, Jumaan AO, Winston CA, Shefer A.** 2005. Impact of varicella vaccination on health care utilization. Jama **294:**797-802.

102. **Preblud SR, Orenstein WA, Bart KJ.** 1984. Varicella: clinical manifestations, epidemiology and health impact in children. Pediatr Infect Dis **3:**505-509.

103. **Marin M, Guris D, Chaves SS, Schmid S, Seward JF.** 2007. Prevention of varicella: recommendations of the Advisory Committee on Immunization Practices (ACIP). MMWR Recomm Rep **56:**1-40.

104. **Chaves SS, Gargiullo P, Zhang JX, Civen R, Guris D, Mascola L, Seward JF.** 2007. Loss of vaccine-induced immunity to varicella over time. N Engl J Med **356:**1121-1129.

105. **Lopez AS, Guris D, Zimmerman L, Gladden L, Moore T, Haselow DT, Loparev VN, Schmid DS, Jumaan AO, Snow SL.** 2006. One dose of varicella vaccine does not prevent school outbreaks: is it time for a second dose? Pediatrics **117:**e1070-1077.

106. **Shapiro ED, Vazquez M, Esposito D, Holabird N, Steinberg SP, Dziura J, LaRussa PS, Gershon AA.** 2011. Effectiveness of 2 doses of varicella vaccine in children. J Infect Dis **203:**312-315.

107. **Seward JF, Marin M, Vazquez M.** 2008. Varicella vaccine effectiveness in the US vaccination program: a review. J Infect Dis **197 Suppl 2:**S82-89.

108. **Nader S, Bergen R, Sharp M, Arvin AM.** 1995. Age-related differences in cell-mediated immunity to varicella-zoster virus among children and adults immunized with live attenuated varicella vaccine. J Infect Dis **171:**13-17.

109. **Habermehl P, Lignitz A, Knuf M, Schmitt HJ, Slaoui M, Zepp F.** 1999. Cellular immune response of a varicella vaccine following simultaneous DTaP and VZV vaccination. Vaccine **17:**669-674.

110. **Watson B, Rothstein E, Bernstein H, Arbeter A, Arvin A, Chartrand S, Clements D, Kumar ML, Reisinger K, Blatter M, et al.** 1995. Safety and cellular and humoral immune responses of a booster dose of varicella vaccine 6 years after primary immunization. J Infect Dis **172:**217-219.

111. **Zerboni L, Nader S, Aoki K, Arvin AM.** 1998. Analysis of the persistence of humoral and cellular immunity in children and adults immunized with varicella vaccine. J Infect Dis **177:**1701-1704.

112. **Kuter B, Matthews H, Shinefield H, Black S, Dennehy P, Watson B, Reisinger K, Kim LL, Lupinacci L, Hartzel J, Chan I.** 2004. Ten year follow-up of healthy children who received one or two injections of varicella vaccine. Pediatr Infect Dis J **23:**132-137.

113. **Grossberg R, Harpaz R, Rubtcova E, Loparev V, Seward JF, Schmid DS.** 2006. Secondary transmission of varicella vaccine virus in a chronic care facility for children. J Pediatr **148:**842-844.

114. **Levin MJ, Gershon AA, Weinberg A, Song LY, Fentin T, Nowak B.** 2006. Administration of live varicella vaccine to HIV-infected children with current or past significant depression of CD4(+) T cells. J Infect Dis **194:**247-255.

115. **Gershon AA, Chen J, Davis L, Krinsky C, Cowles R, Reichard R, Gershon M.** 2012. Latency of varicella zoster virus in dorsal root, cranial, and enteric ganglia in vaccinated children. Trans Am Clin Climatol Assoc **123:**17-33; discussion 33-15.

116. **Krause PR, Klinman DM.** 2000. Varicella vaccination: evidence for frequent reactivation of the vaccine strain in healthy children. Nat Med **6:**451-454.

117. **Hardy I, Gershon AA, Steinberg SP, LaRussa P.** 1991. The incidence of zoster after immunization with live attenuated varicella vaccine. A study in children with leukemia. Varicella Vaccine Collaborative Study Group. N Engl J Med **325:**1545-1550.

118. **Weinberg A, Zhang JH, Oxman MN, Johnson GR, Hayward AR, Caulfield MJ, Irwin MR, Clair J, Smith JG, Stanley H, Marchese RD, Harbecke R, Williams HM, Chan IS, Arbeit RD, Gershon AA, Schodel F, Morrison VA, Kauffman CA, Straus SE, Schmader KE, Davis LE, Levin MJ.** 2009. Varicella-zoster virus-specific immune responses to herpes zoster in elderly participants in a trial of a clinically effective zoster vaccine. J Infect Dis **200:**1068-1077.

119. **Wareham DW, Breuer J.** 2007. Herpes zoster. BMJ **334:**1211-1215.

120. **Oxman MN.** 1995. Immunization to reduce the frequency and severity of herpes zoster and its complications. Neurology **45:**S41-46.

121. **Keating GM.** 2013. Shingles (herpes zoster) vaccine (zostavax((R))): a review of its use in the prevention of herpes zoster and postherpetic neuralgia in adults aged >/=50 years. Drugs **73:**1227-1244.

122. **Long MD, Martin C, Sandler RS, Kappelman MD.** 2013. Increased risk of herpes zoster among 108 604 patients with inflammatory bowel disease. Aliment Pharmacol Ther **37:**420-429.

123. **Zhang JX, Joesoef RM, Bialek S, Wang C, Harpaz R.** 2013. Association of physical trauma with risk of herpes zoster among Medicare beneficiaries in the United States. J Infect Dis **207:**1007-1011.

124. **Schmader K, George LK, Burchett BM, Hamilton JD, Pieper CF.** 1998. Race and stress in the incidence of herpes zoster in older adults. J Am Geriatr Soc **46:**973-977.

125. **Insinga RP, Itzler RF, Pellissier JM, Saddier P, Nikas AA.** 2005. The incidence of herpes zoster in a United States administrative database. J Gen Intern Med **20:**748-753.

126. **Fleming DM, Cross KW, Cobb WA, Chapman RS.** 2004. Gender difference in the incidence of shingles. Epidemiol Infect **132:**1-5.

127. **Opstelten W, Van Essen GA, Schellevis F, Verheij TJ, Moons KG.** 2006. Gender as an independent risk factor for herpes zoster: a population-based prospective study. Ann Epidemiol **16:**692-695.

128. **Ultsch B, Siedler A, Rieck T, Reinhold T, Krause G, Wichmann O.** 2011. Herpes zoster in Germany: quantifying the burden of disease. BMC Infect Dis **11:**173.

129. **Gialloreti LE, Merito M, Pezzotti P, Naldi L, Gatti A, Beillat M, Serradell L, di Marzo R, Volpi A.** 2010. Epidemiology and economic burden of herpes zoster and post-herpetic neuralgia in Italy: a retrospective, population-based study. BMC Infect Dis **10:**230.

130. **Schwab IR.** 1997. Herpes zoster sine herpete. A potential cause of iridoplegic granulomatous iridocyclitis. Ophthalmology **104:**1421-1425.

131. **Furuta Y, Ohtani F, Mesuda Y, Fukuda S, Inuyama Y.** 2000. Early diagnosis of zoster sine herpete and antiviral therapy for the treatment of facial palsy. Neurology **55:**708-710.

132. **Cohrs RJ, Mehta SK, Schmid DS, Gilden DH, Pierson DL.** 2008. Asymptomatic reactivation and shed of infectious varicella zoster virus in astronauts. J Med Virol **80:**1116-1122.

133. **Volpi A.** 2007. Severe complications of herpes zoster. Herpes **14 Suppl 2:**35-39.

134. **Liesegang TJ.** 2008. Herpes zoster ophthalmicus natural history, risk factors, clinical presentation, and morbidity. Ophthalmology **115:**S3-12.

135. **Gilden D, Cohrs RJ, Mahalingam R, Nagel MA.** 2009. Varicella zoster virus vasculopathies: diverse clinical manifestations, laboratory features, pathogenesis, and treatment. Lancet Neurol **8:**731-740.

136. **Gilden D, Nagel MA, Ransohoff RM, Cohrs RJ, Mahalingam R, Tanabe JL.** 2009. Recurrent varicella zoster virus myelopathy. J Neurol Sci **276:**196-198.

137. **Holland-Cunz S, Goppl M, Rauch U, Bar C, Klotz M, Schafer KH.** 2006. Acquired intestinal aganglionosis after a lytic infection with varicella-zoster virus. J Pediatr Surg **41:**e29-31.

138. **Johnson RW, Wasner G, Saddier P, Baron R.** 2008. Herpes zoster and postherpetic neuralgia: optimizing management in the elderly patient. Drugs Aging **25:**991-1006.

139. **Li Q, Chen N, Yang J, Zhou M, Zhou D, Zhang Q, He L.** 2009. Antiviral treatment for preventing postherpetic neuralgia. Cochrane Database Syst Rev doi:10.1002/14651858.CD006866.pub2**:**CD006866.

140. **Mehta N, Bucior I, Bujanover S, Shah R, Gulati A.** 2016. Relationship between pain relief, reduction in pain-associated sleep interference, and overall impression of improvement in patients with postherpetic neuralgia treated with extended-release gabapentin. Health Qual Life Outcomes **14:**54.

141. **Moore RA, Wiffen PJ, Derry S, Toelle T, Rice AS.** 2014. Gabapentin for chronic neuropathic pain and fibromyalgia in adults. Cochrane Database Syst Rev **4:**CD007938.

142. **Johnson RW, Rice AS.** 2014. Clinical practice. Postherpetic neuralgia. N Engl J Med **371:**1526-1533.

143. **Watson CP, Tyler KL, Bickers DR, Millikan LE, Smith S, Coleman E.** 1993. A randomized vehicle-controlled trial of topical capsaicin in the treatment of postherpetic neuralgia. Clin Ther **15:**510-526.

144. **Amanna IJ, Carlson NE, Slifka MK.** 2007. Duration of humoral immunity to common viral and vaccine antigens. N Engl J Med **357:**1903-1915.

145. **Levin MJ, Smith JG, Kaufhold RM, Barber D, Hayward AR, Chan CY, Chan IS, Li DJ, Wang W, Keller PM, Shaw A, Silber JL, Schlienger K, Chalikonda I, Vessey SJ, Caulfield MJ.** 2003. Decline in varicella-zoster virus (VZV)-specific cell-mediated immunity with increasing age and boosting with a high-dose VZV vaccine. J Infect Dis **188:**1336-1344.

146. **Asanuma H, Sharp M, Maecker HT, Maino VC, Arvin AM.** 2000. Frequencies of memory T cells specific for varicella-zoster virus, herpes simplex virus, and cytomegalovirus by intracellular detection of cytokine expression. J Infect Dis **181:**859-866.

147. **Malavige GN, Rohanachandra LT, Jones L, Crack L, Perera M, Fernando N, Guruge D, Ogg GS.** 2010. IE63-specific T-cell responses associate with control of subclinical varicella zoster virus reactivation in individuals with malignancies. Br J Cancer **102:**727-730.

148. **Steain M, Sutherland JP, Rodriguez M, Cunningham AL, Slobedman B, Abendroth A.** 2014. Analysis of T cell responses during active varicella-zoster virus reactivation in human ganglia. J Virol **88:**2704-2716.

149. **Steain M, Gowrishankar K, Rodriguez M, Slobedman B, Abendroth A.** 2011. Upregulation of CXCL10 in human dorsal root ganglia during experimental and natural varicella-zoster virus infection. J Virol **85:**626-631.

150. **Harpaz R, Ortega-Sanchez IR, Seward JF.** 2008. Prevention of herpes zoster: recommendations of the Advisory Committee on Immunization Practices (ACIP). MMWR Recomm Rep **57:**1-30; quiz CE32-34.

151. **Oxman MN, Levin MJ, Johnson GR, Schmader KE, Straus SE, Gelb LD, Arbeit RD, Simberkoff MS, Gershon AA, Davis LE, Weinberg A, Boardman KD, Williams HM, Zhang JH, Peduzzi PN, Beisel CE, Morrison VA, Guatelli JC, Brooks PA, Kauffman CA, Pachucki CT, Neuzil KM, Betts RF, Wright PF, Griffin MR, Brunell P, Soto NE, Marques AR, Keay SK, Goodman RP, Cotton DJ, Gnann JW, Jr., Loutit J, Holodniy M, Keitel WA, Crawford GE, Yeh SS, Lobo Z, Toney JF, Greenberg RN, Keller PM, Harbecke R, Hayward AR, Irwin MR, Kyriakides TC, Chan CY, Chan IS, Wang WW, Annunziato PW, Silber JL.** 2005. A vaccine to prevent herpes zoster and postherpetic neuralgia in older adults. N Engl J Med **352:**2271-2284.

152. **Sutradhar SC, Wang WW, Schlienger K, Stek JE, Xu J, Chan IS, Silber JL.** 2009. Comparison of the levels of immunogenicity and safety of Zostavax in adults 50 to 59 years old and in adults 60 years old or older. Clin Vaccine Immunol **16:**646-652.

153. **Administration USFaD.** 2011. FDA approves Zostavax vaccine to prevent shingles in individuals 50 to 59 years of age. wwwfdagovNewsEvents/Newsroom/PressAnnouncements/ucm248390htm.

154. **Morrison VA, Johnson GR, Schmader KE, Levin MJ, Zhang JH, Looney DJ, Betts R, Gelb L, Guatelli JC, Harbecke R, Pachucki C, Keay S, Menzies B, Griffin MR, Kauffman CA, Marques A, Toney J, Boardman K, Su SC, Li X, Chan IS, Parrino J, Annunziato P, Oxman MN, Shingles Prevention Study G.** 2015. Long-term persistence of zoster vaccine efficacy. Clin Infect Dis **60:**900-909.

155. **Levin MJ, Oxman MN, Zhang JH, Johnson GR, Stanley H, Hayward AR, Caulfield MJ, Irwin MR, Smith JG, Clair J, Chan IS, Williams H, Harbecke R, Marchese R, Straus SE, Gershon A, Weinberg A.** 2008. Varicella-zoster virus-specific immune responses in elderly recipients of a herpes zoster vaccine. J Infect Dis **197:**825-835.

156. **Laing KJ, Russell RM, Dong L, Schmid DS, Stern M, Magaret A, Haas JG, Johnston C, Wald A, Koelle DM.** 2015. Zoster Vaccination Increases the Breadth of CD4+ T Cells Responsive to Varicella Zoster Virus. J Infect Dis **212:**1022-1031.

157. **Jing L, Laing KJ, Dong L, Russell RM, Barlow RS, Haas JG, Ramchandani MS, Johnston C, Buus S, Redwood AJ, White KD, Mallal SA, Phillips EJ, Posavad CM, Wald A, Koelle DM.** 2016. Extensive CD4 and CD8 T Cell Cross-Reactivity between Alphaherpesviruses. J Immunol **196:**2205-2218.

158. **Mills R, Tyring SK, Levin MJ, Parrino J, Li X, Coll KE, Stek JE, Schlienger K, Chan IS, Silber JL.** 2010. Safety, tolerability, and immunogenicity of zoster vaccine in subjects with a history of herpes zoster. Vaccine **28:**4204-4209.

159. **Schmader KE, Levin MJ, Gnann JW, Jr., McNeil SA, Vesikari T, Betts RF, Keay S, Stek JE, Bundick ND, Su SC, Zhao Y, Li X, Chan IS, Annunziato PW, Parrino J.** 2012. Efficacy, safety, and tolerability of herpes zoster vaccine in persons aged 50-59 years. Clin Infect Dis **54:**922-928.

160. **Kerzner B, Murray AV, Cheng E, Ifle R, Harvey PR, Tomlinson M, Barben JL, Rarrick K, Stek JE, Chung MO, Schodel FP, Wang WW, Xu J, Chan IS, Silber JL, Schlienger K.** 2007. Safety and immunogenicity profile of the concomitant administration of ZOSTAVAX and inactivated influenza vaccine in adults aged 50 and older. J Am Geriatr Soc **55:**1499-1507.

161. **Wyman MJ, Stabi KL.** 2013. Concomitant administration of pneumococcal-23 and zoster vaccines provides adequate herpes zoster coverage. Ann Pharmacother **47:**1064-1068.

162. **Sanford M, Keating GM.** 2010. Zoster vaccine (Zostavax): a review of its use in preventing herpes zoster and postherpetic neuralgia in older adults. Drugs Aging **27:**159-176.

163. **Harpaz R, Ortega-Sanchez IR, Seward JF, Advisory Committee on Immunization Practices Centers for Disease C, Prevention.** 2008. Prevention of herpes zoster: recommendations of the Advisory Committee on Immunization Practices (ACIP). MMWR Recomm Rep **57:**1-30; quiz CE32-34.

164. **Perella D, Fiks AG, Jumaan A, Robinson D, Gargiullo P, Pletcher J, Forke CM, Schmid DS, Renwick M, Mankodi F, Watson B, Spain CV.** 2009. Validity of reported varicella history as a marker for varicella zoster virus immunity among unvaccinated children, adolescents, and young adults in the post-vaccine licensure era. Pediatrics **123:**e820-828.

165. **Lal H, Cunningham AL, Godeaux O, Chlibek R, Diez-Domingo J, Hwang SJ, Levin MJ, McElhaney JE, Poder A, Puig-Barbera J, Vesikari T, Watanabe D, Weckx L, Zahaf T, Heineman TC, Group ZOES.** 2015. Efficacy of an adjuvanted herpes zoster subunit vaccine in older adults. N Engl J Med **372:**2087-2096.

166. **Harper DR, Kangro HO, Heath RB.** 1990. Antibody responses in recipients of varicella vaccine assayed by immunoblotting. J Med Virol **30:**61-67.

167. **Arvin AM, Kinney-Thomas E, Shriver K, Grose C, Koropchak CM, Scranton E, Wittek AE, Diaz PS.** 1986. Immunity to varicella-zoster viral glycoproteins, gp I (gp 90/58) and gp III (gp 118), and to a nonglycosylated protein, p 170. J Immunol **137:**1346-1351.

168. **Coffman RL, Sher A, Seder RA.** 2010. Vaccine adjuvants: putting innate immunity to work. Immunity **33:**492-503.

169. **Leroux-Roels I, Leroux-Roels G, Clement F, Vandepapeliere P, Vassilev V, Ledent E, Heineman TC.** 2012. A phase 1/2 clinical trial evaluating safety and immunogenicity of a varicella zoster glycoprotein e subunit vaccine candidate in young and older adults. J Infect Dis **206:**1280-1290.

170. **Stadtmauer EA, Sullivan KM, Marty FM, Dadwal SS, Papanicolaou GA, Shea TC, Mossad SB, Andreadis C, Young JA, Buadi FK, El Idrissi M, Heineman TC, Berkowitz EM.** 2014. A phase 1/2 study of an adjuvanted varicella-zoster virus subunit vaccine in autologous hematopoietic cell transplant recipients. Blood **124:**2921-2929.

171. **Berkowitz EM, Moyle G, Stellbrink HJ, Schurmann D, Kegg S, Stoll M, El Idrissi M, Oostvogels L, Heineman TC, Zoster HZsSG.** 2015. Safety and immunogenicity of an adjuvanted herpes zoster subunit candidate vaccine in HIV-infected adults: a phase 1/2a randomized, placebo-controlled study. J Infect Dis **211:**1279-1287.

172. **Redman RL, Nader S, Zerboni L, Liu C, Wong RM, Brown BW, Arvin AM.** 1997. Early reconstitution of immunity and decreased severity of herpes zoster in bone marrow transplant recipients immunized with inactivated varicella vaccine. J Infect Dis **176:**578-585.

173. **Hata A, Asanuma H, Rinki M, Sharp M, Wong RM, Blume K, Arvin AM.** 2002. Use of an inactivated varicella vaccine in recipients of hematopoietic-cell transplants. N Engl J Med **347:**26-34.

174. **Myers MG, Duer HL, Hausler CK.** 1980. Experimental infection of guinea pigs with varicella-zoster virus. J Infect Dis **142:**414-420.

175. **Myers MG, Stanberry LR, Edmond BJ.** 1985. Varicella-zoster virus infection of strain 2 guinea pigs. J Infect Dis **151:**106-113.

176. **Myers MG, Connelly BL, Stanberry LR.** 1991. Varicella in hairless guinea pigs. J Infect Dis **163:**746-751.

177. **Lowry PW, Sabella C, Koropchak CM, Watson BN, Thackray HM, Abbruzzi GM, Arvin AM.** 1993. Investigation of the pathogenesis of varicella-zoster virus infection in guinea pigs by using polymerase chain reaction. J Infect Dis **167:**78-83.

178. **Matsunaga Y, Yamanishi K, Takahashi M.** 1982. Experimental infection and immune response of guinea pigs with varicella-zoster virus. Infect Immun **37:**407-412.

179. **Gan L, Wang M, Chen JJ, Gershon MD, Gershon AA.** 2014. Infected peripheral blood mononuclear cells transmit latent varicella zoster virus infection to the guinea pig enteric nervous system. J Neurovirol **20:**442-456.

180. **Milligan KL, Jain AK, Garrett JS, Knutsen AP.** 2012. Gastric ulcers due to varicella-zoster reactivation. Pediatrics **130:**e1377-1381.

181. **Keene JK, Lowe DK, Grosfeld JL, Fitzgerald JF, Gonzales-Crussi F.** 1978. Disseminated varicella complicating ulcerative colitis. Jama **239:**45-46.

182. **Sadzot-Delvaux C, Merville-Louis MP, Delree P, Marc P, Piette J, Moonen G, Rentier B.** 1990. An in vivo model of varicella-zoster virus latent infection of dorsal root ganglia. J Neurosci Res **26:**83-89.

183. **Brunell PA, Ren LC, Cohen JI, Straus SE.** 1999. Viral gene expression in rat trigeminal ganglia following neonatal infection with varicella-zoster virus. J Med Virol **58:**286-290.

184. **Wroblewska Z, Valyi-Nagy T, Otte J, Dillner A, Jackson A, Sole DP, Fraser NW.** 1993. A mouse model for varicella-zoster virus latency. Microb Pathog **15:**141-151.

185. **Annunziato P, LaRussa P, Lee P, Steinberg S, Lungu O, Gershon AA, Silverstein S.** 1998. Evidence of latent varicella-zoster virus in rat dorsal root ganglia. J Infect Dis **178 Suppl 1:**S48-51.

186. **Kennedy PG, Grinfeld E, Bell JE.** 2000. Varicella-zoster virus gene expression in latently infected and explanted human ganglia. J Virol **74:**11893-11898.

187. **Mahalingam R, Wellish M, Lederer D, Forghani B, Cohrs R, Gilden D.** 1993. Quantitation of latent varicella-zoster virus DNA in human trigeminal ganglia by polymerase chain reaction. J Virol **67:**2381-2384.

188. **Meier JL, Holman RP, Croen KD, Smialek JE, Straus SE.** 1993. Varicella-zoster virus transcription in human trigeminal ganglia. Virology **193:**193-200.

189. **Kennedy PG, Grinfeld E, Bontems S, Sadzot-Delvaux C.** 2001. Varicella-Zoster virus gene expression in latently infected rat dorsal root ganglia. Virology **289:**218-223.

190. **Fleetwood-Walker SM, Quinn JP, Wallace C, Blackburn-Munro G, Kelly BG, Fiskerstrand CE, Nash AA, Dalziel RG.** 1999. Behavioural changes in the rat following infection with varicella-zoster virus. J Gen Virol **80 (Pt 9):**2433-2436.

191. **Dalziel RG, Bingham S, Sutton D, Grant D, Champion JM, Dennis SA, Quinn JP, Bountra C, Mark MA.** 2004. Allodynia in rats infected with varicella zoster virus--a small animal model for post-herpetic neuralgia. Brain Res Brain Res Rev **46:**234-242.

192. **Ku C-C, Besser J, Abendroth A, Grose C, Arvin AM.** 2005. Varicella-Zoster Virus Pathogenesis and Immunobiology: New Concepts Emerging from Investigations with the SCIDhu Mouse Model. J Virol **79:**2651-2658.

193. **Zerboni L, Ku CC, Jones CD, Zehnder JL, Arvin AM.** 2005. Varicella-zoster virus infection of human dorsal root ganglia in vivo. Proc Natl Acad Sci U S A **102:**6490-6495.

194. **Moffat JF, Stein MD, Kaneshima H, Arvin AM.** 1995. Tropism of varicella-zoster virus for human CD4+ and CD8+ T lymphocytes and epidermal cells in SCID-hu mice. J Virol **69:**5236-5242.

195. **Reichelt M, Zerboni L, Arvin AM.** 2008. Mechanisms of Varicella-Zoster Virus Neuropathogenesis in Human Dorsal Root Ganglia. J Virol **82:**3971-3983.

196. **Cohen JI, Moskal T, Shapiro M, Purcell RH.** 1996. Varicella in Chimpanzees. J Med Virol **50:**289-292.

197. **Provost PJ, Keller PM, Banker FS, Keech BJ, Klein HJ, Lowe RS, Morton DH, Phelps AH, McAleer WJ, Ellis RW.** 1987. Successful infection of the common marmoset (Callithrix jacchus) with human varicella-zoster virus. J Virol **61:**2951-2955.

198. **Felsenfeld AD, Schmidt NJ.** 1979. Varicella-zoster virus immunizes patas monkeys against simian varicella-like disease. J Gen Virol **42:**171-178.

199. **Willer DO, Ambagala AP, Pilon R, Chan JK, Fournier J, Brooks J, Sandstrom P, Macdonald KS.** 2012. Experimental infection of Cynomolgus Macaques (Macaca fascicularis) with human varicella-zoster virus. J Virol **86:**3626-3634.

200. **Meyer C, Engelmann F, Arnold N, Krah DL, Ter Meulen J, Haberthur K, Dewane J, Messaoudi I.** 2015. Abortive Intrabronchial Infection of Rhesus Macaques with

Varicella-Zoster Virus Provides Partial Protection against Simian Varicella Virus Challenge. J Virol **89:**1781-1793.

201. **Clarkson MJ, Thorpe E, McCarthy K.** 1967. A virus disease of captive vervet monkeys (Cercopithecus aethiops) caused by a new herpesvirus. Arch Gesamte Virusforsch **22:**219-234.

202. **Blakely GA, Lourie B, Morton WG, Evans HH, Kaufmann AF.** 1973. A varicella-like disease in macaque monkeys. J Infect Dis **127:**617-625.

203. **Felsenfeld AD, Schmidt NJ.** 1977. Antigenic relationships among several simian varicella-like viruses and varicella-zoster virus. Infect Immun **15:**807-812.

204. **Gray WL, Oakes JE.** 1984. Simian varicella virus DNA shares homology with human varicella-zoster virus DNA. Virology **136:**241-246.

205. **Gray WL.** 2004. Simian varicella: a model for human varicella-zoster virus infections. Rev Med Virol **14:**363-381.

206. **Mahalingam R, Gray WL.** 2007. The simian varicella virus genome contains an invertible 665 base pair terminal element that is absent in the varicella zoster virus genome. Virology.

207. **Roberts ED, Baskin GB, Soike K, Gibson SV.** 1984. Pathologic changes of experimental simian varicella (Delta herpesvirus) infection in African green monkeys (Cercopithecus aethiops). Am J Vet Res **45:**523-530.

208. **White TM, Mahalingam R, Traina-Dorge V, Gilden DH.** 2002. Persistence of simian varicella virus DNA in CD4(+) and CD8(+) blood mononuclear cells for years after intratracheal inoculation of African green monkeys. Virology **303:**192-198.

209. **White TM, Mahalingam R, Traina-Dorge V, Gilden DH.** 2002. Simian varicella virus DNA is present and transcribed months after experimental infection of adult African green monkeys. J Neurovirol **8:**191-203.

210. **Mahalingam R, Traina-Dorge V, Wellish M, Smith J, Gilden DH.** 2002. Naturally acquired simian varicella virus infection in African green monkeys. J Virol **76:**8548-8550.

211. **Mahalingam R, Smith D, Wellish M, Wolf W, Dueland AN, Cohrs R, Soike K, Gilden D.** 1991. Simian varicella virus DNA in dorsal root ganglia. Proc Natl Acad Sci U S A **88:**2750-2752.

212. **Mahalingam R, Clarke P, Wellish M, Dueland AN, Soike KF, Gilden DH, Cohrs R.** 1992. Prevalence and distribution of latent simian varicella virus DNA in monkey ganglia. Virology **188:**193-197.

213. **Gray WL, Gusick NJ, Fletcher TM, Soike KF.** 1995. Simian varicella virus antibody response in experimental infection of African green monkeys. J Med Primatol **24:**246-251.

214. **Mahalingam R, Wellish M, Soike K, White T, Kleinschmidt-DeMasters BK, Gilden DH.** 2001. Simian varicella virus infects ganglia before rash in experimentally infected monkeys. Virology **279:**339-342.

215. **Kolappaswamy K, Mahalingam R, Traina-Dorge V, Shipley ST, Gilden DH, Kleinschmidt-Demasters BK, McLeod CG, Jr., Hungerford LL, DeTolla LJ.** 2007. Disseminated simian varicella virus infection in an irradiated rhesus macaque (Macaca mulatta). J Virol **81:**411-415.

216. **Mahalingam R, Traina-Dorge V, Wellish M, Lorino R, Sanford R, Ribka EP, Alleman SJ, Brazeau E, Gilden DH.** 2007. Simian varicella virus reactivation in cynomolgus monkeys. Virology.

217. **Messaoudi I, Barron A, Wellish M, Engelmann F, Legasse A, Planer S, Gilden D, Nikolich-Zugich J, Mahalingam R.** 2009. Simian varicella virus infection of rhesus macaques recapitulates essential features of varicella zoster virus infection in humans. PLoS Pathog **5:**e1000657.

218. **Mahalingam R, Traina-Dorge V, Wellish M, Deharo E, Singletary ML, Ribka EP, Sanford R, Gilden D.** 2010. Latent simian varicella virus reactivates in monkeys treated with tacrolimus with or without exposure to irradiation. J Neurovirol **16:**342-354.

219. **Haberthur K, Engelmann F, Park B, Barron A, Legasse A, Dewane J, Fischer M, Kerns A, Brown M, Messaoudi I.** 2011. CD4 T Cell Immunity Is Critical for the Control of Simian Varicella Virus Infection in a Nonhuman Primate Model of VZV Infection. PLoS Pathog **7:**e1002367.

220. **Meyer C, Kerns A, Barron A, Kreklywich C, Streblow DN, Messaoudi I.** 2011. Simian varicella virus gene expression during acute and latent infection of rhesus macaques. J Neurovirol **17:**600-612.

221. **Haberthur K, Meyer C, Arnold N, Engelmann F, Jeske DR, Messaoudi I.** 2014. Intrabronchial infection of rhesus macaques with simian varicella virus results in a robust immune response in the lungs. J Virol **88:**12777-12792.

222. **Haberthur K, Kraft A, Arnold N, Park B, Meyer C, Asquith M, Dewane J, Messaoudi I.** 2013. Genome-wide analysis of T cell responses during acute and latent simian varicella virus infections in rhesus macaques. J Virol **87:**11751-11761.

223. **Ouwendijk WJ, Mahalingam R, de Swart RL, Haagmans BL, van Amerongen G, Getu S, Gilden D, Osterhaus AD, Verjans GM.** 2013. T-Cell tropism of simian varicella virus during primary infection. PLoS Pathog **9:**e1003368.

224. **Ouwendijk WJ, Getu S, Mahalingam R, Gilden D, Osterhaus AD, Verjans GM.** 2015. Characterization of the immune response in ganglia after primary simian varicella virus infection. J Neurovirol doi:10.1007/s13365-015-0408-1.

225. **Ouwendijk WJ, Abendroth A, Traina-Dorge V, Getu S, Steain M, Wellish M, Andeweg AC, Osterhaus AD, Gilden D, Verjans GM, Mahalingam R.** 2013. T-Cell Infiltration Correlates with CXCL10 Expression in Ganglia of Cynomolgus Macaques with Reactivated Simian Varicella Virus. J Virol **87:**2979-2982.

226. **Whitmer T, Malouli D, Uebelhoer LS, DeFilippis VR, Fruh K, Verweij MC.** 2015. The ORF61 Protein Encoded by Simian Varicella Virus and Varicella-Zoster Virus Inhibits NF-kappaB Signaling by Interfering with IkappaBalpha Degradation. J Virol **89:**8687-8700.

227. **Verweij MC, Wellish M, Whitmer T, Malouli D, Lapel M, Jonjic S, Haas JG, DeFilippis VR, Mahalingam R, Fruh K.** 2015. Varicella Viruses Inhibit Interferon-Stimulated JAK-STAT Signaling through Multiple Mechanisms. PLoS Pathog **11:**e1004901.

228. **Meyer C, Kerns A, Haberthur K, Dewane J, Walker J, Gray W, Messaoudi I.** 2013. Attenuation of the adaptive immune response in rhesus macaques infected with simian varicella virus lacking open reading frame 61. J Virol **87:**2151-2163.

229. **Moffat J, Ku CC, Zerboni L, Sommer M, Arvin A.** 2007. VZV: pathogenesis and the disease consequences of primary infection. *In* Arvin A, Campadelli-Fiume G, Mocarski E, Moore PS, Roizman B, Whitley R, Yamanishi K (ed), Human Herpesviruses: Biology, Therapy, and Immunoprophylaxis, Cambridge.

230. **Feldman S.** 1994. Varicella-zoster virus pneumonitis. Chest **106:**22S-27S.

231. **Mohsen AH, McKendrick M.** 2003. Varicella pneumonia in adults. Eur Respir J **21:**886-891.

232. **Chiner E, Ballester I, Betlloch I, Blanquer J, Aguar MC, Blanquer R, Fernandez-Fabrellas E, Andreu AL, Briones M, Sanz F.** 2010. Varicella-zoster virus pneumonia in an adult population: has mortality decreased? Scand J Infect Dis **42:**215-221.

233. **Barr T, Girke T, Sureshchandra S, Nguyen C, Grant K, Messaoudi I.** 2016. Alcohol Consumption Modulates Host Defense in Rhesus Macaques by Altering Gene Expression in Circulating Leukocytes. J Immunol **196:**182-195.

234. **Suzuki K, Hu D, Bustos T, Zlotogora J, Richieri-Costa A, Helms JA, Spritz RA.** 2000. Mutations of PVRL1, encoding a cell-cell adhesion molecule/herpesvirus receptor, in cleft lip/palate-ectodermal dysplasia. Nat Genet **25:**427-430.

235. **Takeuchi O, Akira S.** 2009. Innate immunity to virus infection. Immunol Rev **227:**75-86.

236. **Hashimoto S, Kobayashi A, Kooguchi K, Kitamura Y, Onodera H, Nakajima H.** 2000. Upregulation of two death pathways of perforin/granzyme and FasL/Fas in septic acute respiratory distress syndrome. Am J Respir Crit Care Med **161:**237-243.
237. **Ramana CV, Chatterjee-Kishore M, Nguyen H, Stark GR.** 2000. Complex roles of Stat1 in regulating gene expression. Oncogene **19:**2619-2627.

238. **Doi T, Lukosiute A, Ruttenstock E, Dingemann J, Puri P.** 2011. Expression of Iroquois genes is up-regulated during early lung development in the nitrofen-induced pulmonary hypoplasia. J Pediatr Surg **46:**62-66.

239. **Gronostajski RM.** 2000. Roles of the NFI/CTF gene family in transcription and development. Gene **249:**31-45.

240. **Kim TH, Kim SH, Seo JY, Chung H, Kwak HJ, Lee SK, Yoon HJ, Shin DH, Park SS, Sohn JW.** 2011. Blockade of the Wnt/beta-catenin pathway attenuates bleomycin-induced pulmonary fibrosis. Tohoku J Exp Med **223:**45-54.

241. **Laity JH, Lee BM, Wright PE.** 2001. Zinc finger proteins: new insights into structural and functional diversity. Curr Opin Struct Biol **11:**39-46.

242. **Martic G, Karetsou Z, Kefala K, Politou AS, Clapier CR, Straub T, Papamarcaki T.** 2005. Parathymosin affects the binding of linker histone H1 to nucleosomes and remodels chromatin structure. J Biol Chem **280:**16143-16150.

243. **Heng TS, Painter MW, Immunological Genome Project C.** 2008. The Immunological Genome Project: networks of gene expression in immune cells. Nat Immunol **9:**1091-1094.

244. **ImmGen C.** 2016. Open-source ImmGen: mononuclear phagocytes. Nat Immunol **17:**741.

245. **Genster N, Ma YJ, Munthe-Fog L, Garred P.** 2014. The pattern recognition molecule ficolin-1 exhibits differential binding to lymphocyte subsets, providing a novel link between innate and adaptive immunity. Mol Immunol **57:**181-190.

246. **Razorenova OV, Castellini L, Colavitti R, Edgington LE, Nicolau M, Huang X, Bedogni B, Mills EM, Bogyo M, Giaccia AJ.** 2014. The apoptosis repressor with a CARD domain (ARC) gene is a direct hypoxia-inducible factor 1 target gene and promotes survival and proliferation of VHL-deficient renal cancer cells. Mol Cell Biol **34:**739-751.

247. **Marino M, Stoilova T, Giorgi C, Bachi A, Cattaneo A, Auricchio A, Pinton P, Zito E.** 2015. SEPN1, an endoplasmic reticulum-localized selenoprotein linked to skeletal muscle pathology, counteracts hyperoxidation by means of redox-regulating SERCA2 pump activity. Hum Mol Genet **24:**1843-1855.

248. **Kasamatsu J, Azuma M, Oshiumi H, Morioka Y, Okabe M, Ebihara T, Matsumoto M, Seya T.** 2014. INAM plays a critical role in IFN-gamma production by NK cells

interacting with polyinosinic-polycytidylic acid-stimulated accessory cells. J Immunol **193:**5199-5207.

249. **Nauta AJ, Bottazzi B, Mantovani A, Salvatori G, Kishore U, Schwaeble WJ, Gingras AR, Tzima S, Vivanco F, Egido J, Tijsma O, Hack EC, Daha MR, Roos A.** 2003. Biochemical and functional characterization of the interaction between pentraxin 3 and C1q. Eur J Immunol **33:**465-473.

250. **Yatagai Y, Sakamoto T, Yamada H, Masuko H, Kaneko Y, Iijima H, Naito T, Noguchi E, Hirota T, Tamari M, Konno S, Nishimura M, Hizawa N.** 2014. Genomewide association study identifies HAS2 as a novel susceptibility gene for adult asthma in a Japanese population. Clin Exp Allergy **44:**1327-1334.

251. **Dziegiel P, Jelen M, Muszczynska B, Maciejczyk A, Szulc A, Podhorska-Okolow M, Cegielski M, Zabel M.** 2004. Role of metallothionein expression in non-small cell lung carcinomas. Rocz Akad Med Bialymst **49 Suppl 1:**43-45.

252. **Zuo W, Zhang T, Wu DZ, Guan SP, Liew AA, Yamamoto Y, Wang X, Lim SJ, Vincent M, Lessard M, Crum CP, Xian W, McKeon F.** 2015. p63(+)Krt5(+) distal airway stem cells are essential for lung regeneration. Nature **517:**616-620.

253. **Keegan A, Dorsey N, Qi XL, Smith E, Dasgupta P.** 2013. Insulin Receptor Substrate-2 negatively regulates alternative macrophage activation and allergic lung inflammation. Journal of Immunology **190**.

254. **Hishikawa D, Shindou H, Harayama T, Ogasawara R, Suwabe A, Shimizu T.** 2013. Identification of Sec14-like 3 as a novel lipid-packing sensor in the lung. FASEB J **27:**5131-5140.

255. **Joaquin M, Watson RJ.** 2003. Cell cycle regulation by the B-Myb transcription factor. Cell Mol Life Sci **60:**2389-2401.

256. **Wierstra I, Alves J.** 2007. FOXM1, a typical proliferation-associated transcription factor. Biol Chem **388:**1257-1274.

257. **Zhou L, Cai X, Han X, Xu N, Chang DC.** 2014. CDK1 switches mitotic arrest to apoptosis by phosphorylating Bcl-2/Bax family proteins during treatment with microtubule interfering agents. Cell Biol Int **38:**737-746.

258. **Fabbro M, Zhou BB, Takahashi M, Sarcevic B, Lal P, Graham ME, Gabrielli BG, Robinson PJ, Nigg EA, Ono Y, Khanna KK.** 2005. Cdk1/Erk2- and Plk1-dependent phosphorylation of a centrosome protein, Cep55, is required for its recruitment to midbody and cytokinesis. Dev Cell **9:**477-488.

259. **Tang Z, Shu H, Oncel D, Chen S, Yu H.** 2004. Phosphorylation of Cdc20 by Bub1 provides a catalytic mechanism for APC/C inhibition by the spindle checkpoint. Mol Cell **16:**387-397.

260. **Bradley K, McConnell-Breul S, Crystal RG.** 1974. Lung collagen heterogeneity. Proc Natl Acad Sci U S A **71:**2828-2832.

261. **Mirakaj V, Thix CA, Laucher S, Mielke C, Morote-Garcia JC, Schmit MA, Henes J, Unertl KE, Kohler D, Rosenberger P.** 2010. Netrin-1 dampens pulmonary inflammation during acute lung injury. Am J Respir Crit Care Med **181:**815-824.

262. **Hay JG, Danel C, Chu CS, Crystal RG.** 1995. Human CC10 gene expression in airway epithelium and subchromosomal locus suggest linkage to airway disease. Am J Physiol **268:**L565-575.

263. **Huang QQ, Brozovich FV, Jin JP.** 1999. Fast skeletal muscle troponin T increases the cooperativity of transgenic mouse cardiac muscle contraction. J Physiol **520 Pt 1:**231-242.

264. **Dong Z, Meller J, Succop P, Wang J, Wikenheiser-Brokamp K, Starnes S, Lu S.** 2014. Secretory phospholipase A2-IIa upregulates HER/HER2-elicited signaling in lung cancer cells. Int J Oncol **45:**978-984.

265. **Liao SF, Alman MJ, Vanzant ES, Miles ED, Harmon DL, McLeod KR, Boling JA, Matthews JC.** 2008. Basal expression of nucleoside transporter mRNA differs among small intestinal epithelia of beef steers and is differentially altered by ruminal or abomasal infusion of starch hydrolysate. J Dairy Sci **91:**1570-1584.

266. **Neesen J, Kirschner R, Ochs M, Schmiedl A, Habermann B, Mueller C, Holstein AF, Nuesslein T, Adham I, Engel W.** 2001. Disruption of an inner arm dynein heavy chain gene results in asthenozoospermia and reduced ciliary beat frequency. Hum Mol Genet **10:**1117-1128.

267. **Hormi-Carver KK, Shi W, Liu CW, Berndt N.** 2004. Protein phosphatase 1alpha is required for murine lung growth and morphogenesis. Dev Dyn **229:**791-801.

268. **Costa ML, Escaleira R, Cataldo A, Oliveira F, Mermelstein CS.** 2004. Desmin: molecular interactions and putative functions of the muscle intermediate filament protein. Braz J Med Biol Res **37:**1819-1830.

269. **Openshaw PJ.** 1989. Flow cytometric analysis of pulmonary lymphocytes from mice infected with respiratory syncytial virus. Clin Exp Immunol **75:**324-328.

270. **Weinfurter JT, Brunner K, Capuano SV, 3rd, Li C, Broman KW, Kawaoka Y, Friedrich TC.** 2011. Cross-reactive T cells are involved in rapid clearance of 2009 pandemic H1N1 influenza virus in nonhuman primates. PLoS Pathog **7:**e1002381.

271. **Goulding J, Bogue R, Tahiliani V, Croft M, Salek-Ardakani S.** 2012. CD8 T cells are essential for recovery from a respiratory vaccinia virus infection. J Immunol **189:**2432-2440.

272. **Liu B, Mori I, Hossain MJ, Dong L, Takeda K, Kimura Y.** 2004. Interleukin-18 improves the early defence system against influenza virus infection by augmenting natural killer cell-mediated cytotoxicity. J Gen Virol **85:**423-428.

273. **Kaiser L, Fritz RS, Straus SE, Gubareva L, Hayden FG.** 2001. Symptom pathogenesis during acute influenza: interleukin-6 and other cytokine responses. J Med Virol **64:**262-268.

274. **Josset L, Engelmann F, Haberthur K, Kelly S, Park B, Kawoaka Y, Garcia-Sastre A, Katze MG, Messaoudi I.** 2012. Increased viral loads and exacerbated innate host responses in aged macaques infected with the 2009 pandemic H1N1 influenza A virus. J Virol **86:**11115-11127.

275. **Winthrop K, Rivera A, Engelmann F, Rose S, Lewis A, Ku J, Bermudez L, Messaoudi I.** 2016. A Rhesus Macaque Model of Pulmonary Nontuberculous Mycobacterial Disease. Am J Respir Cell Mol Biol **54:**170-176.

276. **Nishioka Y, Manabe K, Kishi J, Wang W, Inayama M, Azuma M, Sone S.** 2007. CXCL9 and 11 in patients with pulmonary sarcoidosis: a role of alveolar macrophages. Clin Exp Immunol **149:**317-326.

277. **Fenwick PS, Macedo P, Kilty IC, Barnes PJ, Donnelly LE.** 2015. Effect of JAK Inhibitors on Release of CXCL9, CXCL10 and CXCL11 from Human Airway Epithelial Cells. PLoS One **10:**e0128757.

278. **Sha Q, Truong-Tran AQ, Plitt JR, Beck LA, Schleimer RP.** 2004. Activation of airway epithelial cells by toll-like receptor agonists. Am J Respir Cell Mol Biol **31:**358-364.

279. **Liu B, Kimura Y.** 2007. Local immune response to respiratory syncytial virus infection is diminished in senescence-accelerated mice. J Gen Virol **88:**2552-2558.

280. **Kumagai Y, Takeuchi O, Kato H, Kumar H, Matsui K, Morii E, Aozasa K, Kawai T, Akira S.** 2007. Alveolar macrophages are the primary interferon-alpha producer in pulmonary infection with RNA viruses. Immunity **27:**240-252.

281. **Harty RN, Pitha PM, Okumura A.** 2009. Antiviral activity of innate immune protein ISG15. J Innate Immun **1:**397-404.

282. **Le Goffic R, Pothlichet J, Vitour D, Fujita T, Meurs E, Chignard M, Si-Tahar M.** 2007. Cutting Edge: Influenza A virus activates TLR3-dependent inflammatory and RIG-I-dependent antiviral responses in human lung epithelial cells. J Immunol **178:**3368-3372.

283. **Janssen R, Pennings J, Hodemaekers H, Buisman A, van Oosten M, de Rond L, Ozturk K, Dormans J, Kimman T, Hoebee B.** 2007. Host transcription profiles upon primary respiratory syncytial virus infection. J Virol **81:**5958-5967.

284. **Muramoto Y, Shoemaker JE, Le MQ, Itoh Y, Tamura D, Sakai-Tagawa Y, Imai H, Uraki R, Takano R, Kawakami E, Ito M, Okamoto K, Ishigaki H, Mimuro H, Sasakawa C, Matsuoka Y, Noda T, Fukuyama S, Ogasawara K, Kitano H, Kawaoka Y.** 2014. Disease severity is associated with differential gene expression at the early and late phases of infection in nonhuman primates infected with different H5N1 highly pathogenic avian influenza viruses. J Virol **88:**8981-8997.

285. **Chowdhury D, Lieberman J.** 2008. Death by a thousand cuts: granzyme pathways of programmed cell death. Annu Rev Immunol **26:**389-420.

286. **Cullen SP, Brunet M, Martin SJ.** 2010. Granzymes in cancer and immunity. Cell Death Differ **17:**616-623.

287. **Bem RA, van Woensel JB, Lutter R, Domachowske JB, Medema JP, Rosenberg HF, Bos AP.** 2010. Granzyme A- and B-cluster deficiency delays acute lung injury in pneumovirus-infected mice. J Immunol **184:**931-938.

288. **Moffat JM, Gebhardt T, Doherty PC, Turner SJ, Mintern JD.** 2009. Granzyme A expression reveals distinct cytolytic CTL subsets following influenza A virus infection. Eur J Immunol **39:**1203-1210.

289. **Cooper DM, Pechkovsky DV, Hackett TL, Knight DA, Granville DJ.** 2011. Granzyme K activates protease-activated receptor-1. PLoS One **6:**e21484.

290. **Damjanovic D, Divangahi M, Kugathasan K, Small CL, Zganiacz A, Brown EG, Hogaboam CM, Gauldie J, Xing Z.** 2011. Negative regulation of lung inflammation and immunopathology by TNF-alpha during acute influenza infection. Am J Pathol **179:**2963-2976.

291. **van der Pol WL, Leijenaar JF, Spliet WG, Lavrijsen SW, Jansen NJ, Braun KP, Mulder M, Timmers-Raaijmakers B, Ratsma K, Dooijes D, van Haelst MM.** 2014. Nemaline myopathy caused byTNNT1 mutations in a Dutch pedigree. Mol Genet Genomic Med **2:**134-137.

292. **Jackson BC, Thompson DC, Wright MW, McAndrews M, Bernard A, Nebert DW, Vasiliou V.** 2011. Update of the human secretoglobin (SCGB) gene superfamily and an example of 'evolutionary bloom' of androgen-binding protein genes within the mouse Scgb gene superfamily. Hum Genomics **5:**691-702.

293. **Yamada A, Suzuki D, Miyazono A, Oshima K, Kamiya A, Zhao B, Takami M, Donnelly RP, Itabe H, Yamamoto M, Kimura S, Kamijo R.** 2009. IFN-gamma down-regulates Secretoglobin 3A1 gene expression. Biochem Biophys Res Commun **379:**964-968.

294. **Chen J, Feng G, Guo Q, Wardenburg JB, Lin S, Inoshima I, Deaton R, Yuan JX, Garcia JG, Machado RF, Otto M, Wunderink RG.** 2013. Transcriptional events during the recovery from MRSA lung infection: a mouse pneumonia model. PLoS One **8:**e70176.

295. **Thebaud B, Ladha F, Michelakis ED, Sawicka M, Thurston G, Eaton F, Hashimoto K, Harry G, Haromy A, Korbutt G, Archer SL.** 2005. Vascular endothelial growth factor gene therapy increases survival, promotes lung angiogenesis, and prevents alveolar damage in hyperoxia-induced lung injury: evidence that angiogenesis participates in alveolarization. Circulation **112:**2477-2486.

296. **Chen L, Acciani T, Le Cras T, Lutzko C, Perl AK.** 2012. Dynamic regulation of platelet-derived growth factor receptor alpha expression in alveolar fibroblasts during realveolarization. Am J Respir Cell Mol Biol **47:**517-527.

297. **Fashner J, Bell AL.** 2011. Herpes zoster and postherpetic neuralgia: prevention and management. Am Fam Physician **83:**1432-1437.

298. **Taha Y, Scott FT, Parker SP, Syndercombe Court D, Quinlivan ML, Breuer J.** 2006. Reactivation of 2 genetically distinct varicella-zoster viruses in the same individual. Clin Infect Dis **43:**1301-1303.

299. **Gowrishankar K, Steain M, Cunningham AL, Rodriguez M, Blumbergs P, Slobedman B, Abendroth A.** 2010. Characterization of the host immune response in human Ganglia after herpes zoster. J Virol **84:**8861-8870.

300. **Kolappaswamy K, Mahalingam R, Traina-Dorge V, Shipley ST, Gilden DH, Kleinschmidt-Demasters BK, McLeod CG, Jr., Hungerford LL, DeTolla LJ.** 2007. Disseminated Simian Varicella Virus Infection in an Irradiated Rhesus Macaque (Macaca mulatta). J Virol **81:**411-415.

301. **Soike KF.** 1992. Simian varicella virus infection in African and Asian monkeys. The potential for development of antivirals for animal diseases. Ann N Y Acad Sci **653:**323-333.

302. **Huber W, Carey VJ, Gentleman R, Anders S, Carlson M, Carvalho BS, Bravo HC, Davis S, Gatto L, Girke T, Gottardo R, Hahne F, Hansen KD, Irizarry RA, Lawrence M, Love MI, MacDonald J, Obenchain V, Oles AK, Pages H, Reyes A, Shannon P, Smyth GK, Tenenbaum D, Waldron L, Morgan M.** 2015. Orchestrating high-throughput genomic analysis with Bioconductor. Nat Methods **12:**115-121.

303. **Langmead B, Salzberg SL.** 2012. Fast gapped-read alignment with Bowtie 2. Nat Methods **9:**357-359.

304. **Kim D, Pertea G, Trapnell C, Pimentel H, Kelley R, Salzberg SL.** 2013. TopHat2: accurate alignment of transcriptomes in the presence of insertions, deletions and gene fusions. Genome Biol **14:**R36.

305. **Cunningham F, Amode MR, Barrell D, Beal K, Billis K, Brent S, Carvalho-Silva D, Clapham P, Coates G, Fitzgerald S, Gil L, Giron CG, Gordon L, Hourlier T, Hunt SE, Janacek SH, Johnson N, Juettemann T, Kahari AK, Keenan S, Martin FJ, Maurel T, McLaren W, Murphy DN, Nag R, Overduin B, Parker A, Patricio M, Perry E, Pignatelli M, Riat HS, Sheppard D, Taylor K, Thormann A, Vullo A, Wilder SP, Zadissa A, Aken BL, Birney E, Harrow J, Kinsella R, Muffato M,**

Ruffier M, Searle SM, Spudich G, Trevanion SJ, Yates A, Zerbino DR, Flicek P. 2015. Ensembl 2015. Nucleic Acids Res **43:**D662-669.

306. **Lawrence M, Huber W, Pages H, Aboyoun P, Carlson M, Gentleman R, Morgan MT, Carey VJ.** 2013. Software for computing and annotating genomic ranges. PLoS Comput Biol **9:**e1003118.

307. **Robinson MD, McCarthy DJ, Smyth GK.** 2010. edgeR: a Bioconductor package for differential expression analysis of digital gene expression data. Bioinformatics **26:**139-140.

308. **Anders S, McCarthy DJ, Chen Y, Okoniewski M, Smyth GK, Huber W, Robinson MD.** 2013. Count-based differential expression analysis of RNA sequencing data using R and Bioconductor. Nat Protoc **8:**1765-1786.

309. **Cohrs RJ, Gilden DH.** 2003. Varicella zoster virus transcription in latently-infected human ganglia. Anticancer Res **23:**2063-2069.

310. **Ito H, Sommer MH, Zerboni L, Baiker A, Sato B, Liang R, Hay J, Ruyechan W, Arvin AM.** 2005. Role of the varicella-zoster virus gene product encoded by open reading frame 35 in viral replication in vitro and in differentiated human skin and T cells in vivo. J Virol **79:**4819-4827.

311. **Ou Y, Davis KA, Traina-Dorge V, Gray WL.** 2007. Simian varicella virus expresses a latency-associated transcript that is antisense to open reading frame 61 (ICP0) mRNA in neural ganglia of latently infected monkeys. J Virol **81:**8149-8156.

312. **Ratner N, Bunge RP, Glaser L.** 1985. A neuronal cell surface heparan sulfate proteoglycan is required for dorsal root ganglion neuron stimulation of Schwann cell proliferation. J Cell Biol **101:**744-754.

313. **Sato M, Nagano T.** 2005. Involvement of filamin A and filamin A-interacting protein (FILIP) in controlling the start and cell shape of radially migrating cortical neurons. Anat Sci Int **80:**19-29.

314. **Yagi H, Nagano T, Xie MJ, Ikeda H, Kuroda K, Komada M, Iguchi T, Tariqur RM, Morikubo S, Noguchi K, Murase K, Okabe M, Sato M.** 2014. Filamin A-interacting protein (FILIP) is a region-specific modulator of myosin 2b and controls spine morphology and NMDA receptor accumulation. Sci Rep **4:**6353.

315. **Shi HX, Yang K, Liu X, Liu XY, Wei B, Shan YF, Zhu LH, Wang C.** 2010. Positive regulation of interferon regulatory factor 3 activation by Herc5 via ISG15 modification. Mol Cell Biol **30:**2424-2436.

316. **Petzold A.** 2015. Glial fibrillary acidic protein is a body fluid biomarker for glial pathology in human disease. Brain Res **1600:**17-31.

317. **Dateki M, Horii T, Kasuya Y, Mochizuki R, Nagao Y, Ishida J, Sugiyama F, Tanimoto K, Yagami K, Imai H, Fukamizu A.** 2005. Neurochondrin negatively

regulates CaMKII phosphorylation, and nervous system-specific gene disruption results in epileptic seizure. J Biol Chem **280:**20503-20508.

318. **Kielar C, Sawiak SJ, Navarro Negredo P, Tse DH, Morton AJ.** 2012. Tensor-based morphometry and stereology reveal brain pathology in the complexin1 knockout mouse. PLoS One **7:**e32636.

319. **Thomas P, Pang Y.** 2012. Membrane progesterone receptors: evidence for neuroprotective, neurosteroid signaling and neuroendocrine functions in neuronal cells. Neuroendocrinology **96:**162-171.

320. **Roisen FJ, Wilson FJ, Yorke G, Inczedy-Marcsek M, Hirabayashi T.** 1983. Immunohistochemical localization of troponin-C in cultured neurons. J Muscle Res Cell Motil **4:**163-175.

321. **Kneussel M, Wagner W.** 2013. Myosin motors at neuronal synapses: drivers of membrane transport and actin dynamics. Nat Rev Neurosci **14:**233-247.

322. **Stoevring B, Jaliashvili I, Thougaard AV, Ensinger C, Hogdall CK, Rasmussen LS, Sellebjerg F, Christiansen M.** 2006. Tetranectin in cerebrospinal fluid of patients with multiple sclerosis. Scand J Clin Lab Invest **66:**577-583.

323. **Zhou X, Michal JJ, Zhang L, Ding B, Lunney JK, Liu B, Jiang Z.** 2013. Interferon induced IFIT family genes in host antiviral defense. Int J Biol Sci **9:**200-208.

324. **Verhelst J, Parthoens E, Schepens B, Fiers W, Saelens X.** 2012. Interferon-inducible protein Mx1 inhibits influenza virus by interfering with functional viral ribonucleoprotein complex assembly. J Virol **86:**13445-13455.

325. **Hoshino A, Kawamura YI, Yasuhara M, Toyama-Sorimachi N, Yamamoto K, Matsukawa A, Lira SA, Dohi T.** 2007. Inhibition of CCL1-CCR8 interaction prevents aggregation of macrophages and development of peritoneal adhesions. J Immunol **178:**5296-5304.

326. **Liu Y, Luo S, He S, Zhang M, Wang P, Li C, Huang W, Hu B, Griffin GE, Shattock RJ, Hu Q.** 2015. Tetherin restricts HSV-2 release and is counteracted by multiple viral glycoproteins. Virology **475:**96-109.

327. **Montague P, McCallion AS, Davies RW, Griffiths IR.** 2006. Myelin-associated oligodendrocytic basic protein: a family of abundant CNS myelin proteins in search of a function. Dev Neurosci **28:**479-487.

328. **Schmitz G, Kaminski WE.** 2002. ABCA2: a candidate regulator of neural transmembrane lipid transport. Cell Mol Life Sci **59:**1285-1295.

329. **Carenini S, Montag D, Schachner M, Martini R.** 1999. Subtle roles of neural cell adhesion molecule and myelin-associated glycoprotein during Schwann cell spiralling in P0-deficient mice. Glia **27:**203-212.

330. **Watanabe E, Hiyama TY, Shimizu H, Kodama R, Hayashi N, Miyata S, Yanagawa Y, Obata K, Noda M.** 2006. Sodium-level-sensitive sodium channel Na(x) is expressed in glial laminate processes in the sensory circumventricular organs. Am J Physiol Regul Integr Comp Physiol **290:**R568-576.

331. **Ashpole NM, Song W, Brustovetsky T, Engleman EA, Brustovetsky N, Cummins TR, Hudmon A.** 2012. Calcium/calmodulin-dependent protein kinase II (CaMKII) inhibition induces neurotoxicity via dysregulation of glutamate/calcium signaling and hyperexcitability. J Biol Chem **287:**8495-8506.

332. **Kabos P, Kabosova A, Neuman T.** 2002. Neuronal injury affects expression of helix-loop-helix transcription factors. Neuroreport **13:**2385-2388.

333. **Sun T, Xiao HS, Zhou PB, Lu YJ, Bao L, Zhang X.** 2006. Differential expression of synaptoporin and synaptophysin in primary sensory neurons and up-regulation of synaptoporin after peripheral nerve injury. Neuroscience **141:**1233-1245.

334. **Morimoto S, Cassell MD, Sigmund CD.** 2002. Neuron-specific expression of human angiotensinogen in brain causes increased salt appetite. Physiol Genomics **9:**113-120.

335. **Gimeno RE.** 2007. Fatty acid transport proteins. Curr Opin Lipidol **18:**271-276.

336. **Ogura M, Takarada T, Nakamichi N, Kawagoe H, Sako A, Nakazato R, Yoneda Y.** 2011. Exacerbated vulnerability to oxidative stress in astrocytic C6 glioma cells with stable overexpression of the glutamine transporter slc38a1. Neurochem Int **58:**504-511.

337. **Lockhart PJ, Holtom B, Lincoln S, Hussey J, Zimprich A, Gasser T, Wszolek ZK, Hardy J, Farrer MJ.** 2002. The human sideroflexin 5 (SFXN5) gene: sequence, expression analysis and exclusion as a candidate for PARK3. Gene **285:**229-237.

338. **Gold ES, Underhill DM, Morrissette NS, Guo J, McNiven MA, Aderem A.** 1999. Dynamin 2 is required for phagocytosis in macrophages. J Exp Med **190:**1849-1856.

339. **Umezu-Goto M, Kishi Y, Taira A, Hama K, Dohmae N, Takio K, Yamori T, Mills GB, Inoue K, Aoki J, Arai H.** 2002. Autotaxin has lysophospholipase D activity leading to tumor cell growth and motility by lysophosphatidic acid production. J Cell Biol **158:**227-233.

340. **Yamao T, Noguchi T, Takeuchi O, Nishiyama U, Morita H, Hagiwara T, Akahori H, Kato T, Inagaki K, Okazawa H, Hayashi Y, Matozaki T, Takeda K, Akira S, Kasuga M.** 2002. Negative regulation of platelet clearance and of the macrophage phagocytic response by the transmembrane glycoprotein SHPS-1. J Biol Chem **277:**39833-39839.

341. **Dufour JH, Dziejman M, Liu MT, Leung JH, Lane TE, Luster AD.** 2002. IFN-gamma-inducible protein 10 (IP-10; CXCL10)-deficient mice reveal a role for IP-10 in effector T cell generation and trafficking. J Immunol **168:**3195-3204.

342. **Villa C, Venturelli E, Fenoglio C, Clerici F, Marcone A, Benussi L, Ghidoni R, Gallone S, Cortini F, Scalabrini D, Serpente M, Binetti G, Cappa S, Mariani C, Rainero I, Bresolin N, Scarpini E, Galimberti D.** 2009. CCL8/MCP-2 association analysis in patients with Alzheimer's disease and frontotemporal lobar degeneration. J Neurol **256:**1379-1381.

343. **Wiley SR, Schooley K, Smolak PJ, Din WS, Huang CP, Nicholl JK, Sutherland GR, Smith TD, Rauch C, Smith CA, et al.** 1995. Identification and characterization of a new member of the TNF family that induces apoptosis. Immunity **3:**673-682.

344. **Warke RV, Becerra A, Zawadzka A, Schmidt DJ, Martin KJ, Giaya K, Dinsmore JH, Woda M, Hendricks G, Levine T, Rothman AL, Bosch I.** 2008. Efficient dengue virus (DENV) infection of human muscle satellite cells upregulates type I interferon response genes and differentially modulates MHC I expression on bystander and DENV-infected cells. J Gen Virol **89:**1605-1615.

345. **Li S, Xie Y, Zhang W, Gao J, Wang M, Zheng G, Yin X, Xia H, Tao X.** 2015. Interferon alpha-inducible protein 27 promotes epithelial-mesenchymal transition and induces ovarian tumorigenicity and stemness. J Surg Res **193:**255-264.

346. **Barnard DC, Patton JG.** 2000. Identification and characterization of a novel serine-arginine-rich splicing regulatory protein. Mol Cell Biol **20:**3049-3057.

347. **Huang X, Beullens M, Zhang J, Zhou Y, Nicolaescu E, Lesage B, Hu Q, Wu J, Bollen M, Shi Y.** 2009. Structure and function of the two tandem WW domains of the pre-mRNA splicing factor FBP21 (formin-binding protein 21). J Biol Chem **284:**25375-25387.

348. **Nordmann A, Wixler L, Boergeling Y, Wixler V, Ludwig S.** 2012. A new splice variant of the human guanylate-binding protein 3 mediates anti-influenza activity through inhibition of viral transcription and replication. FASEB J **26:**1290-1300.

349. **Wilczynska KM, Singh SK, Adams B, Bryan L, Rao RR, Valerie K, Wright S, Griswold-Prenner I, Kordula T.** 2009. Nuclear factor I isoforms regulate gene expression during the differentiation of human neural progenitors to astrocytes. Stem Cells **27:**1173-1181.

350. **Kiefer JC.** 2007. Back to basics: Sox genes. Dev Dyn **236:**2356-2366.

351. **Kaltschmidt B, Kaltschmidt C.** 2009. NF-kappaB in the nervous system. Cold Spring Harb Perspect Biol **1:**a001271.

352. **Barton DE, Arquint M, Roder J, Dunn R, Francke U.** 1987. The myelin-associated glycoprotein gene: mapping to human chromosome 19 and mouse chromosome 7 and expression in quivering mice. Genomics **1:**107-112.

353. **Hamacher M, Pippirs U, Kohler A, Muller HW, Bosse F.** 2001. Plasmolipin: genomic structure, chromosomal localization, protein expression pattern, and putative association with Bardet-Biedl syndrome. Mamm Genome **12:**933-937.

354. **Kruer MC, Paisan-Ruiz C, Boddaert N, Yoon MY, Hama H, Gregory A, Malandrini A, Woltjer RL, Munnich A, Gobin S, Polster BJ, Palmeri S, Edvardson S, Hardy J, Houlden H, Hayflick SJ.** 2010. Defective FA2H leads to a novel form of neurodegeneration with brain iron accumulation (NBIA). Ann Neurol **68:**611-618.

355. **Mandich P, Grandis M, Geroldi A, Acquaviva M, Varese A, Gulli R, Ciotti P, Bellone E.** 2008. Gap junction beta 1 (GJB1) gene mutations in Italian patients with X-linked Charcot-Marie-Tooth disease. J Hum Genet **53:**529-533.

356. **Kutzleb C, Petrasch-Parwez E, Kilimann MW.** 2007. Cellular and subcellular localization of paralemmin-1, a protein involved in cell shape control, in the rat brain, adrenal gland and kidney. Histochem Cell Biol **127:**13-30.

357. **Yonezawa T, Ohtsuka A, Yoshitaka T, Hirano S, Nomoto H, Yamamoto K, Ninomiya Y.** 2003. Limitrin, a novel immunoglobulin superfamily protein localized to glia limitans formed by astrocyte endfeet. Glia **44:**190-204.

358. **Watanabe K, Hasegawa Y, Yamashita H, Shimizu K, Ding Y, Abe M, Ohta H, Imagawa K, Hojo K, Maki H, Sonoda H, Sato Y.** 2004. Vasohibin as an endothelium-derived negative feedback regulator of angiogenesis. J Clin Invest **114:**898-907.

359. **Copie-Bergman C, Gaulard P, Maouche-Chretien L, Briere J, Haioun C, Alonso MA, Romeo PH, Leroy K.** 1999. The MAL gene is expressed in primary mediastinal large B-cell lymphoma. Blood **94:**3567-3575.

360. **Ferraro A, Schepis F, Leone V, Federico A, Borbone E, Pallante P, Berlingieri MT, Chiappetta G, Monaco M, Palmieri D, Chiariotti L, Santoro M, Fusco A.** 2013. Tumor suppressor role of the CL2/DRO1/CCDC80 gene in thyroid carcinogenesis. J Clin Endocrinol Metab **98:**2834-2843.

361. **Digweed M, Gunthert U, Schneider R, Seyschab H, Friedl R, Sperling K.** 1995. Irreversible repression of DNA synthesis in Fanconi anemia cells is alleviated by the product of a novel cyclin-related gene. Mol Cell Biol **15:**305-314.

362. **Birkedal U, Christensen-Dalsgaard M, Krogh N, Sabarinathan R, Gorodkin J, Nielsen H.** 2015. Profiling of ribose methylations in RNA by high-throughput sequencing. Angew Chem Int Ed Engl **54:**451-455.

363. **Letourneau PC.** 2009. Actin in axons: stable scaffolds and dynamic filaments. Results Probl Cell Differ **48:**65-90.

364. **Muller L, de Escauriaza MD, Lajoie P, Theis M, Jung M, Muller A, Burgard C, Greiner M, Snapp EL, Dudek J, Zimmermann R.** 2010. Evolutionary gain of function for the ER membrane protein Sec62 from yeast to humans. Mol Biol Cell **21:**691-703.

365. **Takashima H, Boerkoel CF, De Jonghe P, Ceuterick C, Martin JJ, Voit T, Schroder JM, Williams A, Brophy PJ, Timmerman V, Lupski JR.** 2002. Periaxin mutations cause a broad spectrum of demyelinating neuropathies. Ann Neurol **51:**709-715.

366. **Fricker LD, McKinzie AA, Sun J, Curran E, Qian Y, Yan L, Patterson SD, Courchesne PL, Richards B, Levin N, Mzhavia N, Devi LA, Douglass J.** 2000. Identification and characterization of proSAAS, a granin-like neuroendocrine peptide precursor that inhibits prohormone processing. J Neurosci **20:**639-648.

367. **Rauwel B, Jang SM, Cassano M, Kapopoulou A, Barde I, Trono D.** 2015. Release of human cytomegalovirus from latency by a KAP1/TRIM28 phosphorylation switch. Elife **4**.

368. **Lopez-Hernandez T, Sirisi S, Capdevila-Nortes X, Montolio M, Fernandez-Duenas V, Scheper GC, van der Knaap MS, Casquero P, Ciruela F, Ferrer I, Nunes V, Estevez R.** 2011. Molecular mechanisms of MLC1 and GLIALCAM mutations in megalencephalic leukoencephalopathy with subcortical cysts. Hum Mol Genet **20:**3266-3277.

369. **Whitmarsh AJ, Kuan CY, Kennedy NJ, Kelkar N, Haydar TF, Mordes JP, Appel M, Rossini AA, Jones SN, Flavell RA, Rakic P, Davis RJ.** 2001. Requirement of the JIP1 scaffold protein for stress-induced JNK activation. Genes Dev **15:**2421-2432.

370. **Zak M, Bress A, Pfister M, Blin N.** 2011. Temporal expression pattern of Fkbp8 in rodent cochlea. Cell Physiol Biochem **28:**1023-1030.

371. **Mamalaki A, Boutou E, Hurel C, Patsavoudi E, Tzartos S, Matsas R.** 1995. The BM88 antigen, a novel neuron-specific molecule, enhances the differentiation of mouse neuroblastoma cells. J Biol Chem **270:**14201-14208.

372. **Terauchi A, Timmons KM, Kikuma K, Pechmann Y, Kneussel M, Umemori H.** 2015. Selective synaptic targeting of the excitatory and inhibitory presynaptic organizers FGF22 and FGF7. J Cell Sci **128:**281-292.

373. **Surpili MJ, Delben TM, Kobarg J.** 2003. Identification of proteins that interact with the central coiled-coil region of the human protein kinase NEK1. Biochemistry **42:**15369-15376.

374. **Chergui K, Svenningsson P, Greengard P.** 2005. Physiological role for casein kinase 1 in glutamatergic synaptic transmission. J Neurosci **25:**6601-6609.

375. **Monteggia LM, Gideons E, Kavalali ET.** 2013. The role of eukaryotic elongation factor 2 kinase in rapid antidepressant action of ketamine. Biol Psychiatry **73:**1199-1203.

376. **Kele J, Andersson ER, Villaescusa JC, Cajanek L, Parish CL, Bonilla S, Toledo EM, Bryja V, Rubin JS, Shimono A, Arenas E.** 2012. SFRP1 and SFRP2 dose-dependently regulate midbrain dopamine neuron development in vivo and in embryonic stem cells. Stem Cells **30:**865-875.

377. **Marsland BJ, Battig P, Bauer M, Ruedl C, Lassing U, Beerli RR, Dietmeier K, Ivanova L, Pfister T, Vogt L, Nakano H, Nembrini C, Saudan P, Kopf M, Bachmann MF.** 2005. CCL19 and CCL21 induce a potent proinflammatory differentiation program in licensed dendritic cells. Immunity **22:**493-505.

378. **Satoh J, Tabunoki H, Yamamura T, Arima K, Konno H.** 2007. Human astrocytes express aquaporin-1 and aquaporin-4 in vitro and in vivo. Neuropathology **27:**245-256.

379. **Saarela J, Jung G, Hermann M, Nimpf J, Schneider WJ.** 2008. The patatin-like lipase family in Gallus gallus. BMC Genomics **9:**281.

380. **Larsson J, Forsberg M, Brannvall K, Zhang XQ, Enarsson M, Hedborg F, Forsberg-Nilsson K.** 2008. Nuclear receptor binding protein 2 is induced during neural progenitor differentiation and affects cell survival. Mol Cell Neurosci **39:**32-39.

381. **Shang YC, Chong ZZ, Wang S, Maiese K.** 2012. Wnt1 inducible signaling pathway protein 1 (WISP1) targets PRAS40 to govern beta-amyloid apoptotic injury of microglia. Curr Neurovasc Res **9:**239-249.

382. **Sugino T, Nozaki K, Hashimoto N.** 2000. Activation of mitogen-activated protein kinases in gerbil hippocampus with ischemic tolerance induced by 3-nitropropionic acid. Neurosci Lett **278:**101-104.

383. **Doxakis E, Huang EJ, Davies AM.** 2004. Homeodomain-interacting protein kinase-2 regulates apoptosis in developing sensory and sympathetic neurons. Curr Biol **14:**1761-1765.

384. **Harder JM, Ding Q, Fernandes KA, Cherry JD, Gan L, Libby RT.** 2012. BCL2L1 (BCL-X) promotes survival of adult and developing retinal ganglion cells. Mol Cell Neurosci **51:**53-59.

385. **Gondi CS, Dinh DH, Klopfenstein JD, Gujrati M, Rao JS.** 2009. MMP-2 downregulation mediates differential regulation of cell death via ErbB-2 in glioma xenografts. Int J Oncol **35:**257-263.

386. **Erlich S, Shohami E, Pinkas-Kramarski R.** 2000. Closed head injury induces up-regulation of ErbB-4 receptor at the site of injury. Mol Cell Neurosci **16:**597-608.

387. **Tu-Sekine B, Raben DM.** 2011. Regulation and roles of neuronal diacylglycerol kinases: a lipid perspective. Crit Rev Biochem Mol Biol **46:**353-364.

388. **Hawryluk GW, Cusimano MD.** 2006. The role of recombinant activated factor VII in neurosurgery: hope or hype? J Neurosurg **105:**859-868.

389. **Perez-Janices N, Blanco-Luquin I, Tunon MT, Barba-Ramos E, Ibanez B, Zazpe-Cenoz I, Martinez-Aguillo M, Hernandez B, Martinez-Lopez E, Fernandez AF, Mercado MR, Cabada T, Escors D, Megias D, Guerrero-Setas D.** 2015. EPB41L3,

TSP-1 and RASSF2 as new clinically relevant prognostic biomarkers in diffuse gliomas. Oncotarget **6:**368-380.

390. **Tsujikawa M, Malicki J.** 2004. Intraflagellar transport genes are essential for differentiation and survival of vertebrate sensory neurons. Neuron **42:**703-716.

391. **Infante C, Ramos-Morales F, Fedriani C, Bornens M, Rios RM.** 1999. GMAP-210, A cis-Golgi network-associated protein, is a minus end microtubule-binding protein. J Cell Biol **145:**83-98.

392. **Surapureddi S, Viswakarma N, Yu S, Guo D, Rao MS, Reddy JK.** 2006. PRIC320, a transcription coactivator, isolated from peroxisome proliferator-binding protein complex. Biochem Biophys Res Commun **343:**535-543.

393. **Camarena V, Cao L, Abad C, Abrams A, Toledo Y, Araki K, Araki M, Walz K, Young JI.** 2014. Disruption of Mbd5 in mice causes neuronal functional deficits and neurobehavioral abnormalities consistent with 2q23.1 microdeletion syndrome. EMBO Mol Med **6:**1003-1015.

394. **Pettersson M, Dannaeus K, Nilsson K, Jonsson JI.** 2000. Isolation of MYADM, a novel hematopoietic-associated marker gene expressed in multipotent progenitor cells and up-regulated during myeloid differentiation. J Leukoc Biol **67:**423-431.

395. **Davis AE, 3rd, Cai S, Liu D.** 2004. The biological role of the C1 inhibitor in regulation of vascular permeability and modulation of inflammation. Adv Immunol **82:**331-363.

396. **North RA.** 2004. P2X3 receptors and peripheral pain mechanisms. J Physiol **554:**301-308.

397. **Watson AP, Evans RL, Egland KA.** 2013. Multiple functions of sushi domain containing 2 (SUSD2) in breast tumorigenesis. Mol Cancer Res **11:**74-85.

398. **Kzhyshkowska J, Gratchev A, Goerdt S.** 2007. Human chitinases and chitinase-like proteins as indicators for inflammation and cancer. Biomark Insights **2:**128-146.

399. **Richter F, Meurers BH, Zhu C, Medvedeva VP, Chesselet MF.** 2009. Neurons express hemoglobin alpha- and beta-chains in rat and human brains. J Comp Neurol **515:**538-547.

400. **Zhou ZD, Chan CH, Ma QH, Xu XH, Xiao ZC, Tan EK.** 2011. The roles of amyloid precursor protein (APP) in neurogenesis: Implications to pathogenesis and therapy of Alzheimer disease. Cell Adh Migr **5:**280-292.

401. **Hermann JS, Skroblin P, Bertinetti D, Hanold LE, von der Heide EK, Wagener EM, Zenn HM, Klussmann E, Kennedy EJ, Herberg FW.** 2015. Neurochondrin is an atypical RIIalpha-specific A-kinase anchoring protein. Biochim Biophys Acta doi:10.1016/j.bbapap.2015.04.018.

402. **Nakayama T, Yaoi T, Yasui M, Kuwajima G.** 1998. N-copine: a novel two C2-domain-containing protein with neuronal activity-regulated expression. FEBS Lett **428:**80-84.

403. **Matsuda K, Park CH, Sunden Y, Kimura T, Ochiai K, Kida H, Umemura T.** 2004. The vagus nerve is one route of transneural invasion for intranasally inoculated influenza a virus in mice. Vet Pathol **41:**101-107.

404. **Gesser RM, Koo SC.** 1996. Oral inoculation with herpes simplex virus type 1 infects enteric neuron and mucosal nerve fibers within the gastrointestinal tract in mice. J Virol **70:**4097-4102.

405. **Thompson RL, Sawtell NM.** 2000. Replication of herpes simplex virus type 1 within trigeminal ganglia is required for high frequency but not high viral genome copy number latency. J Virol **74:**965-974.

406. **Song HS, Back JH, Jin DK, Chung PW, Moon HS, Suh BC, Kim YB, Kim BM, Woo HY, Lee YT, Park KY.** 2008. Cardiac troponin T elevation after stroke: relationships between elevated serum troponin T, stroke location, and prognosis. J Clin Neurol **4:**75-83.

407. **Hasirci B, Okay M, Agircan D, Kocer A.** 2013. Elevated troponin level with negative outcome was found in ischemic stroke. Cardiovasc Psychiatry Neurol **2013:**953672.

408. **Kang JH, Ho JD, Chen YH, Lin HC.** 2009. Increased risk of stroke after a herpes zoster attack: a population-based follow-up study. Stroke **40:**3443-3448.

409. **Wirrell E, Hill MD, Jadavji T, Kirton A, Barlow K.** 2004. Stroke after varicella vaccination. J Pediatr **145:**845-847.

410. **van Velzen M, Laman JD, Kleinjan A, Poot A, Osterhaus AD, Verjans GM.** 2009. Neuron-interacting satellite glial cells in human trigeminal ganglia have an APC phenotype. J Immunol **183:**2456-2461.

411. **Trudler D, Farfara D, Frenkel D.** 2010. Toll-like receptors expression and signaling in glia cells in neuro-amyloidogenic diseases: towards future therapeutic application. Mediators Inflamm **2010**.

412. **Kawai T, Akira S.** 2010. The role of pattern-recognition receptors in innate immunity: update on Toll-like receptors. Nat Immunol **11:**373-384.

413. **Clarner T, Janssen K, Nellessen L, Stangel M, Skripuletz T, Krauspe B, Hess FM, Denecke B, Beutner C, Linnartz-Gerlach B, Neumann H, Vallieres L, Amor S, Ohl K, Tenbrock K, Beyer C, Kipp M.** 2015. CXCL10 triggers early microglial activation in the cuprizone model. J Immunol **194:**3400-3413.

414. **Muller M, Carter S, Hofer MJ, Campbell IL.** 2010. Review: The chemokine receptor CXCR3 and its ligands CXCL9, CXCL10 and CXCL11 in neuroimmunity--a tale of conflict and conundrum. Neuropathol Appl Neurobiol **36:**368-387.

415. **Whitaker-Dowling PA, Wilcox DK, Widnell CC, Youngner JS.** 1983. Interferon-mediated inhibition of virus penetration. Proc Natl Acad Sci U S A **80:**1083-1086.

416. **Campadelli-Fiume G, Amasio M, Avitabile E, Cerretani A, Forghieri C, Gianni T, Menotti L.** 2007. The multipartite system that mediates entry of herpes simplex virus into the cell. Rev Med Virol **17:**313-326.

417. **Fazakerley JK, Walker R.** 2003. Virus demyelination. J Neurovirol **9:**148-164.

418. **Martin JR.** 1984. Intra-axonal virus in demyelinative lesions of experimental herpes simplex type 2 infection. J Neurol Sci **63:**63-74.

419. **Malmquist SJ, Abramsson A, McGraw HF, Linbo TH, Raible DW.** 2013. Modulation of dorsal root ganglion development by ErbB signaling and the scaffold protein Sorbs3. Development **140:**3986-3996.

420. **Kennedy PG, Major EO, Williams RK, Straus SE.** 1994. Down-regulation of glial fibrillary acidic protein expression during acute lytic varicella-zoster virus infection of cultured human astrocytes. Virology **205:**558-562.

421. **Jones M, Dry IR, Frampton D, Singh M, Kanda RK, Yee MB, Kellam P, Hollinshead M, Kinchington PR, O'Toole EA, Breuer J.** 2014. RNA-seq analysis of host and viral gene expression highlights interaction between varicella zoster virus and keratinocyte differentiation. PLoS Pathog **10:**e1003896.

422. **Jones JO, Arvin AM.** 2003. Microarray analysis of host cell gene transcription in response to varicella-zoster virus infection of human T cells and fibroblasts in vitro and SCIDhu skin xenografts in vivo. J Virol **77:**1268-1280.

423. **Mahalingam R, Messaoudi I, Gilden D.** 2010. Simian varicella virus pathogenesis. Curr Top Microbiol Immunol **342:**309-321.

424. **Arnold N, Girke T, Sureshchandra S, Messaoudi I.** 2016. Acute simian varicella infection causes robust and sustained changes in gene expression in the sensory ganglia. J Virol doi:10.1128/JVI.01272-16.

425. **Girke T.** 2015. systemPipeR:NGS workflow and report generation environment.

426. **Komatsu T, Nagata K.** 2012. Replication-uncoupled histone deposition during adenovirus DNA replication. J Virol **86:**6701-6711.

427. **Conn KL, Hendzel MJ, Schang LM.** 2008. Linker histones are mobilized during infection with herpes simplex virus type 1. J Virol **82:**8629-8646.

428. **Lieberman PM.** 2008. Chromatin organization and virus gene expression. J Cell Physiol **216:**295-302.

429. **Halazonetis TD, Georgopoulos K, Greenberg ME, Leder P.** 1988. c-Jun dimerizes with itself and with c-Fos, forming complexes of different DNA binding affinities. Cell **55:**917-924.

430. **Provost E, Weier CA, Leach SD.** 2013. Multiple ribosomal proteins are expressed at high levels in developing zebrafish endoderm and are required for normal exocrine pancreas development. Zebrafish **10:**161-169.

431. **Jackson RJ, Hellen CU, Pestova TV.** 2010. The mechanism of eukaryotic translation initiation and principles of its regulation. Nat Rev Mol Cell Biol **11:**113-127.

432. **Tetsuka T, Uranishi H, Imai H, Ono T, Sonta S, Takahashi N, Asamitsu K, Okamoto T.** 2000. Inhibition of nuclear factor-kappaB-mediated transcription by association with the amino-terminal enhancer of split, a Groucho-related protein lacking WD40 repeats. J Biol Chem **275:**4383-4390.

433. **Stauffer DR, Howard TL, Nyun T, Hollenberg SM.** 2001. CHMP1 is a novel nuclear matrix protein affecting chromatin structure and cell-cycle progression. J Cell Sci **114:**2383-2393.

434. **Shor B, Wu J, Shakey Q, Toral-Barza L, Shi C, Follettie M, Yu K.** 2010. Requirement of the mTOR kinase for the regulation of Maf1 phosphorylation and control of RNA polymerase III-dependent transcription in cancer cells. J Biol Chem **285:**15380-15392.

435. **Friedman JR, Fredericks WJ, Jensen DE, Speicher DW, Huang XP, Neilson EG, Rauscher FJ, 3rd.** 1996. KAP-1, a novel corepressor for the highly conserved KRAB repression domain. Genes Dev **10:**2067-2078.

436. **Morey L, Brenner C, Fazi F, Villa R, Gutierrez A, Buschbeck M, Nervi C, Minucci S, Fuks F, Di Croce L.** 2008. MBD3, a component of the NuRD complex, facilitates chromatin alteration and deposition of epigenetic marks. Mol Cell Biol **28:**5912-5923.

437. **Tokumitsu H, Brickey DA, Glod J, Hidaka H, Sikela J, Soderling TR.** 1994. Activation mechanisms for Ca2+/calmodulin-dependent protein kinase IV. Identification of a brain CaM-kinase IV kinase. J Biol Chem **269:**28640-28647.

438. **Moser SC, Bensaddek D, Ortmann B, Maure JF, Mudie S, Blow JJ, Lamond AI, Swedlow JR, Rocha S.** 2013. PHD1 links cell-cycle progression to oxygen sensing through hydroxylation of the centrosomal protein Cep192. Dev Cell **26:**381-392.

439. **Ballabio E, Mariotti M, De Benedictis L, Maier JA.** 2004. The dual role of endothelial differentiation-related factor-1 in the cytosol and nucleus: modulation by protein kinase A. Cell Mol Life Sci **61:**1069-1074.

440. **Lord SJ, Rajotte RV, Korbutt GS, Bleackley RC.** 2003. Granzyme B: a natural born killer. Immunol Rev **193:**31-38.

441. **Schoggins JW, Rice CM.** 2011. Interferon-stimulated genes and their antiviral effector functions. Curr Opin Virol **1:**519-525.

442. **Honda K, Taniguchi T.** 2006. IRFs: master regulators of signalling by Toll-like receptors and cytosolic pattern-recognition receptors. Nat Rev Immunol **6:**644-658.

443. **Ostermann G, Weber KS, Zernecke A, Schroder A, Weber C.** 2002. JAM-1 is a ligand of the beta(2) integrin LFA-1 involved in transendothelial migration of leukocytes. Nat Immunol **3:**151-158.

444. **Paz PE, Wang S, Clarke H, Lu X, Stokoe D, Abo A.** 2001. Mapping the Zap-70 phosphorylation sites on LAT (linker for activation of T cells) required for recruitment and activation of signalling proteins in T cells. Biochem J **356:**461-471.

445. **Xue L, Chiang L, Kang C, Winoto A.** 2008. The role of the PI3K-AKT kinase pathway in T-cell development beyond the beta checkpoint. European Journal of Immunology **38:**3200-3207.

446. **Yamazaki T, Hamano Y, Tashiro H, Itoh K, Nakano H, Miyatake S, Saito T.** 1999. CAST, a novel CD3epsilon-binding protein transducing activation signal for interleukin-2 production in T cells. J Biol Chem **274:**18173-18180.

447. **Zhu MH, Berry JA, Russell SM, Leonard WJ.** 1998. Delineation of the regions of interleukin-2 (IL-2) receptor beta chain important for association of Jak1 and Jak3. Jak1-independent functional recruitment of Jak3 to Il-2Rbeta. J Biol Chem **273:**10719-10725.

448. **Randow F, Lehner PJ.** 2009. Viral avoidance and exploitation of the ubiquitin system. Nat Cell Biol **11:**527-534.

449. **Kristie TM, Liang Y, Vogel JL.** 2010. Control of alpha-herpesvirus IE gene expression by HCF-1 coupled chromatin modification activities. Biochim Biophys Acta **1799:**257-265.

450. **Kalpana GV, Marmon S, Wang W, Crabtree GR, Goff SP.** 1994. Binding and stimulation of HIV-1 integrase by a human homolog of yeast transcription factor SNF5. Science **266:**2002-2006.

451. **Butin-Israeli V, Drayman N, Oppenheim A.** 2010. Simian virus 40 infection triggers a balanced network that includes apoptotic, survival, and stress pathways. J Virol **84:**3431-3442.

452. **Fahmi H, Cochet C, Hmama Z, Opolon P, Joab I.** 2000. Transforming growth factor beta 1 stimulates expression of the Epstein-Barr virus BZLF1 immediate-early gene product ZEBRA by an indirect mechanism which requires the MAPK kinase pathway. J Virol **74:**5810-5818.

453. **Breen KC, Bruce M, Anderton BH.** 1991. Beta amyloid precursor protein mediates neuronal cell-cell and cell-surface adhesion. J Neurosci Res **28:**90-100.

454. **Prokunina-Olsson L, Kaplan LM, Schadt EE, Collins FS.** 2009. Alternative splicing of TCF7L2 gene in omental and subcutaneous adipose tissue and risk of type 2 diabetes. PLoS One **4:**e7231.

455. **Agiostratidou G, Muros RM, Shioi J, Marambaud P, Robakis NK.** 2006. The cytoplasmic sequence of E-cadherin promotes non-amyloidogenic degradation of A beta precursors. J Neurochem **96:**1182-1188.

456. **Brown GD.** 2006. Dectin-1: a signalling non-TLR pattern-recognition receptor. Nat Rev Immunol **6:**33-43.

457. **Dansako H, Yamane D, Welsch C, McGivern DR, Hu F, Kato N, Lemon SM.** 2013. Class A scavenger receptor 1 (MSR1) restricts hepatitis C virus replication by mediating toll-like receptor 3 recognition of viral RNAs produced in neighboring cells. PLoS Pathog **9:**e1003345.

458. **Lu YC, Yeh WC, Ohashi PS.** 2008. LPS/TLR4 signal transduction pathway. Cytokine **42:**145-151.

459. **Kerkhoff E, Simpson JC, Leberfinger CB, Otto IM, Doerks T, Bork P, Rapp UR, Raabe T, Pepperkok R.** 2001. The Spir actin organizers are involved in vesicle transport processes. Curr Biol **11:**1963-1968.

460. **Heider MR, Munson M.** 2012. Exorcising the exocyst complex. Traffic **13:**898-907.

461. **Zeisel MB, Koutsoudakis G, Schnober EK, Haberstroh A, Blum HE, Cosset FL, Wakita T, Jaeck D, Doffoel M, Royer C, Soulier E, Schvoerer E, Schuster C, Stoll-Keller F, Bartenschlager R, Pietschmann T, Barth H, Baumert TF.** 2007. Scavenger receptor class B type I is a key host factor for hepatitis C virus infection required for an entry step closely linked to CD81. Hepatology **46:**1722-1731.

462. **Miller JL, de Wet BJ, Martinez-Pomares L, Radcliffe CM, Dwek RA, Rudd PM, Gordon S.** 2008. The mannose receptor mediates dengue virus infection of macrophages. PLoS Pathog **4:**e17.

463. **Gianni T, Salvioli S, Chesnokova LS, Hutt-Fletcher LM, Campadelli-Fiume G.** 2013. alphavbeta6- and alphavbeta8-integrins serve as interchangeable receptors for HSV gH/gL to promote endocytosis and activation of membrane fusion. PLoS Pathog **9:**e1003806.

464. **Stief TW, Radtke KP, Heimburger N.** 1987. Inhibition of urokinase by protein C-inhibitor (PCI). Evidence for identity of PCI and plasminogen activator inhibitor 3. Biol Chem Hoppe Seyler **368:**1427-1433.

465. **DePoli P, Bacon-Baguley T, Kendra-Franczak S, Cederholm MT, Walz DA.** 1989. Thrombospondin interaction with plasminogen. Evidence for binding to a specific region of the kringle structure of plasminogen. Blood **73:**976-982.

466. **Huber R, Romisch J, Paques EP.** 1990. The crystal and molecular structure of human annexin V, an anticoagulant protein that binds to calcium and membranes. EMBO J **9:**3867-3874.

467. **de Boer JP, Creasey AA, Chang A, Abbink JJ, Roem D, Eerenberg AJ, Hack CE, Taylor FB, Jr.** 1993. Alpha-2-macroglobulin functions as an inhibitor of fibrinolytic, clotting, and neutrophilic proteinases in sepsis: studies using a baboon model. Infect Immun **61:**5035-5043.

468. **Szabo R, Netzel-Arnett S, Hobson JP, Antalis TM, Bugge TH.** 2005. Matriptase-3 is a novel phylogenetically preserved membrane-anchored serine protease with broad serpin reactivity. Biochem J **390:**231-242.

469. **Bengtsson-Olivecrona G, Sletten K.** 1990. Primary structure of the bovine analogues to human apolipoproteins CII and CIII. Studies on isoforms and evidence for proteolytic processing. Eur J Biochem **192:**515-521.

470. **Kang JY, Sung SH, Lee YJ, Choi TI, Choi SJ.** 2014. Impact of ENPP1 K121Q on change of insulin resistance after web-based intervention in Korean men with diabetes and impaired fasting glucose. J Korean Med Sci **29:**1353-1359.

471. **Kuribayashi F, de Boer M, Leusen JH, Verhoeven AJ, Roos D.** 1996. A novel polymorphism in the coding region of CYBB, the human gp91-phox gene. Hum Genet **97:**611-613.

472. **Huberle A, Beyeen AD, Ockinger J, Ayturan M, Jagodic M, de Graaf KL, Fissolo N, Marta M, Olofsson P, Hultqvist M, Holmdahl R, Olsson T, Weissert R.** 2009. Advanced intercross line mapping suggests that ncf1 (ean6) regulates severity in an animal model of guillain-barre syndrome. J Immunol **182:**4432-4438.

473. **Guindalini C, Lee KS, Andersen ML, Santos-Silva R, Bittencourt LR, Tufik S.** 2010. The influence of obstructive sleep apnea on the expression of glycerol-3-phosphate dehydrogenase 1 gene. Exp Biol Med (Maywood) **235:**52-56.

474. **Hymowitz SG, Christinger HW, Fuh G, Ultsch M, O'Connell M, Kelley RF, Ashkenazi A, de Vos AM.** 1999. Triggering cell death: The crystal structure of Apo2L/TRAIL in a complex with death receptor 5. Molecular Cell **4:**563-571.

475. **Pias EK, Ekshyyan OY, Rhoads CA, Fuseler J, Harrison L, Aw TY.** 2003. Differential effects of superoxide dismutase isoform expression on hydroperoxide-induced apoptosis in PC-12 cells. Journal of Biological Chemistry **278:**13294-13301.

476. **Fu J, Yang QY, Sai K, Chen FR, Pang JCS, Ng HK, Kwan AL, Chen ZP.** 2013. TGM2 inhibition attenuates ID1 expression in CD44-high glioma-initiating cells. Neuro-Oncology **15:**1353-1365.

477. **Walsh D, Mathews MB, Mohr I.** 2013. Tinkering with translation: protein synthesis in virus-infected cells. Cold Spring Harb Perspect Biol **5:**a012351.

478. **Lee AS, Burdeinick-Kerr R, Whelan SP.** 2013. A ribosome-specialized translation initiation pathway is required for cap-dependent translation of vesicular stomatitis virus mRNAs. Proc Natl Acad Sci U S A **110:**324-329.

479. **Walsh D, Mohr I.** 2004. Phosphorylation of eIF4E by Mnk-1 enhances HSV-1 translation and replication in quiescent cells. Genes Dev **18:**660-672.

480. **Walsh D, Perez C, Notary J, Mohr I.** 2005. Regulation of the translation initiation factor eIF4F by multiple mechanisms in human cytomegalovirus-infected cells. J Virol **79:**8057-8064.

481. **Liang Y, Vogel JL, Narayanan A, Peng H, Kristie TM.** 2009. Inhibition of the histone demethylase LSD1 blocks alpha-herpesvirus lytic replication and reactivation from latency. Nat Med **15:**1312-1317.

482. **Ambagala AP, Bosma T, Ali MA, Poustovoitov M, Chen JJ, Gershon MD, Adams PD, Cohen JI.** 2009. Varicella-zoster virus immediate-early 63 protein interacts with human antisilencing function 1 protein and alters its ability to bind histones h3.1 and h3.3. J Virol **83:**200-209.

483. **Helin E, Matikainen S, Julkunen I, Heino J, Hyypia T, Vainionpaa R.** 2002. Measles virus enhances the expression of cellular immediate-early genes and DNA-binding of transcription factor AP-1 in lung epithelial A549 cells. Arch Virol **147:**1721-1732.

484. **Sadowska B, Barrucco R, Khalili K, Safak M.** 2003. Regulation of human polyomavirus JC virus gene transcription by AP-1 in glial cells. J Virol **77:**665-672.

485. **Huttunen P, Heino J, Hyypia T.** 1997. Echovirus 1 replication, not only virus binding to its receptor, VLA-2, is required for the induction of cellular immediate-early genes. J Virol **71:**4176-4180.

486. **Bagga S, Bouchard MJ.** 2014. Cell cycle regulation during viral infection. Methods Mol Biol **1170:**165-227.

487. **Jiang W, Wang Q, Chen S, Gao S, Song L, Liu P, Huang W.** 2013. Influenza A virus NS1 induces G0/G1 cell cycle arrest by inhibiting the expression and activity of RhoA protein. J Virol **87:**3039-3052.

488. **Yuan X, Wu J, Shan Y, Yao Z, Dong B, Chen B, Zhao Z, Wang S, Chen J, Cong Y.** 2006. SARS coronavirus 7a protein blocks cell cycle progression at G0/G1 phase via the cyclin D3/pRb pathway. Virology **346:**74-85.

489. **Goh WC, Rogel ME, Kinsey CM, Michael SF, Fultz PN, Nowak MA, Hahn BH, Emerman M.** 1998. HIV-1 Vpr increases viral expression by manipulation of the cell cycle: a mechanism for selection of Vpr in vivo. Nat Med **4:**65-71.

490. **Chami M, Oules B, Paterlini-Brechot P.** 2006. Cytobiological consequences of calcium-signaling alterations induced by human viral proteins. Biochim Biophys Acta **1763:**1344-1362.

491. **Namazue J, Kato T, Okuno T, Shiraki K, Yamanishi K.** 1989. Evidence for attachment of fatty acid to varicella-zoster virus glycoproteins and effect of cerulenin on the maturation of varicella-zoster virus glycoproteins. Intervirology **30:**268-277.

492. **Gao TT, Qin ZL, Ren H, Zhao P, Qi ZT.** 2015. Inhibition of IRS-1 by hepatitis C virus infection leads to insulin resistance in a PTEN-dependent manner. Virol J **12:**12.

493. **Rasheed S, Yan JS, Lau A, Chan AS.** 2008. HIV replication enhances production of free fatty acids, low density lipoproteins and many key proteins involved in lipid metabolism: a proteomics study. PLoS One **3:**e3003.

494. **Reiss CS, Komatsu T.** 1998. Does nitric oxide play a critical role in viral infections? J Virol **72:**4547-4551.

495. **Sen N, Mukherjee G, Arvin AM.** 2015. Single cell mass cytometry reveals remodeling of human T cell phenotypes by varicella zoster virus. Methods **90:**85-94.

496. **Mogensen TH.** 2009. Pathogen recognition and inflammatory signaling in innate immune defenses. Clin Microbiol Rev **22:**240-273, Table of Contents.

497. **Yu WC, Chan RW, Wang J, Travanty EA, Nicholls JM, Peiris JS, Mason RJ, Chan MC.** 2011. Viral replication and innate host responses in primary human alveolar epithelial cells and alveolar macrophages infected with influenza H5N1 and H1N1 viruses. J Virol **85:**6844-6855.

498. **Catusse J, Spinks J, Mattick C, Dyer A, Laing K, Fitzsimons C, Smit MJ, Gompels UA.** 2008. Immunomodulation by herpesvirus U51A chemokine receptor via CCL5 and FOG-2 down-regulation plus XCR1 and CCR7 mimicry in human leukocytes. Eur J Immunol **38:**763-777.

499. **Alcami A, Symons JA, Collins PD, Williams TJ, Smith GL.** 1998. Blockade of chemokine activity by a soluble chemokine binding protein from vaccinia virus. J Immunol **160:**624-633.

500. **Wilson JF, Marsa GW, Johnson RE.** 1972. Herpes zoster in Hodgkin's disease. Clinical, histologic, and immunologic correlations. Cancer **29:**461-465.

501. **Arvin AM.** 2000. Varicella-Zoster virus: pathogenesis, immunity, and clinical management in hematopoietic cell transplant recipients. Biol Blood Marrow Transplant **6:**219-230.

502. **Rusthoven JJ, Ahlgren P, Elhakim T, Pinfold P, Reid J, Stewart L, Feld R.** 1988. Varicella-zoster infection in adult cancer patients. A population study. Arch Intern Med **148:**1561-1566.

503. **Schmader K, Studenski S, MacMillan J, Grufferman S, Cohen HJ.** 1990. Are stressful life events risk factors for herpes zoster? J Am Geriatr Soc **38:**1188-1194.

504. **Randall J. Cohrs SKMDSSDHGDLP.** 2008. Asymptomatic reactivation and shed of infectious varicella zoster virus in astronauts. Journal of Medical Virology **80:**1116-1122.

505. **Uchakin PN, Parish DC, Dane FC, Uchakina ON, Scheetz AP, Agarwal NK, Smith BE.** 2011. Fatigue in medical residents leads to reactivation of herpes virus latency. Interdiscip Perspect Infect Dis **2011:**571340.

506. **Terada K, Kawano S, Yoshihiro K, Morita T.** 1994. Varicella-zoster virus (VZV) reactivation is related to the low response of VZV-specific immunity after chickenpox in infancy. J Infect Dis **169:**650-652.

507. **Oxman MN.** 2009. Herpes zoster pathogenesis and cell-mediated immunity and immunosenescence. J Am Osteopath Assoc **109:**S13-17.

508. **Vermont CL, Jol-van der Zijde EC, Hissink Muller P, Ball LM, Bredius RG, Vossen AC, Lankester AC.** 2014. Varicella zoster reactivation after hematopoietic stem cell transplant in children is strongly correlated with leukemia treatment and suppression of host T-lymphocyte immunity. Transpl Infect Dis **16:**188-194.

509. **Onozawa M, Hashino S, Takahata M, Fujisawa F, Kawamura T, Nakagawa M, Kahata K, Kondo T, Ota S, Tanaka J, Imamura M, Asaka M.** 2006. Relationship between preexisting anti-varicella-zoster virus (VZV) antibody and clinical VZV reactivation in hematopoietic stem cell transplantation recipients. J Clin Microbiol **44:**4441-4443.

510. **Park HB, Kim KC, Park JH, Kang TY, Lee HS, Kim TH, Jun JB, Bae SC, Yoo DH, Craft J, Jung S.** 2004. Association of reduced CD4 T cell responses specific to varicella zoster virus with high incidence of herpes zoster in patients with systemic lupus erythematosus. J Rheumatol **31:**2151-2155.

511. **Mahalingam R, Traina-Dorge V, Wellish M, Lorino R, Sanford R, Ribka EP, Alleman SJ, Brazeau E, Gilden DH.** 2007. Simian varicella virus reactivation in cynomolgus monkeys. Virology **368:**50-59.

512. **Traina-Dorge V, Doyle-Meyers LA, Sanford R, Manfredo J, Blackmon A, Wellish M, James S, Alvarez X, Midkiff C, Palmer BE, Deharo E, Gilden D, Mahalingam R.** 2015. Simian Varicella Virus Is Present in Macrophages, Dendritic Cells, and T Cells in Lymph Nodes of Rhesus Macaques after Experimental Reactivation. J Virol **89:**9817-9824.

513. **Zhang D, Zhao T, Ang HS, Chong P, Saiki R, Igarashi K, Yang H, Vardy LA.** 2012. AMD1 is essential for ESC self-renewal and is translationally down-regulated on differentiation to neural precursor cells. Genes Dev **26:**461-473.

514. **Keller LC, Geimer S, Romijn E, Yates J, 3rd, Zamora I, Marshall WF.** 2009. Molecular architecture of the centriole proteome: the conserved WD40 domain protein POC1 is required for centriole duplication and length control. Mol Biol Cell **20:**1150-1166.

515. **Wieczorek E, Brand M, Jacq X, Tora L.** 1998. Function of TAF(II)-containing complex without TBP in transcription by RNA polymerase II. Nature **393:**187-191.

516. **Rapino C, Bianchi G, Di Giulio C, Centurione L, Cacchio M, Antonucci A, Cataldi A.** 2005. HIF-1alpha cytoplasmic accumulation is associated with cell death in old rat cerebral cortex exposed to intermittent hypoxia. Aging Cell **4:**177-185.

517. **Iacobas DA, Urban-Maldonado M, Iacobas S, Scemes E, Spray DC.** 2003. Array analysis of gene expression in connexin-43 null astrocytes. Physiol Genomics **15:**177-190.

518. **Johnson ES, Ma PC, Ota IM, Varshavsky A.** 1995. A proteolytic pathway that recognizes ubiquitin as a degradation signal. J Biol Chem **270:**17442-17456.

519. **Flynn JM, Neher SB, Kim YI, Sauer RT, Baker TA.** 2003. Proteomic discovery of cellular substrates of the ClpXP protease reveals five classes of ClpX-recognition signals. Mol Cell **11:**671-683.

520. **Wang CC, Kadota M, Nishigaki R, Kazuki Y, Shirayoshi Y, Rogers MS, Gojobori T, Ikeo K, Oshimura M.** 2004. Molecular hierarchy in neurons differentiated from mouse ES cells containing a single human chromosome 21. Biochem Biophys Res Commun **314:**335-350.

521. **Liu Z, Li H, Hu X, Yu L, Liu H, Han R, Colella R, Mower GD, Chen Y, Qiu M.** 2008. Control of precerebellar neuron development by Olig3 bHLH transcription factor. J Neurosci **28:**10124-10133.

522. **O'Keeffe GW, Gutierrez H, Howard L, Laurie CW, Osorio C, Gavalda N, Wyatt SL, Davies AM.** 2016. Region-specific role of growth differentiation factor-5 in the establishment of sympathetic innervation. Neural Dev **11:**4.

523. **Arimoto K, Funami K, Saeki Y, Tanaka K, Okawa K, Takeuchi O, Akira S, Murakami Y, Shimotohno K.** 2010. Polyubiquitin conjugation to NEMO by triparite motif protein 23 (TRIM23) is critical in antiviral defense. Proc Natl Acad Sci U S A **107:**15856-15861.

524. **Kwon J, Cho HJ, Han SH, No JG, Kwon JY, Kim H.** 2010. A novel LZAP-binding protein, NLBP, inhibits cell invasion. J Biol Chem **285:**12232-12240.

525. **Lan L, Ui A, Nakajima S, Hatakeyama K, Hoshi M, Watanabe R, Janicki SM, Ogiwara H, Kohno T, Kanno S, Yasui A.** 2010. The ACF1 complex is required for DNA double-strand break repair in human cells. Mol Cell **40:**976-987.

526. **Blackmore TM, Mercer CF, Paterno GD, Gillespie LL.** 2008. The transcriptional cofactor MIER1-beta negatively regulates histone acetyltransferase activity of the CREB-binding protein. BMC Res Notes **1:**68.

527. **Aslam A, Mittal S, Koch F, Andrau JC, Winkler GS.** 2009. The Ccr4-NOT deadenylase subunits CNOT7 and CNOT8 have overlapping roles and modulate cell proliferation. Mol Biol Cell **20:**3840-3850.

528. **Ikeda M, Ikeda M.** 2014. Bmal1 is an essential regulator for circadian cytosolic Ca(2)(+) rhythms in suprachiasmatic nucleus neurons. J Neurosci **34:**12029-12038.

529. **Emanuele MJ, Stukenberg PT.** 2007. Xenopus Cep57 is a novel kinetochore component involved in microtubule attachment. Cell **130:**893-905.

530. **Lohi H, Kujala M, Makela S, Lehtonen E, Kestila M, Saarialho-Kere U, Markovich D, Kere J.** 2002. Functional characterization of three novel tissue-specific anion exchangers SLC26A7, -A8, and -A9. J Biol Chem **277:**14246-14254.

531. **Maden M.** 2007. Retinoic acid in the development, regeneration and maintenance of the nervous system. Nat Rev Neurosci **8:**755-765.

532. **Manteniotis S, Lehmann R, Flegel C, Vogel F, Hofreuter A, Schreiner BS, Altmuller J, Becker C, Schobel N, Hatt H, Gisselmann G.** 2013. Comprehensive RNA-Seq expression analysis of sensory ganglia with a focus on ion channels and GPCRs in Trigeminal ganglia. PLoS One **8:**e79523.

533. **Toth C, Shim SY, Wang J, Jiang Y, Neumayer G, Belzil C, Liu WQ, Martinez J, Zochodne D, Nguyen MD.** 2008. Ndel1 promotes axon regeneration via intermediate filaments. PLoS One **3:**e2014.

534. **Kuja-Panula J, Kiiltomaki M, Yamashiro T, Rouhiainen A, Rauvala H.** 2003. AMIGO, a transmembrane protein implicated in axon tract development, defines a novel protein family with leucine-rich repeats. J Cell Biol **160:**963-973.

535. **Rege TA, Hagood JS.** 2006. Thy-1 as a regulator of cell-cell and cell-matrix interactions in axon regeneration, apoptosis, adhesion, migration, cancer, and fibrosis. FASEB J **20:**1045-1054.

536. **Baum PD, Garriga G.** 1997. Neuronal migrations and axon fasciculation are disrupted in ina-1 integrin mutants. Neuron **19:**51-62.

537. **Ono Y, Nakatani T, Minaki Y, Kumai M.** 2010. The basic helix-loop-helix transcription factor Nato3 controls neurogenic activity in mesencephalic floor plate cells. Development **137:**1897-1906.

538. **Goodfellow SJ, Rebello MR, Toska E, Zeef LA, Rudd SG, Medler KF, Roberts SG.** 2011. WT1 and its transcriptional cofactor BASP1 redirect the differentiation pathway of an established blood cell line. Biochem J **435:**113-125.

539. **Torres-Peraza JF, Engel T, Martin-Ibanez R, Sanz-Rodriguez A, Fernandez-Fernandez MR, Esgleas M, Canals JM, Henshall DC, Lucas JJ.** 2013. Protective neuronal induction of ATF5 in endoplasmic reticulum stress induced by status epilepticus. Brain **136:**1161-1176.

540. **Gaboli M, Kotsi PA, Gurrieri C, Cattoretti G, Ronchetti S, Cordon-Cardo C, Broxmeyer HE, Hromas R, Pandolfi PP.** 2001. Mzf1 controls cell proliferation and tumorigenesis. Genes Dev **15:**1625-1630.

541. **Kurumizaka H, Ikawa S, Nakada M, Eda K, Kagawa W, Takata M, Takeda S, Yokoyama S, Shibata T.** 2001. Homologous-pairing activity of the human DNA-repair proteins Xrcc3.Rad51C. Proc Natl Acad Sci U S A **98:**5538-5543.

542. **Nagasawa K, Higashi T, Hosokawa N, Kaufman RJ, Nagata K.** 2007. Simultaneous induction of the four subunits of the TRAP complex by ER stress accelerates ER degradation. EMBO Rep **8:**483-489.

543. **Maze I, Wenderski W, Noh KM, Bagot RC, Tzavaras N, Purushothaman I, Elsasser SJ, Guo Y, Ionete C, Hurd YL, Tamminga CA, Halene T, Farrelly L, Soshnev AA, Wen D, Rafii S, Birtwistle MR, Akbarian S, Buchholz BA, Blitzer RD, Nestler EJ, Yuan ZF, Garcia BA, Shen L, Molina H, Allis CD.** 2015. Critical Role of Histone Turnover in Neuronal Transcription and Plasticity. Neuron **87:**77-94.

544. **Angelastro JM, Mason JL, Ignatova TN, Kukekov VG, Stengren GB, Goldman JE, Greene LA.** 2005. Downregulation of activating transcription factor 5 is required for differentiation of neural progenitor cells into astrocytes. J Neurosci **25:**3889-3899.

545. **Oda K, Shiratsuchi T, Nishimori H, Inazawa J, Yoshikawa H, Taketani Y, Nakamura Y, Tokino T.** 1999. Identification of BAIAP2 (BAI-associated protein 2), a novel human homologue of hamster IRSp53, whose SH3 domain interacts with the cytoplasmic domain of BAI1. Cytogenet Cell Genet **84:**75-82.

546. **Kondoh H, Lleonart ME, Gil J, Wang J, Degan P, Peters G, Martinez D, Carnero A, Beach D.** 2005. Glycolytic enzymes can modulate cellular life span. Cancer Res **65:**177-185.

547. **Miura T, Nishinaka T, Terada T.** 2008. Different functions between human monomeric carbonyl reductase 3 and carbonyl reductase 1. Mol Cell Biochem **315:**113-121.

548. **Yik JH, Chen R, Pezda AC, Zhou Q.** 2005. Compensatory contributions of HEXIM1 and HEXIM2 in maintaining the balance of active and inactive positive transcription elongation factor b complexes for control of transcription. J Biol Chem **280:**16368-16376.

549. **Bekris LM, Galloway NM, Millard S, Lockhart D, Li G, Galasko DR, Farlow MR, Clark CM, Quinn JF, Kaye JA, Schellenberg GD, Leverenz JB, Seubert P, Tsuang DW, Peskind ER, Yu CE.** 2011. Amyloid precursor protein (APP) processing genes and cerebrospinal fluid APP cleavage product levels in Alzheimer's disease. Neurobiol Aging **32:**556 e513-523.

550. **Parker AE, Van de Weyer I, Laus MC, Oostveen I, Yon J, Verhasselt P, Luyten WH.** 1998. A human homologue of the Schizosaccharomyces pombe rad1+ checkpoint gene encodes an exonuclease. J Biol Chem **273:**18332-18339.

551. **Lieberman HB, Hopkins KM, Nass M, Demetrick D, Davey S.** 1996. A human homolog of the Schizosaccharomyces pombe rad9+ checkpoint control gene. Proc Natl Acad Sci U S A **93:**13890-13895.

552. **Post S, Weng YC, Cimprich K, Chen LB, Xu Y, Lee EY.** 2001. Phosphorylation of serines 635 and 645 of human Rad17 is cell cycle regulated and is required for G(1)/S checkpoint activation in response to DNA damage. Proc Natl Acad Sci U S A **98:**13102-13107.

553. **Kumar RA, Pilz DT, Babatz TD, Cushion TD, Harvey K, Topf M, Yates L, Robb S, Uyanik G, Mancini GM, Rees MI, Harvey RJ, Dobyns WB.** 2010. TUBA1A mutations cause wide spectrum lissencephaly (smooth brain) and suggest that multiple neuronal migration pathways converge on alpha tubulins. Hum Mol Genet **19:**2817-2827.

554. **Yamaguchi M, Yu S, Qiao R, Weissmann F, Miller DJ, VanderLinden R, Brown NG, Frye JJ, Peters JM, Schulman BA.** 2015. Structure of an APC3-APC16 complex: insights into assembly of the anaphase-promoting complex/cyclosome. J Mol Biol **427:**1748-1764.

555. **Lindsay RM.** 1988. Nerve growth factors (NGF, BDNF) enhance axonal regeneration but are not required for survival of adult sensory neurons. J Neurosci **8:**2394-2405.

556. **Buckingham BP, Inman DM, Lambert W, Oglesby E, Calkins DJ, Steele MR, Vetter ML, Marsh-Armstrong N, Horner PJ.** 2008. Progressive ganglion cell degeneration precedes neuronal loss in a mouse model of glaucoma. J Neurosci **28:**2735-2744.

557. **Mazzoni EO, Mahony S, Peljto M, Patel T, Thornton SR, McCuine S, Reeder C, Boyer LA, Young RA, Gifford DK, Wichterle H.** 2013. Saltatory remodeling of Hox chromatin in response to rostrocaudal patterning signals. Nat Neurosci **16:**1191-1198.

558. **Buonamici S, Trimarchi T, Ruocco MG, Reavie L, Cathelin S, Mar BG, Klinakis A, Lukyanov Y, Tseng JC, Sen F, Gehrie E, Li M, Newcomb E, Zavadil J, Meruelo D, Lipp M, Ibrahim S, Efstratiadis A, Zagzag D, Bromberg JS, Dustin ML, Aifantis I.** 2009. CCR7 signalling as an essential regulator of CNS infiltration in T-cell leukaemia. Nature **459:**1000-1004.

559. **Neujahr DC, Chen C, Huang X, Markmann JF, Cobbold S, Waldmann H, Sayegh MH, Hancock WW, Turka LA.** 2006. Accelerated memory cell homeostasis during T cell depletion and approaches to overcome it. J Immunol **176:**4632-4639.

560. **Blumenthal DT, Shacham-Shmueli E, Bokstein F, Schmid DS, Cohrs RJ, Nagel MA, Mahalingam R, Gilden D.** 2011. Zoster sine herpete: virologic verification by detection of anti-VZV IgG antibody in CSF. Neurology **76:**484-485.

561. **Ljungman P, Lonnqvist B, Gahrton G, Ringden O, Sundqvist VA, Wahren B.** 1986. Clinical and subclinical reactivations of varicella-zoster virus in immunocompromised patients. J Infect Dis **153:**840-847.

562. **Birlea M, Arendt G, Orhan E, Schmid DS, Bellini WJ, Schmidt C, Gilden D, Cohrs RJ.** 2011. Subclinical reactivation of varicella zoster virus in all stages of HIV infection. J Neurol Sci **304:**22-24.

563. **Onunu AN, Uhunmwangho A.** 2004. Clinical spectrum of herpes zoster in HIV-infected versus non-HIV infected patients in Benin City, Nigeria. West Afr J Med **23:**300-304.

564. **Drylewicz J, Schellens IM, Gaiser R, Nanlohy NM, Quakkelaar ED, Otten H, van Dorp S, Jacobi R, Ran L, Spijkers S, Koning D, Schuurman R, Meijer E, Pietersma FL, Kuball J, van Baarle D.** 2016. Rapid reconstitution of CD4 T cells and NK cells protects against CMV-reactivation after allogeneic stem cell transplantation. J Transl Med **14:**230.

565. **Meyer C, Dewane J, Kerns A, Haberthur K, Barron A, Park B, Messaoudi I.** 2013. Age and immune status of rhesus macaques impact simian varicella virus gene expression in sensory ganglia. J Virol **87:**8294-8306.

566. **St Leger AJ, Hendricks RL.** 2011. CD8+ T cells patrol HSV-1-infected trigeminal ganglia and prevent viral reactivation. J Neurovirol **17:**528-534.

567. **Vallortigara J, Chassande O, Higueret P, Enderlin V.** 2009. Thyroid hormone receptor alpha plays an essential role in the normalisation of adult-onset hypothyroidism-related hypoexpression of synaptic plasticity target genes in striatum. J Neuroendocrinol **21:**49-56.

568. **Martin EA, Muralidhar S, Wang Z, Cervantes DC, Basu R, Taylor MR, Hunter J, Cutforth T, Wilke SA, Ghosh A, Williams ME.** 2015. The intellectual disability gene Kirrel3 regulates target-specific mossy fiber synapse development in the hippocampus. Elife **4:**e09395.

569. **Ray A, Treloar HB.** 2012. IgSF8: a developmentally and functionally regulated cell adhesion molecule in olfactory sensory neuron axons and synapses. Mol Cell Neurosci **50:**238-249.

570. **Westerlund N, Zdrojewska J, Padzik A, Komulainen E, Bjorkblom B, Rannikko E, Tararuk T, Garcia-Frigola C, Sandholm J, Nguyen L, Kallunki T, Courtney MJ, Coffey ET.** 2011. Phosphorylation of SCG10/stathmin-2 determines multipolar stage exit and neuronal migration rate. Nat Neurosci **14:**305-313.

571. **Franke K, Otto W, Johannes S, Baumgart J, Nitsch R, Schumacher S.** 2012. miR-124-regulated RhoG reduces neuronal process complexity via ELMO/Dock180/Rac1 and Cdc42 signalling. EMBO J **31:**2908-2921.

572. **Eriksson KS, Zhang S, Lin L, Lariviere RC, Julien JP, Mignot E.** 2008. The type III neurofilament peripherin is expressed in the tuberomammillary neurons of the mouse. BMC Neurosci **9:**26.

573. **Yorimitsu T, Sato K, Takeuchi M.** 2014. Molecular mechanisms of Sar/Arf GTPases in vesicular trafficking in yeast and plants. Front Plant Sci **5:**411.

574. **Molyneux SD, Waterhouse PD, Shelton D, Shao YW, Watling CM, Tang QL, Harris IS, Dickson BC, Tharmapalan P, Sandve GK, Zhang X, Bailey SD, Berman H, Wunder JS, Izsvak Z, Lupien M, Mak TW, Khokha R.** 2014. Human somatic cell mutagenesis creates genetically tractable sarcomas. Nat Genet **46:**964-972.

575. **Strezoska Z, Pestov DG, Lau LF.** 2000. Bop1 is a mouse WD40 repeat nucleolar protein involved in 28S and 5. 8S RRNA processing and 60S ribosome biogenesis. Mol Cell Biol **20:**5516-5528.

576. **Schmader K.** 1998. Postherpetic neuralgia in immunocompetent elderly people. Vaccine **16:**1768-1770.